



Field-Trip Guide to the Vents, Dikes, Stratigraphy, and Structure of the Columbia River Basalt Group, Eastern Oregon and Southeastern Washington



Scientific Investigations Report 2017–5022–N

Cover. Palouse Falls, Washington. The Palouse River originates in Idaho and flows westward before it enters the Snake River near Lyons Ferry, Washington. About 10 kilometers north of this confluence, the river has eroded through the Wanapum Basalt and upper portion of the Grande Ronde Basalt to produce Palouse Falls, where the river drops 60 meters (198 feet) into the plunge pool below. The river's course was created during the cataclysmic Missoula floods of the Pleistocene as ice dams along the Clark Fork River in Idaho periodically broke and reformed. These events released water from Glacial Lake Missoula, with the resulting floods into Washington creating the Channeled Scablands and Glacial Lake Lewis. Palouse Falls was created by headward erosion of these floodwaters as they spilled over the basalt into the Snake River. After the last of the floodwaters receded, the Palouse River began to follow the scabland channel it resides in today. Photograph by Stephen P. Reidel.

Field-Trip Guide to the Vents, Dikes, Stratigraphy, and Structure of the Columbia River Basalt Group, Eastern Oregon and Southeastern Washington

By Victor E. Camp, Stephen P. Reidel, Martin E. Ross, Richard J. Brown, and
Stephen Self

Scientific Investigations Report 2017–5022–N

**U.S. Department of the Interior
U.S. Geological Survey**

U.S. Department of the Interior
RYAN K. ZINKE, Secretary

U.S. Geological Survey
William H. Werkheiser, Acting Director

U.S. Geological Survey, Reston, Virginia: 2017

For more information on the USGS—the Federal source for science about the Earth, its natural and living resources, natural hazards, and the environment—visit <https://www.usgs.gov> or call 1–888–ASK–USGS.

For an overview of USGS information products, including maps, imagery, and publications, visit <https://www.usgs.gov/pubprod/>.

Any use of trade, firm, or product names is for descriptive purposes only and does not imply endorsement by the U.S. Government.

Although this information product largely is in the public domain, it may also contain copyrighted materials as noted in the text. Permission to reproduce copyrighted items must be secured from the copyright owner.

Suggested citation:

Camp, V.E., Reidel, S.P., Ross, M.E., Brown, R.J., and Self, S., 2017, Field-trip guide to the vents, dikes, stratigraphy, and structure of the Columbia River Basalt Group, eastern Oregon and southeastern Washington: U.S. Geological Survey Scientific Investigations Report 2017–5022–N, 88 p., <https://doi.org/10.3133/sir20175022N>.

ISSN 2328-0328 (online)

Preface

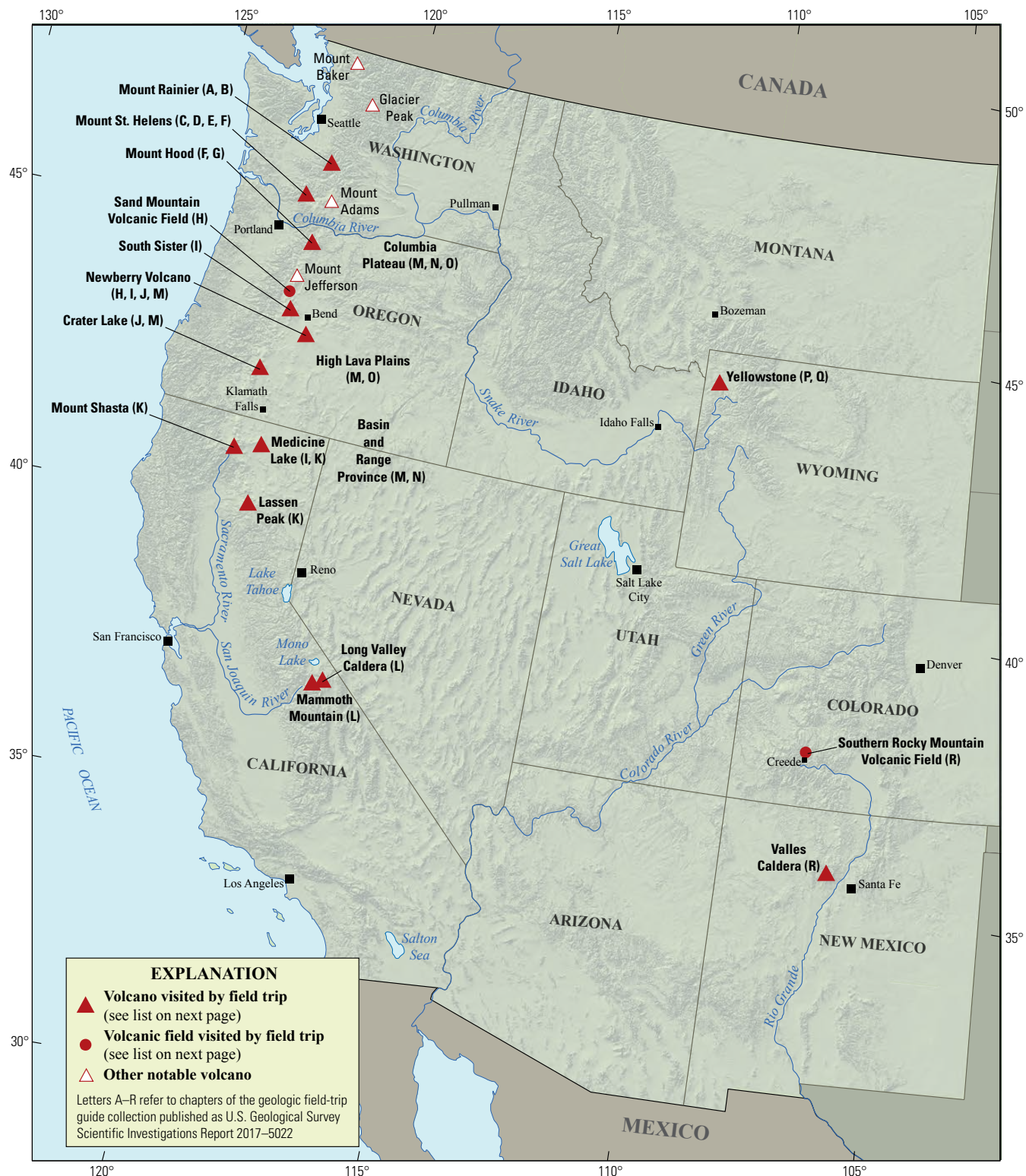
The North American Cordillera is home to a greater diversity of volcanic provinces than any comparably sized region in the world. The interplay between changing plate-margin interactions, tectonic complexity, intra-crustal magma differentiation, and mantle melting have resulted in a wealth of volcanic landscapes. Field trips in this series visit many of these landscapes, including (1) active subduction-related arc volcanoes in the Cascade Range; (2) flood basalts of the Columbia Plateau; (3) bimodal volcanism of the Snake River Plain-Yellowstone volcanic system; (4) some of the world's largest known ignimbrites from southern Utah, central Colorado, and northern Nevada; (5) extension-related volcanism in the Rio Grande Rift and Basin and Range Province; and (6) the spectacular eastern Sierra Nevada featuring Long Valley Caldera and the iconic Bishop Tuff. Some of the field trips focus on volcanic eruptive and emplacement processes, calling attention to the fact that the western United States provides opportunities to examine a wide range of volcanological phenomena at many scales.

The 2017 Scientific Assembly of the International Association of Volcanology and Chemistry of the Earth's Interior (IAVCEI) in Portland, Oregon, marks the first time that the U.S. volcanological community has hosted this quadrennial meeting since 1989, when it was held in Santa Fe, New Mexico. The 1989 field-trip guides are still widely used by students and professionals alike. This new set of field guides is similarly a legacy collection that summarizes decades of advances in our understanding of magmatic and tectonic processes of volcanic western North America.

The field of volcanology has flourished since the 1989 IAVCEI meeting, and it has profited from detailed field investigations coupled with emerging new analytical methods. Mapping has been enhanced by plentiful major- and trace-element whole-rock and mineral data, technical advances in radiometric dating and collection of isotopic data, GPS (Global Positioning System) advances, and the availability of lidar (light detection and ranging) imagery. Spectacularly effective microbeam instruments, geodetic and geophysical data collection and processing, paleomagnetic determinations, and modeling capabilities have combined with mapping to provide new information and insights over the past 30 years. The collective works of the international community have made it possible to prepare wholly new guides to areas across the western United States. These comprehensive field guides are available, in large part, because of enormous contributions from many experienced geologists who have devoted entire careers to their field areas. Early career scientists are carrying forward and refining their foundational work with impressive results.

Our hope is that future generations of scientists as well as the general public will use these field guides as introductions to these fascinating areas and will be enticed toward further exploration and field-based research.

Michael Dungan, University of Oregon
Judy Fierstein, U.S. Geological Survey
Cynthia Gardner, U.S. Geological Survey
Dennis Geist, National Science Foundation
Anita Grunder, Oregon State University
John Wolff, Washington State University
Field-trip committee, IAVCEI 2017



Map of the western United States showing volcanoes and volcanic fields visited by geologic field trips scheduled in conjunction with the 2017 meeting of the International Association of Volcanology and Chemistry of the Earth's Interior (IAVCEI) in Portland, Oregon, and available as chapters in U.S. Geological Survey Scientific Investigations Report 2017–5022.

0 100 200 300 400 MILES
0 100 200 300 400 KILOMETERS

Chapter letter	Title
A	Field-Trip Guide to Volcanism and Its Interaction with Snow and Ice at Mount Rainier, Washington
B	Field-Trip Guide to Subaqueous Volcaniclastic Facies in the Ancestral Cascades Arc in Southern Washington State—The Ohanapecosh Formation and Wildcat Creek Beds
C	Field-Trip Guide for Exploring Pyroclastic Density Current Deposits from the May 18, 1980, Eruption of Mount St. Helens, Washington
D	Field-Trip Guide to Mount St. Helens, Washington—An overview of the Eruptive History and Petrology, Tephra Deposits, 1980 Pyroclastic Density Current Deposits, and the Crater
E	Field-Trip Guide to Mount St. Helens, Washington—Recent and Ancient Volcaniclastic Processes and Deposits
F	Geologic Field-Trip Guide of Volcaniclastic Sediments from Snow- and Ice-Capped Volcanoes—Mount St. Helens, Washington, and Mount Hood, Oregon
G	Field-Trip Guide to Mount Hood, Oregon, Highlighting Eruptive History and Hazards
H	Field-Trip Guide to Mafic Volcanism of the Cascade Range in Central Oregon—A Volcanic, Tectonic, Hydrologic, and Geomorphic Journey
I	Field-Trip Guide to Holocene Silicic Lava Flows and Domes at Newberry Volcano, Oregon, South Sister Volcano, Oregon, and Medicine Lake Volcano, California
J	Geologic Field-Trip Guide to Mount Mazama, Crater Lake Caldera, and Newberry Volcano, Oregon
K	Geologic Field-Trip Guide to Volcanoes of the Cascades Arc in Northern California
L	Geologic Field-Trip Guide to Long Valley Caldera, California
M	Field-Trip Guide to a Volcanic Transect of the Pacific Northwest
N	Field-Trip Guide to the Vents, Dikes, Stratigraphy, and Structure of the Columbia River Basalt Group, Eastern Oregon and Southeastern Washington
O	Field-Trip Guide to Flood Basalts, Associated Rhyolites, and Diverse Post-Plume Volcanism in Eastern Oregon
P	Field-Trip Guide to the Volcanic and Hydrothermal Landscape of Yellowstone Plateau, Montana and Wyoming
Q	Field-Trip Guide to the Petrology of Quaternary Volcanism on the Yellowstone Plateau, Idaho and Wyoming
R	Field-Trip Guide to Continental Arc to Rift Volcanism of the Southern Rocky Mountains—Southern Rocky Mountain, Taos Plateau, and Jemez Volcanic Fields of Southern Colorado and Northern New Mexico

Contributing Authors

Boise State University

Brittany D. Brand
Nicholas Pollock

Colgate University

Karen Harpp
Alison Koleszar

Durham University

Richard J. Brown

East Oregon University

Mark L. Ferns

ETH Zurich

Olivier Bachmann

Georgia Institute of Technology

Josef Dufek

GNS Science, New Zealand

Natalia I. Deligne

Hamilton College

Richard M. Conrey

Massachusetts Institute of Technology

Timothy Grove

National Science Foundation

Dennis Geist (also with Colgate University and University of Idaho)

New Mexico Bureau of Geology and Mineral Resources

Paul W. Bauer
William C. McIntosh
Matthew J. Zimmerer

New Mexico State University

Emily R. Johnson

Northeastern University

Martin E. Ross

Oregon Department of Geology and Mineral Industries

William J. Burns
Lina Ma
Ian P. Madin
Jason D. McClaughry

Oregon State University

Adam J.R. Kent

Portland State University

Jonathan H. Fink
Martin J. Streck
Ashley R. Streig

San Diego State University

Victor E. Camp

Smithsonian Institution

Lee Siebert

Universidad Nacional Autónoma de San Luis Potosí

Damiano Sarocchi

University of California, Davis

Kari M. Cooper

University of Liverpool

Peter B. Kokelaar

University of Northern Colorado

Steven W. Anderson

University of Oregon

Ilya N. Binderman
Michael A. Dungan
Daniele McKay (also with Oregon State University and Oregon State University, Cascades)

University of Portland

Kristin Sweeney

University of Tasmania

Martin Jutzeler
Jocelyn McPhie

University of Utah

Jamie Farrell

U.S. Army Corps of Engineers

Keith I. Kelso

U.S. Forest Service

Gordon E. Grant (also with Oregon State University)
Robert A. Jensen

U.S. Geological Survey

Charles R. Bacon
Andrew T. Calvert
Christine F. Chan
Robert L. Christiansen
Michael A. Clyne
Michael A. Cosca
Julie M. Donnelly-Nolan

Benjamin J. Drenth

William C. Evans
Judy Fierstein
Cynthia A. Gardner
V.J.S. Grauch

Christopher J. Harpel
Wes Hildreth
Richard P. Hoblitt

Peter W. Lipman
Jacob B. Lowenstern
Jon J. Major
Seth C. Moran

Lisa A. Morgan
Leah E. Morgan
L.J. Patrick Muffler
James E. O'Connor

John S. Pallister
Thomas C. Pierson
Joel E. Robinson
Juliet Ryan-Davis

Kevin M. Scott
William E. Scott
Wayne (Pat) Shanks
David R. Sherrod

Thomas W. Sisson
Mark Evan Stelten
Weston Thelen
Ren A. Thompson

Kenzie J. Turner
James W. Vallance
Alexa R. Van Eaton
Jorge A. Vazquez

Richard B. Waitt
Heather M. Wright

U.S. Nuclear Regulatory Commission

Stephen Self (also with University of California, Berkeley)

Washington State University

Joseph R. Boro
Owen K. Neill
Stephen P. Reidel
John A. Wolff

Acknowledgments

Juliet Ryan-Davis and Kate Sullivan created the overview map, and Vivian Nguyen created the cover design for this collection of field-trip guide books. The field trip committee is grateful for their contributions.

Acknowledgments

Much of our understanding of the Columbia River flood-basalt province comes from a foundation of field investigations and mapping projects that are often underappreciated. In this regard, we wish to acknowledge the following workers whose field contributions have proved particularly beneficial to the authors of this field-trip guide: Jim Evans, Mark Ferns, Peter Hooper, Jenda Johnson, Martin Streck, Don Swanson, and Tom Wright. We thank Brennan Jordan and Rick Carlson for providing thorough and comprehensive reviews that greatly improved the manuscript, and John Wolff for further suggestions and editorial guidance. The guide benefited greatly from careful editing provided by Carolyn Donlin and Katherine Jacques.

Contents

Preface	iii
Contributing Authors	vi
Introduction	1
Physiography and Regional Setting	1
Stratigraphy of the Columbia River Basalt Group.....	3
Main Eruptive Phase.....	5
Waning Eruptive Phase.....	9
Paleomagnetic Stratigraphy.....	10
Petrochemical Stratigraphy.....	10
Stratigraphic Evidence for the Northward Migration of Flood-Basalt Eruption	13
Feeder Dikes.....	13
Dike Emplacement.....	13
Fissure-Fed Eruptions	15
Physical Volcanology.....	15
Giant Pāhoehoe Sheet Flows.....	15
Compound Flow Fields and Constituent Flow Lobes	16
Flow Emplacement.....	16
Deformation and Crustal Stress During and After the CRBG Eruptions	18
Petrogenesis	19
Road Log.....	23
Day 1 Overview—Malheur River Gorge.....	24
Day 1—Road Log	25
Day 2 Overview—Steens Mountain.....	28
Day 2—Road Log	28
Day 3 Overview—Baker City to Enterprise, Oregon.....	34
Day 3—Road Log:.....	36
Day 4 Overview—Grande Ronde and Snake River Canyons	39
Day 4—Road Log	40
Day 5 Overview—Proximal Pyroclastic Deposits of the Roza Member.....	54
Day 5—Road Log	54
Day 6 Overview—Geology of the Pasco Basin	61

Day 6—Road Log.....	62
Day 7 Overview—Geology and Structure of the Yakima Fold Belt.....	70
Day 7—Road Log.....	70
References Cited.....	77

Figures

1. Map of the distribution and physiographic features of the Columbia River flood-basalt province.....	2
2. Generalized basalt and paleomagnetic stratigraphy of the Columbia River Basalt Group.....	4
3. Graphs of Columbia River Basalt Group unit ages versus volume at both log and linear scales	5
4. Distribution maps for the seven formations of the Columbia River Basalt Group	7
5. Surface exposure map of the Columbia River Basalt Group main-phase lavas with eruption ages between ~16.7 and 15.6 Ma and contemporaneous rhyolite from 16.5 to 14 Ma	8
6. Photographs of the Saddle Mountains Basalt intracanyon outcrops exposed in the Snake River Canyon south of Asotin, Washington.....	9
7. Map of the eastern Columbia Basin showing the gradual pinching out to the west of progressively younger magnetostratigraphic units of the Grande Ronde Basalt	11
8. Variation diagrams showing the chemical range of analyses for each formation and selected members of the Columbia River Basalt Group	12
9. Map of the main dike swarms of the Columbia River flood-basalt province.....	14
10. Composite diagram showing various intraflow features that can be found in Columbia River Basalt sheet flows	17
11. Plot of $^{87}\text{Sr}/^{86}\text{Sr}$ versus $^{143}\text{Nd}/^{144}\text{Nd}$ for the main Columbia River Basalt Group formations	20
12. Compositional fields for 688 analyses of Steens Basalt, Imnaha Basalt, and Grande Ronde Basalt of the Columbia River Basalt Group main phase, plotted on the total alkali versus silica diagram of La Bas and others (1986)	21
13. Map of the field-trip route through eastern Oregon and southeastern Washington State	23
14. Old and updated distribution maps for the Columbia River Basalt Province	24
15. Map of field-trip stops for Day 1.....	25
16. Stratigraphic correlations of the basalt of Malheur Gorge, and its three stratigraphic units with Steens Basalt to the south and Imnaha and Grande Ronde Basalt to the north.....	26
17. Plot of chemical correlations between the basalt of Malheur Gorge/Hunter Creek Basalt and the main-phase Columbia River Basalt Group units lower Steens Basalt, Imnaha Basalt, and Grande Ronde Basalt	27
18. Map of field-trip stops for Day 2.....	29
19. Map of channel-fill deposits of the Devine Canyon Ash-flow Tuff in the vicinity of Steens Loop Road east of Frenchglen, Oregon	29
20. The Steens Mountain summit region, with notable physiographic features and mapped feeder dikes of Steens Basalt	31
21. Composite stratigraphic and paleomagnetic section of Steens Basalt at Steens Mountain	32

22.	Oblique aerial view of the Steens Mountain summit region, looking N20°W	33
23.	Map of field-trip stops for Day 3.....	34
24.	Map of the location of the middle Miocene-to-Pliocene La Grande-Owyhee eruptive axis and related grabens.....	35
25.	The Little Sheep Creek vent exposure	38
26.	Map of field-trip stops for Day 4.....	39
27.	Photograph from Stop 1 looking azimuth 332° across the Grouse Flat syncline	41
28.	Geologic map of the Troy, Oregon area	42
29.	Stratigraphic chart for the Troy area.....	43
30.	Photograph from Stop 2 looking azimuth 330° across the Grande Ronde River 3.6 km northeast of Troy	43
31.	Photograph looking azimuth 350° over Stop 3.	45
32.	Photograph looking azimuth 050° showing the intracanyon phase of the flow of Wenaha at Stop 4 above Grouse Creek.....	46
33.	Photograph of the undulatory Roza Member dike margin exposed parallel to roadcut at Rattlesnake Grade.....	47
34.	Photograph of the Roza Member dike exposed along Rattlesnake Grade showing marginal banded zones and columnar joints	47
35.	Map showing the extent of the Umatilla Member.....	49
36.	Photographs showing the vent complex for the flow of Joseph Creek, Teepee Butte Member	51
37.	Photographs of the major features of the flow of Joseph Creek vent complex	52
38.	Compositional variations across flow of Joseph Creek dike section B–B', Teepee Butte Member vent complex	53
39.	Map of field-trip stops for Day 5.....	54
40.	Sketch maps of the Columbia River flood-basalt province, showing the extent of the Roza Member and the Roza vent system.....	55
41.	Photo-interpretation of the pyroclastic edifice at the Texas Draw vent.....	56
42.	Pyroclastic deposits of the Rock Creek vent accumulations.....	57
43.	Interpretations of man-made cuts through the Roza Member at Winona illustrating how the tephra fall deposit has been dissected into a number of mounds, and the complex stratigraphic relations between pyroclastic rocks and lavas	59
44.	Photograph of successive stages of canyon development of the ancestral Salmon-Clearwater River recorded in Saddle Mountains Basalt intracanyon flows exposed at Devils Canyon, Washington.....	60
45.	Map of field-trip stops for Day 6.....	61
46.	Google Earth image of the Wallula Fault Zone near Wallula Gap	62
47.	Photograph showing the Two Sisters	63
48.	Photographs of basalt of Goose Island dike, Ice Harbor Member.....	64
49.	Graphs of TiO ₂ composition of the Umatilla Member in the Columbia Basin.....	66
50.	Photograph of thrust fault on the Little Badger Mountain anticline, Kennewick, Washington.....	67
51.	Aerial photograph of Rattlesnake Mountain.....	68
52.	Photograph of Umtanum Ridge, an anticlinal ridge similar to Rattlesnake Mountain	69
53.	Chemical composition of the Sentinel Bluffs Member in Sentinel Gap of the Saddle Mountains and the Sentinel Bluffs Member at Bingen, Washington	71
54.	Map of field-trip stops for Day 7	72

55.	Diagram of the Laurel Fault Zone exposed along Interstate 84 at Fairbanks Gap, Oregon	73
56.	Columbia Hills Fault Zone as viewed from Stop 3 along Washington State Route 14....	74
57.	Comparison of the stratigraphy from Bingen/White Salmon along State Route 14 east of Bingen, and Dog Mountain, which is west of Bingen.....	76
58.	Photograph of Mitchell Point, viewed across the river from Washington State Route 14	77

Conversion Factors

Inch/Pound to SI

Multiply	By	To obtain
Length		
inch (in.)	2.54	centimeter (cm)
inch (in.)	25.4	millimeter (mm)
foot (ft)	0.3048	meter (m)
mile (mi)	1.609	kilometer (km)
mile, nautical (nmi)	1.852	kilometer (km)
yard (yd)	0.9144	meter (m)
Area		
acre	4,047	square meter (m^2)
acre	0.4047	hectare (ha)
acre	0.4047	square hectometer (hm^2)
acre	0.004047	square kilometer (km^2)
square foot (ft^2)	929.0	square centimeter (cm^2)
square foot (ft^2)	0.09290	square meter (m^2)
square inch (in^2)	6.452	square centimeter (cm^2)
section (640 acres or 1 square mile)	259.0	square hectometer (hm^2)
square mile (mi^2)	259.0	hectare (ha)
square mile (mi^2)	2.590	square kilometer (km^2)
Volume		
cubic foot (ft^3)	28.32	cubic decimeter (dm^3)
cubic foot (ft^3)	0.02832	cubic meter (m^3)
cubic yard (yd^3)	0.7646	cubic meter (m^3)
cubic mile (mi^3)	4.168	cubic kilometer (km^3)
acre-foot (acre-ft)	1,233	cubic meter (m^3)
acre-foot (acre-ft)	0.001233	cubic hectometer (hm^3)

Temperature in degrees Celsius ($^{\circ}C$) may be converted to degrees Fahrenheit ($^{\circ}F$) as follows:

$$^{\circ}F = (1.8 \times ^{\circ}C) + 32$$

Temperature in degrees Fahrenheit ($^{\circ}F$) may be converted to degrees Celsius ($^{\circ}C$) as follows:

$$^{\circ}C = (^{\circ}F - 32) / 1.8$$

Field-Trip Guide to the Vents, Dikes, Stratigraphy, and Structure of the Columbia River Basalt Group, Eastern Oregon and Southeastern Washington

By Victor E. Camp¹, Stephen P. Reidel², Martin E. Ross³, Richard J. Brown⁴, and Stephen Self⁵

Introduction

The Columbia River Basalt Group (CRBG) covers an area of more than 210,000 km² with an estimated volume of 210,000 km³ (Reidel and others, 2013a). As the youngest continental flood-basalt province on Earth (16.7–5.5 Ma), it is well preserved, with a coherent and detailed stratigraphy exposed in the deep canyonlands of eastern Oregon and southeastern Washington. The Columbia River flood-basalt province (CRFBP) is often cited as a model for the study of similar provinces worldwide.

This field-trip guide explores the main source region of the CRBG and is written for trip participants attending the 2017 International Association of Volcanology and Chemistry of the Earth's Interior (IAVCEI) Scientific Assembly in Portland, Oregon, USA. The first part of the guide provides an overview of the geologic features common in the CRFBP and the stratigraphic terminology used in the CRBG. The accompanying road log examines the stratigraphic evolution, eruption history, and structure of the province through a field examination of the lavas, dikes, and pyroclastic rocks of the CRBG.

Physiography and Regional Setting

Basaltic lavas of the CRFBP were generated in a back-arc setting between the active Cascade volcanic arc and the Rocky Mountains. The province covers most of eastern Washington and eastern Oregon, a significant part of western Idaho, and extends southward into northernmost Nevada (fig. 1). Some flows advanced westward through a lowland gap in the Cascade arc, spreading into the Willamette Valley and Coast Ranges, and farther west into offshore forearc basins beyond

the coastline of northwestern Oregon (Beeson and others, 1979; Niem and Niem, 1985; Wells and others, 2009).

The major physiographic feature of the northern part of the province is the Columbia Basin, a broad structural basin lying between the Cascades arc and the Idaho batholith, covering more than 150,000 km² of the province (fig. 1). The Columbia Basin is bounded to the south by the Blue Mountains, which define the transition between the northern and southern parts of the province. In southeastern Oregon, the southern part of the province is sometimes referred to as the Oregon Plateau (for example, Carlson and Hart, 1987) despite the fact that it is characterized by high-relief topography of fault-bounded mountains and basins (fig. 1). Lying west of the Oregon Plateau is the younger Oregon High Lava Plains, a late Miocene to recent bimodal terrain of tholeiitic basalt and rhyolite (Jordan and others, 2004; Ford and others, 2013). The thickest accumulation of the CRBG is located beneath the central part of the Columbia Basin where subsidence began in the Eocene, but where Miocene subsidence generated a basalt pile of subaerial flows more than 4 km thick (Reidel and others, 1989a). In the southern part of the province, the thickest accumulation is at Steens Mountain where the oldest formation (Steens Basalt) is nearly 1 km thick (Johnson and others, 1998).

The middle Miocene flood-basalt stratigraphy unconformably overlies a variety of older rock types. To the northeast and east, these basement rocks are composed of a cratonic assemblage of Proterozoic and Paleozoic rocks intruded by Cretaceous granite (for example, Reidel and others, 1989a, 2013b); however, the southern part of the province is underlain primarily by Paleogene volcanic and volcaniclastic rocks, which in turn are underlain by a Mesozoic to Paleozoic assemblage of accreted oceanic terranes (Walker and MacLeod, 1991; Scarberry and others, 2010; Schwartz and others, 2010; LaMaskin and others, 2011). The southern part of the province in eastern Oregon is partly overlain by a younger, diverse assemblage of tholeiitic, silicic, calc-alkaline, and mildly alkaline volcanic rocks of late Miocene to Pliocene age that are best exposed in the La Grande, Baker, and Oregon-Idaho grabens (Cummings and others, 2000; Hooper and others, 2002; Ferns and McClaughry, 2013). These rocks are largely contemporaneous

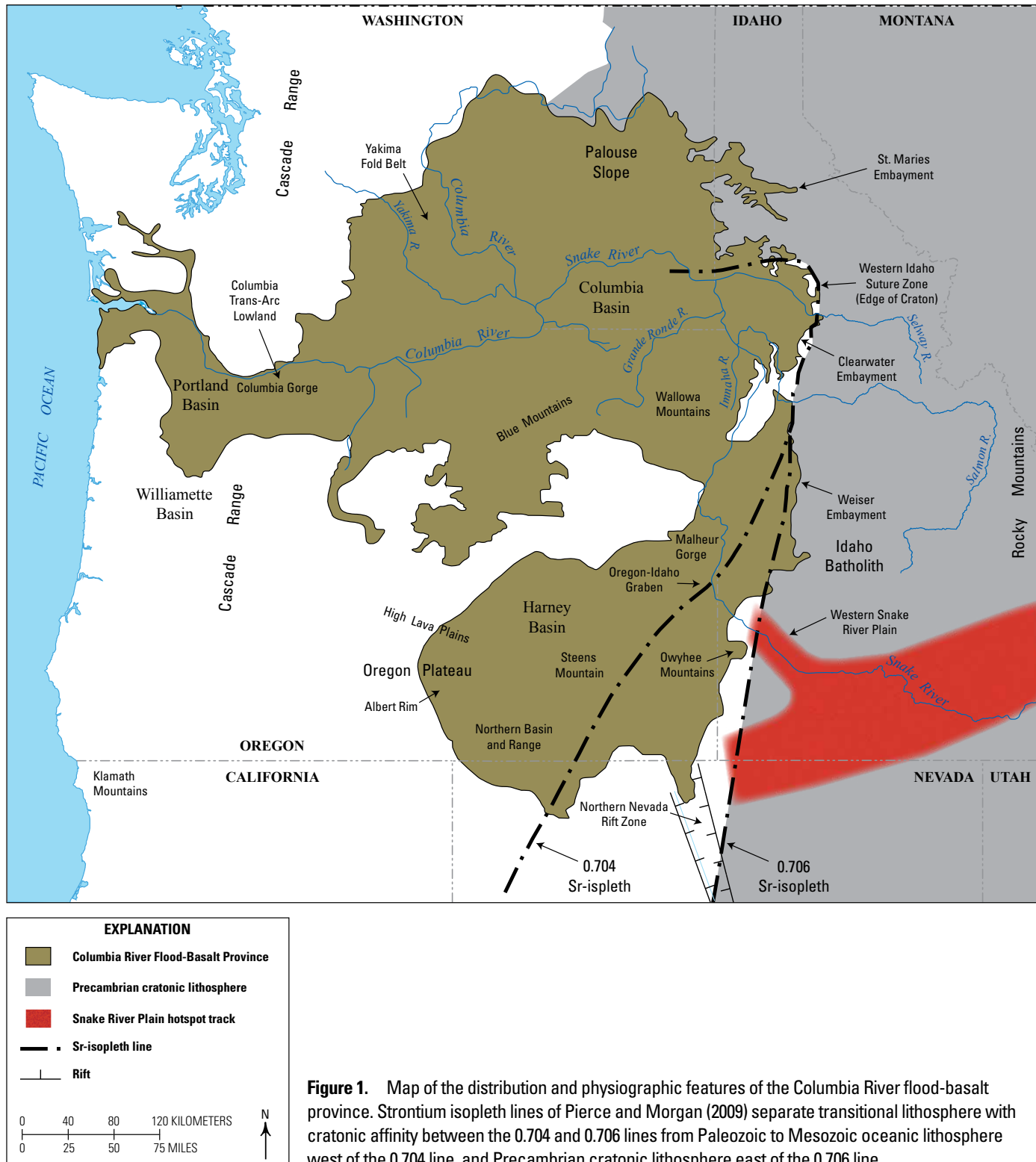
¹Department of Geological Sciences, San Diego State University.

²School of the Environment, Washington State University.

³Department of Marine and Environmental Sciences, Northeastern University.

⁴Department of Earth Sciences, Durham University.

⁵Department of Earth and Planetary Science, University of California, Berkeley.



with the Saddle Mountains Basalt but typically postdate CRBG lavas in any given location, and appear to be related to a later period of crustal stretching (Hooper and others, 2007).

Although the CRBG was created in a discrete volcanic event of tholeiitic flood-basalt volcanism, from 16.7 to 5.5 Ma, it is also part of a long-lived volcanic record in the Cascadia back-arc region. This record includes calc-alkaline to alkaline volcanism associated with the John Day and Clarno Formations and equivalent rocks (~50–22 Ma), and volcanism along the La Grande-Owyhee eruptive axis of Ferns and McClaughry (2013) that varies in composition from an older period of calc-alkaline volcanism (~14–10 Ma) to a younger period of alkali volcanism (~10–2 Ma). A well-established hiatus or waning in volcanism, between ~22–20 Ma and 16.7 Ma, separates John Day/Clarno-age calc-alkaline volcanism from the initiation of tholeiitic CRBG volcanism (McKee and others, 1970; McQuarrie and Oskin, 2010; Coble and Mahood, 2012). The volcanic record in the back-arc region continues to this day with bimodal volcanism along the Oregon High Lava Plains (~10 Ma to recent) and Snake River Plain (~15 Ma to recent), where tholeiitic basalt erupts periodically along age-progressive rhyolite trends to the west-northwest and east-northeast, respectively. The fact that the CRBG is embedded in a long and continuing record of diverse volcanism in a back-arc setting is an important distinction separating this flood-basalt event from all others in the geologic record.

Stratigraphy of the Columbia River Basalt Group

The first regional map of the CRFBP was produced by Aaron Waters (1961). Based on the field recognition of extensive flows and groups of flows, Waters (1961) generated a gross stratigraphy for the province, subdividing it into two main stratigraphic units, the Picture Gorge Basalt and younger Yakima basalt subgroup. Several workers added stratigraphic detail to Yakima basalt subgroup with further subdivisions in the 1960s and early 1970s (for example, Mackin, 1961; Bingham and Grolier, 1966; Schmincke, 1967; Wright and others, 1973). By the mid-1970s, an integrated approach to geologic mapping had evolved, where flow identification by conventional field work was combined with rapid x-ray fluorescence (XRF) analyses and the field identification of paleomagnetic polarities for flows and groups of flows. This integrated approach was used in the publication of several regional maps for the province (for example, Grolier and Bingham, 1971, 1978; Swanson and others, 1980, 1981), and it was instrumental in helping to establish a detailed revision of the CRBG stratigraphic nomenclature (Swanson and others, 1979). Continued refinement of the stratigraphy in the northern segment of the CRFBP (Columbia Basin and Blue Mountains) is evident in a variety of papers published in

Geological Society of America Special Papers 239 (Reidel and Hooper, 1989) and 497 (Reidel and others, 2013c).

South of the Blue Mountains in southeastern Oregon (fig. 1), early workers noted that the volume of the Steens Basalt was as great as the volume of many individual CRBG formations (Carlson and Hart, 1987), and that the Steens Basalt also shares a common isotopic source component with Imnaha Basalt, which at that time, was recognized as the oldest formation of the CRBG (Carlson and others, 1981; Carlson, 1984; Hart and Carlson, 1987). Hooper and others (2002) and Camp and others (2003) established a conformable stratigraphic connection between the Steens and Imnaha Basalt. In 2013, the Steens Basalt was formally recognized as the earliest formation of the CRBG stratigraphy, resulting in the southern extension of the province into southeastern Oregon (fig. 1; Camp and others, 2013).

A precedent was established by Swanson and others (1979) to exclude lithostratigraphic units from CRBG stratigraphy that are not fundamentally basaltic. The nomenclature is meant to be flexible and there are no set rules on what can be accepted, but rather a malleable set of evolving criteria that can be assessed and weighed by current workers. The only fixed requirement is that lithostratigraphic units must conform to the Code of Stratigraphic Nomenclature (North American Commission on Stratigraphic Nomenclature, 2005). For the CRBG, some criteria that might be considered are (1) chemical affinity, (2) stratigraphic continuity, (3) physical volcanology, with particular emphasis on large-volume sheet flows, (4) a vent source by fissure eruption closely related in time, space, and orientation to other CRBG source regions, and (or) (5) other criteria linking the unit to the same petrogenetic environment.

Today, the CRBG contains seven formations and numerous formal and informal members (fig. 2). The combined stratigraphic column contains more than 350 extensive and mappable tholeiitic sheet flows, and perhaps thousands of smaller flows and flow lobes (Reidel and others, 2013a). From oldest to youngest, the volumetrically significant and (or) most studied formations are the Steens Basalt, Imnaha Basalt, Grande Ronde Basalt, Wanapum Basalt and Saddle Mountains Basalt. Picture Gorge Basalt and Prineville Basalt are also given formation status, but they are more localized to north-central Oregon and interbedded in part with the Grande Ronde Basalt (fig. 2). The Grande Ronde Basalt is composed of 25 formal and informal members. The only formations where all members are formalized are the well-exposed Wanapum and Saddle Mountains Basalts. Of the six Wanapum Basalt members, the most intensely studied include, from oldest to youngest, the Frenchman Springs, Roza, and Priest Rapids Members. Of the nine Saddle Mountains Basalt members, the most intensely studied include, from oldest to youngest, the Umatilla, Asotin/Wilbur Creek, Pomona, Elephant Mountain, Ice Harbor, and Lower Monumental Members.

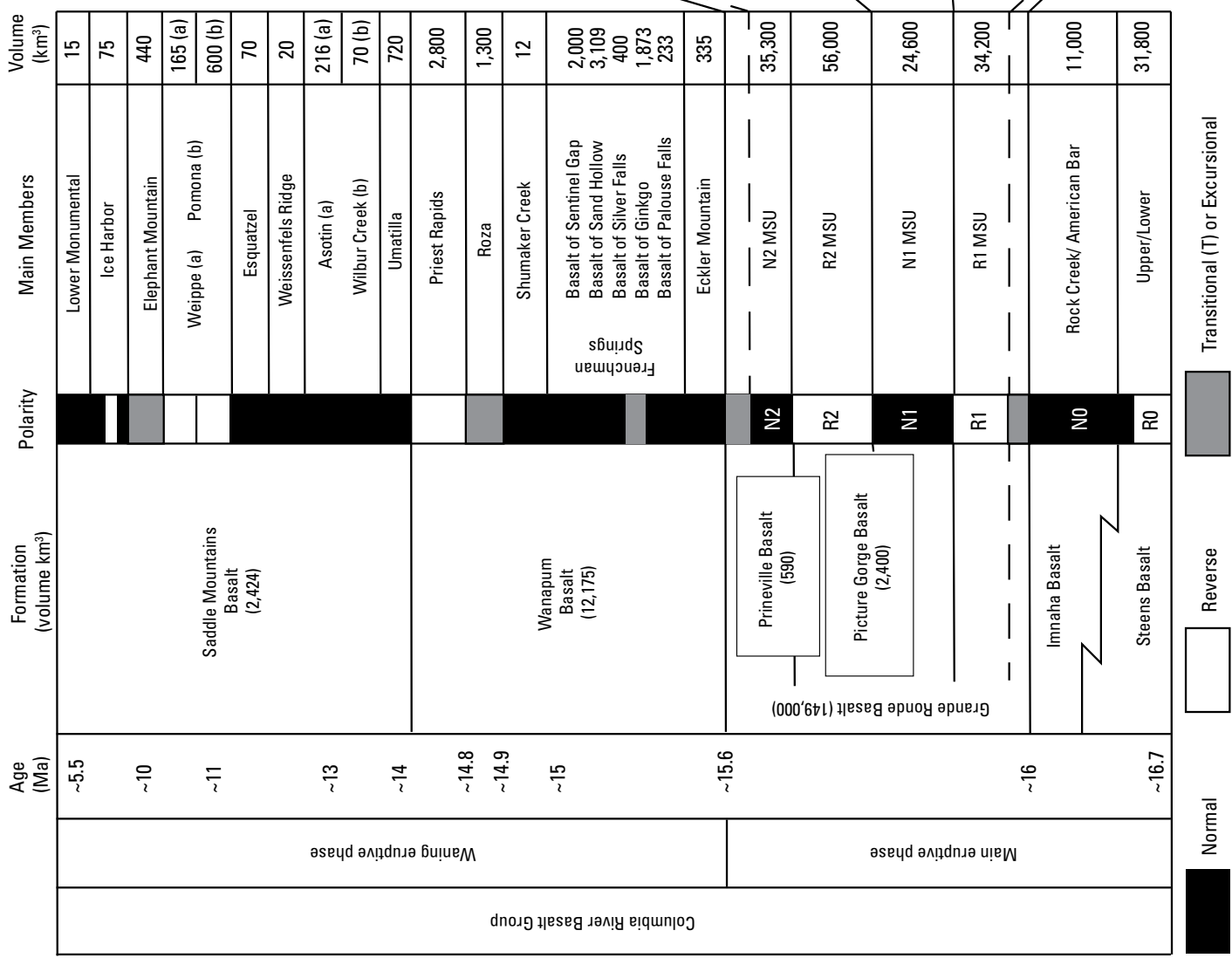


Figure 2. Generalized basalt and paleomagnetic stratigraphy of the Columbia River Basalt Group. R0 through N2 refer to magnetostratigraphic units (MSUs) of the main eruptive phase. Modified from Reidel (2015) with ages from Barry and others (2010, 2013).

Main Members	Volume (km ³)
Sentinel Bluffs Member	10,150
Winter Water Member	7,800
Fields Spring Member	290
Indian Ridge Member	1,200
Member of Armstrong Canyon	800
Member of Ortley	13,800
Member of Buttermilk Canyon	990
Slack Canyon Member	310
Meyer Ridge Member	580
Member of Grouse Creek	7,050
Wapsilla Ridge Member	40,250
Member of Mount Horrible	8,150
Cold Springs Ridge Member	5,275
Hoskin Gulch Member	4,700
China Creek Member	6,100
Member of Frye Point	4,800
Member of Downey Gulch	7,500
Member of Brady Gulch	Note 1
Member of Kendrik Grade	Note 1
Member of Center Creek	5,250
Member of Skelton Creek	4,000
Member of Rogersburg	6,400
Teepee Butte Member	7,600
Member of Birch Creek	1,900
Buckhorn Springs Member	5,304

Main Eruptive Phase

The CRBG eruptions continued for more than 11 million years, from ~16.7 to 5.5 Ma; however, about 93 percent of the flood-basalt volume erupted in only ~1.1 million years (m.y.; 16.7–15.6 Ma). We refer to these eruptions as the “main eruptive phase,” generated during a period of nearly constant basalt eruption with relatively little time between effusive events (figs. 2 and 3). The entire volume of Steens Basalt, Imnaha Basalt, Grande Ronde Basalt, Picture Gorge Basalt, and Prineville Basalt erupted over this short time interval (figs. 3 and 4), with the peak of the main eruptive phase occurring during the eruption of Grande Ronde Basalt, when ~71 percent of the flood-basalt volume (mostly basaltic

andesites) erupted in about 400,000 years (Barry and others, 2013). The time interval for the Grande Ronde eruptions was estimated by Barry and others (2013) at ~16–15.6 Ma, but this interval might be too young because (1) it overlaps with the age range of ash beds found in the Wanapum Basalt that have been correlated with tephra deposits of known age between 16 and 15.4 Ma (Ladderdud and others, 2015), and (2) it is, for the most part, younger than the age range of 16.05 to 16.02 Ma derived from the Littlefield Rhyolite that sits above lavas chemically equivalent to the Grande Ronde Basalt in the Malheur Gorge of eastern Oregon (Webb and others, 2016).

These main-phase eruptions were, in part, contemporaneous with initial eruptions of rhyolite at the western end of the Snake

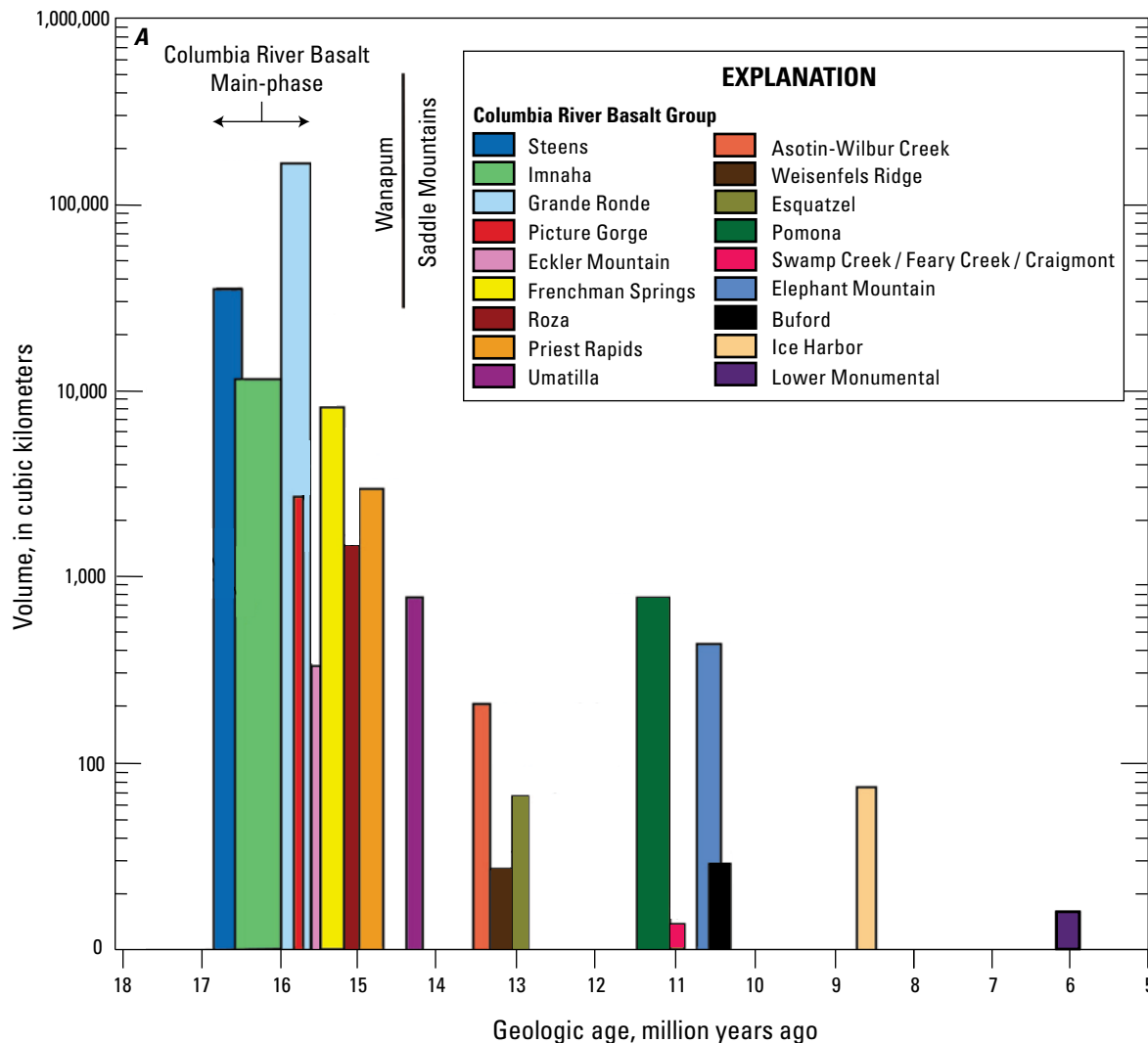


Figure 3. Graphs of Columbia River Basalt Group unit ages versus volume at both log (A) and linear (B) scales, modified from Barry and others (2013).

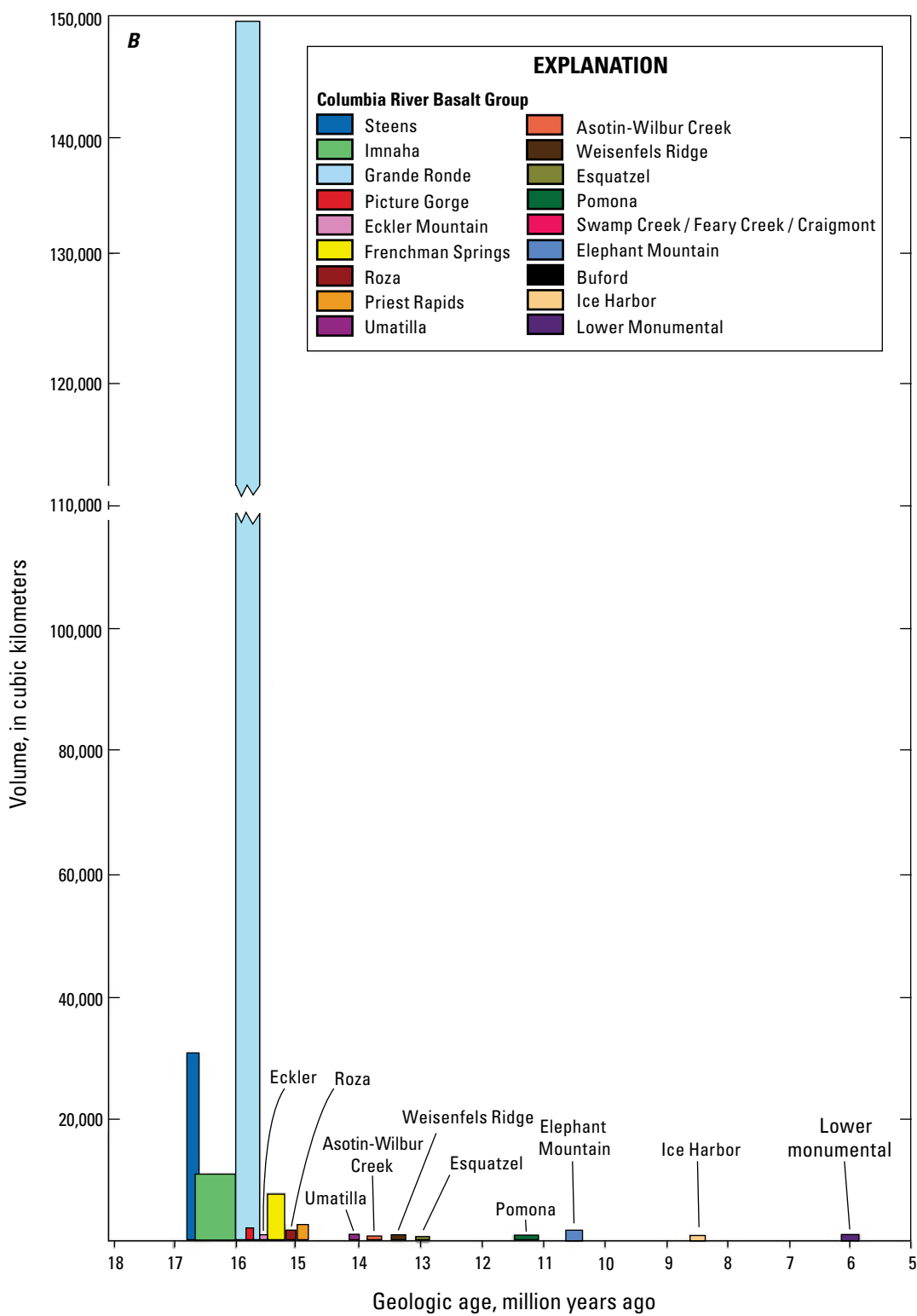


Figure 3.—Continued

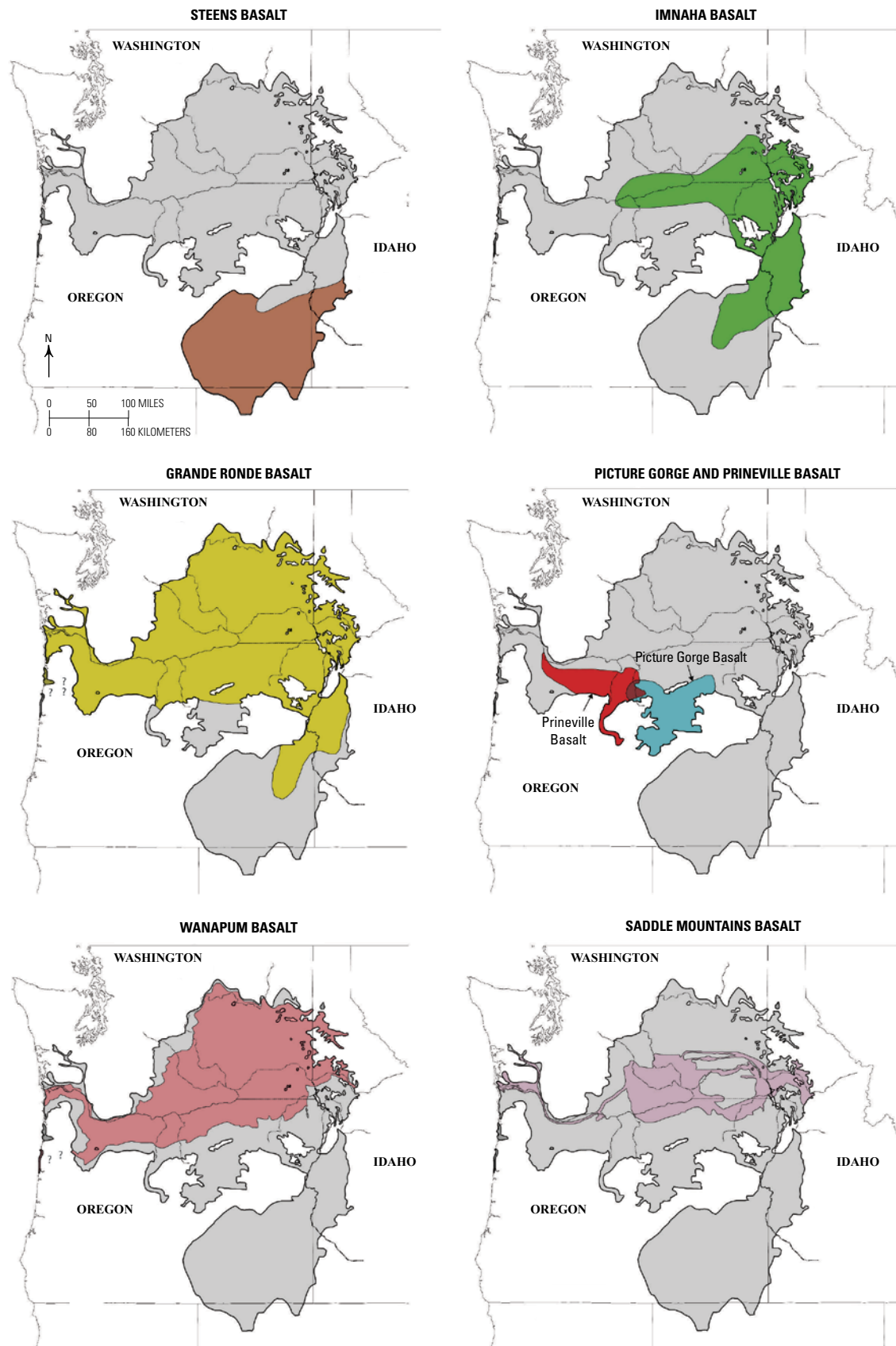


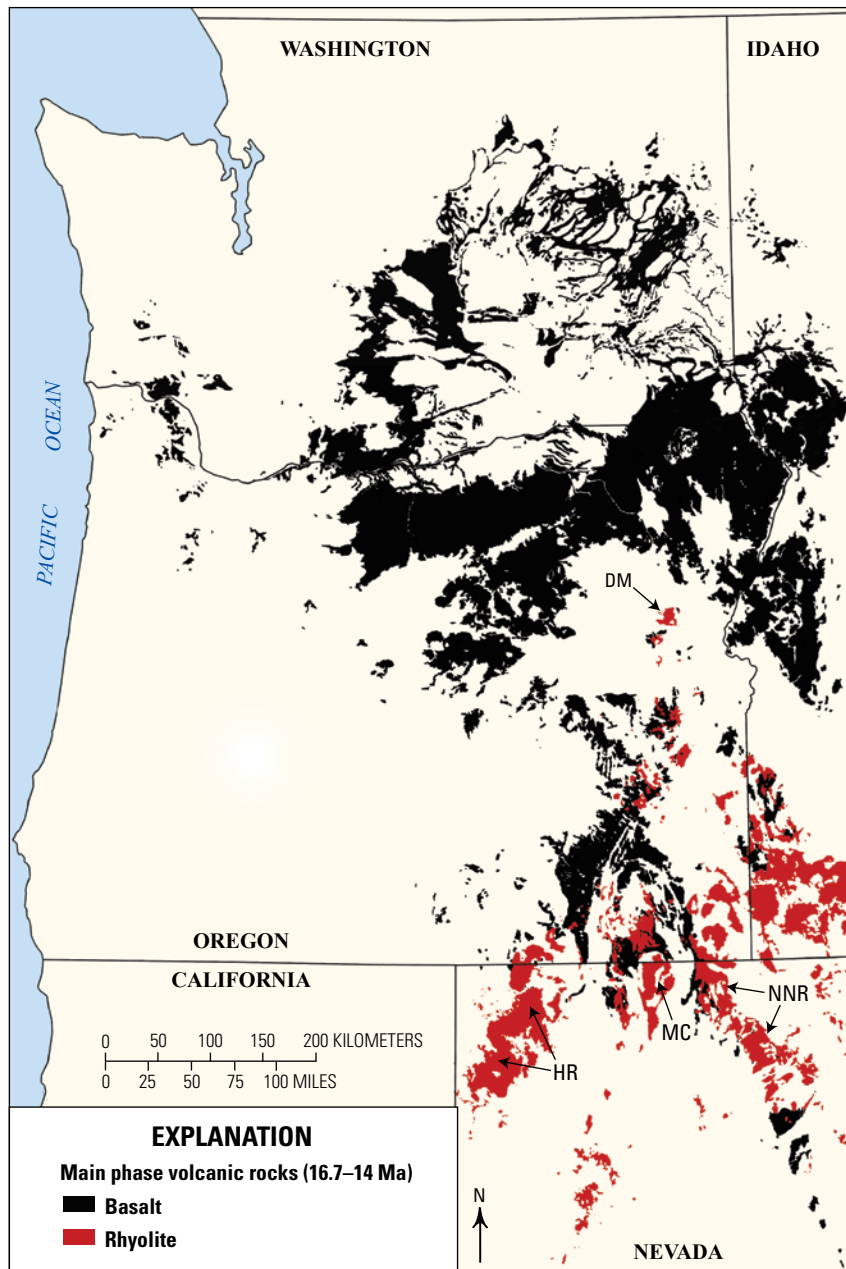
Figure 4. Distribution maps for the seven formations of the Columbia River Basalt Group (modified from Reidel, 2015).

River Plain hot spot track (for example, Coble and Mahood, 2015; Mahood and Benson, 2016). The southern part of the CRFBP could therefore be described as a bimodal province during the early stage of volcanism (fig. 5). In any given area, however, the greatest volume of rhyolite eruptions appear to have followed the initial basalt eruptions (for example, Benson and Mahood, 2016). The eruption of the Steens Basalt at ~16.7 Ma was partly contemporaneous with small-volume eruptions of interbedded rhyolitic tuff having similar ages derived from $^{40}\text{Ar}/^{39}\text{Ar}$ feldspar analyses (Mahood and Benson, 2016). The eruption of the Steens Basalt with minor rhyolite was followed by the eruption of voluminous rhyolitic ash flows. These began to erupt across the Oregon-Nevada border region between 16.5 and 16.4 Ma from the High Rock caldera complex, the McDermitt caldera, the Hawkes

Valley/Lone Mountain rhyolite center, and the Santa Rosa-Calico Volcanic complex (Rytuba and McKee, 1984; Brueske and Hart, 2008; Wypych and others, 2011; Benson and others, 2013, 2016; Coble and Mahood, 2015).

Although the oldest rhyolite ages (~16.7–16.4 Ma) are largely restricted to a narrow region at the western end of the Snake River Plain hot spot track (fig. 1), slightly younger rhyolites (~16–15 Ma) are spread over a much wider area (fig. 5) to include felsic rocks as far north as Baker City, Oregon (Shervais and Hanan, 2008; Streck and others, 2015), and as far south as the northern Nevada rift and unnamed rhyolites in northern Nevada (John and others, 2000; Best and others, 1989). However, recent $^{40}\text{Ar}/^{39}\text{Ar}$ data suggest that a few small-volume rhyolites in the greater Dooley Mountain area near Baker City might be as old

Figure 5. Surface exposure map of the Columbia River Basalt Group main-phase lavas with eruption ages between ~16.7 and 15.6 Ma (Stoons, Imnaha, and Grande Ronde Basalts) and contemporaneous rhyolite from 16.5 to 14 Ma (red). The southern part of the flood-basalt province is largely bimodal, with rhyolitic rocks lying above a broad region of crustal melting that extends beyond the western end of the Snake River Plain hot spot track (that is, the Oregon-Nevada border region). Rhyolitic centers noted in the text are the High Rock caldera complex (HR), the McDermitt caldera (MC), the northern Nevada rift (NNR), and at Dooley Mountain (DM; optional stop for Day 3).



as 16.5 Ma (Streck and others, 2016). A compilation of rhyolites by Benson and others (2016) suggests that the broad region of 16.7–15 Ma felsic volcanism accumulated to a minimum volume of 7,000 km³.

Waning Eruptive Phase

The Wanapum and Saddle Mountains Basalts (~7 percent of the CRBG volume) were generated during the waning stage of the flood-basalt eruptions, where significant time gaps can be recognized between individual members and flows, particularly between Saddle Mountains flows. The volume of single Wanapum flows is similar to that of the large-volume Grande Ronde flows which commonly exceed 1,000 km³. In contrast, Saddle Mountains flows are of smaller volumes (<600 km³), with

significantly greater time gaps between eruptions, often exceeding 1–2 million years.

After erupting in the eastern part of the Columbia Basin, Wanapum lavas typically travelled many hundreds of kilometers from their vents as large pāhoehoe sheet flows. They advanced westward down a west-dipping paleoslope that continued to develop concurrently with the CRBG eruptions (Swanson and others, 1980, 1981; Camp, 1995). The surface extent of most Wanapum flows covered 50 percent or more of the Columbia Basin. In contrast, individual Saddle Mountains flows covered a much smaller surface area, and their westward advance was restricted in part to large canyons of the ancestral Clearwater, Snake, and Columbia River systems, created by erosion during the large time-gaps between successive eruptions (fig. 6).

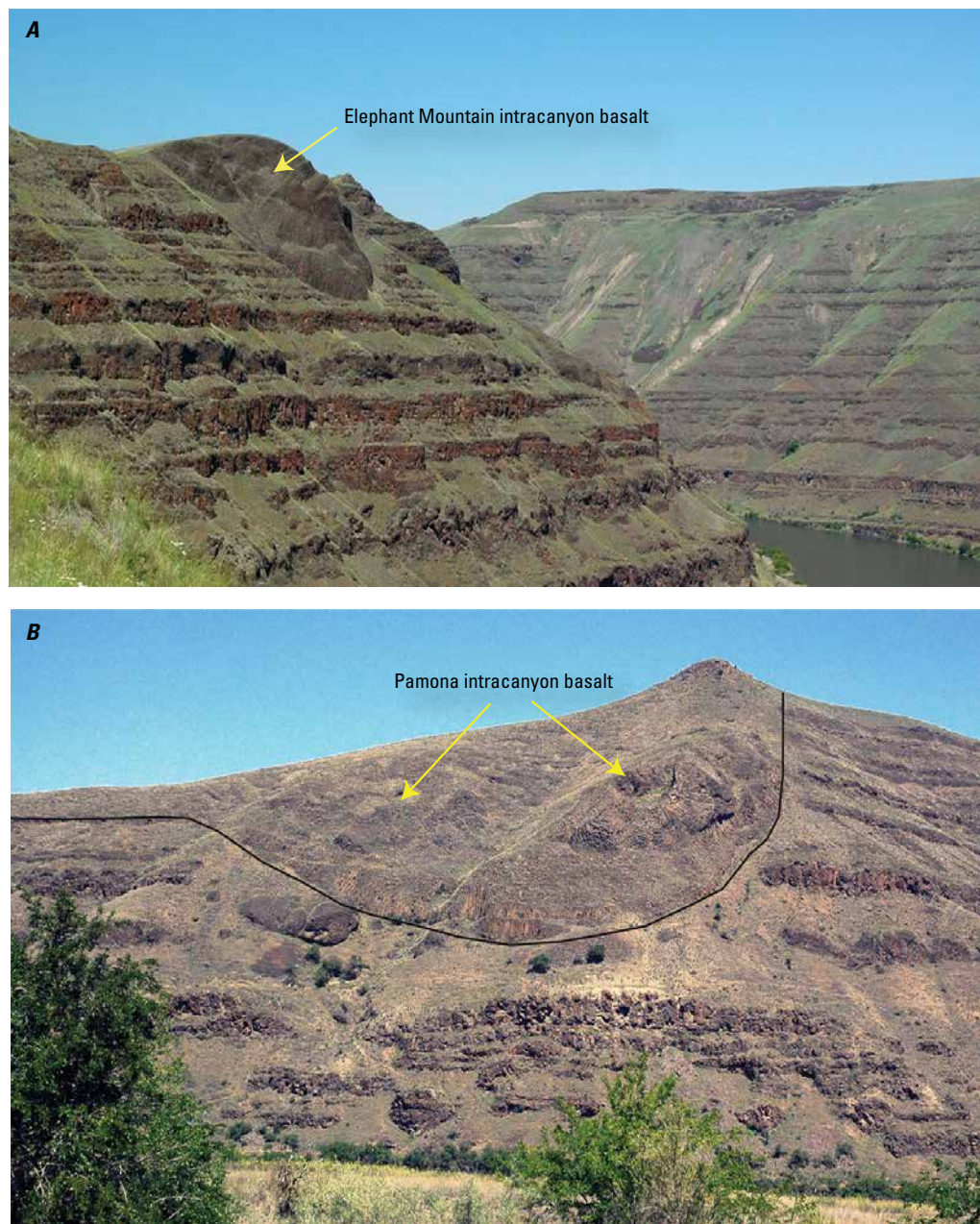


Figure 6. Photographs of the Saddle Mountains Basalt intracanyon outcrops exposed in the Snake River Canyon south of Asotin, Washington. A, Elephant Mountain Member filling a part of the ancestral Snake River canyon that eroded through Grande Ronde lava flows of MSU R2, ~8 km south of Asotin, Washington. B, Intracanyon Pomona Member filling a part of the ancestral Snake River canyon eroded through Grande Ronde Basalt R2 lava flows, ~4 km south of Asotin, Washington.

Paleomagnetic Stratigraphy

Continuity of the main-phase eruptions affords the possibility of using magnetic reversals as a stratigraphic tool (fig. 2). Current data suggests that a continuous paleomagnetic record may exist for the Steens, Imnaha, Grande Ronde, Picture Gorge, and Prineville Basalts, with an informal magnetostatigraphic subdivision into six magnetostatigraphic units (MSUs), from oldest to youngest, R0 through N2, (R, reverse polarity; N, normal polarity). The base of this section is recorded in the Steens Basalt, which contains the two oldest MSUs, R0 and N0, with a well-studied polarity transition between them (Watkins and Baksi, 1974; Mankinen and others, 1985, 1987; Jarboe and others, 2008). Precise $^{40}\text{Ar}/^{39}\text{Ar}$ dating by Jarboe and others (2010) suggest that the magnetic transition may correspond with a polarity reversal dated elsewhere at 16.72 Ma (Gradstein and others, 2004).

A few flows at the base and the top of the Imnaha Basalt stratigraphy have reverse or transitional polarity, but all other flows have normal polarity (for example, Hooper and others, 1984), which suggests that they are stratigraphically equivalent to the uppermost flows of Steens Basalt (that is, N0). Such a conclusion is consistent with two observations: (1) Imnaha Basalt flows of normal polarity typically lie beneath R1 flows of Grande Ronde Basalt in southeastern Washington (for example, Reidel, 1983), and (2) flows in the Malheur Gorge region of eastern Oregon that are chemically equivalent to Imnaha Basalt sit directly above flows of lower Steens Basalt chemistry (that is, R0; Hooper and others, 2002).

The Grande Ronde Basalt has been subdivided into four MSUs (Swanson and others, 1979), R1 to N2. Regional mapping of these units throughout the Columbia Basin (fig. 7) shows that they pinch-out progressively to the east (Swanson and others, 1980, 1981; Camp, 1981; Camp and Hooper, 1981; Kauffman and others, 2009). This is consistent with the development of the west-dipping paleoslope described earlier (see Waning Eruptive Phase), and it suggests that a period of epeirogenic change took place during the Grande Ronde eruptions. Some workers have argued that this was the result of regional uplift to the east (Swanson and Wright, 1976; Hooper and Camp, 1981; Camp and Hooper, 1981; Camp, 1995), but Reidel and others (1989a, 1994a, 2013b) argue that subsidence may have been the main tectonic cause. The Picture Gorge and Prineville Basalts are, in places, interbedded with Grande Ronde Basalt in the southern Columbia Basin, with Picture Gorge erupting during N1 and R2 time (Bailey, 1989) and Prineville during R2 and N2 time (Reidel and others, 2013a).

The development and mapping of a presumably contiguous paleomagnetic record from the Imnaha through the Grande Ronde Basalt is based largely on field determinations using a portable fluxgate magnetometer. Although the repetition of results suggest that the magnetic polarity data is generally consistent, it should also be viewed with caution, in part because of the possibility that original polarities could be overprinted by a younger polarity field. Recent and more precise laboratory results, for example, suggest that the identification of the N2 MSU may have to be redefined to

include paleomagnetic variants and a repositioning of the R2-N2 reversal (Hagstrum and others, 2010). There is also a general lack of paleomagnetic data in the southernmost outcrop area of Imnaha Basalt, leaving the possibility open for additional, yet unrecognized polarity reversals in that region.

Petrochemical Stratigraphy

Early studies relied on field criteria and petrographic characteristics to establish a generalized stratigraphy for the CRFBP, which was later refined by more detailed paleomagnetic and geochemical investigations. One of the most important petrographic aspects in the identification and correlation of flows lies in recognizing the presence or absence of plagioclase phenocrysts and (or) olivine microphenocrysts. For example, the oldest formations of the Steens and Imnaha Basalts, as well as Picture Gorge Basalt, are well known for their abundant, large plagioclase phenocrysts. Plagioclase phenocrysts are also a characteristic of several Wanapum and Saddle Mountains flows. The larger volume of CRBG flows is aphyric, however. This includes most of the Grande Ronde lavas, although a few Grande Ronde flows are characterized by plagioclase microphenocrysts or phenocrysts as much as 7 mm across.

Since the 1970s, major- and trace-element geochemistry has proven to be instrumental in recognizing and correlating flows over vast distances, leading to the establishment of a very detailed and coherent stratigraphy for the CRBG (for example, Wright and others, 1973, 1989; Swanson and others, 1979, 1981; Swanson and Wright, 1981; Reidel, 1983; Beeson and others, 1985; Mangan and others, 1986; Hooper, 2000; Hooper and others, 1984, 2007; Reidel and others 2013a). With careful sampling techniques, fresh, unaltered samples can readily be obtained in most lava flows, thus resulting in consistent geochemical signatures across the entire distribution areas of most flows. An exception to consistent trends exists in flows that appear to be the product of multiple injections associated with flow inflation (see section on Flow Emplacement). Major and trace-element geochemistry has been most effective in the identification of Wanapum and Saddle Mountains members and flows, where their chemical fields can be largely isolated on binary plots, as shown for example, in figure 8.

The remaining formations are chemically more uniform, making it more difficult to differentiate distinct chemical groups that are stratigraphically extensive enough to warrant formal member status. Two informal members have been recognized in the Steens Basalt based on such geochemical distinctions (Camp and others, 2013): the lower Steens Basalt of primitive, homogeneous tholeiite, and the upper Steens Basalt of increasingly more diverse flows of tholeiite, alkali basalt, and basaltic trachyandesite. Similarly, Hooper and others (1984) recognized two distinct chemical groups in the Imnaha Basalt: the slightly more silica-rich American Bar-type, composed of flows located predominantly at the base of the sequence, and the generally less-evolved Rock Creek-type, with flows located at the top of the sequence.

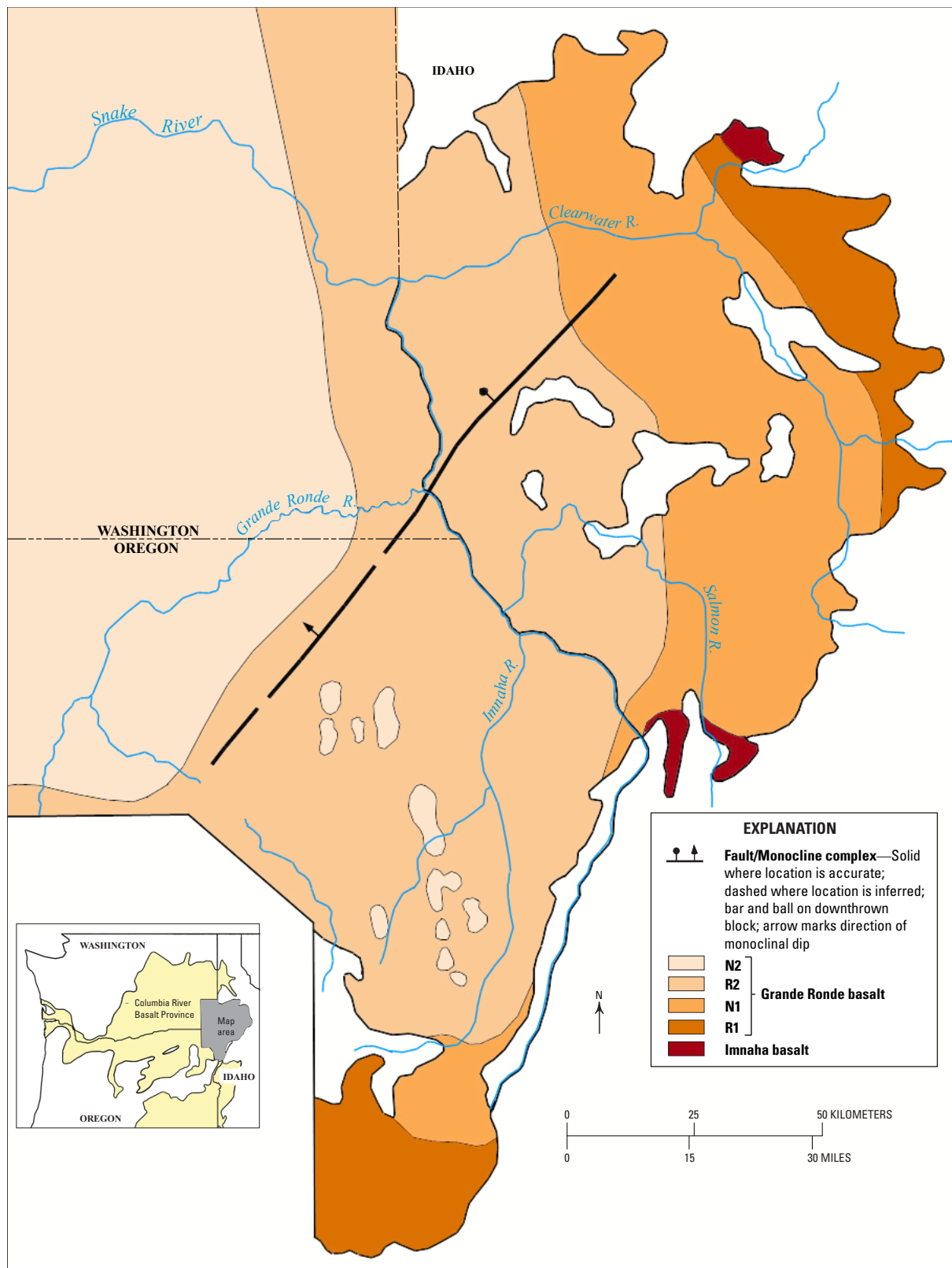


Figure 7. Map of the eastern Columbia Basin showing the gradual pinching out to the west of progressively younger magnetostriatigraphic units (MSU) of the Grande Ronde Basalt, from oldest to youngest: R1, N1, R2, and N2, where N is normal polarity and R is reverse polarity (Swanson and others 1980, 1981; Camp and Hooper, 1981; Hooper and Camp, 1981; Lewis and others, 2006). These onlapping relations are the result of an actively growing paleoslope during Grande Ronde time associated with uplift to the east, and coeval with subsidence of the Columbia Basin to the west.

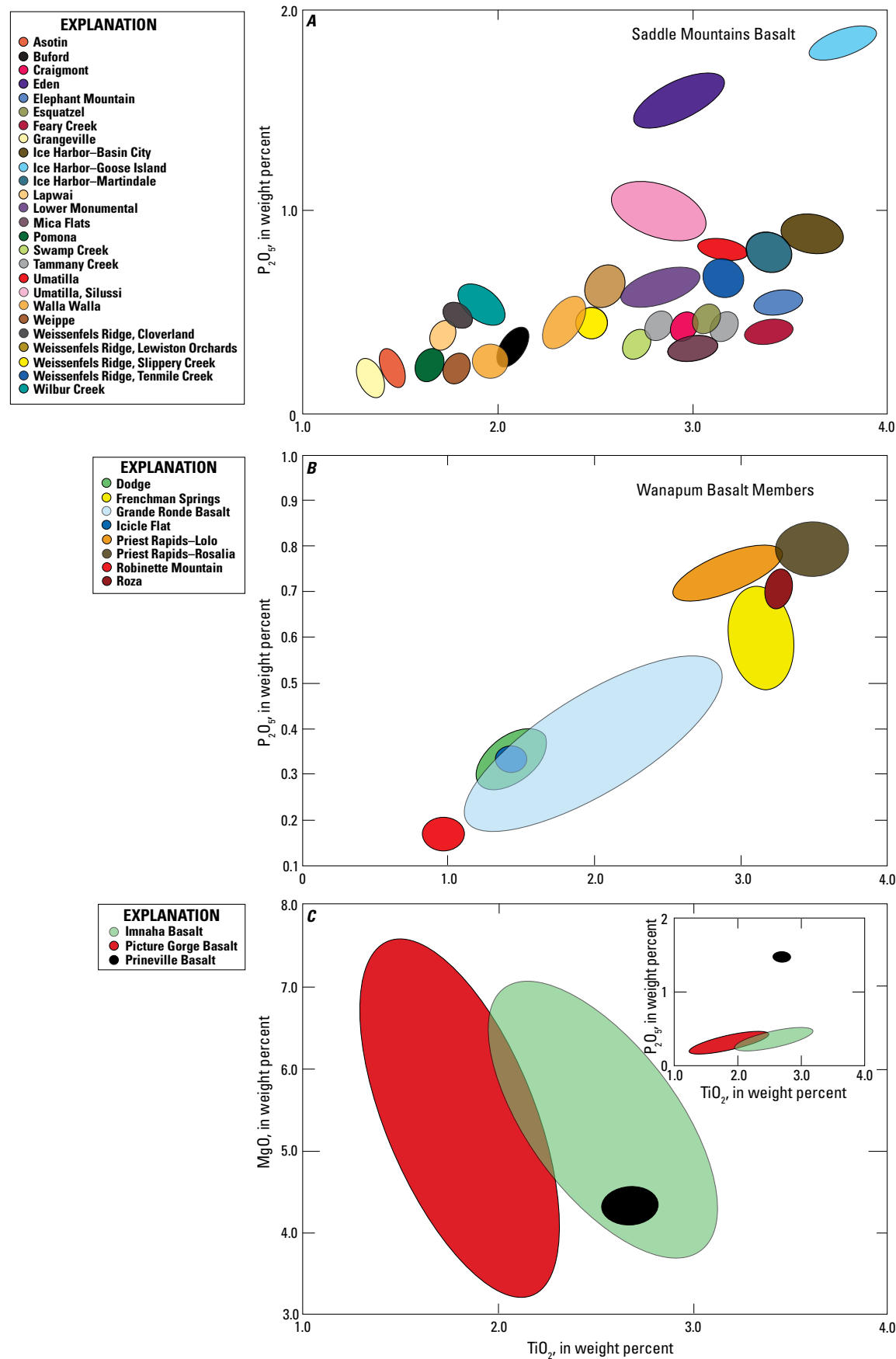


Figure 8. Variation diagrams showing the chemical range of analyses for each formation and selected members of the Columbia River Basalt Group. Rosalia and Lolo chemical types of the Priest Rapids Member (modified after Reidel, 2015).

Despite the fact that Grande Ronde Basalt flows have relatively uniform lithologies with only a few distinctive flows, considerable effort has been given to recognizing stratigraphically consistent (that is, mappable) chemical units (Reidel, 1982, 1983, 2005; Mangan and others, 1986; Reidel and others, 1989b; Reidel and Tolan, 2013). This effort has resulted in the recognition of 25 mappable units that have been designated as informal or formal members of the Grande Ronde Basalt through the integrated application of geochemistry, paleomagnetic polarity, and stratigraphic position (Reidel and Tolan, 2013).

Stratigraphic Evidence for the Northward Migration of Flood-Basalt Eruption

Development of a consistent petrochemical and paleomagnetic stratigraphy has allowed workers to map the distribution of formations accurately at reconnaissance scale. Mapping relations and dike distributions for each unit demonstrate that the CRBG eruptions migrated northward with time (fig. 4), with progressively younger CRBG formations and their MSUs becoming progressively thicker to the north.

Steens Basalt, the oldest formation, is restricted to southeastern Oregon. The Imnaha Basalt of the American Bar-type is present in the Malheur Gorge of east-central Oregon. The younger Imnaha Rock Creek-type is missing in this area, but present farther north in northeastern Oregon and southeastern Washington. A few flows with Grande Ronde Basalt chemistry (basalt of Birch Creek of Hooper and others, 2002) are also present in the Malheur Gorge with the formation thickening to the north. Each of the four Grande Ronde MSUs appear progressively to the north, with R2 and N2 restricted to northeastern Oregon and southeastern Washington. The Wanapum and Saddle Mountains Basalts are largely constrained to eastern Washington, but with a small volume in adjacent Idaho and in northernmost Oregon. This progression of younger units that thicken initially to the north and later to the northwest is consistent with a rapid northward migration of basaltic volcanism in concert with the development of a north- to northwestward-dipping paleoslope during the CRBG eruptions (Swanson and others, 1980, 1981; Camp, 1995). Although a large database of $^{40}\text{Ar}/^{39}\text{Ar}$ ages suggests that basalt volcanism was closely followed by equally rapid northward migration of rhyolitic volcanism (for example, Benson and others, 2016), more recent data calls this conclusion into question (Streck and others, 2016).

A distance of ~450 km can be measured between the geographic center of the oldest Steens eruptions in southeastern Oregon (that is, MSU R0) and the center of the youngest Grande Ronde MSU in southeastern Washington (that is, N2). This distance suggests an average migration rate of ~0.4 meters per year (m/yr) over the ~1.1 m.y. interval of the main phase eruptions. Camp (1995) suggested that northward migration was also contemporaneous with paleoslope generation due to thermal uplift at a rate of 0.67 millimeters per year (mm/yr) during the peak of the main-phase eruptions. This rapid northward migration of volcanism and uplift has been attributed to emplacement of

a northward-propagating plume head (Camp and Ross, 2004; Hooper and others, 2007; Camp and Hanan, 2008; Darold and Humphreys, 2013). James and others (2011) provide an alternative explanation associated with shallow-mantle flow to the north around a tear in the Farallon-Juan de Fuca plate. A similar model by Liu and Stegman (2012) attributes the migration of volcanism to mantle flow through a northward propagating tear in the plate. Hales and others (2005) do not address the northward migration of volcanism, but they provide an alternative model of delamination to explain flood-basalt volcanism in the Chief Joseph dike swarm and more localized uplift in and around the Wallowa Mountains.

Feeder Dikes

A defining characteristic of all flood-basalt provinces is the prolonged eruption of enormous outpourings of lava from extensive fissure systems preserved today in massive dike swarms. Three such areas fed the bulk of the CRBG eruptions (fig. 9): (1) the Steens Mountain dike swarm of southeastern Oregon (the dominant source for Steens Basalt; 15 percent of the CRBG volume), (2) the Monument dike swarm of north-central Oregon (Picture Gorge Basalt; 1 percent of CRBG volume), and (3) the massive Chief Joseph dike swarm of northeastern Oregon and southeastern Washington (Imnaha, Grande Ronde, Wanapum, and Saddle Mountains Basalt; 84 percent of the CRBG volume). Dikes for the small-volume Prineville Basalt (<<1 percent of CRBG volume) have not been found, but are thought to be located in the vicinity of Prineville Basalt outcrops located west of the Monument dike swarm (fig. 9).

Most of the CRBG feeder dikes have been linked with their respective formations, and many with their specific members, through the integration of field mapping combined with petrographic, geochemical and paleomagnetic correlations (for example, Swanson and others, 1975; Camp and others, 1982; Martin, 1989; Ross, 1989; Reidel, 1998, 2005). The same northward migration evident in the flood-basalt stratigraphy is also present in the dike distribution pattern. The oldest dikes of the Steens Basalt are restricted to southeastern Oregon. Both Imnaha and Grande Ronde dikes occur throughout the Chief Joseph dike swarm, but with a greater percentage of Imnaha dikes in the southern part of the swarm and a progressively higher percentage of Grande Ronde dikes in the northern part. Like their respective flows, dikes of Wanapum and Saddle Mountains Basalts are restricted to the northern part of the Chief Joseph dike swarm in northeastern-most Oregon and southeastern Washington.

Dike Emplacement

The great majority of CRBG dikes have north-northwest trends. Although dikes in the Chief Joseph swarm have an overall trend of $N10^\circ\text{W} \pm 10^\circ$, dikes west of the Hite fault (fig. 9) appear to have a more westerly orientation of $N30\text{--}50^\circ\text{W}$, which Reidel and others (2013b) attribute to trends inherited from basement structures. Picture Gorge dikes in the Monument swarm were

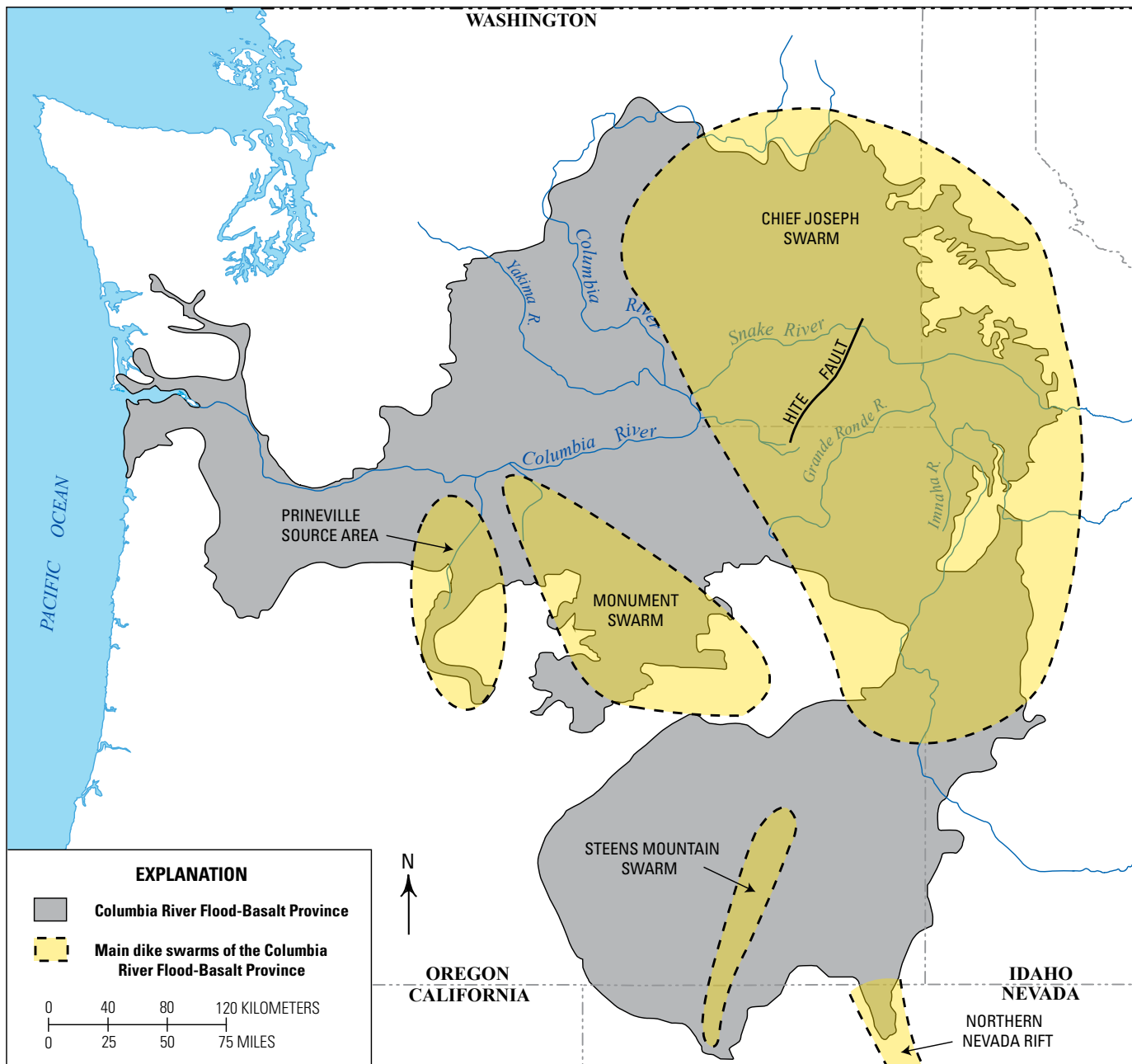


Figure 9. Map of the main dike swarms of the Columbia River flood-basalt province. The Chief Joseph dike swarm erupted ~84 percent of the flood-basalt volume (~175,000 km³), which includes the Imnaha, Grande Ronde, Wanapum, and Saddle Mountains Basalts. Although widespread, the greatest concentration of dikes in the Chief Joseph swarm occurs in the central region of the outcrop area (northeastern Oregon and southeastern Washington). The majority of Steens Basalt erupted from the Steens Mountain dike swarm in southeastern Oregon, and Picture Gorge Basalt from the Monument dike swarm of north-central Oregon. Dikes of Prineville Basalt have not been found, but are thought to be present in the vicinity of Prineville Basalt outcrops west of the Monument swarm.

active during the eruption of Grande Ronde Basalt from the Chief Joseph swarm, but the dikes have a more westerly trend, at N30–35°W.

Some of the earliest Steens Basalt flows may have erupted from a broader set of dikes lying across the Steens Basalt outcrop area. For example, some northerly trending dikes of Steens Basalt are present in the northern part of the northern Nevada rift (Santa Rosa Range), in the Pine Forest Range of northern Nevada, and in the Owyhee Mountains of western Idaho (Colgan and others, 2006; Brueseke and Hart, 2008; Camp and others, 2013). The main source of Steens Basalt dikes, however, is from the Steens Mountain shield volcano, where dike trends are typically N20°E, distinctly different from the north-northwest trends maintained in all other CRBG dike swarms. This north-northeast trend parallels both younger and older structures, leading Camp and others (2013) to suggest that dike orientation at Steens Mountain was inherited from basement structures which were reactivated a second time during the period of crustal extension that created the Steens Mountain front-range fault at ~12–10 Ma.

During the main eruptive phase (16.7–15.6 Ma), the dominant north-northwest trend of CRBG dikes was parallel to the trend for contemporaneous dikes found throughout the length of the northern Nevada rift system. This elongated belt of short-lived magmatism, referred to as the Nevada-Columbia Basin magmatic belt (Camp and others, 2015), extends over a north-south distance greater than 1,000 km. Dike intrusion along the belt from 16.7–15 Ma was contemporaneous with the initiation of Basin and Range extension (Colgan, 2013; Camp and others, 2015). The dominant north-northwest trends of dike emplacement, however, differ by 45° from the north-northeast trend of contemporaneous normal faults produced by Basin and Range extension (for example, Colgan, 2013). This observation prompted Camp and others (2015) to conclude that dike emplacement was not the result of crustal extension, but rather the product of forceful dike injection. Such a model is consistent with the paucity of extensional strain in the CRBG source area during flood-basalt volcanism, as inferred from the lack of extensional faulting together with more quantitative data on rapidly diminishing middle Miocene stress from Nevada northward into eastern Oregon and Washington (for example, McQuarrie and Wernicke, 2005; Payne and others, 2012; McCaffrey and others, 2013, 2016).

Fissure-Fed Eruptions

Contemporaneous dike segments can erupt slightly different compositions along their length, as demonstrated by Martin (1989) for the Roza Member (Wanapum Basalt) dike system, which fed at least five different flow compositions, all falling into the broader Roza compositional field. In some cases, individual flows, like the Cohassett flow of the Sentinel Bluffs Member (Grande Ronde Basalt), are composite lavas of distinct compositional types that erupted simultaneously from different locations along the length of the dike system (Reidel, 2005). Other dikes have multiple glass selvage zones that indicate a history of multiple injections. These observations suggest that compositional variants in fissure-fed

eruptions can be present within and (or) along the length of erupting dikes.

Despite our ability to correlate many dikes with specific members or flows, it is rare to find field locations that expose dike-flow connections where one can then examine the nature of fissure-fed vents and near-vent processes. The significance of such locations lies in the wealth of knowledge that we can gain about eruption style, column height, and the longevity of flood-basalt eruptions, all of which are important in assessing the potential global effect of these eruptions on climate and biological perturbations in the geologic past (for example, Thordarson and Self, 1996).

In addition to visiting several dike locations, this field trip will also examine specific areas of dike-flow connections where we can examine near-vent products and processes associated with the eruption of large pāhoehoe sheet flows. These areas mark the eruption site for three flows of the Teepee Butte Member (Grande Ronde Basalt) exceeding a volume of 5,000 km³ (Reidel and Tolan, 1992) and perhaps as many as five flows of the Roza Member (Wanapum Basalt) with an estimated volume of 1,500 km³ and a fissure length of at least 180 km (Brown and others, 2014). More detailed descriptions of these field stops are included in the Road Log.

Physical Volcanology

Understanding flow morphology and the variety of intraflow features in flood-basalt flows requires consistent use of volcanic nomenclature. Here, we follow the terminology of Self and others (1996) who define a flow lobe as the smallest coherent package of lava, a flow as the product of a single outpouring of lava, and a flow field as lava covering a large area that has many separate outpourings. In the following subsections, we describe two end-member types of flows that can be found in the CRBG, giant pāhoehoe sheet flows and compound flow fields, and discuss current ideas on their emplacement.

Giant Pāhoehoe Sheet Flows

The great majority of the CRBG lavas erupted as extensive pāhoehoe sheet flows, typically from 10 m to >50 m thick, with exceptionally high volumes, particularly in the Grande Ronde Basalt where individual flow fields have average volumes of 1,355 km³ (Reidel and others, 2013a). Such large volumes allow an individual flow to advance away from its vent as a uniform moving sheet of lava, or as a series of sheet-like flow lobes that coalesce into a single flow which appears to cool as a solitary, compositionally homogeneous sheet flow.

The apparent uniform nature of many CRBG sheet flows can be misleading as many, if not most, develop through the invasion of the initial sheet flow by later lava, thus inflating the lobe in height and volume (Reidel and Fecht, 1987; Hon and others, 1994; Self and others, 1996; Thordarson and Self, 1998; Reidel, 1998; Vye-Brown and others, 2013; Brown and others, 2014). Using the

terminology of Walker (1971), large pāhoehoe sheet flows were once thought to be “simple flows” formed by a single outpouring of lava, but instead many of the large-volume CRBG sheet flows subject to flow inflation may have characteristics in common with “compound flows” (for example, Self and others, 1998); the difference, however, is that the injected flow lobes are not marked by distinct disconformities as found in compound flows. In most cases, the later injected lava may coalesce producing a chemically homogeneous flow, but if the injected lobes are compositionally diverse, the flow may be characterized by internal layers of variable composition. In the case of the 100-m-thick Grande Ronde Cohasset flow, for example, several injected layers are recognized by their distinct chemical compositions (Reidel, 2005). Injected lobes can form vesicular zones or sheets that pond near the top of each lobe due to viscosity contrasts with cooler and (or) compositionally diverse lava (Self and others, 1998). Vesicular sheets alone cannot be used to identify inflated lobes, however, since other mechanisms are also capable of producing such zones in thick basaltic lava flows (for example, Goff, 1996).

Intraflow features found at the top and bottom of sheet flows can be highly variable depending on conditions of emplacement, the degree of vesiculation, and rheological behavior (fig. 10). Both flow tops and flow bottoms show evidence of rapid cooling and vesiculation. Flow bottoms are typically narrow regions (<1 m) of fine-grained to glassy basalt; vesicle pipes may be present where the flow encounters vegetation or damp ground. Where flows encounter larger bodies of water, flow bottoms will typically show evidence of lava-water interaction in the form of pillow-palagonite complexes, hyaloclastite, and rarely spiracles (fig. 10). In contrast, flow tops form a chilled, fine-grained to glassy upper crust that is typically a zone of vesicle-rich scoria. In most cases, flow tops display typical pāhoehoe textures, although more highly brecciated textures, hummocky, or rubbly pāhoehoe flow tops are also present. Flow-top thickness can be highly variable, but typically occupies about 10–20 percent of individual flows (Reidel and others, 2013a).

The nonvesicular, cryptocrystalline to crystalline interior of sheet flows will typically contain numerous joints produced by the cooling and contraction of the solidified flow. These so-called “cooling joints” can be subdivided into two main groups: (1) columnar-blocky joints, composed of vertically oriented polygonal columns from 0.5 m to 3 m in diameter; best developed in the lower part of the flow (lower colonnade, fig. 10), and rarely as poorly formed columns in the upper part (upper colonnade, fig. 10), and (2) entablature-colonnade joints, which typically form a more complex pattern in the interior of the flow, varying from numerous, irregular cooling joints bounding small columns (<0.2 m) to randomly oriented joints without clear columns present, to joints bounding small columns that display curvi-columnar (fanning) patterns (fig. 10). The overall jointing pattern in many sheet flows results in a three-tiered aspect to their flow interiors, from lower colonnade, to entablature, to poorly developed upper colonnade (fig. 10). However, sheet flows with a history of multiple lobe injection, will more commonly display more

complex patterns of columnar-blocky and entablature-colonnade jointing.

Compound Flow Fields and Constituent Flow Lobes

Although the great majority of the CRBG eruptions generated thick, extensive sheet flows, the initial CRBG eruptions of the Steens Basalt are distinct in generating thousands of much thinner (~1 to 5 m) anastomosing lava lobes that interfinger and pinch out over short lateral distances (Camp and others, 2013). The thinnest of these lavas (<2 m-thick) more typically occur as distinct sets of stacked pāhoehoe flow lobes that erupted in rapid succession to form compound flow fields that vary in thickness from 10 to 50 m. Most flow fields are chemically distinct, with their constituent flow lobes forming coherent, linear trends on chemical plots, consistent with the near constant eruption of multiple flow units constituting each compound flow (Camp and others, 2013).

All pāhoehoe flow lobes of the Steens Basalt display the same three-part structure common to such flows found in Hawaii and elsewhere (for example, Hon and others, 1994), in which vesicular lower and upper crusts bound a central, vesicle-poor lava core, typically ~1–2 m thick (Bondre and Hart, 2008; Camp and others, 2013). Many of these flow lobes show evidence for flow inflation similar to that displayed in Hawaiian examples (Hon and others, 1994). The lava cores of basalt lobes commonly contain vesicular bands and other bands with variable phenocryst content, both of which might represent pulses of injected lava. Camp and others (2013) noted in their Abert Rim Powerline Road section, ~120 km west of Steens Mountain, the common occurrence of lobes having nearly aphyric cores sandwiched between coarsely porphyritic basal zones and porphyritic vesicular tops, consistent with the injection of aphyric liquids into the cores of inflating flows. They also noted a more dramatic example of an inflated flow at Disaster Peak, Oregon, where sheets, lobes, and pillow-like structures of aphyric lava were injected into the core of a highly plagioclase-phyric flow emplaced as a crystal mush.

Flow Emplacement

The emplacement of CRBG sheet flows and the time required for these flows to cover such huge distances have proved controversial. Shaw and Swanson (1970) originally proposed a very rapid rate of emplacement over the gently sloping plateau surface, where sheet flows covered hundreds of kilometers in weeks or even days, a process requiring turbulent flow. The rationale for rapid rates of emplacement is based on the belief that slower rates would result in rapid heat loss and the solidification of the flows over relatively short lateral distances. It is now recognized that flow inflation evident in Hawaiian pāhoehoe sheet flows (Hon and others, 1994) was also a major process in the much more voluminous CRBG sheet flows. Inflation provides a mechanism for insulating the injected lava from significant heat loss, thus

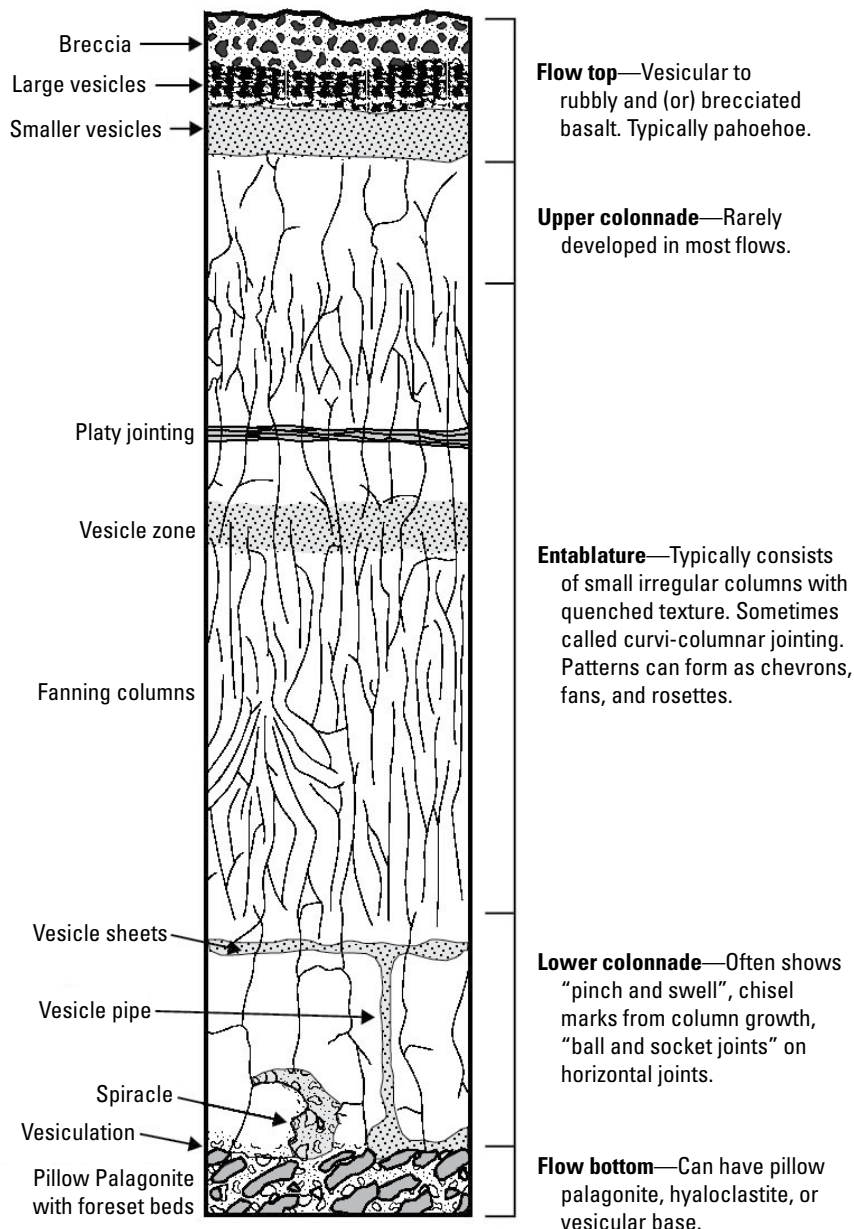


Figure 10. Composite diagram showing various intraflow features that can be found in Columbia River Basalt sheet flows. Modified from Swanson and others (1979) and Reidel and others (2013a).

allowing the sheet flows to travel over great distance in a laminar fashion at slower rates than originally envisioned by Shaw and Swanson (1970).

Although flow inflation is recognized as a common process in CRBG emplacement, there is still a lack of consensus on emplacement rates. Conductive cooling models for the Roza Member (Wanapum Basalt) are consistent with slow emplacement over years to a few decades (Thordarson and Self, 1998). Slow emplacement also appears to be consistent with the heat balance calculations of Keszthelyi and Self (1998) on long basalt lava flows. In contrast, compositional data preserved in CRBG lava flows and phenocrysts are more consistent with shorter timescales of emplacement, from months to years (Reidel and others, 1994b; Ho and Cashman, 1997; Reidel, 1998). Reidel and Fecht (1987) and Reidel (1998, 2005) documented examples where two flows were preserved in individual dikes and vents, yet mixed together to form a single flow more than 200 km from the source, with mixing within less than a meter of the surface. These occurrences are not localized to a small area, but instead occur over a large region of several hundred square kilometers. These authors interpret such mixing as the product of rapid emplacement. More recently, Keszthelyi and others (2006) incorporate aspects of both slow and rapid emplacement. They suggest that a typical CRBG sheet flow of 1,000 km³ could be emplaced as an inflated flow in less than six years, but once the brittle crust is established, injected batches could travel 100 to 300 km from the vent to the flow front in less than 10 days, a velocity similar to that of Shaw and Swanson (1970).

Deformation and Crustal Stress During and After the CRBG Eruptions

The northern segment of the CRFBP is characterized by numerous large folds with trends that vary from east-west to northeast-southwest (Reidel and others, 1989a). These prominent structures are best developed in the Yakima Fold Belt of central Washington and within the Blue Mountains anticlinorium of northeastern Oregon. The Olympic-Wallowa lineament (fig. 1) is a concentration of ~N50°W-trending structural features that extends diagonally across the Yakima Fold Belt and Blue Mountains, from near Puget Sound in the northwestern Washington to the Wallowa Mountains in northeastern Oregon (fig. 1; Raisz, 1945; Hooper and Conrey, 1989; Reidel and others, 1994a; Blakely and others, 2011, 2014).

In contrast to the northern segment of the province, the southern segment on the Oregon Plateau appears to be devoid of significant folding, but instead characterized by minor normal faulting along northwest-southeast trends in the High Lava Plains and Brothers Fault Zone, together with more intense normal faulting along NNE-SSW trends associated with Basin and Range extension south and east of the High Lava Plains (for example, Colgan and others, 2004; Meigs and others, 2009; Scarberry and others, 2010). Although most extensional deformation on the

Oregon Plateau occurred after eruption of the Steens Basalt, field data demonstrate that significant compressional deformation in the northern segment of the CRFBP was contemporaneous with the CRBG eruptions (for example, Swanson and others, 1980; Reidel, 1984; Reidel and others, 1989a).

Ross (1978, 1979) noted the orientation of folds, dikes, and conjugate faults in northeastern Oregon is consistent with a N10°W axis of maximum compression and a complementary N80°E axis of maximum extension. Such a stress regime is applicable to similar structures found throughout the Columbia Basin and Blue Mountains Provinces (Hooper and Camp, 1981). Several workers have suggested that medium- to large-scale clockwise rotation of most of Oregon since ~16 Ma is the cause for compressional stress generating the Yakima Fold Belt of central Washington (for example, Wells and Heller, 1988; Wells and others, 1998; McCaffrey and others, 2013; Wells and McCaffrey, 2013), but this does not explain why the intensity of folding was greatest during the CRBG eruptions (for example, Reidel and others, 1984), and why contemporary earthquake focal mechanisms are oriented north-south (Ludwin and others, 1991).

The evidence for folding and contemporaneous dike emplacement in northeastern Oregon and eastern Washington cannot be readily explained by tectonic rotation. Despite the consistent strain indicators noted in this region by Ross (1978) and Hooper and Camp (1981), contemporary rotation rates (Payne and others, 2012; McCaffrey and others, 2013) combined with paleomagnetic declination anomalies in the CRBG (for example, Wells and Heller, 1988; Wells and McCaffrey, 2013) suggest that there was little or no rotation-derived compression or extension in the main CRBG source region during and after the CRBG eruptions. This is further supported by field evidence that the degree of crustal extension during dike emplacement was <<1 percent (Taubeneck, 1970; Hooper and Conrey, 1989). Additional evidence from northern Nevada demonstrates that the orientation of dikes contemporaneous with the CRBG eruptions was at a high angle to the regional stress orientation (Colgan, 2013). These observations led Camp and others (2015) to suggest that rapid dike emplacement in the CRBG source region and in the northern Nevada rift was fundamentally controlled by a sublithospheric process, which resulted in high magma overpressures and forceful dike injection unrelated to the state of regional crustal stress (see previous discussion; Feeder Dikes).

Large-scale folding was common in the northern part of the CRFBP but absent on the Oregon Plateau. Camp and Hanan (2008) note that such behavior is consistent with crustal deformation associated with plume emplacement, as shown in the model experiments of Burov and Guillou-Frottier (2005) and Burov and others (2007). The experiments show that areas lying above the center of a spreading plume head will remain under extension, but areas lying above the outer part of a spreading plume will be subject to subsidence and compression. Plume subsidence helps to explain a long-unresolved problem of finding a rational explanation for large-scale subsidence of the Columbia Basin coincident with the main phase of basalt eruption (Reidel

and others, 2013b), and north-south compression during plume emplacement provides a rational mechanism to explain why the growth rate of the Yakima folds was greatest during the peak eruptions and rapidly declined as the eruptions ceased (Reidel and others, 1984).

Petrogenesis

Petrogenesis of the CRFBP has been a topic of considerable debate. A shallow-mantle genesis has been invoked in a great variety of models that differ only in the mechanism of melt generation. These include upper mantle melting triggered by either back-arc extension (Carlson and Hart, 1987; Hart and Carlson, 1987; Smith, 1992) or torsional stress of the plate interior (Dickinson, 1997; Tikoff and others, 2008), lithospheric delamination (Hales and others, 2005), convective upwelling of upper mantle along the western edge of North American craton (King and Anderson, 1998), and upper-mantle convection through or around the truncated edge of the Farallon-Juan de Fuca plate (Sigloch and others, 2008; Faccenna and others, 2010; James and others, 2011; Liu and Stegman, 2012; Long and others, 2012).

Models of back-arc extension and torsional stress require a significant degree of lithospheric stretching to produce passive adiabatic upwelling of mantle (White and McKenzie, 1989, 1995); however, passive upwelling is inconsistent with lack of evidence for middle Miocene crustal extension in the source regions of CRBG eruptions (Camp, 2013). The lithospheric delamination model of Hales and others (2005) and the convective upwelling model of King and Anderson (1998) are localized to the Chief Joseph dike swarm and the cratonic boundary, respectively. These models cannot readily explain contemporaneous volcanism over a wider area that includes the Monument dike swarm (Picture Gorge Basalt) to the west, and in the northern Nevada rift system to the south. Models of upper mantle flow through or around the edge of the Farallon-Juan de Fuca plate appear to be more realistic in providing a mechanism for active-mantle upwelling that does not necessarily require significant crustal stretching. Such models can also provide a potential mechanism for the rapid northward migration of flood-basalt volcanism (for example, James and others, 2011; Liu and Stegman, 2012).

These shallow-mantle models lie in contrast to the more widely accepted view that flood-basalt provinces are generated above plumes derived from the deep mantle (for example, Morgan, 1972; Campbell, 2005). Despite the great variety of alternative models, a plume origin remains the favored model by many workers to best explain the field and petrochemical characteristics of the CRFBP and the Snake River Plain hot spot track (for example, Duncan, 1982; Brandon and Goles, 1988, 1995; Draper, 1991; Pierce and Morgan, 1992, 2009; Hooper and Hawkesworth, 1993; Geist and Richards, 1993; Camp, 1995, 2013; Dodson and others, 1997; Pierce and others, 2002; Hooper and others, 2002, 2007; Camp and others 2003; Camp and Ross, 2004; Nash and others, 2006; Shervais and Hanan, 2008; Camp and Hanan, 2008; Wolff and others, 2008; Smith and others, 2009; Wolff and Ramos, 2013; Camp and others, 2015).

Several workers have described trace-element and isotopic evidence for a plume-like component shared by all formations of the main-phase CRBG (Hooper and Hawkesworth, 1993; Camp and Hanan, 2008; Wolff and others 2008; Wolff and Ramos, 2013). Further support for a plume origin comes from (1) high $^3\text{He}/^4\text{He}$ values, indicating a lower-mantle source for basaltic rocks on the Snake River Plain (Graham and others, 2009), and in the Imnaha Basalt on the Columbia Plateau (Dodson and others, 1997), and (2) the seismic resolution of a contemporary low-velocity anomaly beneath the Yellowstone Plateau extending to lower-mantle depths (Obrebski and others, 2011; Humphreys and Schmandt, 2011; Tian and Zhao, 2012). Schmandt and others (2012) note this low-velocity conduit deflects the 660-km mantle discontinuity upward by 12–18 km (Schmandt and others, 2012), as predicted in thermal models of a plume rising through the mantle transition zone (for example, Bina and Helffrich, 1994); however, the 410-km discontinuity remains unaffected, which suggests that the thermal structure of the plume may be vertically heterogeneous and possibly discontinuous (Schmandt and others, 2012).

Despite support for a plume genesis, there is a lack of consensus on the exact location for the center of plume impingement. Plate motion calculations for the middle Miocene plume center vary depending on which hot spot reference model you use (see, for example, Wells and others, 2014). The location of plume impingement could have also been influenced by (1) deflection of the rising plume by the Farallon plate (for example, Pierce and others, 2002; Wells and others, 2014) or along the westward edge of the thick cratonic lithosphere (for example, Jordan, 2005), and (or) (2) the difference vector between plate motion and mantle flow at source depth (Smith and others, 2009).

Some workers prefer the idea of a plume center near the northwestern margin of the western Snake River Plain, where the Oregon-Idaho graben and Chief Joseph dike swarm converge (fig. 1; Shervais and Hanan, 2008; Wolff and others, 2008; Wolff and Ramos, 2013). Others suggest that the plume center was near the Oregon-Nevada border where the oldest ignimbrites (16.5 Ma) can be found lying at the western end of the Snake River Plain hot spot trend (16.5 Ma), in close proximity to the oldest basalt flows (Steens Basalt; 16.7 Ma) of the CRBG (Pierce and Morgan, 1992; Camp and others, 2003; Jordan and others, 2004; Camp and Ross, 2004; Nash and others, 2006; Camp, 2013). In the former model, the northward advance of volcanism results from the northward propagation of dikes from a rather static plume center (Wolff others, 2008, Wolff and Ramos, 2013). In the latter model, the northward advance is associated with a rapidly spreading plume source as it propagated northward against the thick cratonic margin of North America (Camp, 1995, 2013; Camp and Hanan, 2008; Darold and Humphreys, 2013).

The geochemical data supporting a mantle plume source is partly based on the C2 isotopic source component present in the main-phase CRBG lavas. The C2 component was recognized and originally defined by Carlson and others (1981) as sediment-contaminated mantle, but reinterpreted by several workers as a

plume component (Brandon and Goles, 1988, 1995; Hooper and Hawkesworth, 1993; Wolff and others, 2008; Camp and Hanan, 2008; Wolff and Ramos, 2013). Since this isotopic component is least diluted in the Imnaha Basalt, it is sometimes referred to as the “Imnaha component” (for example, Hooper and Hawkesworth, 1993; Wolff and others, 2008).

In Sr-Nd-Pb isotopic space, the Steens, Picture Gorge, and Grande Ronde Basalts lie along mixing trends radiating from Imnaha Basalt (Carlson and others, 1981; Hooper and Hawkesworth, 1993; Brandon and Goles, 1995; Wolff and others, 2008; Camp and Hanan, 2008). Wolff and Ramos (2013) use trace-element and Sr, Pb, and Nd isotope ratios to define the Imnaha (C2) component as a plume-like source (fig. 11), similar to enriched mantle (EM) II type of oceanic island basalt (OIB) source. Isotopic variation in the Imnaha lavas comes mostly from mixing with depleted mantle (DM) (fig. 11). This conclusion is also consistent with trace-element concentrations and normalized trace-element patterns for Imnaha Rock Creek lavas that closely match those from Hawaiian basalts (Hooper

and Hawkesworth, 1993). On the other hand, many of the Imnaha lavas have large-ion lithophile element/high field strength element (LILE/HFSE) ratios that are too high for an EM II OIB source, which suggest an additional lithospheric component, but of smaller proportions, perhaps from the cratonic crust (Wolff and Ramos, 2013). Further evidence for a deep-mantle source for the Imnaha component comes from $^{3}\text{He}/^{4}\text{He}$ of 11.4 ± 0.7 times the atmospheric ratio (R_A ; Dodson and others, 1997). Wolff and Ramos (2013) note that this ratio is significantly elevated compared with mid-oceanic ridge basalt (MORB) and conforms to the “moderately high $^{3}\text{He}/^{4}\text{He}$ ” OIB type of Class and Goldstein (2005).

Even the most primitive CRBG lavas lack the chemical characteristics of a primary magma. If the CRBG melts derive from peridotite, then all erupted lavas must have undergone variable and perhaps extensive degrees of fractional crystallization and (or) crustal contamination, particularly the most evolved lavas of the Grande Ronde Basalt (for example, Carlson and others, 1981; Wolff and Ramos, 2013). An alternative explanation for

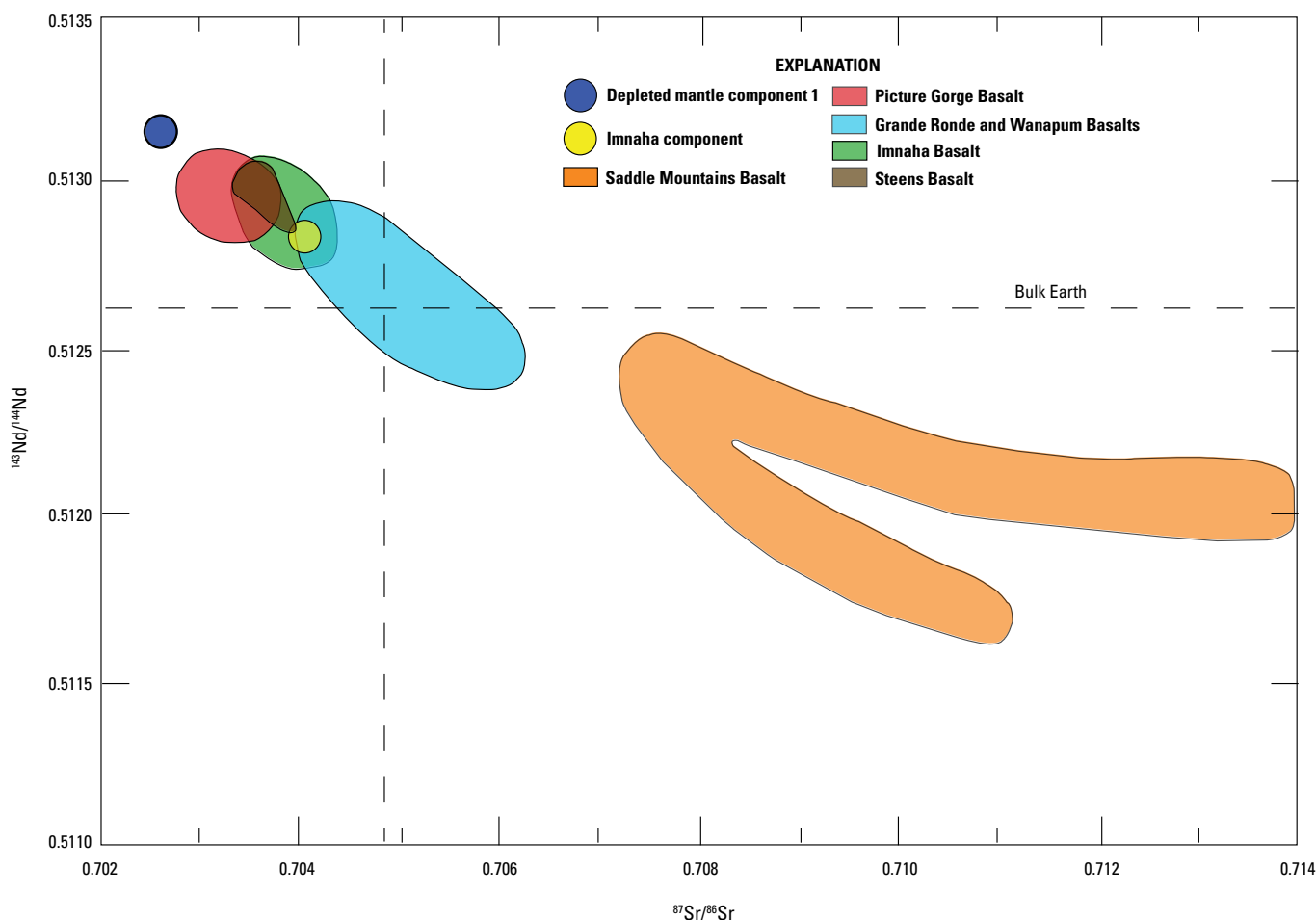


Figure 11. Plot of $^{87}\text{Sr}/^{86}\text{Sr}$ versus $^{143}\text{Nd}/^{144}\text{Nd}$ for the main Columbia River Basalt Group formations. Data from Carlson and others (1981), Hooper and Hawkesworth (1993), Brandon and others (1993), Brandon and Goles (1995), Camp and Hanan (2008). Imnaha component, originally defined by Carlson and others (1981) as a component of depleted mantle contaminated with sediment, but later defined as a plume component (or Imnaha component) by Brandon and others (1993) and Hooper and Hawkesworth (1993).

the derivation of the Grande Ronde lavas is from direct melting of an unusual mantle composition, like pyroxenite (for example, Takahashi and others, 1998). We follow others who contend that the Imnaha Basalt was derived largely from a plume component, and we summarize in the remainder of this section current ideas on the petrogenesis of Steens, Picture Gorge, Grande Ronde, Wanapum and Saddle Mountains Basalt.

The lower Steens Basalt has the most primitive compositions of the main-phase lavas. These lavas are homogeneous, strictly tholeiitic, with a narrow range in both silica content (typically 48–50 percent) and incompatible-element concentrations. The more heterogeneous upper Steens Basalt varies from tholeiitic to alkaline, evolving toward basaltic trachyandesite compositions with significantly higher incompatible-element concentrations. These alkali compositions are atypical of all other lavas in the CRBG. Both Steens and Picture Gorge Basalts lie along isotopic mixing trends between the Imnaha component and a DM source (fig. 11). It seems clear from major-element, trace-element, and isotopic analysis that the upper Steens Basalt and Picture Gorge

Basalt have undergone significant fractional crystallization and variable degrees of crustal assimilation (Gunn and Watkins, 1970; Carlson and others, 1981, 1984; Brandon and others, 1993; Ramos and others, 2005, 2013; Camp and others, 2013).

The Grande Ronde Basalt constitutes 71 percent of the total CRBG volume, 76.5 percent of the main-phase volume, and 85 percent of the volume that erupted from the Chief Joseph dike swarm. The formation is composed of high Fe/Mg, high-silica (52–58 percent) basaltic andesites (fig. 12), which are unusual when compared to the dominant rock types of almost all other flood-basalt provinces. These lavas form a trend in isotopic space that is different than that for Steens and Picture Gorge Basalts, in that they project away from the Imnaha component toward an older lithospheric source (or sources) with $^{87}\text{Sr}/^{86}\text{Sr}$ values as high as 0.706 (for example, fig. 11).

The origin of the Grande Ronde lavas has been a controversial topic. The modeling results of Carlson and others (1981) showed that a MORB-type magma would require a combination of ~20–30 percent assimilation of granitic crust

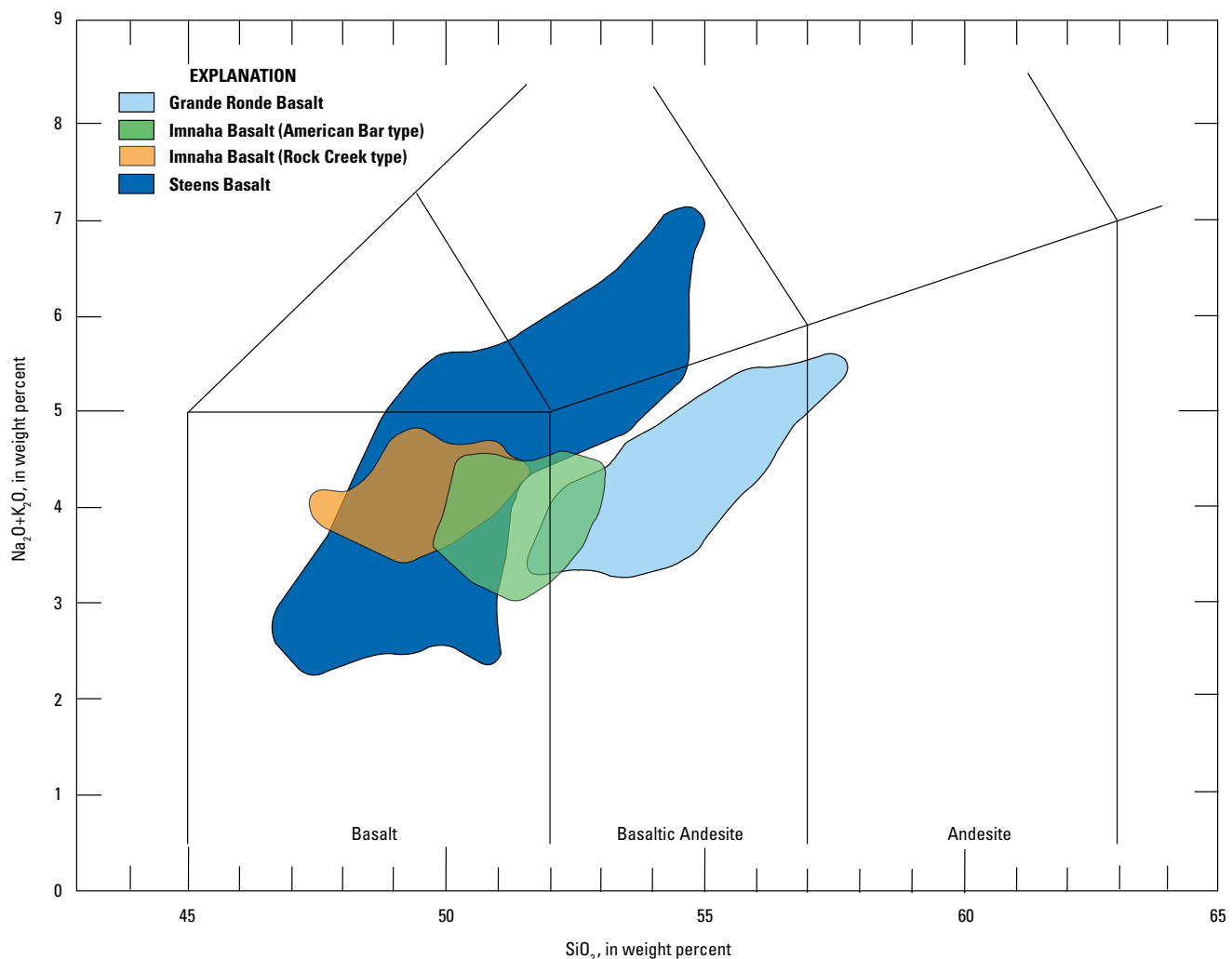


Figure 12. Compositional fields for 688 analyses of Steens Basalt, Imnaha Basalt, and Grande Ronde Basalt of the Columbia River Basalt Group main phase, plotted on the total alkali versus silica diagram of La Bas and others (1986). Fields exclude a few analyses that are clear outliers to the bulk data set. Data from Hooper (2000) and Camp and others (2013).

combined with 30–60 percent fractional crystallization to produce the Grande Ronde Basalt. On the other hand, Carlson (1984) showed that fractional crystallization combined with a smaller amount of crustal assimilation (10–20 percent) would be required if the mafic end-member was derived from the C2 component (that is, Imnaha Basalt). Although some degree of fractional crystallization is needed to explain the chemical variation between the less evolved and more evolved Grande Ronde lavas (for example, Reidel, 1983), several workers have noted that there is little geologic or petrographic evidence that fractional crystallization was a significant factor in generating the Grande Ronde Basalt from peridotite partial melts (Wright and others, 1989; Takahahshi and others, 1998; Hooper and others, 2007; Camp and Hanan, 2008). Wright and others (1989), for example, note that Grande Ronde Basalt flows have small negative Eu anomalies on normalized rare earth element (REE) plots, which do not correlate with either MgO or La/Yb ratio, and are therefore unlikely to result from plagioclase fractionation, but instead may be inherited from a pyroxenite source. Hooper and Hawkesworth (1993) used Sr and Rb distribution coefficients to suggest that fractional crystallization in the Grande Ronde Basalt was minor and could not have exceeded 10 percent. The scarcity of phenocrysts in the great majority of Grande Ronde Basalt flows does not in itself eliminate crystal fractionation as a viable process, but it does require a special mechanism in crustal reservoirs to separate crystallizing phenocrysts.

Camp and Hanan (2008) suggested that the substantial storage time necessary for large-scale fractional crystallization to occur is inconsistent with the enormous volume and rapid eruption rate (~600 km³/km/Ma) of these largely aphyric lavas at the peak of CRBG volcanism. They also note that assimilation is severely limited by the energy required to dissolve crustal rock types. They cite an analysis of enthalpy-composition diagrams demonstrating that an addition of only 10 percent granitic crust to basalt would result in rapid cooling with an abrupt increase in viscosity and a crystal content of 30–40 percent (Glazner, 2007), which seems inconsistent with the rapid eruption and large volume of largely aphyric Grande Ronde Basalt.

Others have cited chemical and experimental evidence that the Grande Ronde Basalt chemistry could be generated instead by large-scale melting of a clinopyroxene-rich source similar to eclogite or a mafic lower crust (Wright and others, 1976, 1989; Swanson and Wight, 1981; Takahahshi and others, 1998; Hooper and others, 2007). In contrast to mantle peridotite, experimental data indicate that the relatively low solidus and liquidus temperatures of a mafic source could result in near complete melting if subjected to elevated temperatures of ~1,480 °C in the upper mantle (Yaxley, 2000). Building on these studies, Camp and Hanan (2008) proposed a model of plume-triggered delamination and the abrupt, near-wholesale melting of mafic lower crust to explain the transition from Imnaha to Grande Ronde chemistry. Under this scenario, older mafic crust underlying Paleozoic-to-Mesozoic oceanic arc terranes and (or) the adjacent Precambrian craton would mix with a small but variable volume of the Imnaha component. The northward advance of volcanism would be

accompanied by delamination during eruption of Grande Ronde Basalt, similar to models proposed by Camp and Hanan (2008) and Darold and Humphreys (2013).

Wolff and Ramos (2013) acknowledge that a high degree of melting of a mafic source at mantle depths could be a plausible mechanism to produce basaltic andesite, but they prefer instead an assimilation and fractional crystallization mechanism to generate the Grande Ronde Basalt, as first proposed by Carlson and others (1981). In their analysis of major-elements, trace-elements, and isotope data, they conclude that the Grande Ronde Basalt was largely the result of mixing between the Imnaha Basalt and a crustal component. In their model calculations, they choose the Idaho batholith as a suitable contaminant to explain the Sr, Nd, and Pb ratios in Grande Ronde Basalt, but the amounts of assimilant required are poorly constrained, from ~10 to 60 percent. Such large amounts of crustal melting and assimilation require significant thermal contributions (for example, Glazner, 2007), which they attribute to a centralized magma system with increasing thermal input to “runaway” conditions (for example, Karlstrom and others, 2010). They follow Wolff and others (2008) in suggesting a location for this magma reservoir near the junction of the western Snake River Plain, the Oregon-Idaho graben, and the southernmost part of the Chief Joseph dike swarm (fig. 1), where magma was injected into the dike swarm travelling laterally to feed flows as much as 400 km to the north.

The waning stage of CRBG volcanism begins with the Wanapum Basalt, which has Sr, Nd, and Pb isotopic values similar to many of the Grande Ronde Basalt lavas (for example, fig. 11). Wanapum Basalt differs, however, in having high MgO, low SiO₂, and enriched trace-element values. It seems likely that these basalt flows were derived by mixing of the Imnaha component with one or more lithospheric components common to Grande Ronde Basalt (for example, Hooper and Hawkesworth, 1993).

Saddle Mountains Basalt lavas are the most isotopically evolved basalts in the CRBG, with the highest ⁸⁷Sr/⁸⁶Sr values and the lowest ¹⁴⁴Nd/¹⁴³Nd of any of the other formations (fig. 11). The data in figure 11 suggest that the Saddle Mountains Basalt could follow a similar mixing model as proposed for the Grande Ronde and Wanapum Basalt, but where the Imnaha component is mixed with a much larger volume of the same lithospheric component found in the older lavas. Such a scenario is inconsistent, however, with isotopic arrays on Pb-Pb plots, which lack well-defined trends linking the Saddle Mountains Basalt to the remainder of the CRBG (Carlson and others, 1981; Carlson, 1984; Church, 1985). Hooper and Hawkesworth (1993) note that Saddle Mountains flows have a wide range in ²⁰⁶Pb/²⁰⁴Pb, ²⁰⁷Pb/²⁰⁴Pb, and ²⁰⁸Pb/²⁰⁴Pb ratios, with most samples plotting on a slope corresponding to an age of ~2 Ga, the presumed age of the lead source component. The overall basaltic composition and trace-element patterns of the Saddle Mountains flows imply a mantle source beneath Precambrian crust of the North American craton. As noted by Hooper and Hawkesworth (1993), Saddle Mountains Basalt has much in common with basalts of the Snake River Plain which erupted above cratonic crust, lying east of the ⁸⁷Sr/⁸⁶Sr = 0.706 line in figure 1.

Road Log

Before launching into the road log, users are encouraged to read the preceding section to become better acquainted with the geologic framework of the CRFBP and the stratigraphic terminology of the CRBG. This will provide the user with the proper context for more specific discussions in the road log.

The road log is subdivided into seven 1-day excursions, with travel-time allotted between each. The excursions are arranged progressively from the oldest to the youngest units found in the heart of the flood-basalt source region. The road log begins in southeastern Oregon, progresses northward into northeastern Oregon and southeastern Washington, and ends in the Pasco Basin and Columbia River Gorge of south-central Washington (fig. 13).

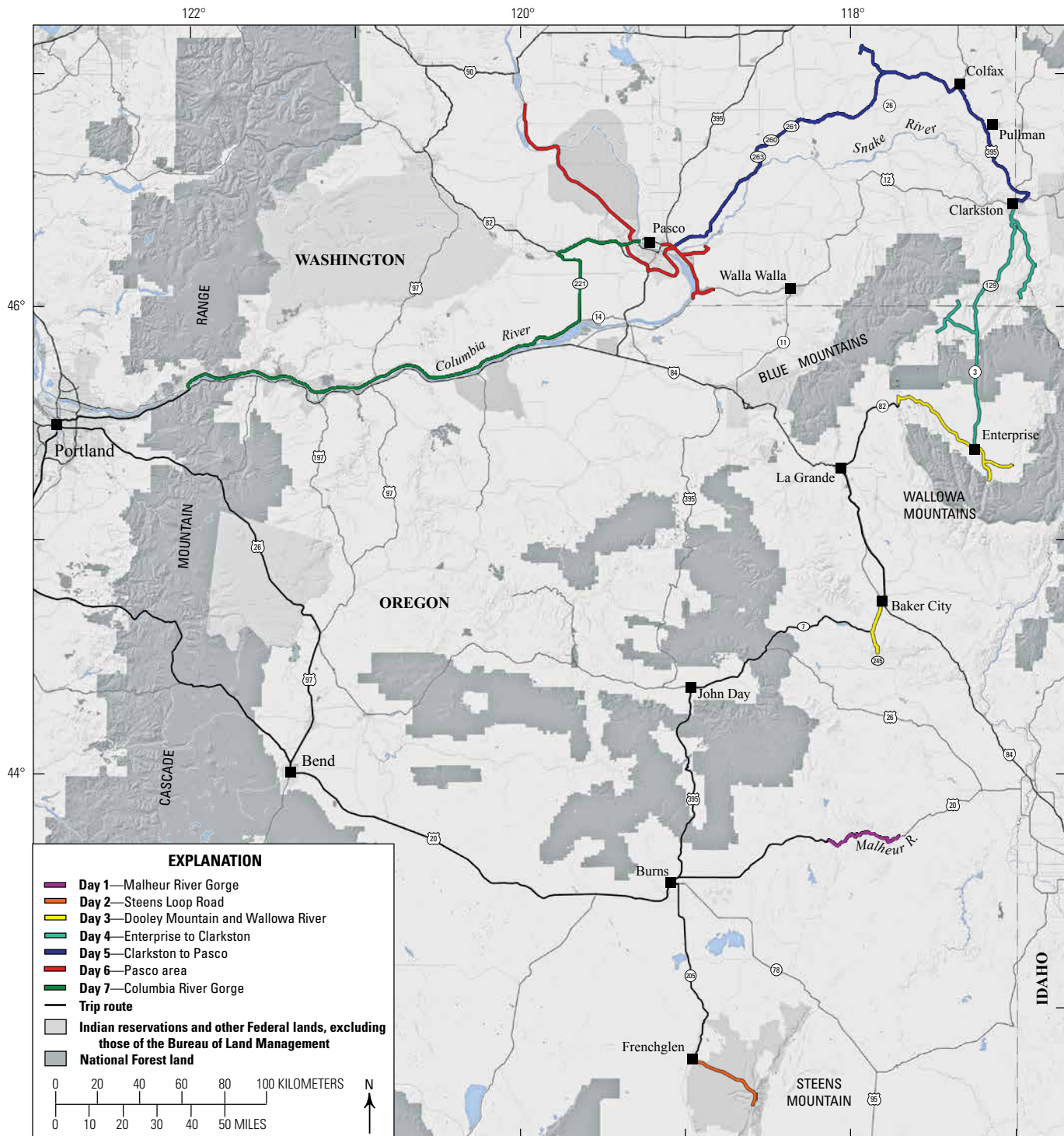


Figure 13. Map of the field-trip route through eastern Oregon and southeastern Washington State.

Numbers at the left of each road-log description are distances in miles from the starting point of each excursion. Numbers in bold at the end of each entry are the distance in miles to the next entry. View directions may be indicated by reference to a clock face, where 12:00 means straight ahead, 3:00 means 90° to the right, and 9:00 means 90° to the left.

Day 1 Overview—Malheur River Gorge

Neogene volcanic rocks in the Malheur River Gorge of east-central Oregon have proved instrumental in helping to establish a direct stratigraphic connection between the Imnaha Basalt of northeastern Oregon and the Steens Basalt of southeastern Oregon. These units resemble one another in containing common plagioclase-phyric flows with abundant, large feldspar phenocrysts (as much as 5 centimeters [cm] in diameter) and distinct but similar compositions that are fundamentally tholeiitic, with a shared source component in strontium-neodymium-lead isotopic space (Brandon and Goles, 1995; Wolff and others, 2008; Camp and Hanan, 2008; and Wolff and Ramos, 2013).

For years, the Imnaha Basalt was established as the oldest formation of the Columbia River Basalt Group until the Steens Basalt was formalized as the oldest formation in 2013 (Camp and others, 2013). The basis for this recognition was largely from the work of Hooper and others (2002) who demonstrated

that Neogene rocks in east-central Oregon, previously mapped as the basalt of Malheur Gorge, could be subdivided into lower flows that are chemically correlative to the Steens Basalt and conformable upper flows that are chemically correlative to the Imnaha and Grande Ronde Basalts. The chemical identification of Steens Basalt as the lowest unit of the basalt of Malheur Gorge was later corroborated by geologic mapping of this succession southward to connect with lava flows derived from the Steens Mountain shield volcano (Camp and others, 2003).

One result of incorporating Steens Basalt into the CRBG was a redefinition of the CRFBP, the distribution of which was expanded southward to the Oregon-Nevada border region (fig. 14; Camp and others, 2013; Reidel and others, 2013a). The updated distribution map demonstrates that the earliest eruptions of flood-basalt volcanism at ~16.7 Ma (Stees Basalt) were essentially coincident in both time and space with the earliest eruptions of rhyolite at the western end of the Snake River Plain hot spot track (fig. 5), which suggests a common origin for both provinces.

The Malheur Gorge also contains exposures of extensive rhyolite ash-flow tuffs and rhyolite lava flows that are both contemporaneous and younger than the main-phase flood-basalt eruptions. All stratigraphic units in the Malheur Gorge were subject to crustal stretching and normal faulting associated with development of the Oregon-Idaho graben after about 15.3 Ma (for example, Cummings and others, 2000).

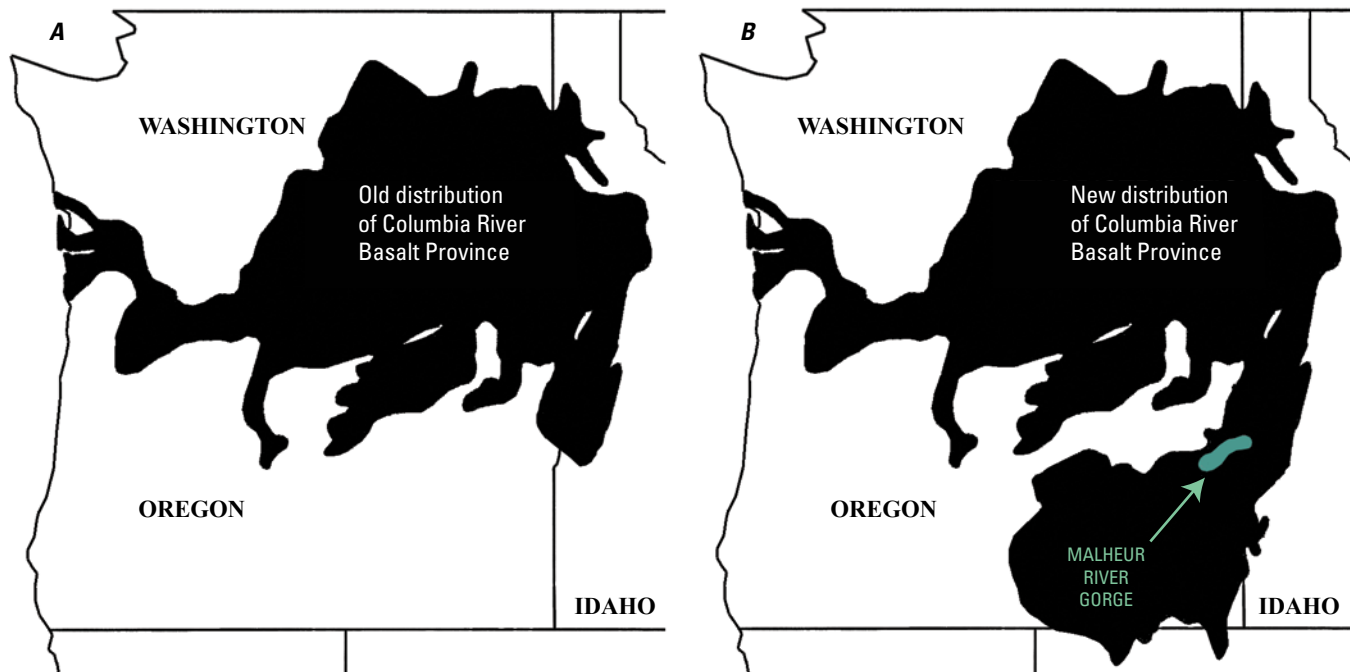


Figure 14. Old (A) and updated (B) distribution maps for the Columbia River Basalt Province. The updated version is based largely on mapping and stratigraphic relations in the Malheur Gorge (Hooper and others, 2002) and south fork of the Malheur River (Camp and others, 2003).

Day 1—Road Log

Depart Portland to Bend, Oregon. Continue eastward on U.S. Highway 20 (U.S. 20) for 185 miles (mi), through Burns to the Malheur River Gorge. Burns lies near the center of the broad Harney Basin of eastern Oregon (fig. 1). We will leave the Harney Basin near the town of Buchanan, about 27 mi east of Burns, ascending into the Stinking Water Mountains before descending gently into the Malheur River Gorge near Juntura, Oregon. Rocks exposed in the Stinking Water Mountains include a variety of middle to late Miocene basaltic and andesitic lava flows, bedded silicic ash and reworked tuffaceous sediments, poorly consolidated lacustrine sediments with diatomite, and fluvial sediments offset along north-trending normal faults. Once you enter Malheur County, about 11 mi (18 km) west of Juntura, you will be in the Mountain Standard Time zone.

- | | | |
|-----|---|-----|
| 0.0 | Stop 1-D1: Devine Canyon Ash-flow Tuff
(43.772812° N, 118.127720° W). Turn north off of U.S. 20 onto a small dirt road with gravel piles 3.3 mi west of Juntura (fig. 15). Stop at the outcrop of west-dipping rimrock about 0.1 mi from the highway. This crystal-rich ash-flow is the Devine Canyon Ash-flow Tuff, which originally covered 18,600 km ² of southeastern Oregon (Greene, 1973; Walker, 1979). The tuff is typically a stony greenish-gray devitrified ash-flow, pumiceous in places, with 10–30 percent phenocrysts of alkali feldspar and quartz. It varies from nonwelded to densely welded with vitric, devitrified, and vapor-phase zones (Wacaster and others, 2011). At this particular outcrop, the Devine Canyon Ash-flow Tuff is welded. It is ~30 m thick, close to its maximum thickness, and it overlies a nonwelded felsic tuff. | 3.3 |
| | | 6.6 |

The ash flow has a $^{40}\text{Ar}/^{39}\text{Ar}$ age of 9.7 Ma (Jordan and others, 2004). It is one of several extensive ash-flows in east-central Oregon that lie stratigraphically above the Steens Basalt; these include the Dinner Creek Welded Tuff, Prater Creek Ash-flow Tuff, and Rattlesnake Ash-flow tuff at 15.2, 8.4, and 7.0 Ma, respectively (Streck and Grunder, 1995; Hooper and others, 2002; Jordan and others, 2004). These ash flows are part of the westward-migrating rhyolites lying along the High Lava Plains trend. 3.3

Oasis Cafe in Juntura. 3.3

Stop 2-D1: View of the Dinner Creek Welded Tuff, Hunter Creek Basalt, and the basalt of Malheur Gorge (43.767113° N, 118.029459° W). Pull off road onto wide berm. The prominent cliff exposed across the river, dipping downstream at 10–15°, is the Dinner Creek Welded Tuff. This tuff is an important marker unit separating the basalt of Malheur Gorge from the younger Hog Creek sequence dominated by rhyolitic units (Ferns and others, 1993). Although the commonly accepted age of the Dinner Creek Welded Tuff in the Malheur Gorge is 15.3 Ma (Hooper and others, 2002), Streck and others (2015) argue that elsewhere it is composed of four separate cooling units of similar composition that range in age from 16 to 15 Ma. The single cooling unit found in the Malheur River Gorge originally covered an area of at least 4,000 km² (Streck and Ferns, 2004), but the four cooling units recognized by Streck and others (2015) covered an original area greater than 25,000 km².

In contrast to the crystal-rich Devine Canyon Ash-flow Tuff, the Dinner Creek Welded Tuff is

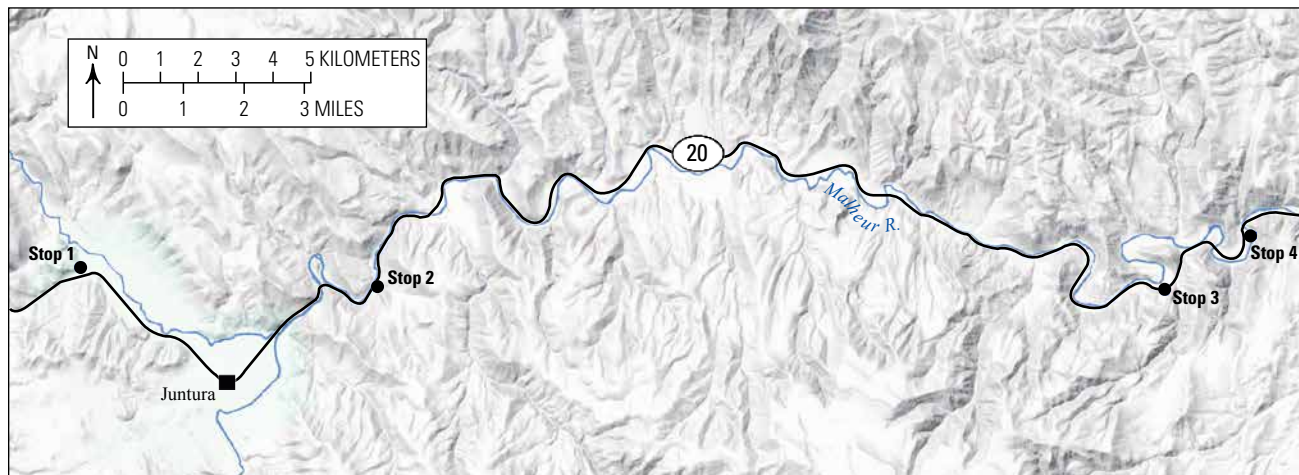


Figure 15. Map of field-trip stops for Day 1. The road log contains four stops along an eastward traverse through the Malheur River Gorge. This 28-mile excursion begins along U.S. 20, 3.3 miles west of the Oasis Cafe in Juntura, Oregon, and ends at the intersection of Highway 20 and old Highway 26.

phenocryst-poor, typically welded, and commonly marked by a basal vitrophyre. This particular exposure is somewhat atypical in containing large cavities filled with lithophysal quartz, some of which are flattened parallel to the base of the flow. The Dinner Creek eruptive center is thought to be near Castle Rock, about 40 km northwest of Juniper (Streck and others, 2015). Minor amounts of mafic globules found in the Dinner Creek Welded Tuff appear to match the Grande Ronde Basalt chemistry, thus providing direct evidence that flood-basalt reservoirs may have existed beneath the rhyolite source region (Streck and others, 2015).

Mafic lava flows exposed below the Dinner Creek Welded Tuff form the basalt of Malheur Gorge, which was subdivided by Hooper and others (2002) into the lower and upper Pole Creek units of plagioclase-phyric basalt overlain by the Birch Creek unit of aphanitic basalt to basaltic andesite. These mafic flows are best exposed to the north-northeast (at 2:00). Hooper and others (2002) demonstrated that these three subunits are chemically and petrographically equivalent to the lower Steens

Basalt (lower Pole Creek), Imnaha Basalt (upper Pole Creek), and Grande Ronde Basalt (Birch Creek), thus establishing for the first time a stratigraphic connection between the Steens Basalt and the CRBG (figs. 16, 17). Lying directly above the Dinner Creek Welded Tuff is the hackly jointed, aphyric Hunter Creek Basalt, composed of flows that are typically tholeiitic ferro-andesites (icelandites), but with a chemical affinity to the Birch Creek/Grande Ronde lavas (Ferns and others, 1993; Hooper and others, 2002). **11.4**

- 18.0 Cross bridge. Malheur River is now on the north side of the road. **1.8**
- 19.8 Gold Creek. Canyon wall at 11:00 exposes basalt of Malheur Gorge overlain by Dinner Creek Welded Tuff and Hunter Creek Basalt. Note the hackly entablature of the Hunter Creek Basalt, which typically weathers to rounded hills of cobble-sized talus. **1.0**
- 20.8 Railroad tunnel north side of the river at 9:00. **3.0**

SOUTH

NORTH

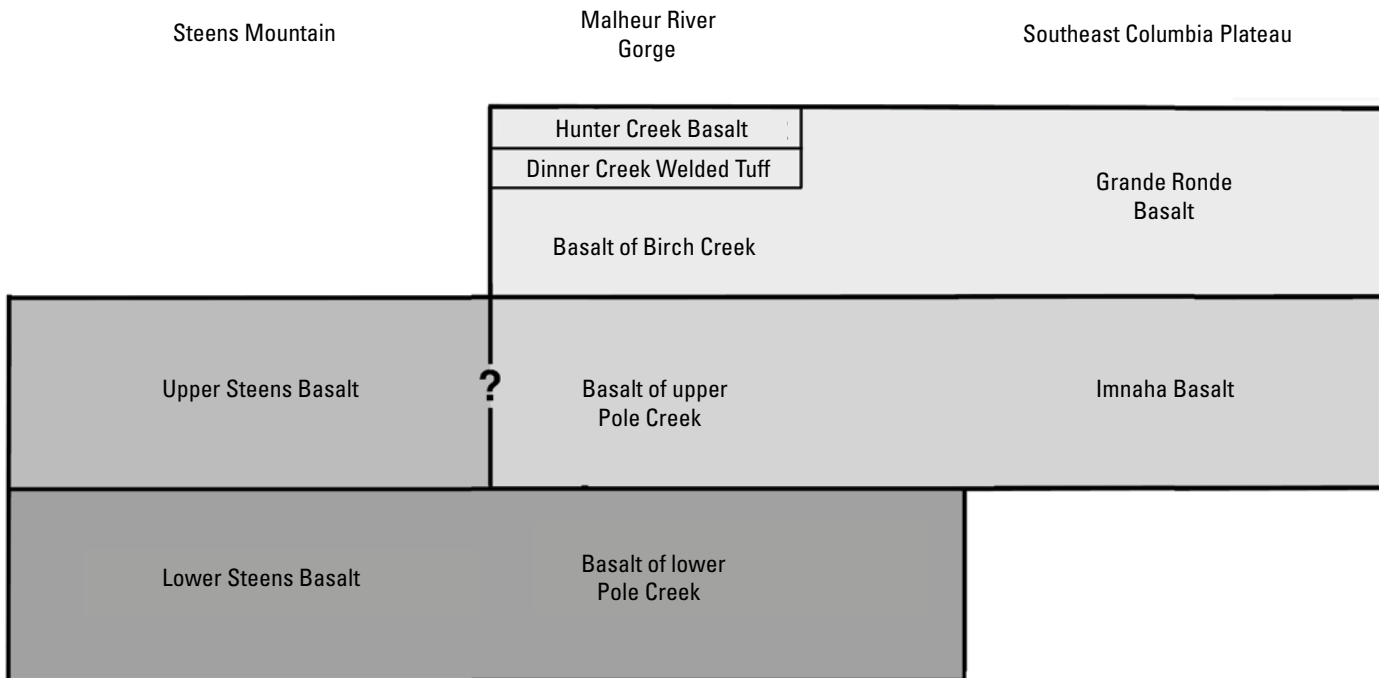


Figure 16. Stratigraphic correlations of the basalt of Malheur Gorge, and its three stratigraphic units (lower Pole Creek, upper Pole Creek, and basalt of Birch Creek) with Steens Basalt to the south and Imnaha and Grande Ronde Basalt to the north. Stratigraphic data from Lees (1994), Binger (1997), Hooper and others (2002), and Camp and others (2003).

- 23.8 **Stop 3-D1: The basalt of Birch Creek and Littlefield Rhyolite; mile marker 212** (44.767488° N, 117.762907° W). The basalt of Birch Creek exposed in the roadcut is fine- to medium-grained and sparsely plagioclase-phyric, with phenocrysts as much as 5 mm in diameter. It contains a 3–4-meter-thick rubbly flow top overlain by 1–2 meters of baked-red, airfall tuff. Note the good exposure of red-oxidized Littlefield Rhyolite on upper canyon wall to the north-northeast. **1.1**
- 26.9 Cross bridge. Malheur River is now on the north side of the road. **1.0**
- 27.9 **Stop 4-D1: Littlefield Rhyolite** (43.772320° N, 117.737114° W). Cross bridge, and immediately turn right onto old Highway 26. The base of the section here is Hunter Creek Basalt overlain by the Littlefield Rhyolite (Kittleman and others, 1965, 1967), a subunit of the Hog Creek sequence of Hooper and others (2002). We will follow the old highway to where all vehicles can comfortably park.

The Littlefield Rhyolite appears to have erupted from north-south linear vents along the western

margin of the Oregon-Idaho graben. It is a low-silica rhyolite (70–72 percent SiO_2), here composed of at least three separate flows covering more than 850 km^2 (Cummings and others, 2000; Hooper and others, 2002; Webb and others, 2016). At this location, the basalt of Malheur Gorge forms the lower 2–3 flows underlying the Littlefield Rhyolite. The rhyolite flows, well-exposed in the cliff face to the south, have a very fine-grained to glassy or devitrified matrix. Some are sparsely plagioclase-phyric. Lees (1994) suggested that the Littlefield Rhyolite may be a rheomorphic ignimbrite with a glassy matrix composed of super-welded ash shards; however, evidence for such an origin is absent in thin section and more consistent with the eruption of a sequence of vitrophyric lava flows (Webb and others, 2016).

Recent $^{40}\text{Ar}/^{39}\text{Ar}$ ages on the Littlefield Rhyolite vary from 16.2 to 16.05 Ma (Webb and others, 2016). This appears to constrain the upper limit of the underlying, Grande Ronde-equivalent Birch Creek lavas in this region to an age older than 16.2 Ma.

Depart the Malheur Gorge by way of U.S. 20 west to Burns, Oregon (about 84 mi).

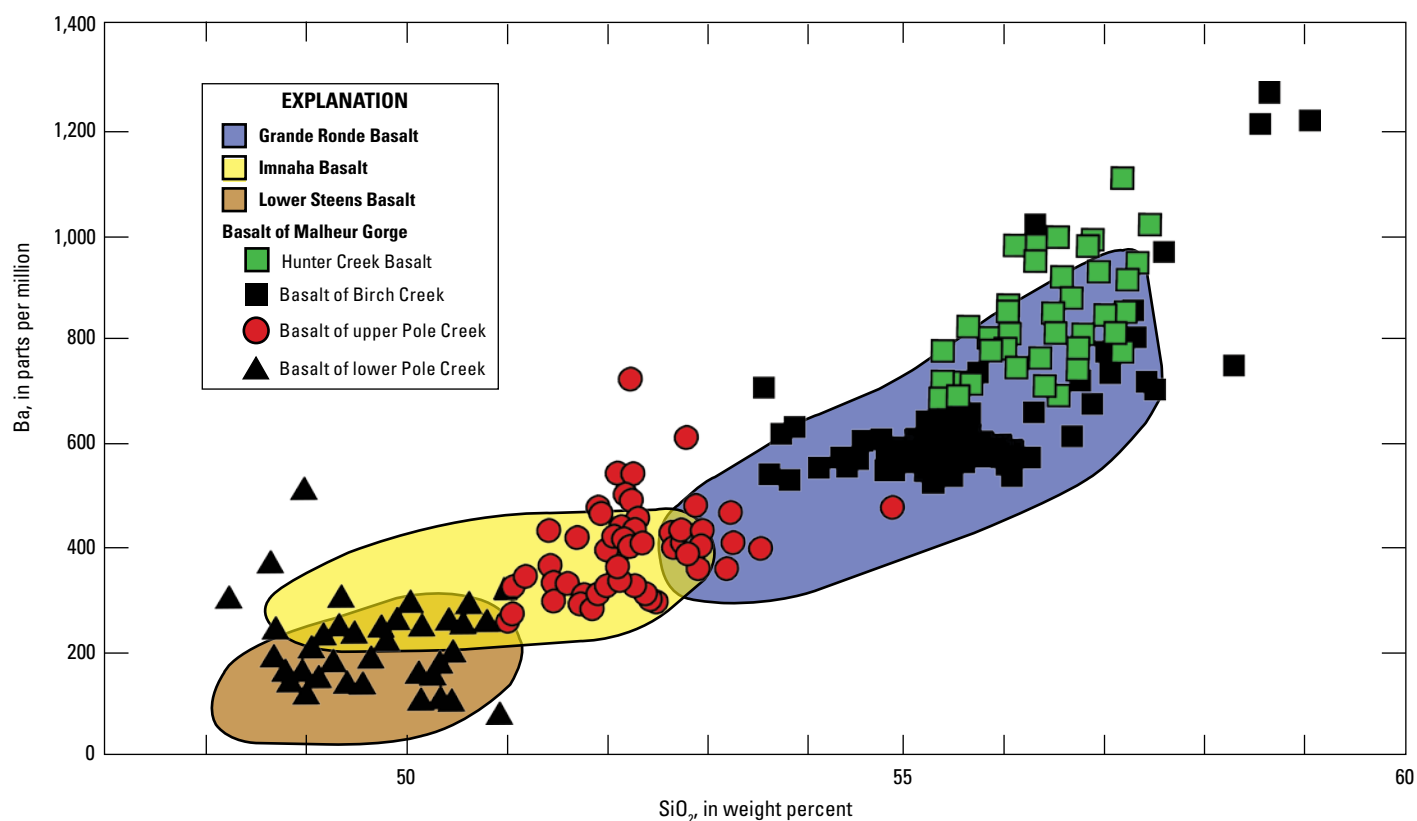


Figure 17. Plot of chemical correlations between the basalt of Malheur Gorge/Hunter Creek Basalt and the main-phase Columbia River Basalt Group units lower Steens Basalt, Imnaha Basalt, and Grande Ronde Basalt (modified from Hooper and others, 2002).

Day 2 Overview—St eens Mountain

Steens Mountain is an impressive topographic feature with a summit elevation of 9,773 ft (2,979 m). Structurally, it is a fault-block mountain, similar to others in the Basin and Range Province, with a gentle western slope but a steep fault escarpment on its eastern slope that descends more than 5,500 ft (>1.6 km) to the Alvord Desert floor below. Although there is evidence for Quaternary fault motion near the base of the escarpment (for example, Hemphill-Haley and others, 1989; Oldow and Singleton, 2008), most movement on the Steens Mountain Fault appears to have occurred between 12 and 10 Ma (Johnson, 1995). Steens Mountain may represent the remains of a middle Miocene shield volcano that was 80–100 km in diameter before being deformed by middle to late Miocene extension and Basin and Range faulting (for example, Mankinen and others, 1987).

The Steens Basalt extends from the Malheur Gorge region in the north, eastward to the Owyhee Mountains of Idaho, beyond Abert Rim to the west, and into northern Nevada to the south (fig. 1). More than 50 high-quality $^{40}\text{Ar}/^{39}\text{Ar}$ ages have been published on the Steens Basalt (tabulated in Camp and others, 2013). These ages, in combination with stratigraphic constraints, suggest that the entire age range of the Steens Basalt is unlikely to be greater than 300,000 years (Barry and others, 2013). The greatest accumulation of basalt was at the Steens Mountain shield volcano, which occurred over a shorter time interval, conservatively estimated at ~50 ka by Camp and others (2013). More recent $^{40}\text{Ar}/^{39}\text{Ar}$ ages from feldspars in interbedded tuffs from the Pueblo Mountains, south of the Steens Mountain summit region, suggest the total duration of Steens Basalt volcanism in this area may have been as much as ~190 ka, from ~16.74 to 16.55 Ma (Mahood and Benson, 2016).

Basalt erupted to a thickness of nearly 1 km from fissures concentrated in the summit area of the shield volcano (Johnson and others, 1998). This rapid eruption occurred during a well-studied paleomagnetic transition (for example, Mankinen and others, 1987), which Jarboe and others (2008, 2010) correlate with the 16.72 Ma transition separating the C5Cr and C5C.3n chronos on the geomagnetic polarity time scale of Gradstein and others (2004). These eruptions mark the initiation of Columbia River flood-basalt volcanism, which began abruptly with Steens lava erupting unabatedly, with an effusion rate estimated at ~0.67 km³/yr by Camp and others (2013) and 0.17 km³/yr by Mahood and Benson (2016).

Day 2—Road Log

Depart Burns, Oregon and travel south to Frenchglen on Oregon Route 205 (O.R. 205; about 60 miles). This highway crosses an elevated ridge known as Wrights Point, about 18 km south of Burns. This topographic feature is a paleo-valley of inverted topography filled by a resistant lava flow of high-alumina olivine tholeiite (HAOT). The lava flow erupted from a vent farther to the west about 2.4 Ma (Walker and Nolf, 1981). Lying beneath the flow are excellent exposures of tuffaceous sedimentary rocks of the Pliocene Harney Formation. Continue an additional 26 mi (42 km) to Frenchglen.

- 0.0 Road log begins at the intersection of O.R. 205 and the Steens Mountain Loop Road at the south end of Frenchglen (fig. 18). The Steens Mountain Loop is a 52 mi gravel road that ascends about 5,500 ft to the Steens Mountain summit area and back along the gentle western slope of the mountain. **3.1**
- 3.1 At intersection, road to the right goes to Page Springs campground and road to the left continues along the Steens Loop Road. Continue to the left past the gate. The sign at the gate will indicate road conditions and closures on Steens Mountain Loop Road, if any. **0.9**
- 4.0 **Stop 1-D2: Channel-fill deposits of Devine Canyon Ash-Flow Tuff** (42.815045° N, 118.848902° W). Road to the left goes to Frazier Reservoir, 0.4 mi to the north. Outcrop at the top of the mesa above the reservoir is the 9.7 Ma Devine Canyon Ash-flow Tuff (Jordan and others, 2004), underlain by brown fluvial sandstone well exposed in the bulldozer cut along the spillway of the reservoir. We observed the Devine Canyon Ash-flow Tuff previously in the Malheur River Gorge at Stop 1-D1, about 75 mi (121 km) to the northeast. Here, numerous exposures of the ash flow occur as elongated, mesa-like outcrops (fig. 19) that have been interpreted as channel-fill deposits on the west flank of the Steens Mountain shield volcano (Evans and Geisler, 2001). These channel-fill deposits pinch out about halfway up the tilted westward slope of Steens Mountain, consistent with Basin and Range extension and the westward tilting before 9.7 Ma. This does not discount, however, a gently dipping west flank to the shield volcano before block faulting began. **3.1**
- 7.1 Bluff at 9:00 is Devine Canyon Ash-flow Tuff. The ash-flow is underlain by a light brown welded pumice flow exposed in shallow ditch to the left of the road. **0.15**
- 7.25 **Optional stop: Channel-fill deposit of Devine Canyon Ash-Flow Tuff** (42.791014° N, 118.797572° W). The eastern end of a channel-fill deposit exposed to the left is composed of Devine Canyon ash-flow that is strongly welded (fig. 19). Steens Basalt is present in the ditch to the right. The 10 vertical meters between Steens Basalt and the welded ash flow is composed of eroded pumice-flow material that is poorly exposed and covered by rock fragments and soil. **0.95**
- 8.2 Canyon at 9:00 exposes Steens Basalt flows inclined by 5° to the northwest. **0.7**
- 8.9 **Stop 2-D2: Younger basalt flow of late Miocene to Pliocene age** (42.784088° N, 118.771246° W). A dark-gray to black basalt flow overlies channel-fill deposits of light-brown to baked oxidized red siltstone present at both ends of the outcrop (fig. 19). This

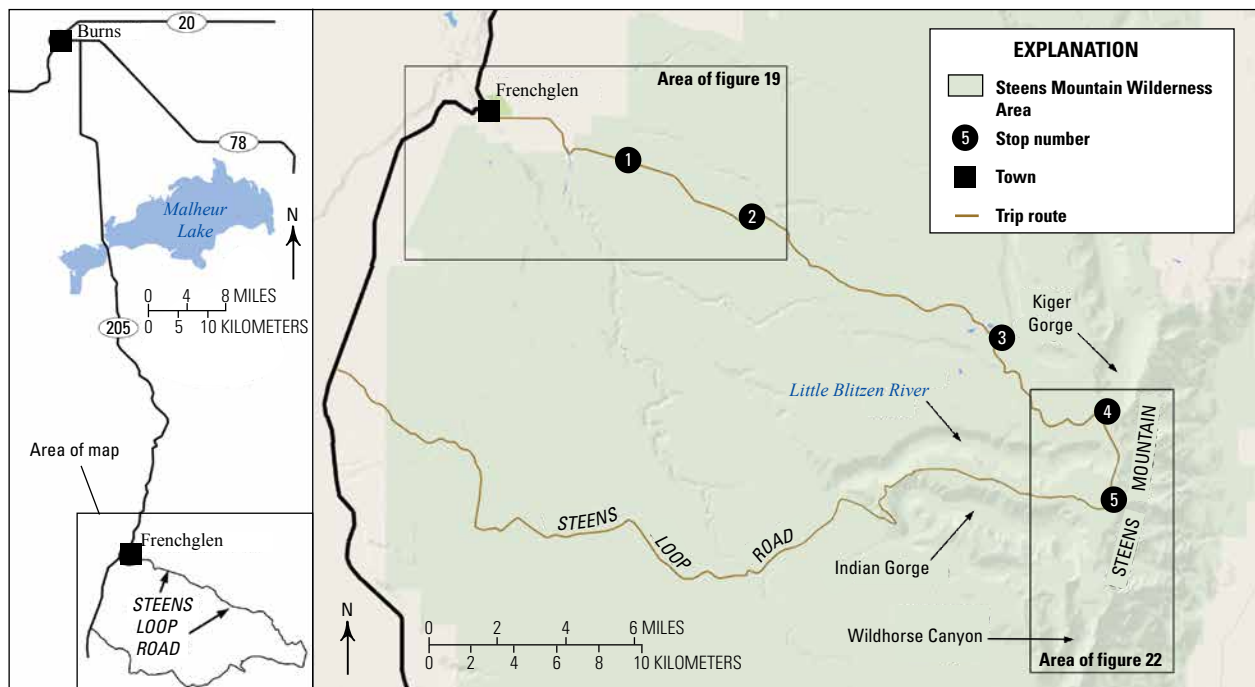


Figure 18. Map of field-trip stops for Day 2. The road log begins at Frenchglen, Oregon, a driving distance of 52.92 miles south of Burns, Oregon. Steens Loop Road ascends along the west flank of the Steens Mountain shield volcano to the summit region and back, a distance of about 52 miles (~83.5 km).

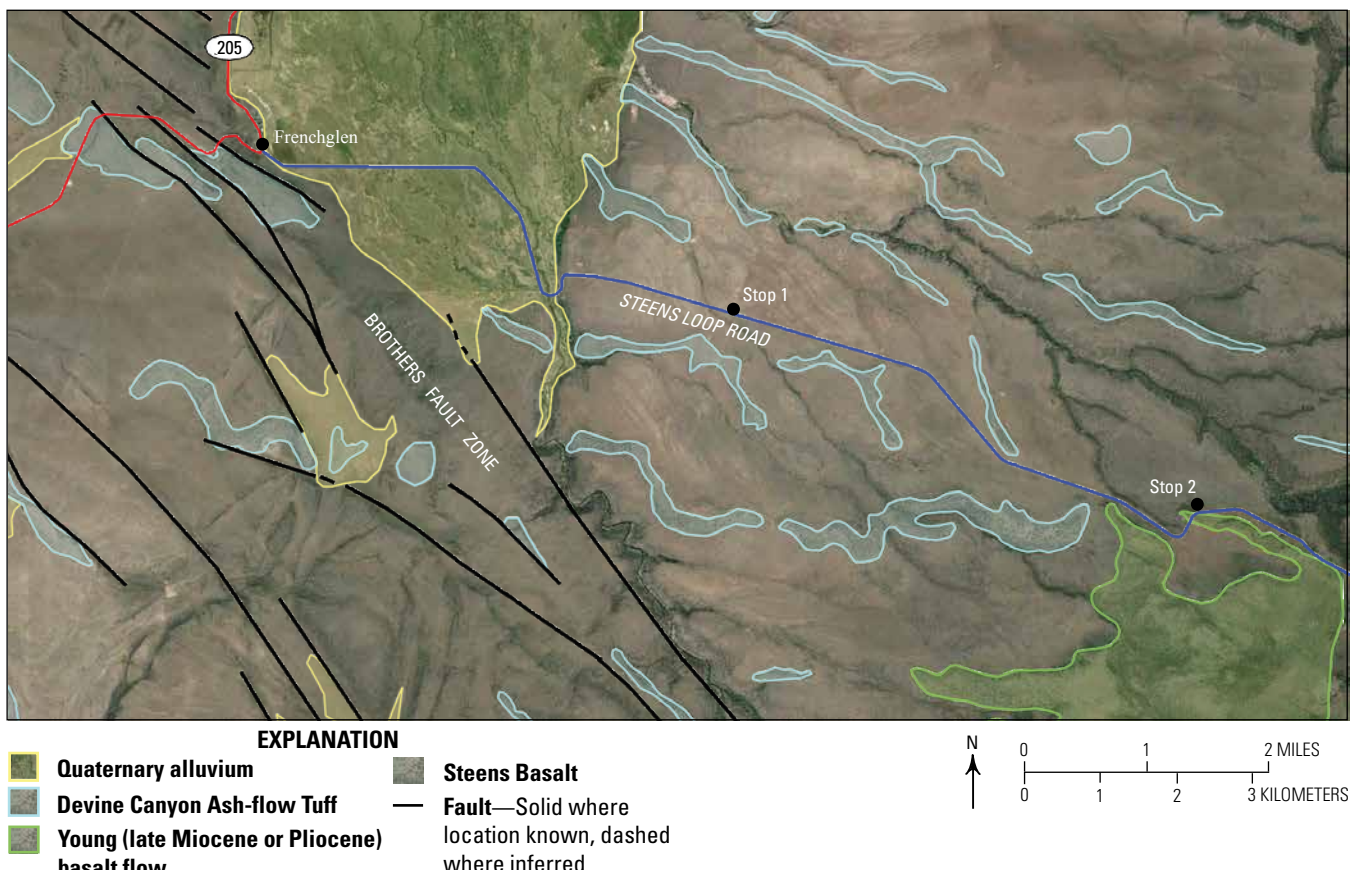
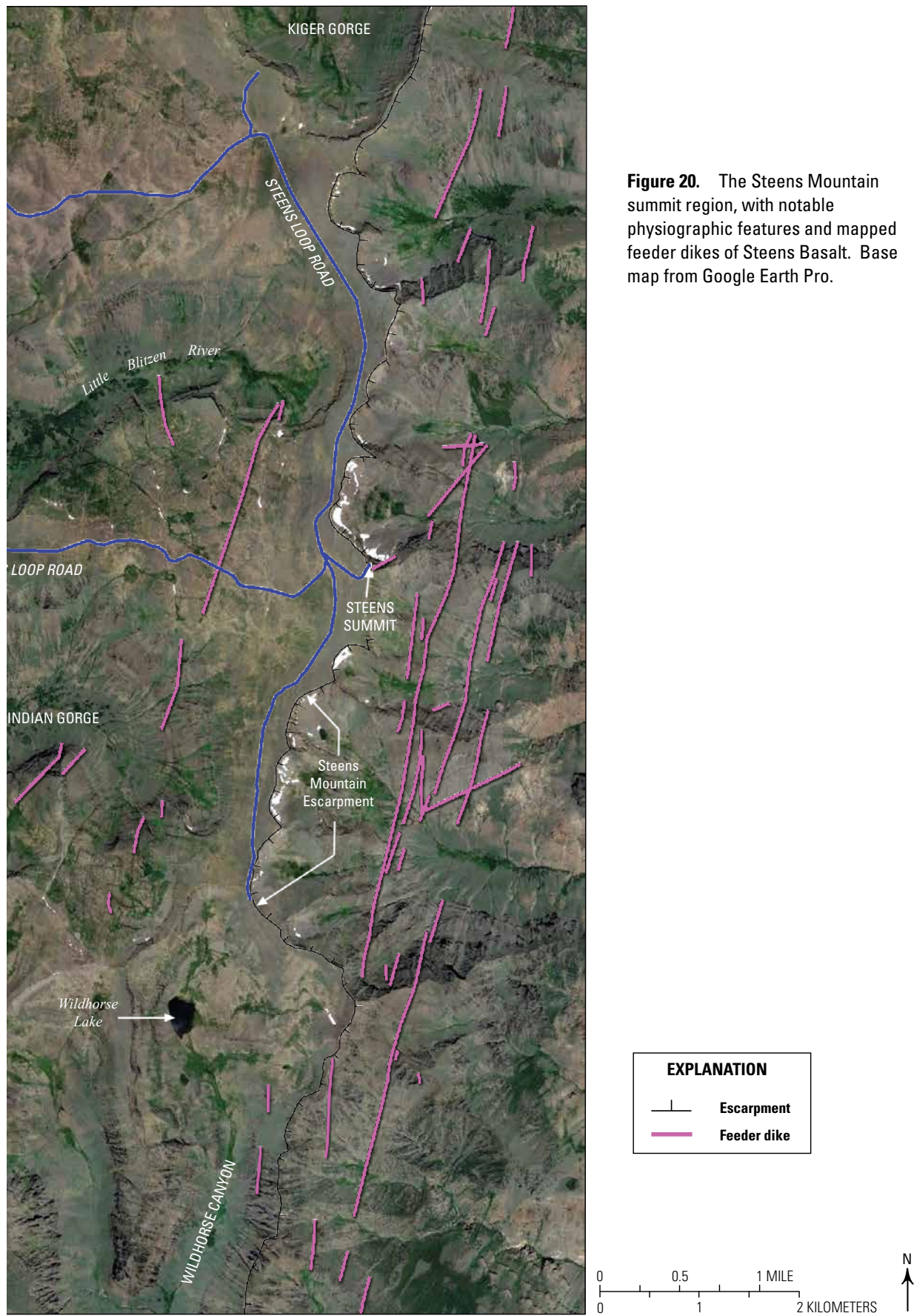
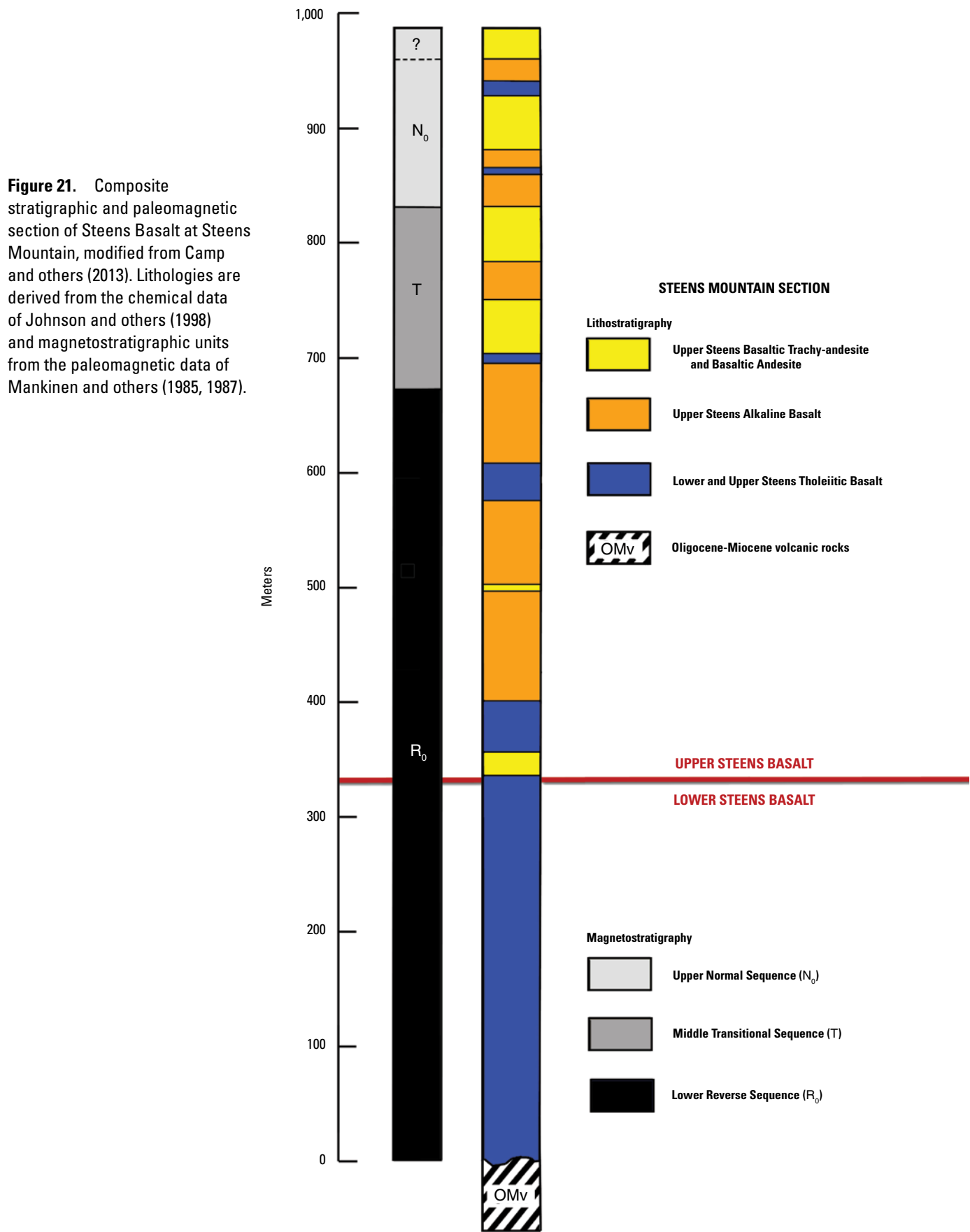


Figure 19. Map of channel-fill deposits of the Devine Canyon Ash-flow Tuff in the vicinity of Steens Loop Road east of Frenchglen, Oregon (modified from Evans and Geilser, 2001). Base map from Google Earth Pro 2016.

- undated basalt flow is younger than Steens Basalt and may be equivalent to the basalt of Hog Wallow in the Krumbo Reservoir 7.5-minute quadrangle to the north (Johnson, 1994), and other low-K tholeiitic basalts of the Oregon High Lava Plains (for example, Jordan and others, 2004). **3.15**
- 12.05 Cattle guard. Large boulders on both sides of the road after cattle guard are glacial erratics that sit above ~10,000-year-old glacial till covering much of the highlands on the west flank of the Steens Mountain shield volcano. **3.9**
- 15.95 Main entrance to Fish Lake campground. **0.75**
- 16.7 **Stop 3-D2: Steens Basalt** (42.735283° N, 118.632870° W). Steens Basalt is well exposed here in several outcrops on both sides of the road after the first group of aspen trees. The undulating plateau surface of the basalt shows evidence of glaciation in the form of glacial striations and sparse glacial erratics. This is a good area for sampling Steens lava. This particular outcrop is olivine-phyric with abundant large plagioclase phenocrysts, 2.5–8 cm in diameter, which form as much as 50 percent of the rock. These large phenocrysts are a characteristic feature of many Steens Basalt flows.
Unlike the typical large-volume sheet flows (simple flows) that characterize the remainder of the CRBG, Steens Basalt is largely composed of thin flow lobes 1–5 m thick with significantly smaller volumes. However, stacked sequences of these flow lobes commonly form 10–50-m-thick compound flows, or flow fields, that display progressive differentiation trends from the bottom to the top of each compound flow (Camp and others, 2013). **1.04**
- 17.74 Gate. A locked gate indicates that Steens Loop Road above this elevation (7,520 ft) may be impassable due to snowdrifts and muddy conditions. If this is the case, a note will be posted at the first gate located near Page Springs campground (mile marker 3.1 on this road log). **2.31**
- 20.05 Little Blitzen Gorge parallels road at 3:00. **1.55**
- 21.6 **Stop 4-D2: Kiger Gorge overlook** (42.708767° N, 118.575197° W). Turn left 3.86 mi from the gate onto the road leading to the Kiger Gorge overlook. Park in small parking area 0.4 mi from Steens Loop Road. The overlook of Kiger Gorge provides a spectacular view of the U-shaped glaciated valley. The north-trending orientation of the gorge is influenced by erosion along a north-south fault that partly cuts through the western wall of the gorge (Evans and Geisler, 2001). The eastern wall is juxtaposed against the headwall of the Steens escarpment (fig. 20), thus forming a knife-edge arête from glacial plucking to both the west and east. The western wall of the gorge exposes a 400–500 m-thick stratigraphic section composed of numerous thin pāhoehoe flow lobes of the more evolved and more chemically heterogeneous sequence of upper Steens Basalt. **1.4**
- 23 South of Kiger Gorge, the Steens Loop Road follows a narrow divide lying along the crest of the Steens Mountain escarpment (fig. 20). The steep head wall of Willow Creek canyon lies to the east, and the U-shaped glaciated headwall of Little Blitzen River canyon lies to the west. This region lies near the center of the Steens Mountain dike swarm. As you drive past Little Blitzen River Gorge to your right, notice the dike exposed in the southern headwall area of the gorge at about 2:00. Several other dikes are exposed in the Steens escarpment area to the left. **1.3**
- 24.3 **Stop 5-D2: East overlook** (42.666209° N, 118.565025° W). Turn left 2.7 mi from the Kiger Gorge Overlook road. Park at East Overlook 0.25 mi from Steens Loop Road. Here, the Steens escarpment descends from an elevation of 9,711 ft (2,960 m) to about 4,060 ft (1,237 m) into the Alvord Desert below. The light-colored evaporite deposits evident on the valley floor represent one of the largest playa lakes in Oregon. Structurally, the Alvord Desert lies in a fault-bounded basin about 200 km long and 15 km wide, with its west side bounded by the Steens Mountain Fault Zone having a vertical displacement of more than 1.5 km.
Numerous thin flows of Steens Basalt are well exposed in the canyon walls east of the overlook. These flows constitute the upper 700 m of the 950-m-thick composite stratigraphic section at Steens Mountain (fig. 21). Most of these flows are upper Steens Basalt. The few lighter-colored flows exposed in the canyon walls appear to correspond with slightly more evolved basaltic trachyandesite found in the upper part of the Steens succession (fig. 21).
This summit region of the Steens Mountain shield volcano is recognized as the central site for the eruption of the upper Steens Basalt (for example, Mankinen and others, 1987), consistent with numerous dikes of upper Steens Basalt exposed in the footwall escarpment, readily observed from the overlook. Exposed dike lengths are typically greater than 2,000 m with dike widths that vary from 5 to 20 m (fig. 22). It is noteworthy that the overall north-northeast strike of the Steens Mountain dike swarm differs from the north-northwest to northwest strike of all other dikes of the CRBG.
Northward from the East Overlook, one can see the entire Steens succession tilted by as much as 10° to the west. A slight angular unconformity at the base of the Steens succession separates it from an older





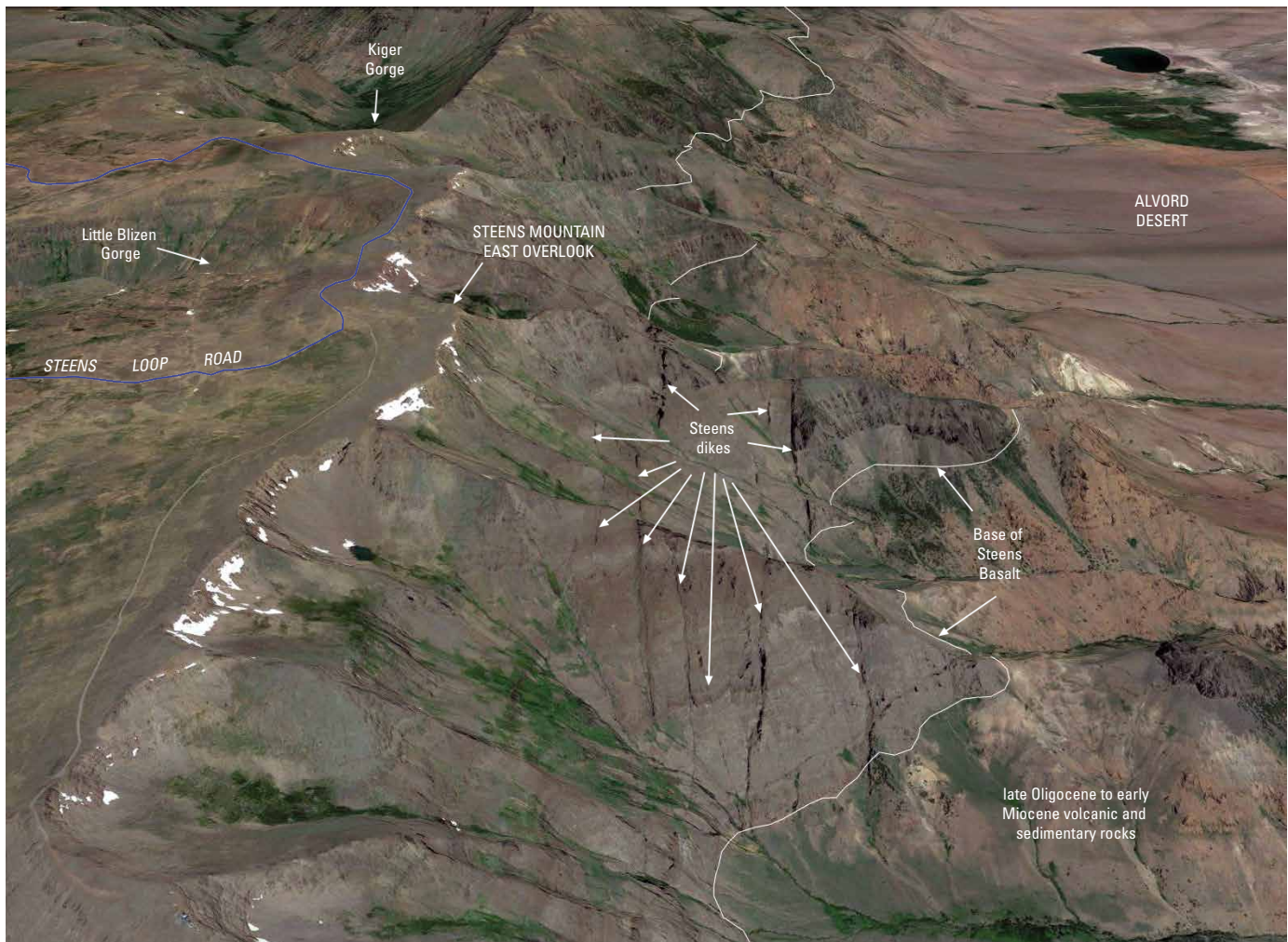


Figure 22. Oblique aerial view of the Steens Mountain summit region, looking N20°W (base image from Google Earth Pro 2016). Nearly 1 kilometer of Steens Basalt lies above late Oligocene to early Miocene volcanic and sedimentary rocks, with numerous Steens Mountain feeder dikes visible from the Steens Mountain overlook.

sequence of late Oligocene to early Miocene volcanic and sedimentary rocks (fig. 22), which are also tilted to the west but at higher angles, from 15° to 25° (Langer, 1991). This suggests that deformation in the vicinity of the Steens Mountain Fault Zone has been periodically active at least since late Oligocene time (Langer, 1991).

Whereas most CRBG dikes were emplaced along north-northwest trends consistent with forceful dike injection in the absence of significant crustal stress (Camp and others, 2015), the dikes at Steens Mountain differ in their orientation along north-northeast trends. Camp and others (2013) and Reidel and others (2013b) suggest that dike emplacement here may be the result of magma rising into a major, north-northeast-trending structural discontinuity that was mapped and defined by Wyld and Wright (2001) as the western Nevada shear zone. The shear zone is best exposed along the eastern escarpment of Pueblo Mountains to the south. Its northward projection beneath the Alvord Desert is coincident with the

north-northeast-trending Sr_i 0.704 line (Shervais and Hanan, 2008) marking a transition from thin crust (25–30 km) of accreted Mesozoic oceanic terranes to the west and increasingly thick and more stable cratonic crust to the east (Eagar and others, 2011). Middle Miocene dike intrusion may have occurred along north-northeast-trending faults coincident with this structural boundary, thus resulting in the eruption of the Steens Basalt and development of the Steens Mountain shield volcano at 16.7 Ma. This long-lived zone of structural weakness was then reactivated at 12–10 Ma during basin and range extension, resulting in normal faulting along the same north-northeast trend to produce the Steens Mountain Fault Zone and related escarpment.

Depart the summit area of Steens Mountain, returning to Burns, Oregon by way of O.R. 205. Continue north on U.S. 395 to John Day, then east on U.S. 26 and O.R. 7 to Baker City, Oregon (about 207 mi).

Day 3 Overview—Baker City to Enterprise, Oregon

Participants on the 2017 IAVCEI field trip will experience a morning viewing of a total solar eclipse from Dooley Mountain, south of Baker City. The remainder of the day will include stops at a Grande Ronde Basalt dike at Minam State Park, a Grande Ronde Basalt vent area in Little Sheep Creek, and an optional stop at Wallowa Lake State Park (fig. 23).

There are no scheduled stops from Baker City through La Grande, Oregon. It is worth noting, however, that this area forms the northernmost part of the middle Miocene to Pliocene La Grande-Owyhee eruptive axis of Ferns and McClaughry (2013). This 300-km-long, north-northwest-trending belt is located midway between the southern part of the Chief Joseph dike swarm to the east and the Monument dike swarm to the west (fig. 24). It contains a diverse assemblage of tholeiitic, calc-alkaline to alkaline, mafic to intermediate rocks together with more evolved

rhyolitic rocks. Although the oldest of these volcanic rocks appear to overlap in age with the latest Grande Ronde to Saddle Mountains Basalts, they typically overlie the CRBG stratigraphy when found in the same geographic area. Middle Miocene to Pliocene crustal stretching along the eruptive axis generated the Oregon-Idaho, Baker, and La Grande grabens (fig. 24), all of which formed after the main-phase eruptions of the CRBG. The degree of extension during the main-phase CRBG eruptions (16.7–15.6 Ma) is estimated to be <<1 percent (Taubeneck, 1970; Hooper and Conrey, 1989). After ~15.5 Ma, however, the degree of extensional strain increased to ~20 percent (Hooper and Conrey, 1989) along the La Grande-Owyhee eruptive axis (Cummings and others, 2000; Ferns and others, 2010; Ferns and McClaughry, 2013). This conversion in both the degree and style of strain was accompanied by an equally abrupt conversion in volcanic activity, resulting in the generation of small-volume eruptions and diverse volcanic assemblages found in the Oregon-Idaho, Baker, and La Grande grabens (Hooper and Conrey, 1989).

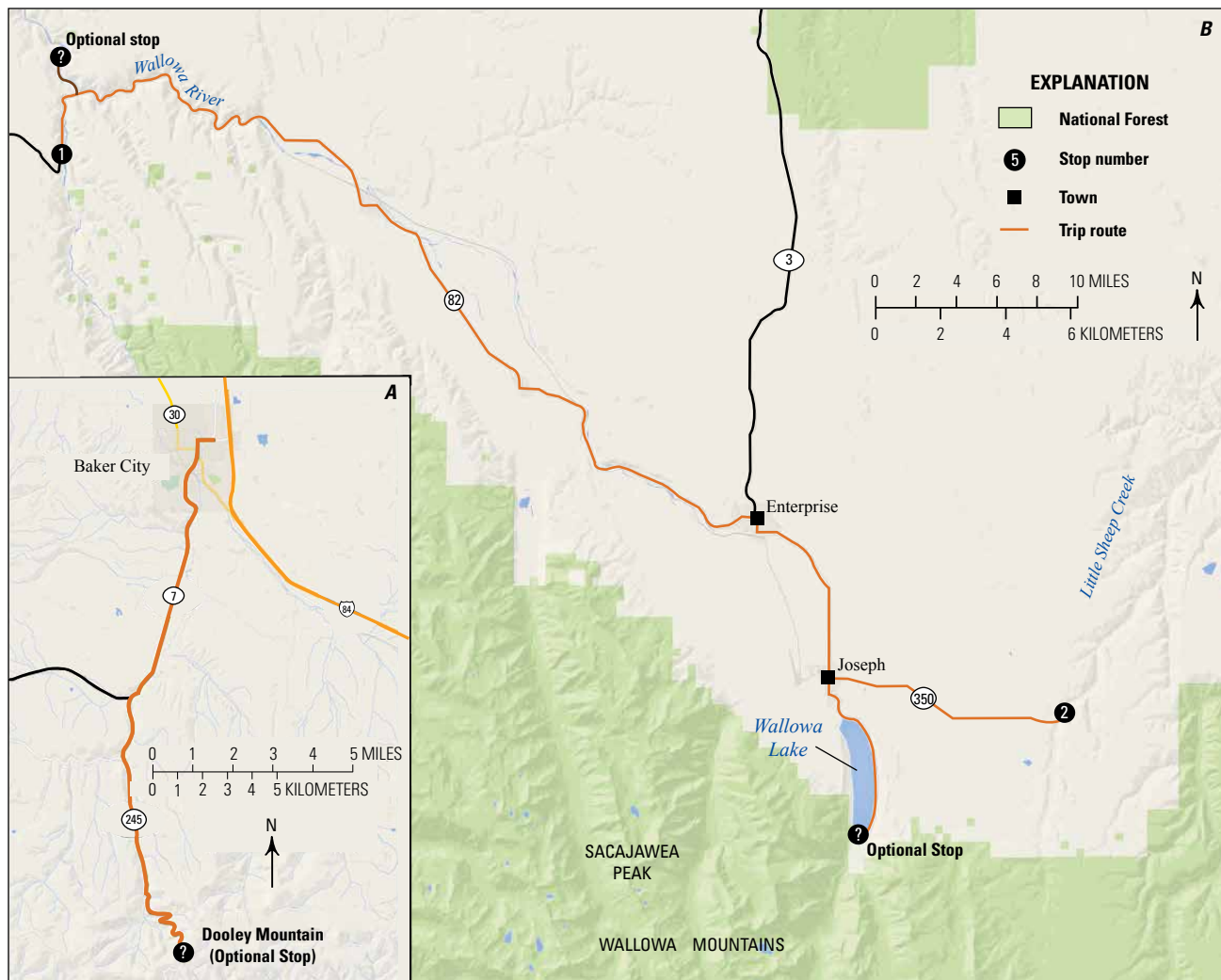


Figure 23. Map of field-trip stops for Day 3. *A*, Location of optional stop at Dooley Mountain. *B*, Location of stops 1 and 2, and the optional stop at Wallowa Lake State Park.

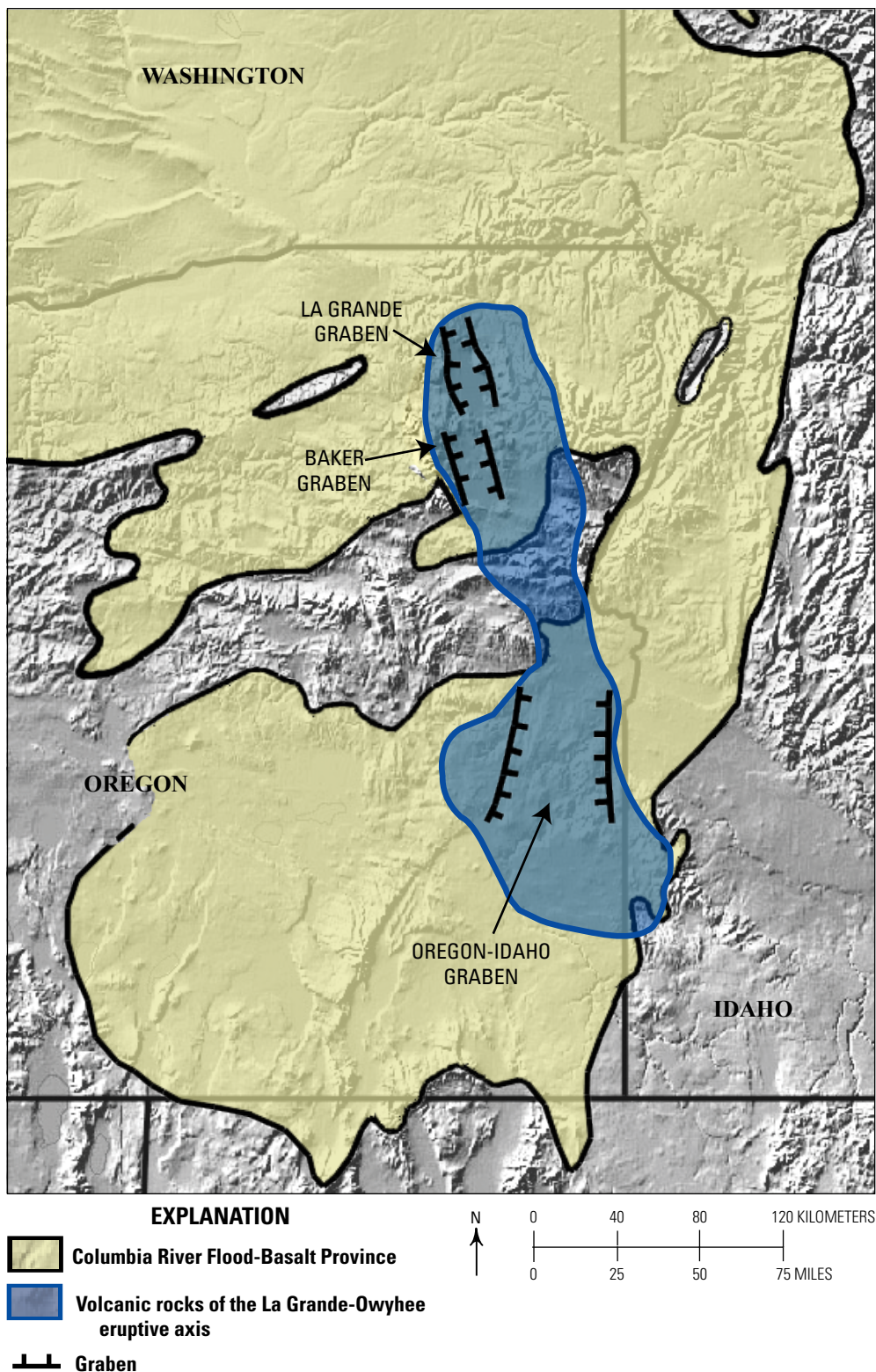


Figure 24. Map of the location of the middle Miocene-to-Pliocene La Grande-Owyhee eruptive axis and related grabens.

Day 3—Road Log:

Optional stop: Dooley Mountain (44.572885° N, 117.839095° W). This optional stop is specifically designated for participants of the 2017 IAVCEI field trip as the viewpoint for the total solar eclipse on August 21, 2017. The eclipse begins at 9:10 a.m., with totality occurring between 10:25 and 10:27 a.m. Safety concerns require the use of approved viewing goggles before and after the period of totality. The final phase of the partial eclipse ends at 11:45 a.m. The designated view stop is at the Dooley Mountain summit pass, 16.68 mi south of the intersection of O.R. 7 and U.S. 30 in Baker City. Take O.R. 7 south for 9.1 mi, turn right onto O.R. 245 for 7.58 mi to the summit pass of Dooley Mountain (fig. 23).

Dooley Mountain forms the northernmost of the felsic vents contemporaneous with the CRBG (fig. 5). Evans (1992) described Dooley Mountain as a rhyolitic dome complex with interbedded rheomorphic and nonwelded ash-flow tuffs. A late-stage rhyolitic dome at Dooley Mountain yielded a K-Ar age of 14.7 Ma (Evans, 1992). This vent complex appears to be the source for an obsidian-clast rhyolite debris-flow deposit that overlies the ~15.3 Ma Dinner Creek Welded Tuff (see Stop 2-D1) east of the Baker graben (Ferns and McClaughry, 2013). Large and others (2015) suggests that Dooley Mountain is a long-lived volcanic center, with ages that range from 15.5 to 14.7 Ma. More recently, Streck and others (2016) report single-crystal Ar-Ar ages for rhyolites in the greater Dooley Mountain area as old as 17–16.53 Ma.

0.0 **STOP 1-D3: Grande Ronde Basalt, Minam Grade** (45.589172° N, 117.732908° W). Road log begins on O.R. 82, at first pullout after the 25 miles per hour (mph) curve sign on Minam Grade, 2.6 mi south of the bridge at the confluence of the Wallowa and Minam Rivers (fig. 23).

This outcrop, covered in wire mesh, exposes a stacked succession of 5–7 flow lobes in Grande Ronde R2 MSU. The flow lobes are thinner than typical Grande Ronde sheet flows, varying in thickness from 2–3 m. Juxtaposed flow fronts and a lensoid cross-section of one flow lobe are evident in the upper half of the exposure. Most of the flow lobes are separated from one another by red, highly pumiceous vitric tuff with subordinate lithic and crystal fragments.

Continuing down the grade, the Grande Ronde flows become thicker (as much as 10 m thick) with greater lateral continuity, more typical of this formation. Note possible invasive relations between flows and tuffs, and at least one good example of a spiracle generated into a Grande Ronde Basalt flow by the explosive force of water-bearing tuffaceous sediment.

2.6 **Optional stop: Grande Ronde dike at Minam State Park** (45.636713° N, 117.731513° W). Turn left onto the road to the Minam State Recreation Area located on the Minam River, 1.5 mi north of the Wallowa Lake Highway (O.R. 82; fig. 23). A Grand Ronde Basalt dike crosses the Minam River valley about 100 m west of the entrance to the park campground (Shubat, 1979). The dike is not readily apparent along the valley floor, but it is best observed about 200 ft higher on the north side of the river. The dike trends N10°W, which is typical of most dikes in the Chief Joseph dike swarm. The dike has reverse magnetic polarity and cuts through the lower part of a 670 m section (2,200 ft) of Grande Ronde MSU R2, most likely feeding one of the upper R2 flows higher in the section. The remaining lavas at the top of this section include Grande Ronde MSU N2, and lava flows of both the Wanapum Basalt (basalt of Dodge and basalt of Powatka) and Saddle Mountains Basalt (Umatilla Member). **1.5 mi (back to O.R. 82)**

- 15.48 O.R. 82 takes left bend onto First Street in Wallowa. **8.0**
- 23.48 Lostine town center. **10.16**
- 33.64 Enterprise town center; O.R. 82 takes left bend onto River Street. **6.31**
- 39.95 Joseph town center; cross street O.R. 350. You have two alternatives here: (1) For the optional stop at Wallowa County Park Boat Landing and Beach, go straight through the intersection on O.R. 351 for 1.5 mi, or (2) turn left on O.R. 351 for 7.8 mi to Stop 2-D3.

41.45 **Optional stop: Wallowa Lake State Park** (45.284128° N, 117.211523° W). This stop provides a visual backdrop of the Wallowa Mountains and opportunity to discuss the Chief Joseph dike swarm, and the structural and uplift history along the Wallowa front-range fault. The Wallowa Mountains contain Late Jurassic plutonic rocks of the Wallowa batholith that intrude older Mesozoic volcanic and sedimentary rocks of accreted oceanic terranes. The plutonic rocks are themselves intruded by numerous dikes of Grande Ronde (mostly) and Imnaha Basalt, with some of the highest peaks in the mountain range capped by remnants of Imnaha Basalt lava flows and rare Grande Ronde Basalt remnants, unconformably overlying the batholithic rocks. These CRBG dikes are part of the Chief Joseph dike swarm, where Grande Ronde Basalt dikes become more prevalent to the north. Petcovic and Grunder (2003) calculate paleo-depths of Grande Ronde Basalt dikes in the Wallowa Mountains as great as 2–5 km.

The northwest-striking Wallowa Fault forms a linear, steep range-front between the northeast flank of the mountain range and the upper Wallowa

River valley. This fault lies near the southeast end of Raisz's (1945) Olympic-Wallowa Lineament (OWL) and has a maximum vertical displacement of about 2,200 m. Initial uplift of the Wallowa Mountains may have occurred during eruption of the Grande Ronde Basalt (Hales and others, 2005), but tilting of some Columbia River Basalt flows by as much as 25° appears to have preceded uplift along the Wallowa Fault (Taubeneck, 1987), with significant uplift occurring after the eruption of the Grande Ronde Basalt. Some workers have suggested that the Wallowa Fault may represent the dextral component of a conjugate system that also includes northeast-striking structures such as the Hite Fault (fig. 8; Hooper and Conrey, 1989; Mann and Meyer, 1993). Such a hypothesis cannot be verified, however, because of the lack of documented evidence for lateral displacement along the fault (Personius and others, 2003).

Workers have long been interested in the dramatic uplift associated with the Wallowa batholith. Hooper and Camp (1981) attributed the uplift of the Wallowa batholith and other prebasalt granitic plutons on the east side of the Columbia Basin to isostatic forces. Hales and others (2005) suggested instead that the Wallowa Mountains underwent uplift of a few hundred meters during the CRBG eruptions, which they attributed to convective downwelling and detachment of the dense plutonic root of the batholith. Darold and Humphreys (2013) expanded on this concept by presenting teleseismic data consistent with a curtain-like structure of presumed Farallon lithosphere beneath the Wallowa batholith. They suggested that arrival of the Yellowstone plume initiated delamination of remnant Farallon lithosphere previously connected to the base of northeastern Oregon, with continued delamination resulting in topographic uplift as the dense Wallowa pluton root began to founder.

48.24

Retrace route back to Joseph, turn right onto state O.R. 350. **14.9 mi.**

STOP 2-D3: Little Sheep Creek vent complex of Grande Ronde MSU R2 (45.335770° N, 117.079779° W).

(**without optional stop**). This site shows a complex interaction between tephra and Grande Ronde lava flows of the R2 MSU (fig. 2). The physical volcanology of tephra disruption by invading lava in this outcrop is described in Brown and others (2015). Grande Ronde Basalt eruptions during R2 time account for ~27 percent of the total CRBG volume. At this location, three of the four members that compose the Grande Ronde R2 are present, from oldest to youngest, the Mount Horrible, Wapshilla Ridge, and Grouse Creek members (Davis and others, 2013). Flows of the Mount Horrible and Grouse Creek members are chemically indistinguishable and must be identified based on their stratigraphic position relative to the Wapshilla Ridge. However, Reidel and Tolan (2013) note that flows of the Wapshilla Ridge, Grouse Creek and Mount Horrible members interfinger, suggesting that there is a compositional transition from the Wapshilla Ridge to Grouse Creek member. In addition, they show the Meyer Ridge and Grouse Creek chemical types have interfingering relations in parts of the CRFBP, consistent with field evidence that all four members of Grande Ronde R2 may have erupted almost simultaneously (Davis and others, 2013).

Evidence for near-simultaneous eruption of the Wapshilla Ridge and Mount Horrible members is present in this outcrop (fig. 25). Here, a vent complex is overlain by a Grouse Creek member flow. Within the complex, a flow of Mount Horrible basalt appears to be invasive into the tuff of Wapshilla Ridge, as indicated by crosscutting relations and soft-sediment deformation. This interfingering of these units suggests that the Mount Horrible and Wapshilla Ridge chemical types may have a cogenetic relation at this location.

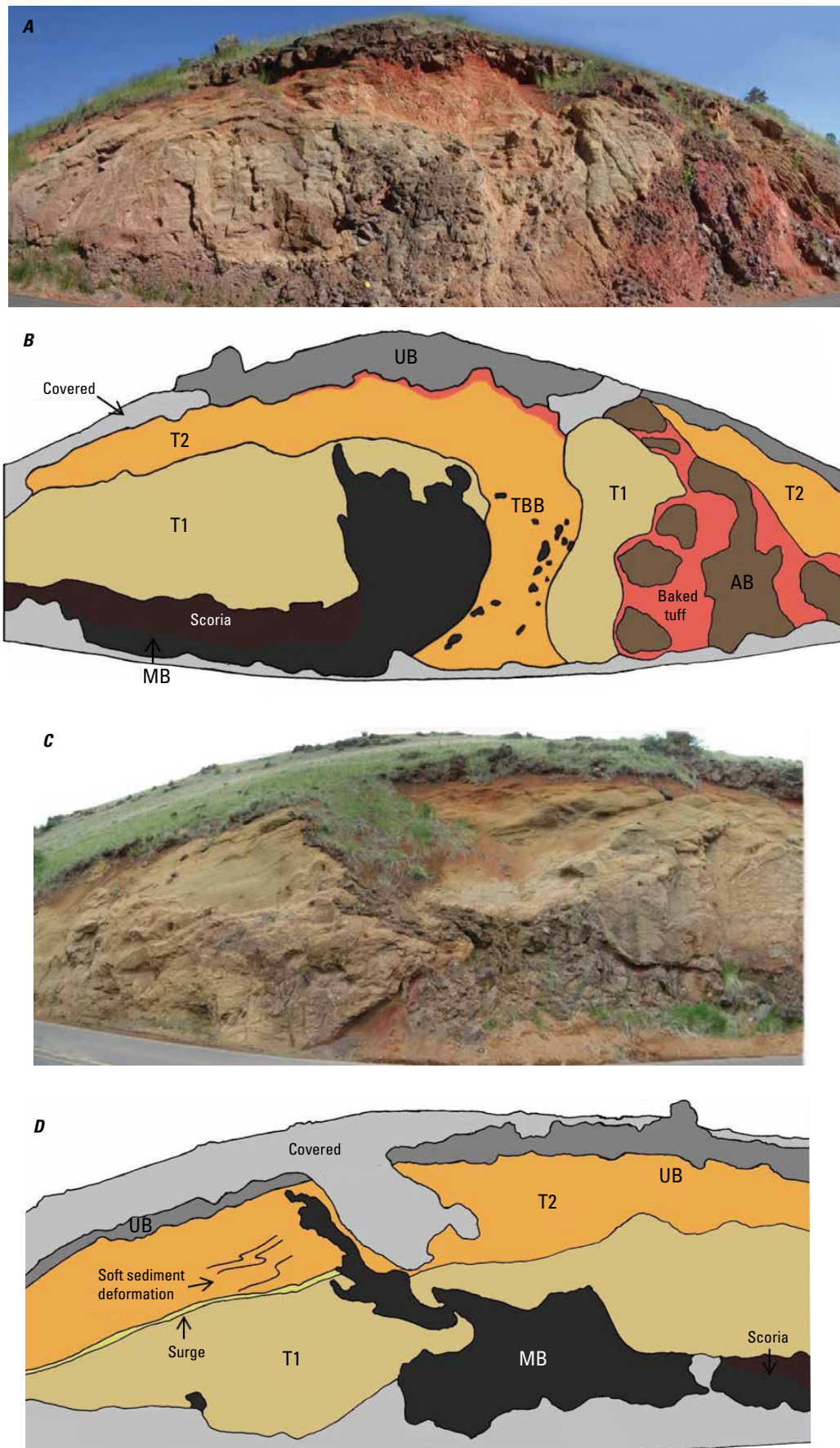


Figure 25. The Little Sheep Creek vent exposure, from Davis and others (2013). *A*, Photograph of the eastern exposure of a lava flow chemically equivalent to the basalt of Mount Horrible intruding into tuff of Wapshilla Ridge. *B*, Sketch map of the eastern exposure. *C*, Photograph of the western exposure of lava with basalt of Mount Horrible chemistry intruding into tuff of Wapshilla Ridge, with soft sediment deformation. *D*, Sketch map of the western exposure. Outcrop heights are roughly 12 meters above road level. T2, upper tuff of Wapshilla Ridge; T1, lower tuff of Wapshilla Ridge; TBB, block bearing tuff of Wapshilla Ridge; UB, upper basalt of Grouse Creek; AB, a'a basalt of Wapshilla Ridge; MB, massive basalt of Mount Horrible.

Day 4 Overview—Grande Ronde and Snake River Canyons

The Grande Ronde and Snake River canyons provide easy access to spectacular exposures of the CRBG across the northern extent of the Chief Joseph dike swarm. Taubeneck (1970) estimated the Chief Joseph swarm may contain as many as 21,000 dikes. Day 4 includes nine stops where a number of features and geologic relations can be observed and discussed (fig. 26). These include (1) stratigraphy and structure of the CRBG along the axis of the Blue Mountains uplift (Stops 1-D4 and 2-D4); (2) dike exposures for the Roza and Elephant Mountain (Wenaha flow) Members of the Wanapum and Saddle Mountains Basalt, respectively (Stops 3-D4 and 5-D4); (3) intracanyon/invasive relations displayed in Saddle Mountains Basalt flows (Stops 4-D4 and 9-D4); (4) the contact relation between the Imnaha and Grande Ronde Basalt, and view of the Grande Ronde type section (Stop 7-D4); and (5) vent exposures for the Teepee Butte and Umatilla Members of the Grande Ronde and Saddle Mountains Basalt, respectively (Stops 8-D4 and 6-D4).

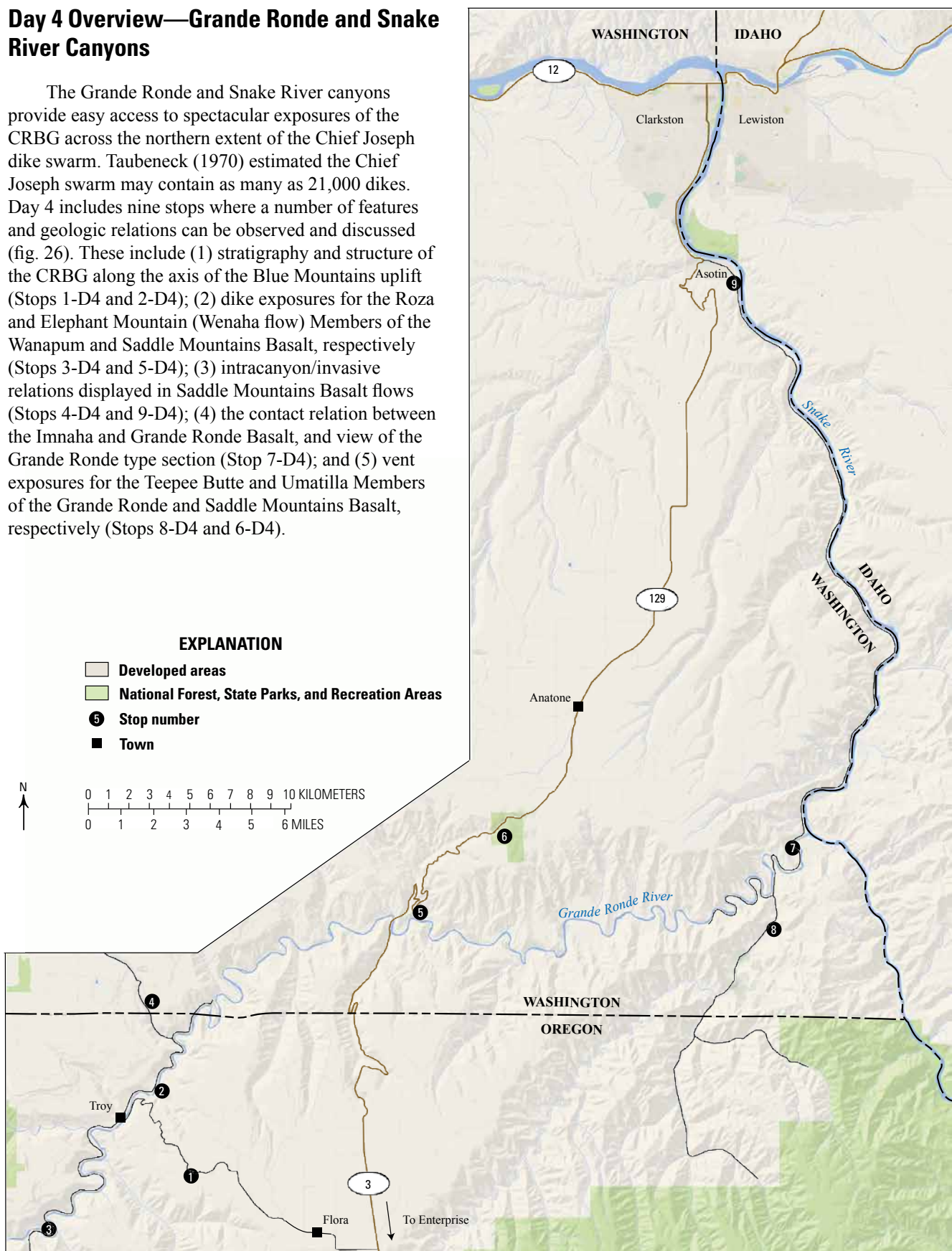


Figure 26. Map of field-trip stops for Day 4. The road log begins 26.5 mi (42.7 km) south of the map in Enterprise, Oregon. The first scheduled stop is at the Troy Basin-Blue Mountains Overlook.

Day 4—Road Log

- 0.0 At junction of O.R. 82 and O.R. 3 in Enterprise, head north on O.R. 3. **2.9**
- 2.9 Road leaves alluvium and is now on R2 Grande Ronde Basalt. Note the flow contact at 3:00 marked by red oxidized zone. **3.5**
- 6.4 Road has dropped through R2 Grande Ronde Basalt and is now on the N1 Grande Ronde Basalt. Note red oxidized flow top. **1.3**
- 7.7 Ant Flat Road. Back in R2 Grande Ronde Basalt. **1.8**
- 9.5 Quarry of R2 GRB at 3:00. **2.0**
- 11.5 Road mileage marker 32. **3.1**
- 14.6 Road mileage marker 29. **0.5**
- 15.1 Road to Starvation Creek. Begin to climb grade. Road is on R2 Grande Ronde Basalt vents. **2.8**
- 17.9 WallowaWhitman National Forest. **2.4**
- 20.3 Summit 4,846 ft. **5.8**
- 26.1 Day Ridge Road. **4.5**
- 30.6 **Optional stop: Joseph view point. View point is located on the Umatilla Member (45.835345° N, 117.263900° W). 1.5**
- 32.1 Road mileage marker 12. **1.0**
- 33.1 Road is now on Buford Flow. **1.2**
- 34.3 Rimrock Inn restaurant. **0.3**
- 34.6 Left (west) on Flora Road. **1.4**
- 36.0 Turn right. **0.4**
- 36.4 Turn left. **1.1**
- 37.5 Turn right in town of Flora. **0.4**
- 37.9 Turn left onto Lost Prairie Road. **2.9**
- 40.8 Turn left onto Troy Road. **1.9**
- 42.7 **STOP 1-D4: Troy Basin-Blue Mountains overlook** (Troy-Flora Road: 45.926844° N, 117.379863° W). This stop provides a general overview of the Troy Basin and Blue Mountains uplift (fig. 27). We are

standing on the southern margin of the south limb of the Grouse Flat syncline (also known as the Troy Basin). The Blue Mountains uplift in the far distance consists of flows of Grande Ronde Basalt folded into the broad, gently east-northeast-plunging anticline (Saddle Butte anticline; Ross, 1978). The Slide Canyon monocline rises at the north edge of Grouse Flat to form the southern front of the Blue Mountains uplift. Flows dip up to 49° S within the monocline before flattening to 1–3° S in the north limb of the Grouse Flat syncline. The axis of the syncline lies on Grouse Flat just north of the river (figs. 27, 28). The surface of Grouse Flat is formed by the Elephant Mountin (Wenaha flow) and Buford Members of the Saddle Mountains Basalt (figs. 28, 29).

Following eruption of the Wenaha flow into the Troy Basin, the ancestral Grande Ronde River developed broad meanders on the surface of the flow. During the initial period of uplift of the Blue Mountains, the river was able to maintain its meanders as it eroded down through the Buford Member and Elephant Mountin (Wenaha) flows, eventually encountering the underlying Grouse Flat sedimentary interbed. The river easily maintained and, perhaps, enlarged its meanders as it eroded into the interbed, the underlying Umatilla Member flows, and the thin Squaw Canyon sedimentary interbed beneath them (figs. 27–29). The result was Bartlett Bench (fig. 27). Subsequently, the main period of Blue Mountains uplift occurred, with the meandering Grande Ronde River becoming entrenched in deep canyons eroded into flows of the Grande Ronde Basalt (figs. 27, 30; Ross, 1980).

The south limb of the Grouse Flat syncline is crossed by a series of north-northeast-trending faults (Grande Ronde Fault System (fig. 28; Ross, 1978, 1989) showing both normal (north side down) and left-lateral strike slip offsets based on displacements of flows and dikes (discussed at Stop 2-D4). **1.1**

- 43.8 North-northeast-trending Horseshoe Bend Fault crosses road with normal offset of 140 m (460 ft) measured here on a flow of basalt of Dodge. **2.0**
- 45.8 North-northeast-trending Courtney Creek Fault crosses road in curve. Normal offset of 175 m (575 ft) measured here on a flow of basalt of Dodge. **1.0**
- 46.8 **STOP 2-D4: Grande Ronde canyon overlook** (45.958370° N, 117.410889° W). Most of the area's stratigraphy is visible in the exposures across the Grand Ronde River from Stop 2-D4 (figs. 29, 30). The steeper, inner canyon walls consist mostly of 15 flows of Grande Ronde Basalt spanning parts of the N1, R2, and N2 MSUs. At the top of the inner canyon wall, these flows are overlain by three flows

of Wanapum Basalt which, in turn, are overlain in succession by two Saddle Mountains Basalt flows, a thick sedimentary interbed, a thick Saddle Mountains Basalt flow, a second sedimentary interbed, and a fourth Saddle Mountains Basalt flow (fig. 29).

Squaw Canyon, immediately below and to the east of the road, is eroded into a northwest-trending fault that intersects a north-northeast-trending fault near the confluence of Squaw Canyon and the Grande Ronde River (fig. 28). The former extends southeast up Squaw Canyon about 2 km before intersecting another north-northeast-trending fault (fig. 28). These are part of the Grande Ronde Fault System extending north-northeast across the south limb of the Grouse Flat syncline (fig. 28). The northeast-trending faults show both left-lateral strike-slip and subsequent normal movements measured on the basalt of Dodge (normal offset as much as 207 m [679 ft]) and a dike consisting of basalt of Dodge with left-lateral offset of 695 m (2,280 ft) in Courtney Creek (fig. 28). These represent the first confirmed strike-slip faults of the CRFBP (Ross, 1975).

Strike-slip offset is suspected along the northwest-trending normal fault in Squaw Canyon but could not be verified. The lower few miles of Courtney Creek and Mud Creek also appear to have eroded into northwest-trending faults, but this could

not be confirmed. Together, the northwest- and north-northeast-trending faults form conjugate sets for which the accompanying stress field is inferred to be a 10° NW principle compressive stress with an associated ENE-WSW extension (Ross, 1975, 1978, 1979, 1989). The origin of this stress is discussed in the introduction.

Evidence in the area supporting the onset of folding of the Grouse Flat syncline during the early stage of Wanapum eruptions includes (1) the largest quantity and thickest of the Wanapum and Saddle Mountains flows are confined to the core of the syncline; and (2) the Elephant Mountain Member (Wenaha flow) thickens into the syncline, as does the underlying Grouse Creek sedimentary interbed. There is limited evidence that a thick N1 flow of Grande Ronde Basalt (Troy flow; Ross, 1978) thins over the Blue Mountain uplift before thickening again north of the axis of the Saddle Butte anticline. This would suggest initiation of the uplift was during the Grande Ronde eruptions. However, owing to the difficulty of tracing the Troy flow across the uplift, this variation in thickness could not be confirmed at more than two outcrops.

Strike-slip faulting within the Grande Ronde Fault System pre-dates eruption of the Wenaha flow as evidenced by the feeder dike intruding into large-scale, en echelon extension gashes located

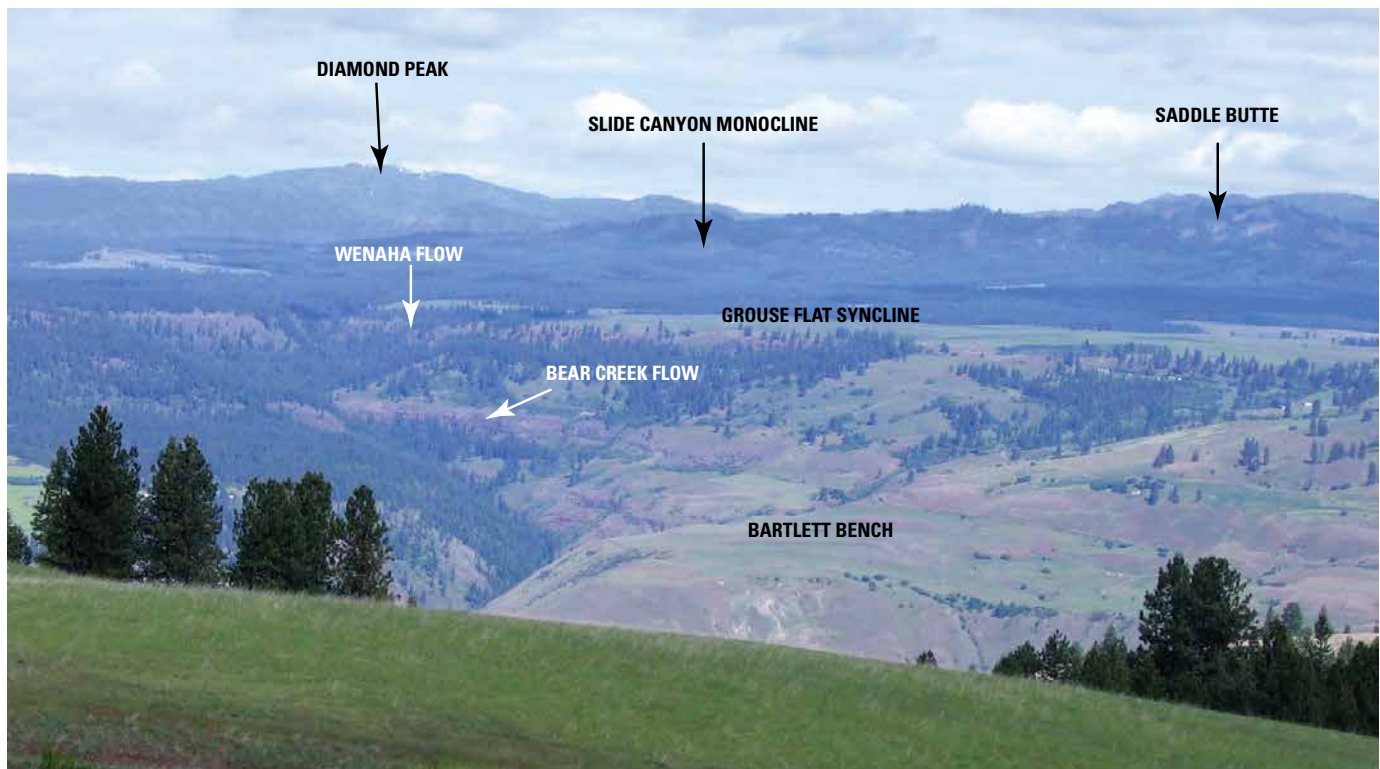


Figure 27. Photograph from Stop 1 looking azimuth 332° across the Grouse Flat syncline (also known as the Troy Basin). The forested highlands beyond the Grouse Creek syncline include Diamond Peak, the Slide Canyon monocline, and Saddle Butte, all of which lie within the larger Blue Mountains Province. The slopes in the foreground steepen northwestward across eroded fault scarps within the Grande Ronde fault system shown in figure 28.

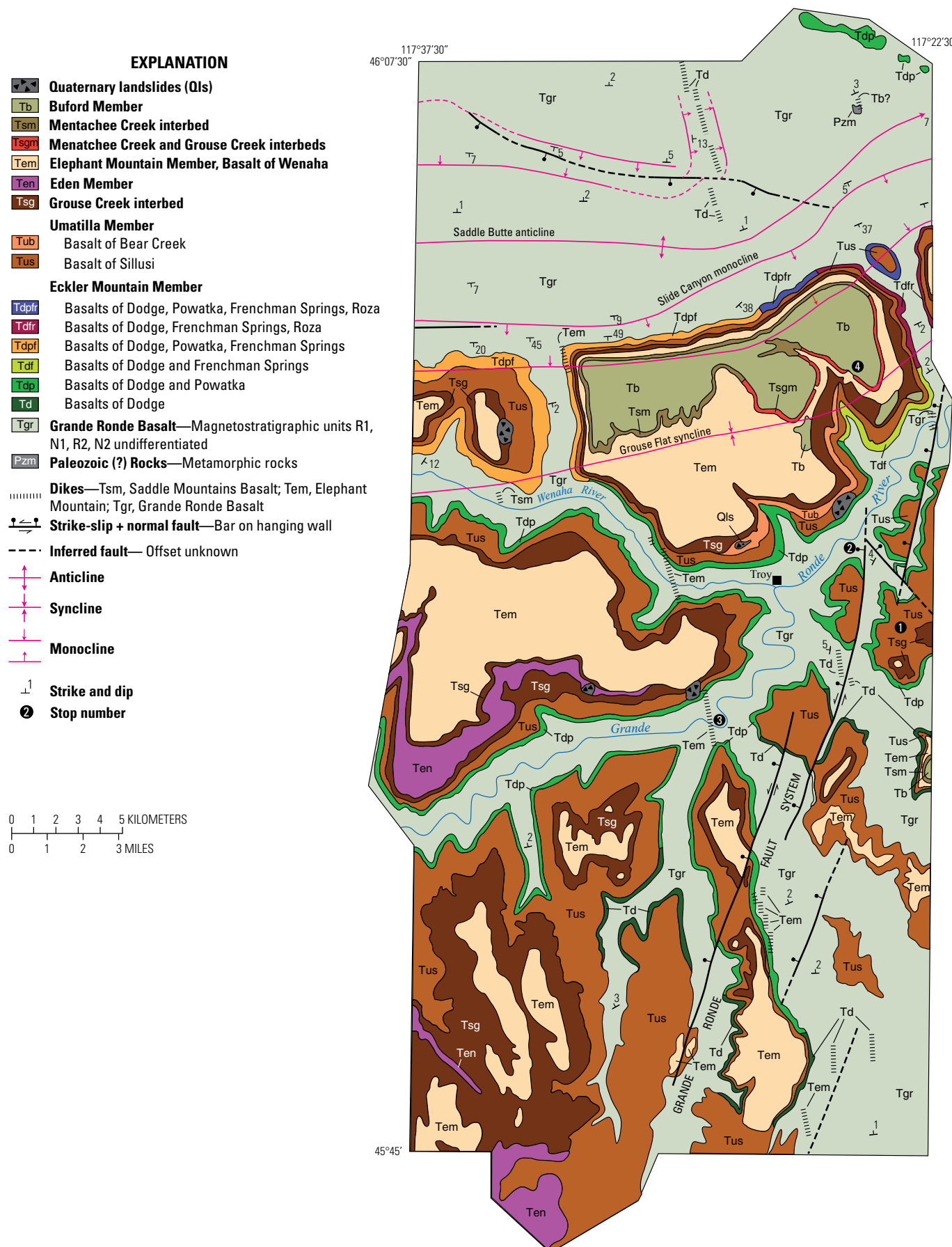


Figure 28. Geologic map of the Troy, Oregon area (after Ross, 1978, 1989).

FORMATION	MEMBER, FLOW, INTERBED
Saddle Mountains Basalt	Buford Member
	Menatchee Creek interbed
	Elephant Mountain Member Wenaha flow (N)
	Eden flow (N)
	Grouse Creek interbed
	Umatilla Member Bear Creek flow (N) Sillusi flow (N)
Wanapum Basalt	Roza Member (T) Basalt of Powatka (N) Frenchman Springs Member (N) Eckler Mountain Member (N) Basalt of Dodge
	Squaw Canyon interbed
Grande Ronde Basalt	As many as 23 flows in Troy area

Figure 29. Stratigraphic chart for the Troy area. N, normal magnetic polarity; T, transitional magnetic polarity. Grande Ronde flows encompass the R1, N1, R2, and N2 magnetostratigraphic intervals with the R1 interval observed only in the extreme northwestern part of the area where it is exposed low in the hanging wall of a normal fault.



Figure 30. Photograph from Stop 2 looking azimuth 330° across the Grande Ronde River 3.6 km northeast of Troy. A, basalt of Troy flow (Grande Ronde Basalt); B, basalt of Dodge flow (lowest Wanapum Basalt); C, basalt of Powatka flow (Wanapum Basalt); D, Frenchman Springs Member (covered, Wanapum Basalt); E, flow of Sillusi (Saddle Mountains Basalt, Umatilla Member); F, flow of Bear Creek (Umatilla Member); G, flow of Wenaha (underlain by Grouse Creek sedimentary interbed); H, Buford member (youngest of Saddle Mountains flows in area). The river follows the Courtney Creek Fault in the lower right corner. The fault shows both left lateral and normal offsets, measured on two dikes and a flow of Dodge respectively. The river is at elevation 488 m and the top of the section is at 1,070 m.

between two of the strike-slip faults where they cross Mud Creek (fig. 28; Ross, 1978). The large lateral gaps between each en echelon segment and their rotation relative the trend of the dike indicates intrusion into fault-related extension gashes rather than segmentation characteristic of dikes in general. Normal movements within the system occurred upon relaxation in the shallow crust following cessation of CRBG volcanism in the area. **1.6**

48.4 Cross bridge over Grande Ronde River and turn left. **1.7**

50.1 Cross bridge over the Wenaha River in Troy. **7.0**

57.1 STOP 3-D4: Flow of Wenaha (Elephant Mountain Member) dike at bridge over Grande Ronde River (45.899667° N, 117.482455° W). A vertical, N10°W trending dike of Wenaha chemistry ($TiO_2 > 3.00$ weight percent) and petrography attains a thickness of 30 m at Stop 3-D4 (fig. 31). Its greatest measured thickness is at least 57 m and possibly 79 m at its southernmost exposure in Mud Creek (fig. 28), making it one of the thickest reported Columbia River Basalt dikes. It extends 32 km north-northwest from its southernmost exposure in Mud Creek to Crooked Creek where it thins to 6.7 m, and appears to terminate at the Slide Canyon monocline (fig. 28).

The dike and flow have identical petrography and chemical compositions distinct from other flows and dikes in the area. Both contain more than 3.00 weight percent TiO_2 , are medium-grained, mostly equigranular, and average less than 2 volume percent plagioclase phenocrysts. Both contain orthopyroxene, more than 2 volume percent olivine, and abundant elongate blades and needle-shaped microphenocrysts of ilmenite. Thin reaction rims of clinopyroxene on orthopyroxene microphenocrysts in the chilled margin of the dike indicate early stage crystallization and resorption of orthopyroxene.

Plagioclase anorthite content in the dike was determined by electron microprobe. The average microphenocryst compositions are $An_{60.1}$ for grain cores and $An_{52.3}$ at their edges, reflecting normal oscillatory zoning. Plagioclase anorthite content of microphenocryst cores decreases by 2.9–5.3 percent from the margin of the dike to its center, whereas the anorthite content of grain margins decrease by 13 percent. Both trends were produced by fractional crystallization during dike intrusion (Ross 1978, 1983).

Chemical variations across the Wenaha dike and three other dikes, including two Dodge dikes, show that chilled dike margins are slightly enriched in felsic components and incompatible elements (SiO_2 , P_2O_5 , TiO_2 , Ba, and K_2O) and depleted in MgO and FeO compared to dike interiors (Ross, 1983). At three sampling stations, SiO_2 decreases as much as

1.13 percent from the margin of the dike to its center, while MgO increases as much as 0.51 percent. This inward felsic to mafic chemical trend is opposite to the plagioclase fractionation trend described above, from more calcic at dike margins to more sodic at dike centers. These chemical trends can best be explained by the relative enrichment of silica and incompatible elements in glass with which they vary sympathetically. **7.0**

64.1 Turn right at Troy and continue east on Troy River Road. **5.6**

69.7 Left onto Grouse Creek Road. **3.4**

73.1 STOP 4-D4: Intracanyon and invasive phases of the flow of Wenaha (Elephant Mountain Member) (Grouse Creek: 46.005007° N, 117.416633° W). The flow of Wenaha (Elephant Mountain Member) is the thickest flow in the area (as much as 146 m [479 ft]), having been fed by the dike seen at Stop 3-D4. Over most of the area it occurs as a sheet flow with a well-developed basal colonnade and thick, spectacularly jointed entablature. It is largely confined to the axis of the Grouse Flat syncline (fig. 28) where it forms prominent cliffs along the margins of Grouse Flat (fig. 27). It also forms isolated hills and ridge tops south of the Grande Ronde River and across the Grand Ronde Fault System, reflecting thinning and erosional stripping from the limb of the syncline.

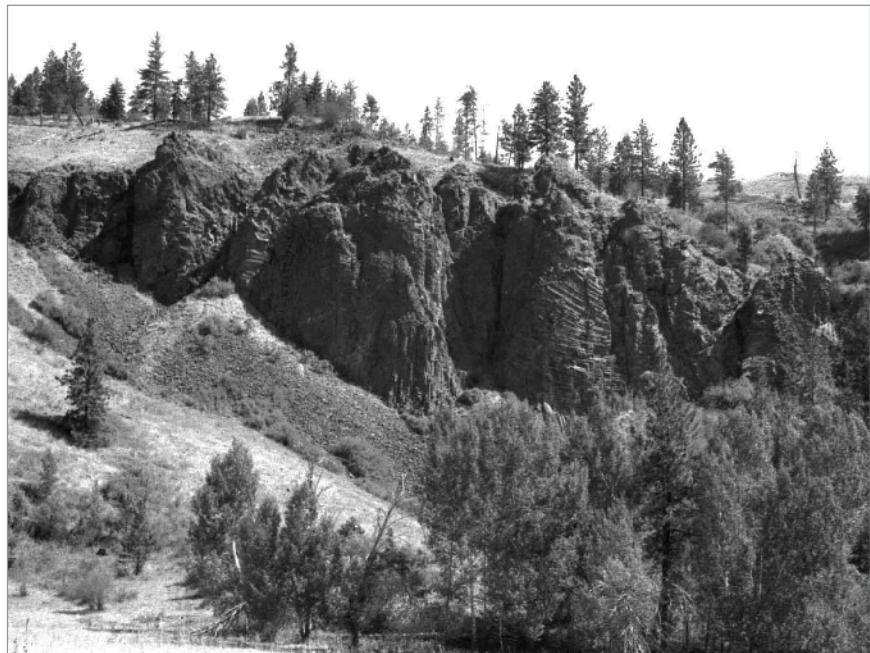
The flow of Wenaha erupted onto the Grouse Creek sedimentary interbed as a subaerial sheet flow that spread east and west from the dike (fig. 28). After advancing 7 km eastward it burrowed into the thick, underlying Grouse Creek sedimentary interbed to form an invasive flow. At nearly the same point, the invasive phase encountered the head of a shallow, east-west-trending, narrow valley eroded into the interbed. The flow exited into the head of the valley to form an intracanyon flow that continued eastward, filling the valley to a depth of at least 76 m (250 ft) (fig. 32). Elsewhere to the north and south, the main body of the invasive phase advanced eastward at a slower pace than the intracanyon phase. Both of these phases are present at Stop 4-D4.

Here, the intracanyon phase forms a prominent, 76-m-high cliff consisting mostly of the spectacularly jointed entablature (fig. 32). The basal colonnade is almost entirely covered in talus. Immediately to the northwest and southeast of the exposure (to left and right of fig. 32) the invasive phase of the flow lacks an entablature, making it more sill-like. At least one thin (30 cm) dike northwest of the intracanyon exposure can be seen extending several meters up from the top of the invasive phase and into the overlying sedimentary interbed. About 1.3 km southeast of Stop 2-D4, joint surfaces several meters above the base of the invasive



Figure 31. Photograph looking azimuth 350° over Stop 3. The feeder dike for the flow of Wenaha (Elephant Mountain Member) is exposed in the north wall of the canyon where it crosses the Grande Ronde River approximately 11 km upstream from Troy. The dike is 30 m thick where it is exposed at the right end of the bridge. The dike exhibits two right-lateral en echelon offsets visible in the canyon wall. Both the flow and dike are characterized by TiO_2 contents in excess of 3.00 weight percent.

Figure 32. Photograph looking azimuth 050° showing the intracanyon phase of the flow of Wenaha at Stop 4 above Grouse Creek. The entablature of the flow forms most of the outcrop, with the top of the basal colonnade barely visible behind the tops of the trees in the foreground. To the right and left of this outcrop the flow is invasive within the Grouse Creek sedimentary interbed. Where invasive, the flow lacks an entablature and columnar jointing is less pronounced in the basal colonnade. To the left and right of this outcrop, thin dikes extend from the flow up into the overlying interbed.



phase are coated with sand injected upward from the underlying wet sediments.

The subaerial sheet phase of the Buford Member flow overlies the Mentachee Creek sedimentary interbed atop the flow of Wenaha at Stop 4-D4, but elsewhere forms intracanyon phases or invades the Grouse Creek sedimentary interbed beneath the Wenaha flow (Stoffel, 1984; Ross, 1989). The Buford Member flow has reversed magnetic polarity, whereas the Wenaha flow has normal polarity. **3.4**

- 76.5 Return to Junction of Grouse Creek Road with Troy River Road. Turn left onto Troy River Road. **1.3**
- 77.8 Washington State line. Troy River Road becomes Grande Ronde Road. **0.2**
- 78.0 Two dikes of Grande Ronde Basalt exposed at river level across Grande Ronde River. **0.9**
- 78.9 Menatchee Creek. **1.8**
- 80.7 A thick, rubbly-topped flow of Grande Ronde Basalt R2 MSU (Troy flow of Ross, 1978) forms thick exposures above the road. The Troy flow (Ross, 1978) is as much as 102 m thick, with at least half consisting of a rubbly flow breccia in its upper part, making it readily recognizable in the field. It tends to be thickest within the core of the Grouse Flat syncline. The high SiO₂ content (55.26 weight percent) of this lava and presence of orthopyroxene indicate it is a basaltic andesite. **6.0**
- 86.7 A dike of Grande Ronde Basalt is exposed as en echelon

segments in the slope above the road. Note the well-developed columnar jointing. En echelon offsets are a common feature of dikes worldwide. They often reflect the deeper magma in a parent dike encountering a rotated stress field as it approaches the surface. As a result the parent dike rises as rotated en echelon segments. **0.2**

- 86.9 Junction of Grande Ronde Road and S.R. 129. Turn left onto S.R. 129. **0.1**
- 87.0 Dike of R2 Grande Ronde Basalt at 9:00. **0.8**
- 87.8 Mazama ash at 9:00. This is an airfall deposit from the eruption of Mount Mazama ~7,700 years ago that included collapse to form Crater Lake (Bacon and Lanphere, 2006). **0.5**
- 88.3 Bend in road. At 0:00 note the breccia zone that traces a fault (about 30 m wide) striking northwest with mainly horizontal movement. The brecciated flow-top back to the south marks the top of N1 Grande Ronde Basalt that may have as little as 1 m of vertical offset. We will pass this fault as we continue up Rattlesnake Grade. **1.2**
- 89.5 **STOP 5-D4: Roza Member dikes** (46.045640° N, 117.238806° W). Park on the gravel on the west side of the road, 300 m (980 ft) to the north of the fourth hairpin (coming from the south). To the east of the road there is a fantastic view down to the Grande Ronde River and Roza Member dikes can be seen in the river gorge. At this stop Roza Member dikes are exposed in the roadcut on the west side of the road. Roza Member dikes are distinctive due to their

geochemistry and the presence of large plagioclase phenocrysts. They outcrop intermittently for 80 km between the Snake River, Washington, and Crow Creek, Oregon. Individual dikes strike N30°W–N33°E, with an overall trend of ~N17°W. Dikes range from 0.13–10 m thick, with a thickness mode of ~2 m. At any one location, as many as 2–16 dikes may be present within zones 25–425 m wide. There is an estimated 20–120 km³ of magma frozen within the Roza Member dike swarm. Proximal pyroclastic deposits along the northern segment of the Roza Member dike/vent system are discussed in the Day 5 description of the field guide.

At Rattlesnake Grade, Roza Member dikes form a composite dike complex (figs. 33, 34). Many of the dikes are intruded next to each other. The dikes are exposed at paleodepths of 300–600 m and cut through rubbly-topped pāhoehoe lavas of the Grande Ronde Basalt. They are commonly sinusoidal, pinch, swell, and bifurcate irregularly, and their margins are strongly controlled by joint patterns in the host lavas. The dikes exhibit thin brown-glassy margins which

show sparse, horizontally oriented pipe-vesicles, each typically <5 mm long. Almost all Roza Member dikes show banded vesicular margins that each consist of as many as eighteen 1–10 cm-thick bands defined by alternating vesicular and nonvesicular zones (fig. 34). The bands become less well-defined inwards toward a middle zone, which can be dense or vesicular.

There are more outcrops of dikes farther down the road in cuts along the lower hairpin bends. Watch for traffic. Farther north along the road, several faults are visible that are related to the fault described at mile-marker 88.3. **3.9**

- 93.4 Fault at 3:00, north of side road. **2.2**
- 95.6 Base of the Meyer Ridge member (Grande Ronde Basalt) R2 MSU. **0.1**
- 95.7 Red oxidized zone with saprolite above. **0.2**
- 95.9 Umatilla Member and Puffer Butte, the volcano for the Umatilla Member. **0.3**



Figure 33. Photograph of the undulatory Roza Member dike margin exposed parallel to roadcut at Rattlesnake Grade. Smooth areas are the thin glassy margins of the dike.



Figure 34. Photograph of the Roza Member dike exposed along Rattlesnake Grade showing marginal banded zones and columnar joints. Dike has intruded into rubbly pāhoehoe of the Grande Ronde lavas.

- 96.2 Fields Spring State Park. **0.4**
- 96.6 Park Road. Turn right. Umatilla Member on left. **0.6**
- 97.2 At 3:00 is the road to Fields Spring Park. **0.3**
- 97.5 Park Camp. **0.2**
- 97.7 **Stop 6-D4: Puffer Butte** (46.067610° N, 117.171096° W). Puffer Butte is the best-exposed vent for the Umatilla Member. The Umatilla Member is the oldest member of the Saddle Mountains Basalt and is one of the most distinct of the CRBG. It was first recognized by Laval (1956), who described two flows from the McNary Dam area in south-central Washington, the younger flow of Sillusi and the older Umatilla flow. Ross (1978, 1989) described a third, very localized cooling unit in the Troy Basin of Oregon, the Bear Creek flow, which is of similar composition to and overlies the Umatilla flow.
- The Umatilla Member covers 15,110 km² and has a volume of 720 km³ (Tolan and others, 1989; Reidel and others, 2013a). The Umatilla Member flows are some of the most physically distinct flows of the CRBG; they are very glassy to fine-grained pāhoehoe flows containing sparse microphenocrysts of plagioclase and olivine. Rare silicic xenoliths occur in the flows in the Pasco Basin. The flows are typically simple sheet flows dominated by small, entablature jointing except along their distal margins. Throughout the extent of the Umatilla Member, both flows typically are more than 90 percent entablature. Flow tops are typically very thin (<5 m).
- The chemical composition of the Umatilla Member is unique for the CRBG, with some of the most evolved trace-element contents of any CRBG flow (Swanson and others, 1979; Hooper, 1985; Wright and others, 1989; Hooper and others, 1995; Reidel, 1998), and with the highest SiO₂ composition of any CRBG flow, from 53 to 58.5 percent (Reidel, 1998; Hooper, 2000). The high SiO₂ content is accompanied by low MgO and CaO concentrations. In addition, the flows have high P₂O₅ concentrations (~1 weight percent) and the highest Ba concentrations (>3,000 parts per million) of any CRBG flow.
- The high SiO₂ is probably the result of crustal contamination (Hooper and others, 1995) as suggested by quartzite xenoliths found in a drill core in the Pasco basin (Reidel and others, 1989a; Reidel, 1998). In addition to the evolved trace-element character of the Umatilla Member, the isotopic data are also consistent with crustal contamination. The unit has ⁸⁷Sr/⁸⁶Sr of 0.7089, εNd of -7, Δ¹⁸O of 6.8, and extraordinarily elevated ²⁰⁷Pb/²⁰⁴Pb and ²⁰⁸Pb/²⁰⁴Pb, consistent with an age of 2.5 Ga for the source component of contamination (Carlson and others, 1981; Carlson, 1984).
- The dike that feeds Puffer Butte is primarily Sillusi in composition (fig. 35). The selvage zones and margins are typically Sillusi-dominated, but the more central-zone compositions, together with a few selvage compositions, deviate toward the Umatilla composition. Samples of predominately Umatilla composition have not been found in the dike. These data suggest that limited mixing between the two compositions might have occurred in the magma chamber before the flow of Sillusi erupted. **1.1**
- 98.8 Return to S.R. 129. **0.7**
- 99.5 Summit. Here a flow of Weissenfels Ridge Member (flow of Tenmile Creek; at 3:00) is overlain by the Buford Member on left and farther ahead. **1.3**
- 100.8 Right on Montgomery Ridge Road. **0.7**
- 101.5 Flow of Tenmile Creek on left. **0.3**
- 101.8 Schumaker Road, turn right. Road has dropped through the flow of Tenmile Creek and is now on the flow of Cleveland (Weissenfels Ridge Member). **0.0**
- 101.8 Only a few hundred feet ahead, Schumaker Road is now on the flow of Slippery Creek (Weissenfels Ridge Member). We will be on this unit predominantly, until the road descends into the Montgomery Gulch. **1.3**
- 103.1 At 2:30 is an excellent view of the shape of Puffer Butte, the Umatilla vent. **1.1**
- 104.2 Weissenfels Ridge Road. **4.1**
- 108.6 Weissenfels Ridge Road junction, stay right toward Snake River. **3.7**
- 112.3 Road junction, turn left toward Snake River Road. Begin to descend grade. On the grade below we will pass through the flow of Slippery Creek and then the flow of Tenmile Creek, both of the Weissenfels Ridge Member; they are separated by a thin interbed. The next flow down is the Asotin Member, which is marked by a flow-top breccia. Below the Asotin is the Umatilla Member, which overlies the R2 Grande Ronde Basalt. **0.3**
- 112.6 Flow of the Weissenfels Ridge Member. **0.2**
- 112.8 Asotin Member. **0.5**
- 113.3 Landslide. **0.6**

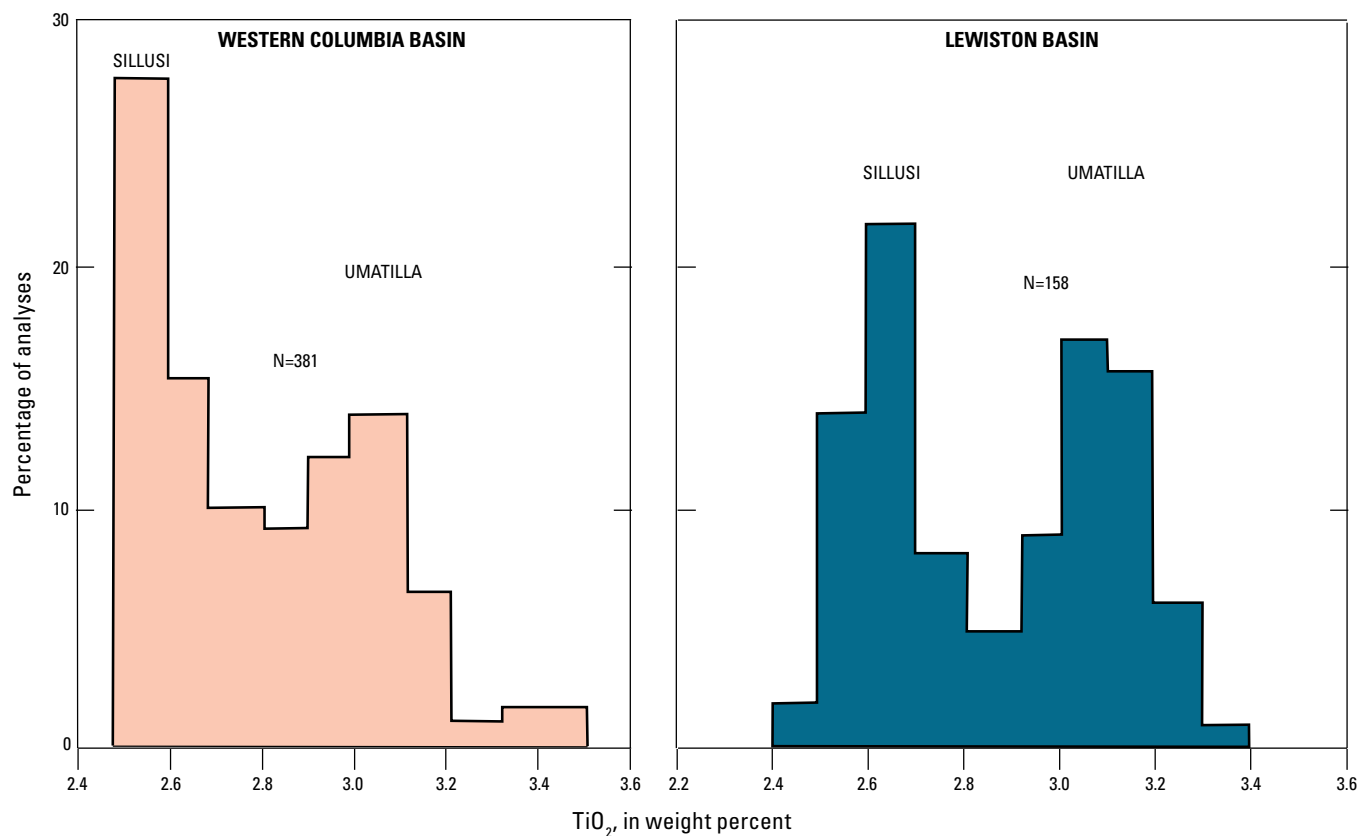
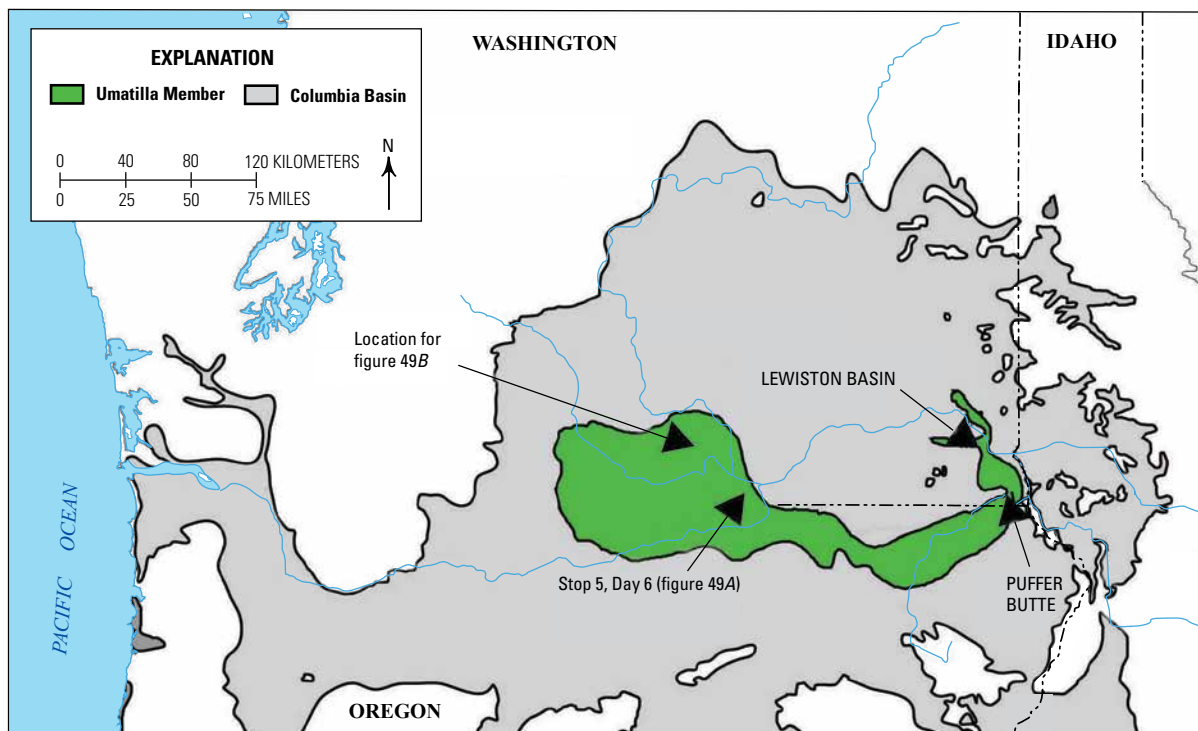


Figure 35. Map showing the extent of the Umatilla Member. Histogram shows that the Lewiston Basin and Columbia Basin have both eruptive units, the Umatilla Member and flow of Sillusi, yet in the Columbia Basin there is mixing of both flows as documented by Reidel (1998).

- 113.9 Out of landslide and into R2 Grande Ronde Basalt. **1.2**
- 115.1 R2/N1 Grande Ronde Basalt contact. **1.4**
- 116.5 Mazama ash in creek for several miles. **0.7**
- 117.2 Road mile marker 3. **2.2**
- 119.4 N1/R1 Grande Ronde Basalt contact. **0.8**
- 120.2 Junction with Snake River Road. Turn right. **4.4**
- 124.6 Pre-Columbia River Basalt Group basaltic andesite. **3.9**
- 128.5 Limekiln Fault across river at 3:00. Note pre-CRBG metasediments and metavolcanics on either side of the fault. **0.5**
- 129.0 Heller Bar. **0.9**
- 129.9 Confluence of Snake and Grande Ronde Rivers. **2.1**
- 132.0 **Stop 7-D4: Contact between the Imnaha Basalt and the Grande Ronde Basalt** (46.074864° N, 116.990323° W). The differences between the Grande Ronde Basalt and the Imnaha Basalt are very apparent at this locality. Although the compositions are very different, this contact suggests very little time between eruptions. Paleomagnetic polarities for the Imnaha Basalt are normal but the overlying Grande Ronde Basalt is transitional in this flow and become reversed above (R1 MSU). The type section for the Grande Ronde Basalt is a few miles down the road where the R1, N1, and R2 MSUs are present. The younger N2 is farther north in the Lewiston Basin and beyond. **0.7**
- 132.7 On the opposite side of the Grande Ronde River is a slope of poorly exposed Imnaha Basalt. The road is in the R1 MSU of Grande Ronde Basalt. **2.0**
- 134.7 Bridge over Grand Ronde River. We will be going through one of the spectacular meanders that give the Grande Ronde River its name. The canyon wall to the west, on the north side of the Grande Ronde River, is the type locality of the Grande Ronde Basalt. Ahead are flood deposits from the cataclysmic floods of the Pleistocene. **0.1**
- 134.8 Notch in meander. Road descends through the Imnaha Basalt with flood deposits on top. Road will leave the Grande Ronde River valley and follow Joseph Canyon. **0.8**
- 135.6 Pleistocene Bonneville flood gravels. **1.8**
- 137.4 Bridge over Joseph Creek. **0.1**

137.5 Stop 8-D4: Dike-vent complex of the Joseph Creek flow, Teepee Butte Member, Grande Ronde Basalt (R1 MSU) (46.041387° N, 117.001558° W). This stop affords the opportunity to see one of the best-preserved vent/dike complexes for the Grande Ronde Basalt (fig. 36); please do not attempt access without the owner's permission. This complex has been described by Reidel and Tolan (1992) and is summarized here.

The Joseph Creek dike is typical of other dikes in the Chief Joseph dike swarm. About 3 km of a nearly continuous basalt dike is exposed in Joseph Canyon. For 300 m on the south side of Joseph Creek, however, the dike forms a series of en echelon segments that trend from N16–18°W to nearly north-south (fig. 37B).

On the north side of Joseph Canyon, the dike can be traced from just above Joseph Creek into a vent complex (fig. 36). The lower part of the dike (where it cuts the Imnaha Basalt) is relatively narrow, averaging about 7 m in width. Here, the dike displays well-developed horizontal columnar joints (column diameter <0.3 m) and has a fine-grained texture. The dike margins are marked by a narrow, 1–5 cm-wide, glassy selvage accompanied by several dike-parallel vesicle layers. Narrow vesicular zones (<1 cm) occupy the center of the dike.

The dike passes through three flows of the Grande Ronde Basalt, two belonging to the Buckhorn Springs member and one belonging to the flow of Limekiln Rapids (Teepee Butte Member). The dike widens from 40 m at the base of the Limekiln Rapids flow to more than 150 m at the paleoground surface. Outwardly, the jointing of the basalt filling this part of the fissure resembles a normal blocky to columnar pattern, typical of basalt flows in the area. The texture coarsens from medium-grained near the margins to nearly diabasic in the central part, which we interpret to be a lava pond.

Dike composition is relatively uniform, but compositionally evolved compositions occur in the selvage zone and probably represent the first erupted lava (fig. 38). No flows with this composition have been found in the Grande Ronde Basalt, suggesting that it represents only a minor volume of lava from the initial eruption.

The vent ramparts (tephra complex; fig. 36) are asymmetrical with the western rampart composed only of lava flows, and the eastern rampart nearly 30 m higher and composed of interbedded tephra and lava flows. There are two types of pāhoehoe flows in the vent ramparts: spatter-fed pāhoehoe and shelly pāhoehoe (fig. 37A). Within the vent complex is a collapse breccia that lies between the eastern margin of the lava pond and fissure wall (fig. 37C); it is composed of angular



Figure 36. Photographs showing the vent complex for the flow of Joseph Creek, Teepee Butte Member. B–B' is the location of figure 38. Inset is a close-up view of the tephra complex. Note tip to left of tephra complex into lava pond; extensional fractures or cracks are vertical lines in tephra. See Reidel and Tolan (1992) for detailed descriptions.

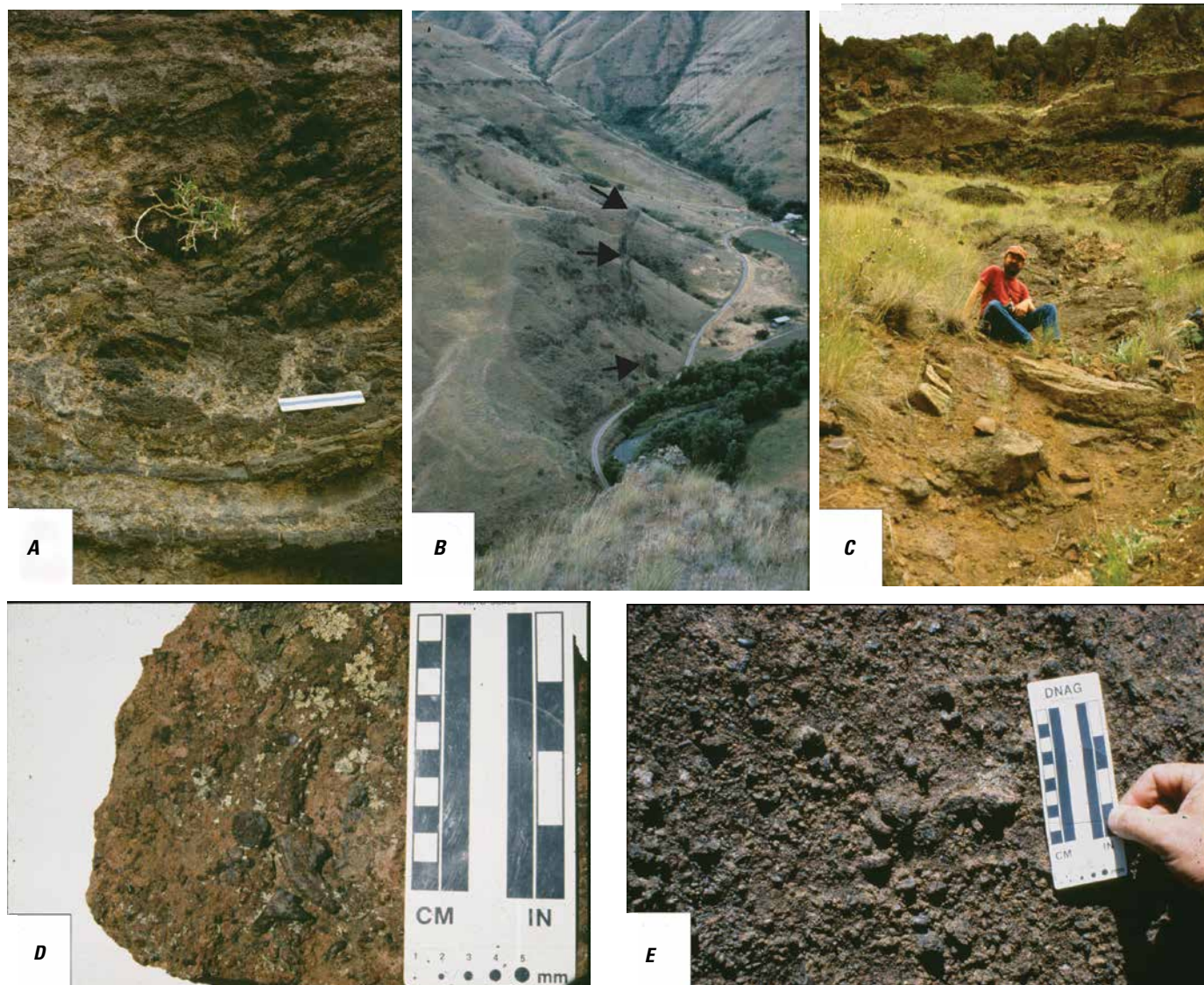


Figure 37. Photographs of the major features of the flow of Joseph Creek vent complex. *A*, Shelly pāhoehoe flows from tephra complex (fig. 36 inset). *B*, Flow of Joseph Creek dike on east side of Joseph Creek. The dike at this location is en echelon at the road and appears to bend slightly. *C*, Collapse or flow-back breccia adjacent to lava pond (fig. 36 inset). *D*, Ribbon bomb in flow of Joseph Creek vent complex. *E*, Pele's tears in flow of Joseph Creek vent complex (fig. 36 inset).

clasts, ranging from several centimeters to more than 1 m. Tephra in the eastern rampart consists of ash- to bomb-size clasts, with the larger clasts (bombs; fig. 37D) proximal to the vent. The most notable aspect of these deposits is the abundance of coarse ash- to lapilli-size Pele's tears (fig. 37C); this is the first reported locality of such pyroclasts in a Grande Ronde Basalt vent (Reidel and Tolan, 1992).

The lower 10 m of the east rampart adjacent to the fissure is tilted several degrees toward the lava pond, and is cut by numerous extension cracks (fig. 36) that opened prior to the last episode of fountaining and were filled by tephra.

Joseph Creek vent deposits are indicative of a Hawaiian-type eruption. Fountaining and effusion

of lava were important parts of the eruptive process. Thick pyroclastic deposits are found only in the eastern rampart, and prevailing westerly winds probably influenced deposition. However, the west side is downslope; any tephra deposited to the west could have been either rafted or bulldozed, and swept away by erupting lava.

Evidence suggests that eruptive activity waxed and waned at the vent locality. At least four major episodes of lava fountaining are preserved at the vent, one in the collapse breccia and three in the east rampart. Each episode erupted thin pāhoehoe flows accompanied by tephra mainly composed of Pele's tears. The tephra deposits and spatter-fed pāhoehoe flows offer direct evidence of repeated fountaining.

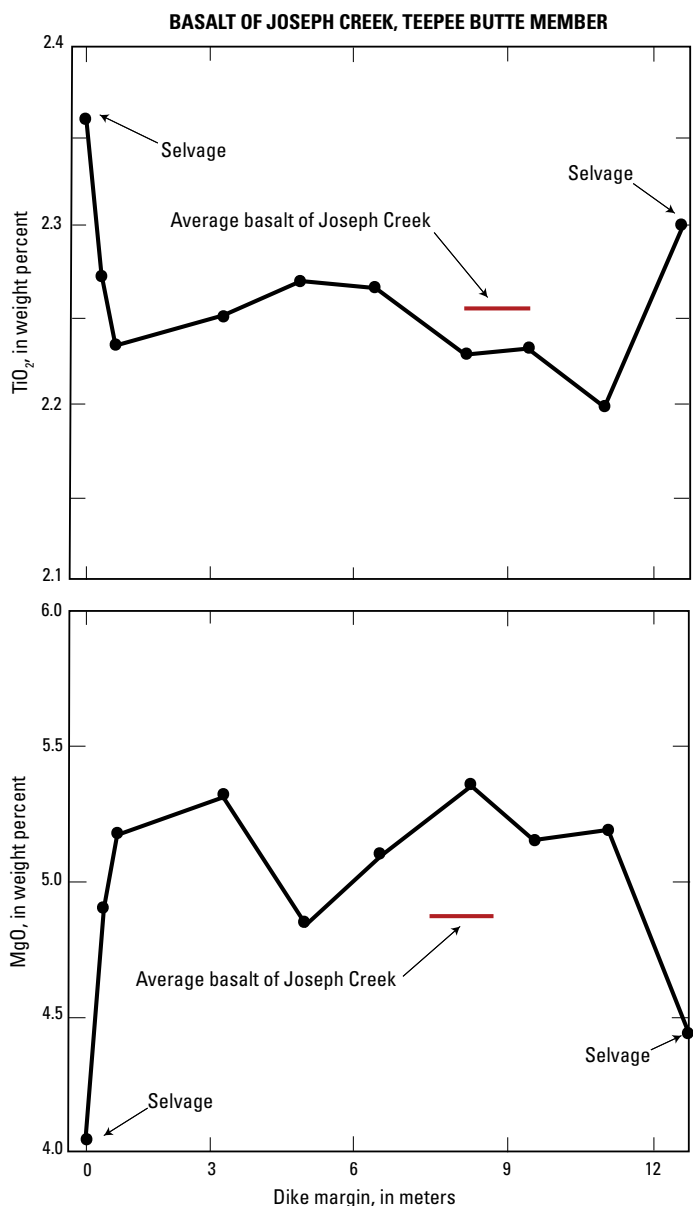


Figure 38. Compositional variations across flow of Joseph Creek dike section B–B' (fig. 36), Teepee Butte Member vent complex.

The final event at the Joseph Creek vent was the formation of a lava pond. The lava pond stands at the same level as the ground surface during Joseph Creek time, yet the unique chemical composition of the lava pond has not been found in vent deposits or basalt flows of the R1 MSU. We infer that no lava flows were erupted from the pond after the change in composition.

Solidification of the lava pond within the Joseph Creek fissure marked the end of Joseph Creek volcanism at this locality. The surface of the lava pond had solidified and stabilized prior to emplacement of the Pruitt Draw flow so that a period of several years separated these eruptions. The Pruitt Draw flow only partly inundated the Joseph Creek vent; it filled the low area between the two ramparts

and caused minor deformation of the eastern rampart.

17.4

Turn around and retrace route.

154.9 Grouse Creek Road (Montgomery Ridge Road). **4.5**

159.4 Road is on N1 Grande Ronde Basalt. Weissenfels Ridge Member dike at 12:00. Elephant Mountain Member intracanyon complex on side of ridge at 1:00. **2.8**

162.2 Bridge. Pomona Member intracanyon flow high on ridge at 9:00. **0.5**

162.7 Elephant Mountain Member intracanyon complex at 2:00. **2.6**

165.3 Excellent exposures of intracanyon Pomona and Elephant Mountain Members on ridge at 3:00. **0.5**

165.8 City of Asotin. **0.5**

166.3 **Stop 9-D4: Ancestral channel of the Clearwater River and intracanyon flows** (46.336929° N, 117.027701° W). On the east side of the river are a series of unusual looking CRBG flows, with well-developed lower colonnades and relatively thick entablatures. These are intracanyon flows of the Pomona and Elephant Mountain Members exposed in a natural cross-section through the canyon of the ancestral Clearwater River. The channel is well exposed on the south side of the exposure where these intracanyon Saddle Mountains Basalt flows overlie N2 Grande Ronde Basalt. These flows can be traced southward intermittently along the Idaho side for about 5 mi (Kauffman and others, 2009). The 9 million year time range of the Saddle Mountains Basalt eruptions (from around 14.5 to 5.5 Ma) was a period of waning volcanism, with the time interval between successive flows often exceeding 1–2 million years, enough to allow erosion of stream channels and even canyons. Several Saddle Mountains flows that erupted in the eastern part of the Columbia Embayment were transported westward down the ancestral Clearwater and Snake River canyons. **0.6**

166.9 Stop sign. Junction with S.R. 129. Continue straight. **0.8**

167.7 Swallow Rock at 2:00. Intracanyon Pomona and Elephant Members. **1.8**

169.5 Base of Swallow Rock. Last exposures of Grande Ronde Basalt. **1.9**

171.6 Bypass to Lewiston Airport. **1.7**

173.3 Junction of S.R. 129 and U.S. 12 in Clarkston.

Day 5 Overview—Proximal Pyroclastic Deposits of the Roza Member

The majority of outcrops in this day's road log (fig. 39) allow examination of the proximal pyroclastic deposits of the Roza Member eruption (Brown and others, 2014). Before ending the day in Tri-Cities, Washington, the final stop will be an examination of intracanyon lavas of the Salmon-Clearwater River system near Lower Monumental Dam, Washington (Swanson and Wright, 1976, 1981).

The Roza Member is a 1,300 km³ tholeiitic flood-basalt flow field covering ~40,350 km² of southeast Washington and northeast Oregon (fig. 40; Martin, 1989; Tolan and others, 1989; Thordarson and Self, 1996, 1998; Reidel and others, 2013a). Providing an accurate age for the Roza Member (henceforth Roza) has proven difficult. Barry and others (2013) suggested it was erupted at 14.98 Ma, but Baksi (2013) suggest that it is a million years older (15.8 Ma). More recent age determinations on sanidine in silicic ash between Wanapum Basalt members, and thus with smaller errors than ages determined on basalt, indicate that the Roza is more likely around 15.8 Ma in age (Ladderud and others, 2015).

The Roza was erupted from a linear vent system that crops out discontinuously for >180 km from just north of Enterprise in northeast Oregon, to north of Rock Creek in southeast Washington (fig. 40A). South of the Snake River, the vent system is represented by dikes and poorly exposed outcrops of pyroclastic deposits and clastogenic lavas, some in monogenetic shield volcanoes. North

of the Snake River, the vent system is marked by many superb outcrops of pyroclastic deposits and spongy to shelly pāhoehoe lavas (for example, Swanson, 1973; Thordarson and Self, 1996, 1998; Brown and others, 2014).

The Roza pyroclastic deposits are the best-exposed proximal deposits of any known flood-basalt eruption. They provide an opportunity to discuss near-vent processes and eruption dynamics of large volume, long-lived basaltic eruptions. The Roza vent system as a whole is comparable to those of historical basaltic fissure eruptions in Iceland; however, some of the edifices apparently differ from Icelandic spatter or scoria cones in morphology and lithology. The Roza agglutinate cones are characterized by moderate slopes (<20°) and are composed of predominantly welded and agglutinated scoria and spatter layers that extend >500 m from the vent. Brown and others (2014) interpreted them as the products of eruptions characterized by vigorous lava fountaining and strongly convecting plumes that may have periodically reached sub-Plinian intensities.

Day 5—Road Log

- 0.0 Begin on the north side of the Red Wolf Bridge (S.R. 128). Turn right onto Down River Road, which is a continuation of S.R. 128. **1.8**
- 1.8 Enter Lewiston. **2.1**
- 3.9 Turn left to access U.S. 95 north. **0.1**

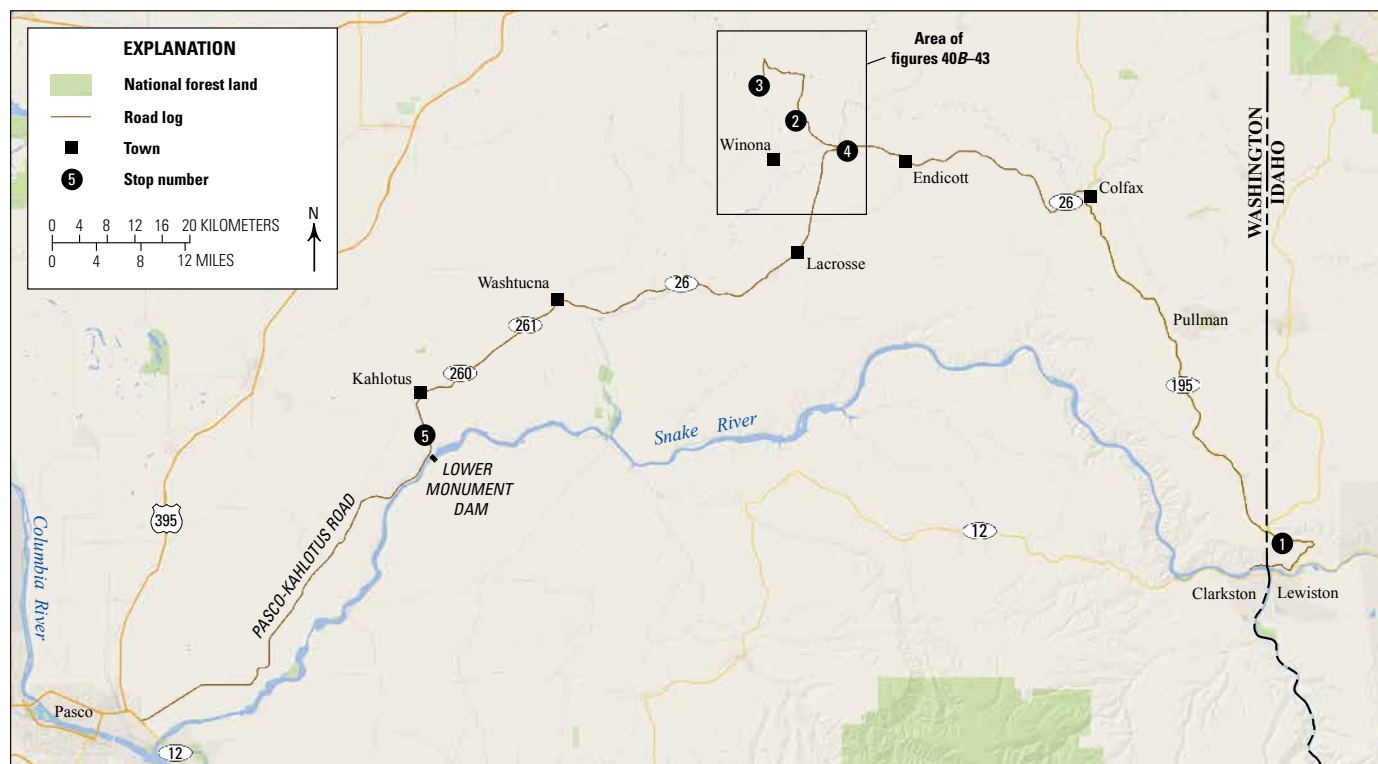


Figure 39. Map of field-trip stops for Day 5.

- 4.0 Enter U.S. 95 north (to Moscow-Pullman). **6.5**
- 10.5 Turn right onto Frontage Road (old Lewiston grade road)

10.5 Stop 1-D5: Overview of Lewiston Basin

(46.461035° N, 117.009638° W). This stop at the top of the Lewiston grade provides an excellent view of the Lewiston Basin, where the confluence of the Snake and Clearwater Rivers forms the lowest point in the state of Idaho at 720 ft (220 m). Structurally, this broad basin is a fault-bounded graben that began to form during emplacement of the CRBG. From this viewpoint, the Vista Fault and “Lewiston structure” form the major structures along the north side of the river, beyond which the Pullman-Moscow plateau stretches farther to the north. The Lewiston structure is a complex faulted anticline with faults along the ridge below us and along the river (Camp, 1976; Camp and Hooper, 1981; Alloway and others, 2013). To the south the Limekiln Fault-Waha monocline forms the other bounding fault. Flows of the CRBG tilt to the north, forming a gentle slope to the Snake/Clearwater Rivers below. Small mounds along this

slope are volcanoes/vents of the Roza Member, Umatilla Member and Elephant Mountain Member, the largest of which is Puffer Butte, which we visited on Day 4.

The uppermost Grande Ronde Basalt flow exposed near the top of the Lewiston grade is MSU R2, overlain by two flows of the Priest Rapids Member of Wanapum Basalt, which in turn are overlain by the Asotin Member of the Saddle Mountains Basalt. An extensive saprolite of residual clay developed at the top of R2 delineates a weathering surface with only local erosion and sedimentation. The saprolite varies in thickness from 5 to 7 m, and marks a significant hiatus between Grande Ronde R2 and the overlying Wanapum Basalt. **0.6**

- 11.1 Exit onto U.S. 195 north to Pullman. **5.7**
- 16.8 Enter Uniontown. **3.3**
- 20.1 Enter Colton. **12.4**
- 32.5 Pullman bypass. Keep left toward Spokane; if you go straight you will go to Pullman. **15.2**

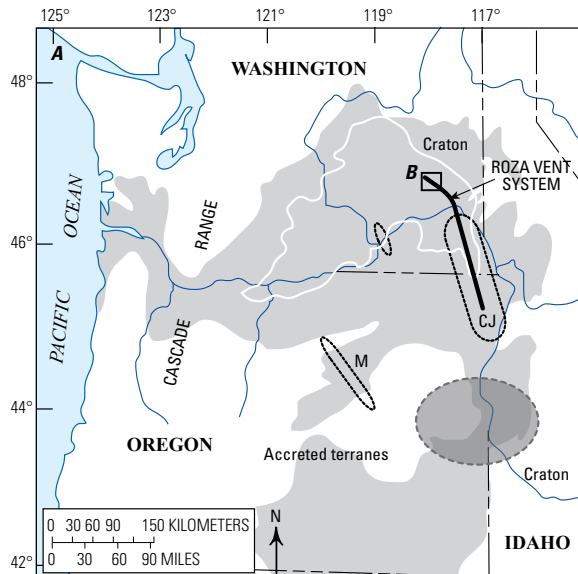
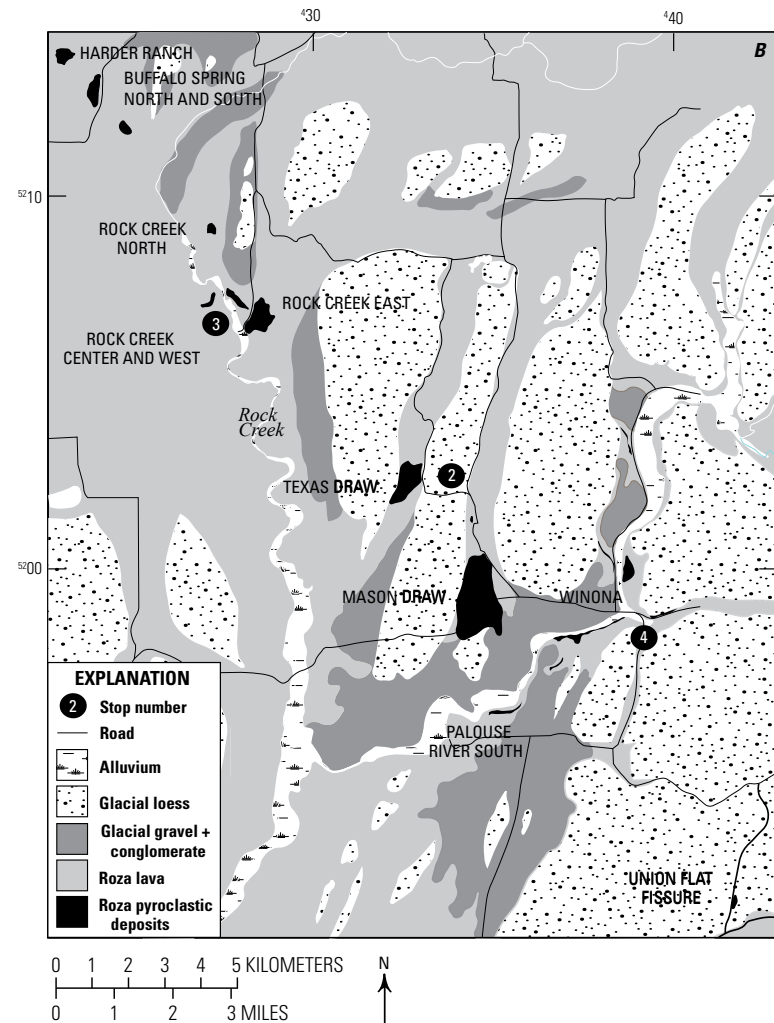


Figure 40. A, Sketch map of the Columbia River flood-basalt province (grey), showing the extent of the Roza Member (solid white line) and the Roza vent system (black solid line). Large grey oval is the inferred position of the Columbia River Basalt Group basaltic magma storage zones/source region according to Wolff and others (2008). Dotted ovals, dike swarms; M, Monument dike swarm; CJ, Chief Joseph dike swarm (including Roza Member dikes). B, Map of the northern end of the Roza vent system showing outcrops of pyroclastic rocks and names of recognized vents. UTM grid zone 11T.



- 47.7 Colfax. U.S. 195 and S.R. 26. This can be confusing. Take the first left across the river, called West Walla Walla Highway. **3.7**
- 51.4 Turn right onto Endicott Road. From this point on, scabland channels carved by the Pleistocene Missoula floods provide the best exposures of the Roza, Priest Rapids, and Asotin Members that are typically covered by a mantle of loess. The stops that we will visit today are exclusively within those flood channels. **15.6**
- 67 Endicott, WA. **5.9**
- 72.9 Winona, WA. **2.0**
- 74.9 Turn right onto Jordan Knott Road. **2.0**
Pyroclastic deposits of the Mason Draw vent segment (fig. 40B) are exposed in the field north of Endicott Road at this junction. These consist of variably dipping, weakly to densely welded scoria and spatter that crop out over an area $>5 \text{ km}^2$. Bedding inclinations and welding fabrics dip $10^\circ\text{--}27^\circ$ mostly to the south, southwest, and northwest, and define an edifice elongated approximately north-south that had a radius of $>500 \text{ m}$. We infer that it built up around a vent located beneath the present valley floor. The edifice is overlain by Roza sheet lobes to the north. The southern end of the Mason Draw edifice is overlain by several meters of thin, spongy, and shelly pāhoehoe lobes that are (poorly) exposed along Endicott Road.
- 76.9 Turn left onto Lamb Road. **0.8**
- 78.1 **Stop 2-D5: Texas Draw pyroclastic edifice** (46.959591° N, 117.862412° W). Stop by the side of road. Examine from a distance the Texas Draw vent area (fig. 41) exposed across the field on the west side of the road, south of Hergert Lake. The pyroclastic rocks here are composed of bedded, weakly to densely agglutinated scoria and spatter exposed over 1.6 km^2 . At the northern end, bedding and welding fabric

orientations define a remnant edifice with slopes dipping $16\text{--}34^\circ$ to the north, west, and south. This was constructed on the western side of an approximately north-south-trending vent that ran along what is now the valley. An eastern counterpart to this edifice is missing and post-pyroclastic Roza Member lavas crop out instead. In detail, the dips and strikes within this edifice are complicated. Dip direction and magnitude change rapidly over distances of tens of meters, and define significant smaller-scale topography. At the southern end of the edifice a 30-m-thick sequence of pyroclastic deposits are exposed. This consists of bedded scoria and spatter that is weakly to densely agglutinated. Several thick beds of densely agglutinated scoria are persistent over hundreds of meters and exhibit columnar joints. The upper $\sim 15 \text{ m}$ consists of densely agglutinated scoria and spatter, and lava-like densely welded spatter. The pyroclastic beds are partly overlain by columnar jointed Roza sheet lobes. **4.2**

- 82.3 Turn left onto Jordan Knott Road. **4.3**
- 86.6 Turn left into Escure Ranch Bureau of Land Management land (rough dirt road). **2.5**
- 89.1 **Stop 3-D5: Pyroclastic deposits of the Rock Creek Center fissure segment** (47.014033° N, 117.946156° W). Parking lot for Escure Ranch and Towell Falls Trailhead. The Rock Creek area hosts superb outcrops of pyroclastic deposits from several vent segments (Brown and others, 2014; fig. 42B,D). Walk north along the eastern side of Rock Creek until you see the large Missoula floods gravel bar and head towards the small shack. The low cliffs behind the shack are the start of the lithologic log in figure 42D.

The $>50 \text{ m}$ -thick sequence of well-preserved pyroclastic deposits drape earlier Roza sheet lobes (fig. 42B,D). The pyroclastic sequence thins southward over the lavas and appears to merge with the pyroclastic deposits of the Rock Creek East vent (fig. 42A). The base of the pyroclastic sequence is marked by 3 m of lava-like densely welded spatter

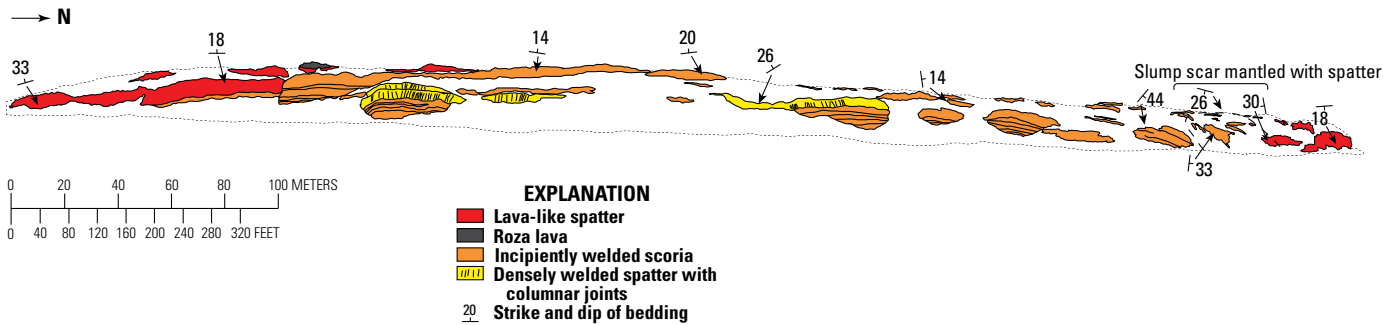
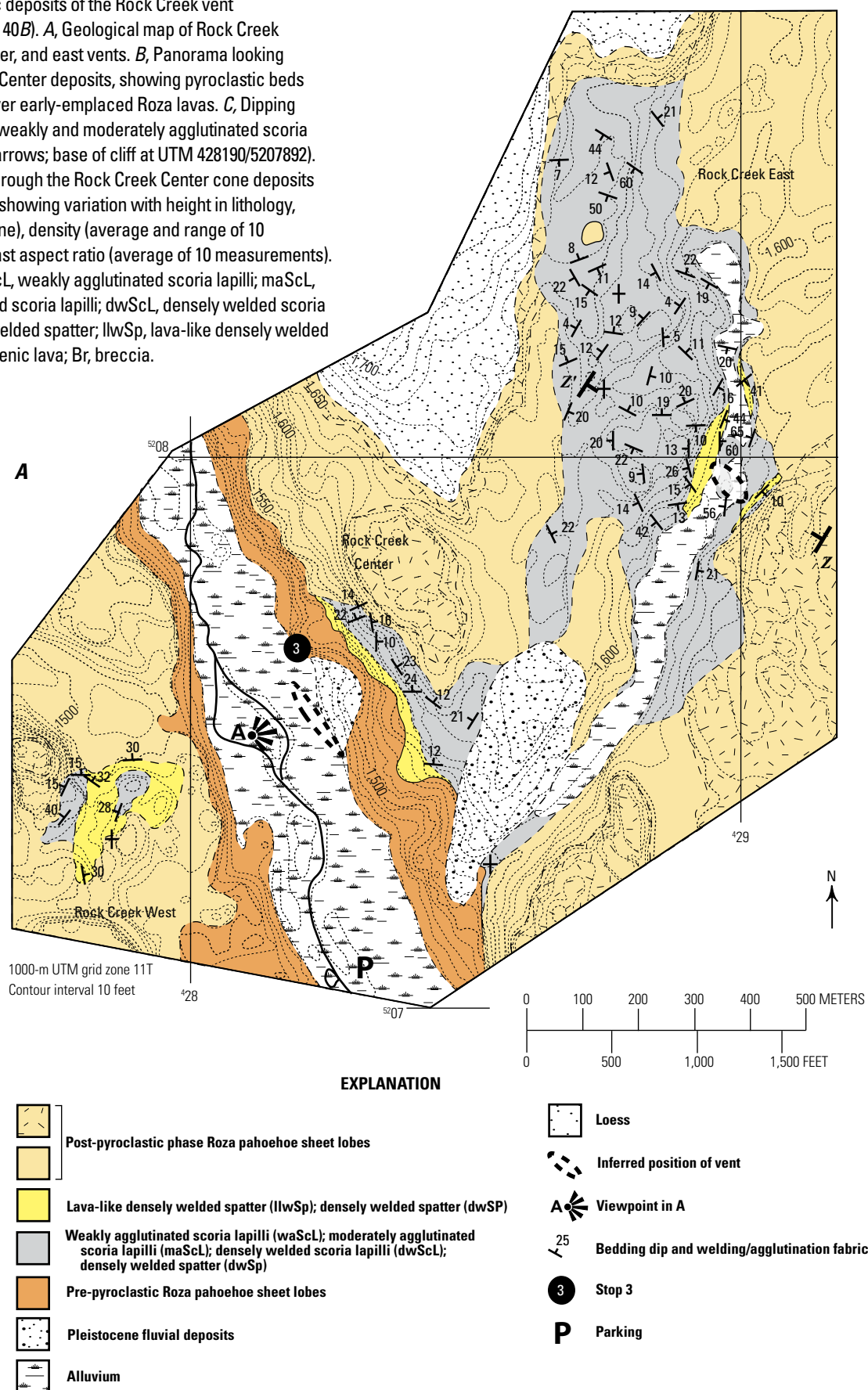


Figure 41. Photo-interpretation of the pyroclastic edifice at the Texas Draw vent (see fig. 40 for location).

Figure 42. Pyroclastic deposits of the Rock Creek vent accumulations (see fig. 40B). A, Geological map of Rock Creek showing the west, center, and east vents. B, Panorama looking east of the Rock Creek Center deposits, showing pyroclastic beds thinning southwards over early-emplaced Roza lavas. C, Dipping beds of predominantly weakly and moderately agglutinated scoria at Rock Creek Center (arrows; base of cliff at UTM 428190/5207892). D, Measured section through the Rock Creek Center cone deposits (UTM 428182/5207894), showing variation with height in lithology, grain size (solid black line), density (average and range of 10 measurements) and clast aspect ratio (average of 10 measurements). ScL, scoria lapilli; waScL, weakly agglutinated scoria lapilli; maScL, moderately agglutinated scoria lapilli; dwScL, densely welded scoria lapilli; dwSp, densely welded spatter; llwSp, lava-like densely welded spatter; clLava, clastogenic lava; Br, breccia.



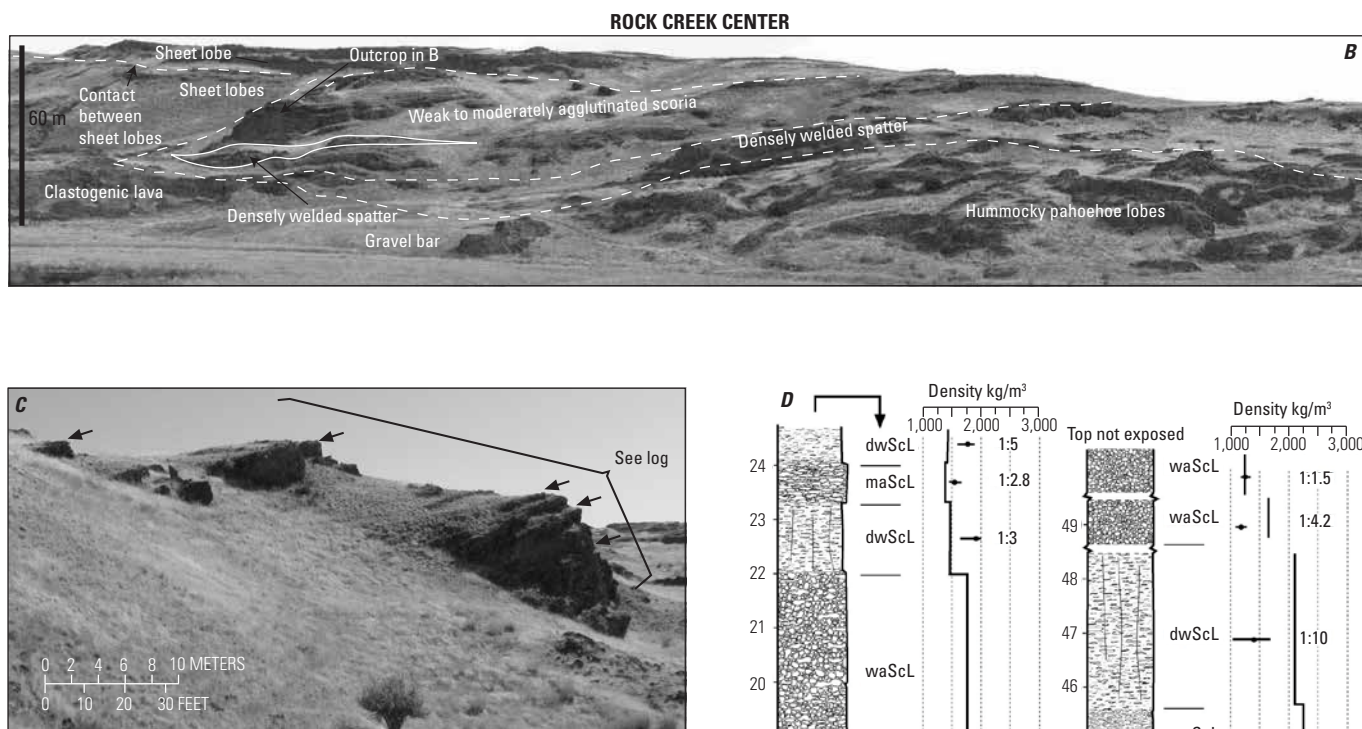


Figure 42.—Continued

and thin clastogenic lava flows. This is overlain by a 1.5-m-thick lava breccia composed of angular blocks and boulders of Roza lava, which, in turn, is overlain by a 2-m-thick scoria lapilli-fall deposit that fines upwards. The upper meter of the fall deposit is densely welded. This is sharply overlain by 6 m of clastogenic lava and lava-like densely welded spatter. The upper ~35 m of the succession is dominated by red, oxidized, weakly and moderately agglutinated scoria in massive or diffusely bedded units that range in thickness from <1 to 15 m thick. Beds in this succession dip 10°–22° to the north, east, and west, and define a half cone with an estimated minimum radius of ~250 m (fig. 42C). The vent that emitted these pyroclastic deposits is inferred to be under Rock Creek. Later-erupted Roza lavas onlap against the cone and may have completely buried it during the eruption.

Retrace route to Winona. Park on the railway sidings in the center of Winona (P on inset in fig. 43) and walk east along Endicott Road for 500 m to Stop 4-D5.

105.3 Stop 4-D5: Roza Member tephra fall deposits
(46.959591° N, 117.862412° W). Tephra fall deposits of the Roza Member are well exposed in roadcuts on the north of the road (Thordarson and Self, 1996; Brown and others, 2014). The axis of the fissure for these deposits is exposed to the west of Winona along the railway line, 1.5 to 2 km away from Stop 4-D5

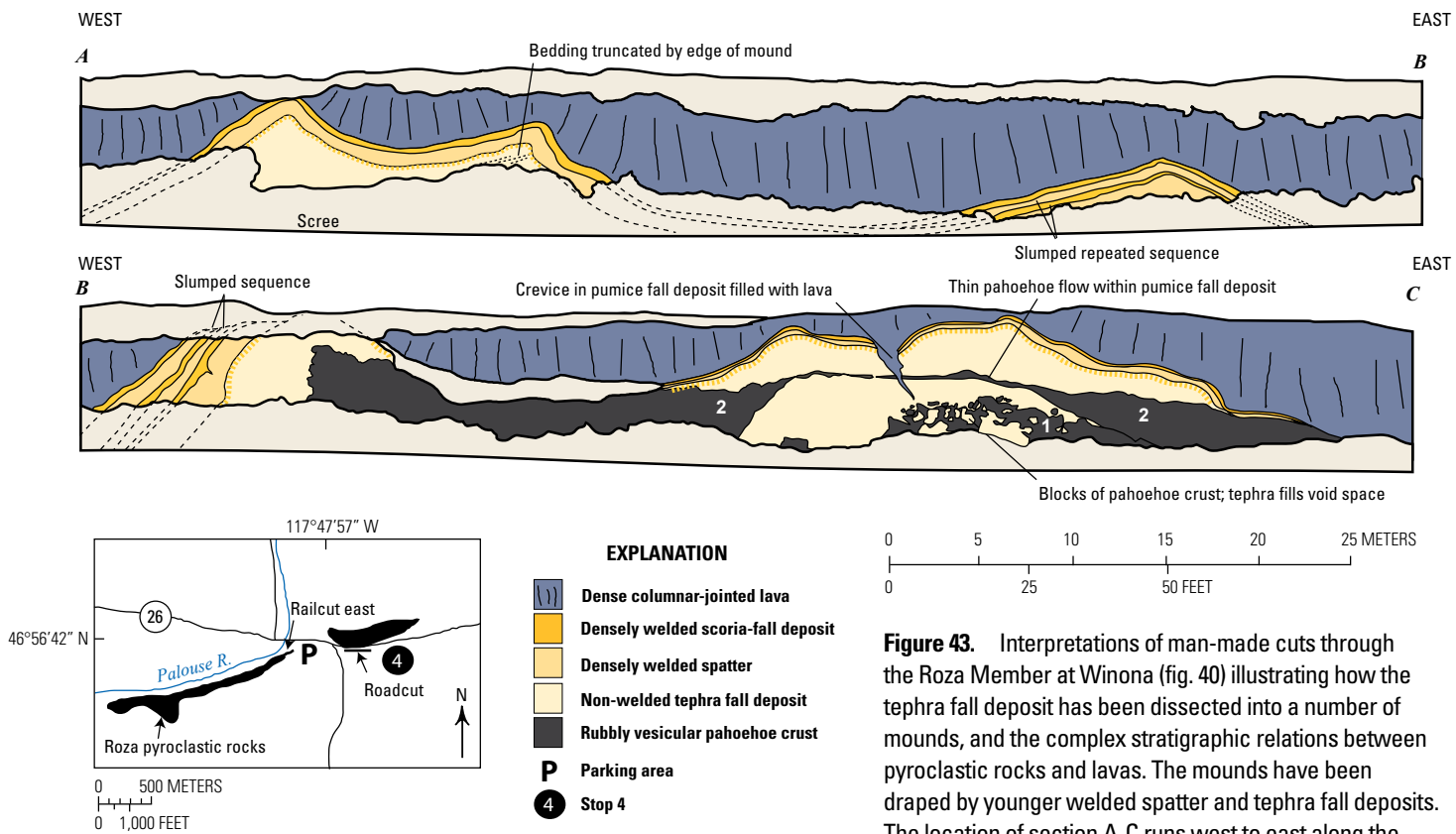


Figure 43. Interpretations of man-made cuts through the Roza Member at Winona (fig. 40) illustrating how the tephra fall deposit has been dissected into a number of mounds, and the complex stratigraphic relations between pyroclastic rocks and lavas. The mounds have been draped by younger welded spatter and tephra fall deposits. The location of section A-C runs west to east along the roadcut noted in the map inset. Lavas labeled 1 and 2 are separate zones of rubbly vesicular pāhoehoe.

(see Brown and others, 2014, fig. 8; Brown and others, 2015, fig. 2). The tephra deposits consist of nonwelded, well sorted, massive to weakly horizontally bedded scoria lapilli. They exhibit unusual geometries and stratigraphic relations with interbedded, thin, highly vesicular, and rubbly pāhoehoe lavas (Brown and others, 2015). The tephra fall deposits have been broken into a series of mounds each as much as 5 m thick, 30 m wide, and spaced ~25–40 m apart (fig. 43). The mounds all occur along the same stratigraphic horizon and feature subhorizontal bedding and are therefore taken to be part of the same fall deposit. The upper mounds are draped by densely welded spatter deposits and the exteriors of the mounds in contact with the spatter have been sintered to depths of 5–10 cm. Brown and others (2015) inferred that the tephra fall deposit was disrupted into mounds by the underlying lava flow, which was still active and undergoing lateral (flow) and vertical (differential inflation) changes. Similar mounds have been observed in three dimensions on historical lava flows elsewhere (for example, Chinyero volcano, Tenerife, Canary Islands, Brown and others, 2015).

Leave Winona, WA; take Winona South Road **2.5**

- 107.8 Intersection Swent Rd, Stormont Road. Bear right on Winona South Road **0.6**
- 109.4 Intersection of Winona South Road and Dynamite Road. Stay on Winona South Road (left). **8.6**
- 116.8 Lacrosse, WA. Take Lacrosse Airport Road to S.R. 26. **2.5**
- 120.1 S.R. 26. Turn right to Washtucna, WA. **19.8**
- 139.9 Washtucna, WA. Turn left on S.R. 261. **6.6**
- 146.5 S.R. 261 on left. This road leads to Palouse Falls. **8.3**
- 154.8 Kahlottus, WA. Turn left on S.R. 263 and Pasco-Kahlottus Highway. **0.6**
- 155.5 Turn left on S.R. 263–Devils Canyon Road toward Lower Monumental Dam. **3.0**
- Stop 5-D5: Saddle Mountains intracanyon flows in the ancestral Salmon-Clearwater River** (46.576503° N, 118.536594° W). Park in turnout on right leading to gate. From this vantage point (fig. 44), we can see an impressive natural cross-section through parts of three

different Saddle Mountains Basalt flows that flowed down the canyon cut by the ancestral Salmon-Clearwater River between 14 and 10.5 Ma (fig. 44; Swanson and Wright, 1976, 1981; Swanson and others, 1980). The earliest flows (Esquatzel Member and Pomona Member) did not fill the canyon and this allowed the river to reoccupy it after these flows were emplaced. At about 10.5 Ma, the Elephant Mountain Member was emplaced (uppermost entablature/colonnade that unconformably lies upon the Esquatzel and Pomona Members) and was voluminous enough to fill and obliterate this canyon of the ancestral Salmon-Clearwater River (Swanson and Wright, 1976, 1981). The Elephant Mountain Member forced the ancestral Salmon-Clearwater River out of this path and caused it to relocate its channel south of its former position to about the present-day location of the Snake River. You will see this new channel when we drive by Lower Monumental Dam in a few miles. **2.4**

Continue on S.R. 263.

160.9 Road turns right to follow Snake River. **0.2**

161.1 Optional stop: Lower Monumental Dam and Wanapum-Grande Ronde Basalt contact

(46.566263° N, 118.542893° W). Note the entablature/colonnade flow that forms the cliffs to the right (north). This is a flow of the basalt of Palouse Falls (Frenchman Springs Member; Martin and others, 2013; Yve-Brown and others, 2013). Here, the Palouse Falls flow directly overlies the Grande Ronde Basalt (Sentinel Bluffs Member). Farther west there is a sedimentary interbed, the Vantage Member of the Ellensburg Formation, between the two members. In the Lewiston Basin there is a saprolite at the contact between the two formations. Across the river is an intracanyon remnant of the 5 Ma Lower Monumental Member (Saddle Mountains Basalt) overlying gravels. After the ancestral Salmon-Clearwater River was abandoned from the location of the previous stop, the river occupied the present Snake River route. **2.6**



Figure 44. Photograph of successive stages of canyon development of the ancestral Salmon-Clearwater River recorded in Saddle Mountains Basalt intracanyon flows exposed at Devils Canyon, Washington. The earliest flows, Esquatzel Member (with prominent lower colonnade and overlying entablature zones) and Pomona Member (with chaotic joint rosettes) did not fill the canyon and this allowed the ancestral Salmon-Clearwater River to reoccupy it. The Elephant Mountain Member was emplaced later and unconformably lies upon the Esquatzel and Pomona Members. Note that the subvertical, knife-edge contact between the Esquatzel and Pomona Members may be created by thermal erosion of a paleo-canyon wall eroded into the former by the latter.

- 163.7 Intersection with Wallace Walker Canyon Road. Continue straight ahead. **0.6**
- 164.3 Pass beneath the railroad trestle at the base of the grade. The Grande Ronde Basalt-Wanapum Basalt contact lies just below the road. **2.4**
- 235.6 Intersection of Pasco-Kahlotus Highway and S.R. 263 (Burr Canyon Road). Turn left (south) toward Pasco. **8.7**
- 246.7 Intersection with Snake River Road. Continue straight ahead. You have just passed Star School, one of the only one-room schoolhouses remaining in Washington. **12.4**
- 187.8 Intersection with Ice Harbor Dam junction. Continue straight ahead. **9.6**
- 197.4 Intersection of Interstate 182 (I-182)/U.S. 12 and the Pasco-Kahlotus Highway. Bear right on I-182 toward Pasco.

Day 6 Overview—Geology of the Pasco Basin

Day 6 will cover the Pasco Basin and vicinity (fig. 45). This leg of the field trip will examine more distal CRBG flows that were seen in the eastern part of the Columbia Basin, and local vents and dikes of the Wanapum and Saddle Mountains Basalts. The Pasco Basin is part of the Yakima Fold Belt and, thus, the growing anticlinal fold has had a major influence on the emplacement of these flows. Mileage for this day begins at the intersection of I-182, U.S. 12, and U.S. 395 (fig. 45). Geologic maps for this area include Reidel (1988), Reidel and Fecht (1994a,b), Schuster (1994, 2005), and Schuster and others (1997). Also see Tolan and others (2009) for additional field guide information.

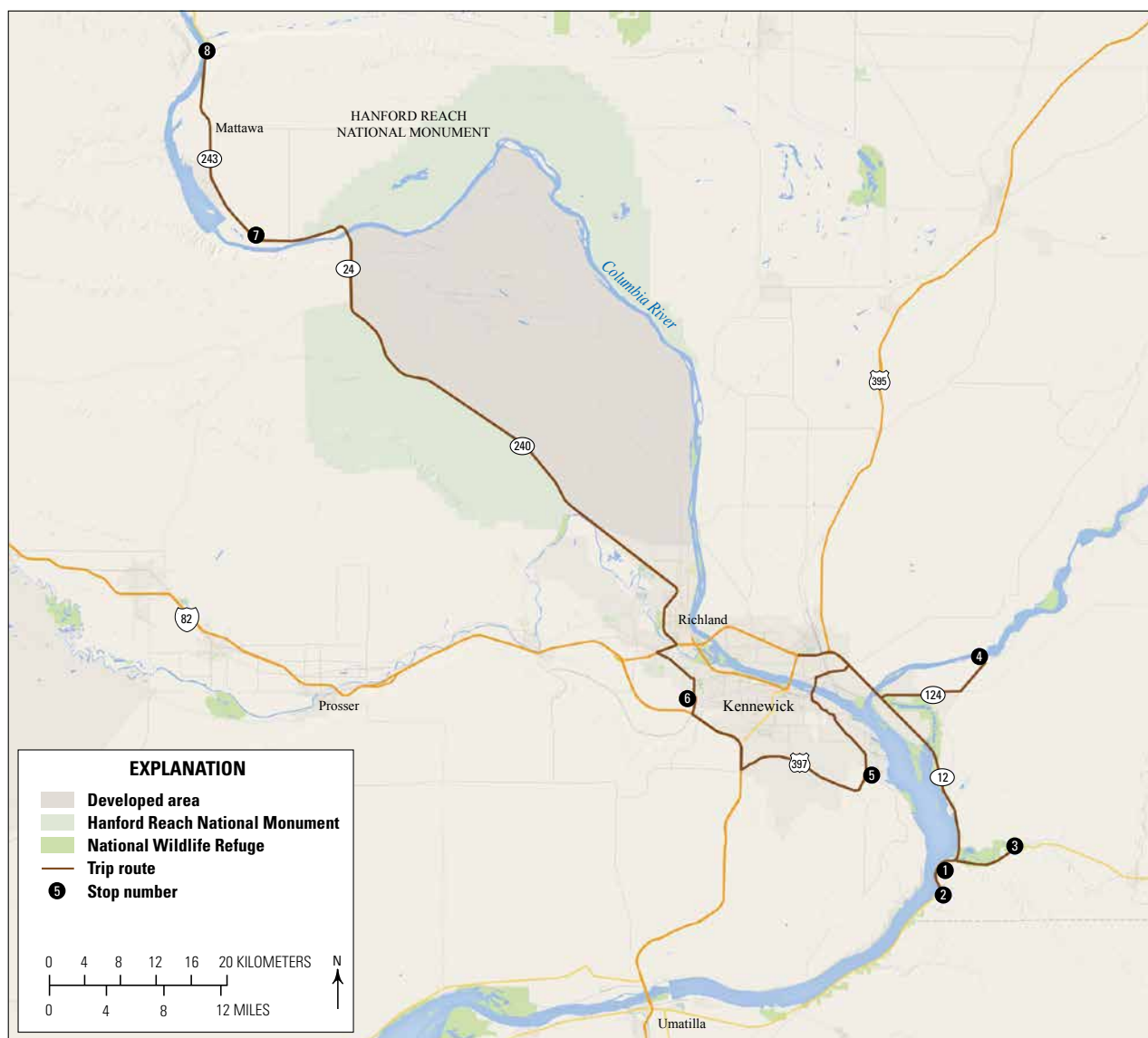


Figure 45. Map of field-trip stops for Day 6.

Day 6—Road Log

- 0.0 Junction of I-182, U.S. 395, and U.S. 12. Proceed straight ahead (east) on U.S. 12. **3.7**
- 3.7 Cross the Snake River. Note the flood gravels along the north bank. About 2 mi to the south, the Snake River flows into the Columbia River. The Ice Harbor Member is exposed at river level about 2 mi up the Snake River to the northeast. Younger flows crop out at progressively greater distances up the river. **0.8**
- 4.5 Junction of U.S. 12 and S.R. 124. **11.7**
- 16.2 Junction of U.S. 12 and U.S. 730. Bear right onto U.S. 730 west. At 11:00, you can see the trace of the main fault at the front of the Horse Heaven Hills just above U.S. 12 to Walla Walla. The area on the south side of the road has been uplifted relative to the north side, juxtaposing Saddle Mountains Basalt to the north against the Frenchman Springs Member to the south (fig. 46). **0.6**
- 16.8 Entrance to the Port of Walla Walla. Flows of the Umatilla through Ice Harbor Members are tilted to the north (30°) in this area. **0.1**
- 16.9 At 3:00 (about 100 yards south of the Pasco–Walla Walla road sign) are excellent examples of vertical strike-slip faults trending $N20^\circ W$ (fig. 46) described in Reidel and others (2013a). Exposed here are three small (5–7.5 cm-thick) secondary fault zones with clay gouge that display excellent subhorizontal slickensides. These zones are associated with the main frontal fault zone of the Horse Heaven Hills that parallels the road to the north. The main displacement on the Horse Heaven Hills Fault is vertical (about 3,300 ft) so that the Ice Harbor, Elephant Mountain, Pomona, and Umatilla Members of the Saddle Mountains Basalt are thrust over by the flows of the Frenchman Springs Member of the Wanapum Basalt. The strike-slip faults are minor features activated by north–south movement along the main fault. In the past they were mistakenly interpreted as the main Wallula Fault Zone but when viewed on aerial photographs, it is clear that they crosscut the Wallula Fault Zone. **0.2**
- 17.1 Basalt pillows in one of the flows of the basalt of Sand Hollow (Frenchman Springs Member, Wanapum Basalt; see Martin and others, 2013). The pillow zone represents an area where this flow entered water. **0.4**

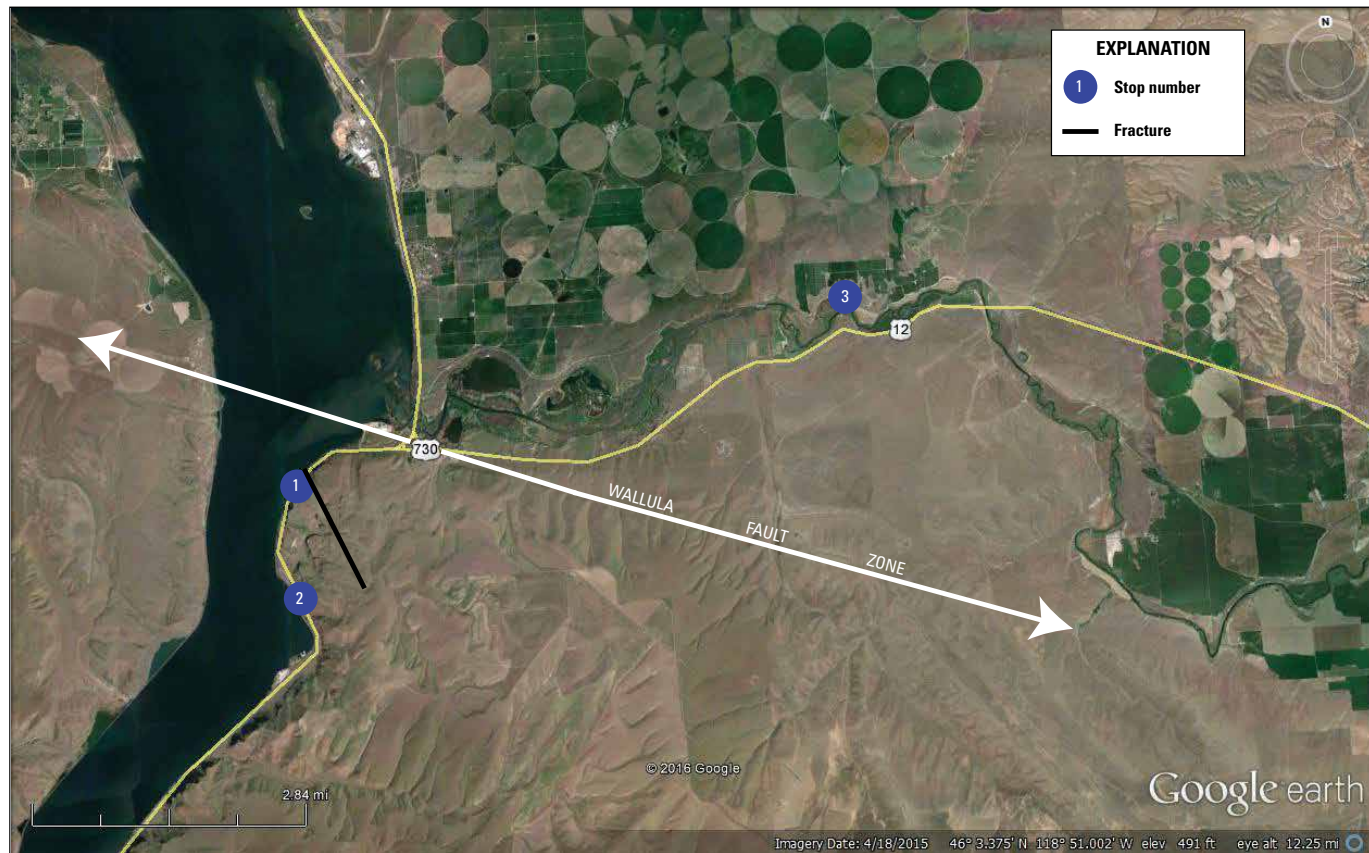


Figure 46. Google Earth image of the Wallula Fault Zone near Wallula Gap. The Wallula Fault Zone forms part of the Olympic-Wallowa Lineament. This map shows the main fault line and the secondary fracture that crosses the main fault and is described in text.

- 17.5 At 9:00, the small valley across the Columbia River is the result of erosion along the trace of the Yellpit Fault, one of the fault segments that make up the frontal fault zone of the Horse Heaven Hills, and a continuation of the Wallula Fault Zone. This fault places Ice Harbor, Elephant Mountain, and Pomona Members of the Saddle Mountains Basalt on the north against the older Frenchman Springs Member of the Wanapum Basalt on the south. The fault trace is overlain by undisturbed sediments that contain the 13,000-year-old Mount St. Helens set 'S' ash. This indicates that the fault has not been active since the ash was deposited. **0.7**
- 18.2 **Stop 1-D6: Twin Sisters** (46.052309° N, 118.934210° W). On the east (left) side of the highway are two basaltic buttes (figs. 46, 47). This famous landmark was described by Meriwether Lewis and William Clark. These buttes are known as the Twin Sisters, and are erosional remnants of the basalt of Sand Hollow (Frenchman Springs Member). Note the well-developed columnar jointing of the colonnade and the overlying irregular or hackly jointing of the entablature. **0.1**
- 18.3 Continue south on U.S. 730.
- 18.3 Mile marker 4.0. Roadcut exposures of the basalt of Ginkgo (Frenchman Springs Member, Wanapum Basalt). **0.1**
- 19.2 **Stop 2-D6:** Contact between the Grande Ronde Basalt and the basalt of Ginkgo (Frenchman Springs Member, Wanapum Basalt) (46.028019°, -118.931640°). Pull into the turnouts on the west (right hand) side of the highway. The outcrops are on the opposite side of the road. Be careful crossing the highway as traffic is very heavy. Here the basalt of Ginkgo (Frenchman Springs Member, Wanapum Basalt) directly overlies the Sentinel Bluffs Member (Grande Ronde Basalt; fig. 46). The basalt of Palouse Falls (Frenchman Springs Member) is not present but the basalt of Museum (Sentinel Bluffs Member, Grande Ronde Basalt) has many more flows than at Lower Monumental Dam (Reidel, 2005). In addition, the youngest Sentinel Bluff Member flows have a transitional magnetic polarity similar to the overlying Ginkgo flow.

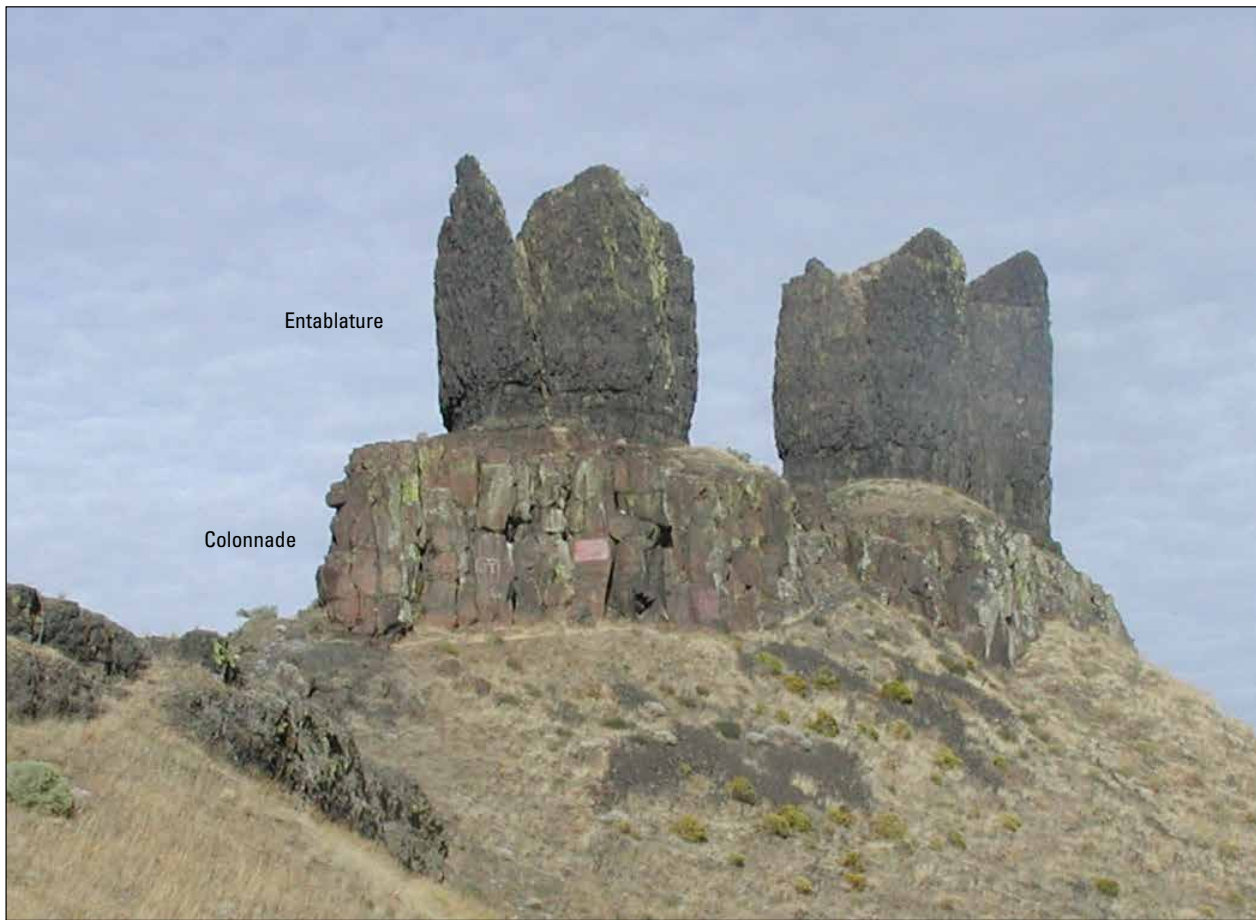


Figure 47. Photograph showing the Two Sisters. This is the colonnade and entablature of a basalt of Sand Hollow flow, Frenchman Springs Member, which was described in the journals of the Lewis and Clark expedition during their Corps of Discovery expedition in 1805 on their way to the coast of Washington and Oregon.

- Turn around to return east on U.S. 730. **1.8**
- 22.0 Junction of U.S. 12 and U.S. 730. Bear right onto U.S. 12 east. **5.0**
- 27.0 Intersection with Oasis Road on north side of U.S. 12. Turn left onto Oasis Road at sign for Cameo Heights Resort. **0.3**
- 27.3 Cross railroad tracks. **0.4**
- 27.7 Quarry on the left. Turn left into the quarry and park. **0.1**
- 27.8 **Stop 3-D6: Dike of the basalt of Goose Island, Ice Harbor Member, Saddle Mountains Basalt** (46.066612° N, 118.833912° W). Swanson and others (1979) recognized a dike of the basalt of Goose Island (Ice Harbor Member) that was exposed at the top of the hill. Since then this has become an active quarry. The exposure (fig. 48A) shows a thin, 8.5 Ma Goose Island dike injected into a fault zone (Reidel and others, 2013a). The host rocks are the Frenchman Springs Members and Umatilla Members, which

were faulted and offset prior to injection of the dike. Figure 48B shows the dark dike intruding the fault breccia, and figure 48C is a close-up view of the dike injected into a cooling joint through the host basalt and flow top of the Frenchman Springs Member. The fault zone appears to have been reactivated after the dike cooled. The exposure indicates that a N35°W fault formed after the Umatilla Member was emplaced but prior to the Ice Harbor Member. After initial faulting, the fault was used as a conduit for the Goose Island dike. Dike emplacement was again followed by fault movement, shattering and brecciating the Goose Island dike that was in the main fault, but leaving undisturbed the dike material that was injected into the surrounding country rock.

Return to U.S. 12. **0.8**

- 28.6 Turn right onto U.S. 12 west. **4.8**
- 33.4 Intersection with U.S. 730. Bear right to continue on U.S. 12 west. Return to Junction of U.S. 12 and U.S. 730. **11.4**

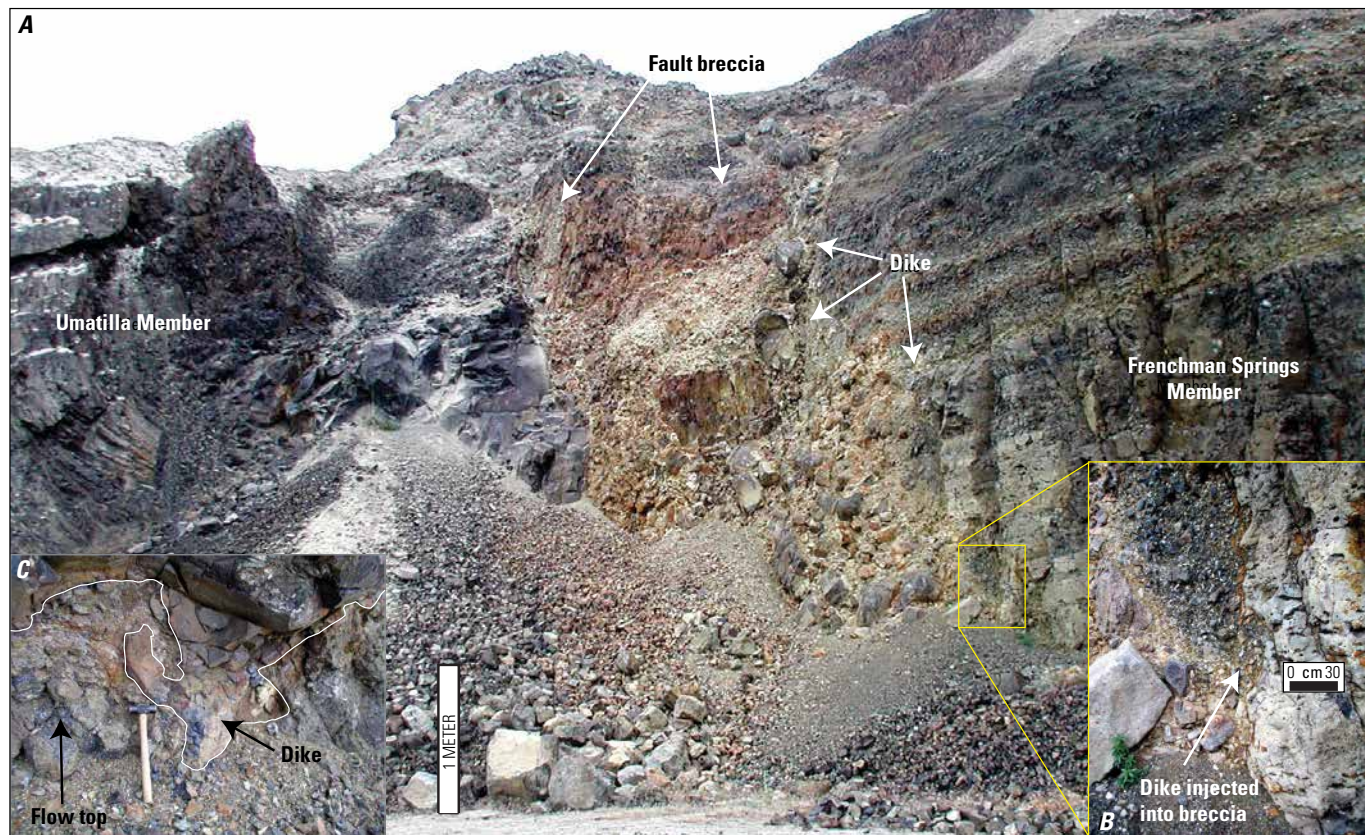


Figure 48. Photographs of basalt of Goose Island dike, Ice Harbor Member. *A*, The exposure shows a thin, 8.5 Ma basalt of Goose Island dike injected into a fault zone. The host rocks are the Frenchman Springs and Umatilla Members, which were faulted and offset prior to injection of the dike. *B*, Dark colored dike intruding the fault breccia. *C*, Close-up showing the way in which the dike was also injected into a cooling joint within the host basalt and flow top of the Frenchman Springs Member. The fault was reactivated after the dike cooled, brecciating the dike (from Reidel and others, 2013b).

- 44.8 Junction of U.S. 12 and U.S. 730. Bear right onto U.S. 12, west toward Pasco. **5.2**
- 46.6 Intersection of U.S. 12 and S.R. 124. Turn right onto S.R. 124. **1.8**
- 50.0 Intersection of S.R. 124 with Monument Drive; turn off for Ice Harbor Dam. Turn left onto Monument Drive. Proceed north on Monument Drive to the Snake River. **2.7**
- 52.7 Snake River. Turn left onto the gravel road that parallels the Snake River downstream from Ice Harbor Dam. **1.1**
- 53.8 **Stop 4-D6: Ice Harbor Member vents** (46.245725° N, 118.881194° W). This locality is on the south shore of the Snake River approximately half a mile downstream from Ice Harbor Dam. Park by the gate and walk to the bluff at the end of the road. The bluff exposes an eroded tuff cone for the basalt of Martindale (Ice Harbor Member, Saddle Mountains Basalt). This 8.5 million year old vent was described by Swanson and others (1975) and Swanson and Wright (1981). It is part of a linear vent system that is more than 90 km long. Swanson and Wright (1981) state the following, “The craggy bluff near the parking area is the remnant of a tuff cone built over a vent for the Basalt of Martindale.... Note the poorly bedded nature of the cone, the palagonitic alteration of most glassy tephra, and the angular unconformity (between tephra below and basalt flow above) visible on the northwest face. A flow of Martindale overlies the cone.”
The tuff cone is approximately 200 m wide and 40 m high; it is built on lava flows belonging to the 10.5 Ma Elephant Mountain Member (Saddle Mountains Basalt). Martindale lava also overlies this cone. The tephra and basalt both dip away from the cone to the north and south; it is generally poorly bedded and varies in size from ash to bombs. The larger clasts are typically white to grey in color and are basaltic pumice. Some of the bombs and blocks are pieces of older lava flows that were ripped loose, brought to the surface, and ejected by the phreatomagmatic eruption that built this cone. The best exposure of the cone flanks is along the trail that follows the river. Basaltic pumice is exposed a few hundred feet along the trail.
If you follow the trail downstream along the bluff, it leads to another old quarry approximately half a mile away, where a flow of Martindale is exposed. In the quarry, the Martindale flow is cut by a feeder dike for the basalt of Goose Island. The basalt of Goose Island is also 8.5 million years old, but overlies the Martindale lava.
At Ice Harbor Dam, the Snake River flows almost due west. The basaltic fissures that fed the vent at this stop cross the river in a north-northwest direction. Comparing modern geologic maps with the maps by Lewis and Clark from 1805, the “very bad rapids or falls” described by Lewis and Clark are aligned with the locations where the Ice Harbor dikes cross the river. Thus, these 8.5 million year old vents formed a major obstacle for Lewis and Clark’s Corps of Discovery.
- The basalt of Martindale vent system provides some insight into the nature of the Olympic-Wallowa Lineament (OWL). Several workers (for example, Hooper and Conrey, 1989; Blakley and others, 2011) have suggested that the OWL is a major strike-slip fault. However, the Martindale vent system can be traced to the north edge of the OWL, and a vent for the basalt of Martindale also occurs directly across the OWL on the south side. This occurrence shows that there has been no strike-slip movement on the OWL in the past 8.5 million years (Reidel and Tolan, 1992; Reidel and others, 2013a). **1.1**
- 54.9 Turn around and return south on Monument Drive to S.R. 124. **2.7**
- 57.6 Intersection of Monument Drive and S.R. 124. Turn right onto S.R. 124. **5.2**
- 62.8 Intersection of S.R. 124 and U.S. 12. Turn right onto U.S. 12 west. **3.7**
- 64.5 A Street. Exit to left. Entering Pasco. **1.8**
- 66.3 Cross Oregon Avenue, which is S.R. 397. **1.2**
- 67.5 S. 10th Avenue. Turn left and continue across bridge into Kennewick. Continue straight. This is now called U.S. 397. **6.8**
- 74.3 Turn right at Finley Road. Continue straight through Finley. **0.2**
- 74.5 Cross Game Farm Road. **1.1**
- 75.6 Turn right on to U.S. 397. **1.1**
- 76.7 Turn left onto gravel road across from sign indicating Finley Road ahead. Drive to gate and park. **0.1**
- 76.8 **Stop 5-D6: Finley quarry** (46.120463° N, 119.043165° W). Finley Quarry is in the Umatilla Member of the Saddle Mountains Basalt (Reidel, 1998); the Pomona Member sits atop the Umatilla and fills a N30°W trending fracture that was eroded prior to emplacement of the Pomona. Here, both the Sillusti and Umatilla flows are present, but the contact between them is marked only by a red-oxidized zone (fig. 49). The Umatilla flow is older and forms the base of the quarry wall. The Sillusti flow sits atop it above the red zone (fig. 49A). As you move north into the Pasco Basin, the Umatilla Member

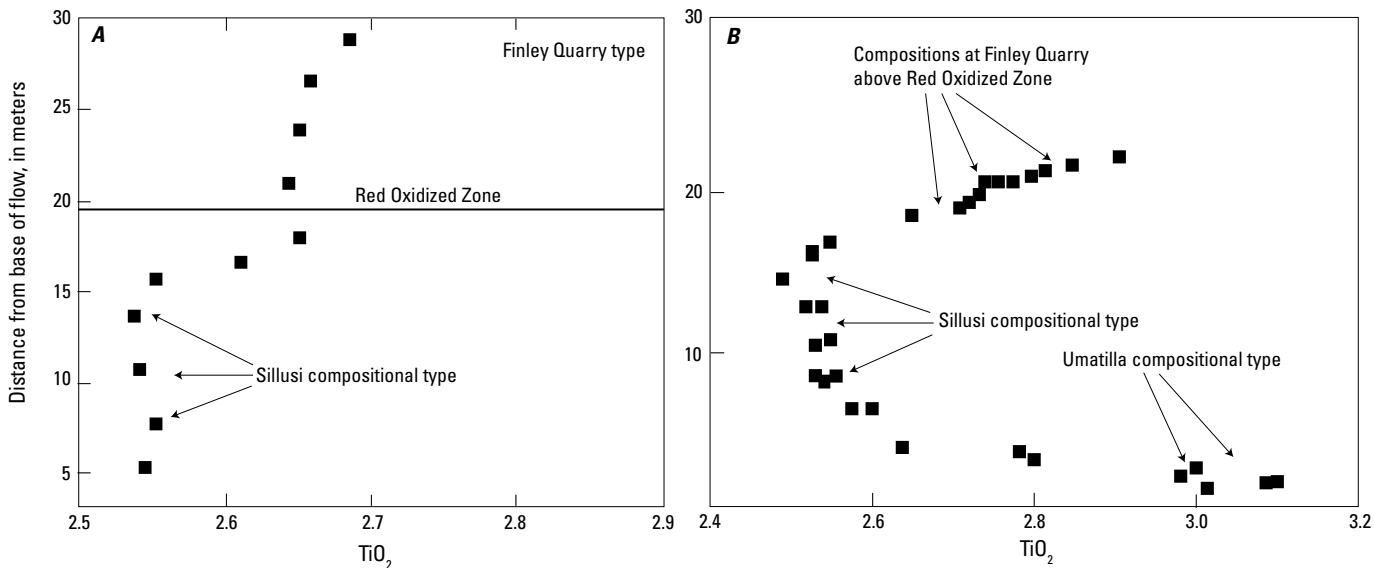


Figure 49. Graphs of TiO_2 composition of the Umatilla Member in the Columbia Basin. *A*, Composition of samples collected through the Umatilla Member exposed in Finley Quarry. *B*, Composition of Umatilla Member samples collected from cored-borehole RRL-4 on the U.S. Department of Energy's Hanford Site.

has been penetrated in boreholes at the Hanford Site. In the boreholes, the two flows have mixed, with Sillusi in the center and Umatilla at the top and bottom. Between the center and the margins, there is complete mixing with an increasing component of Sillusi toward the center (fig. 49B). Reidel (1998) has described the Umatilla Member and its components in detail.

Return to U.S. 397 and turn left and continue on U.S. 397 west. **1.5**

- 78.3 Nine Canyon Road. Continue straight. **0.6**
- 78.9 Roadcuts show Pomona Member over Umatilla Member with Rattlesnake Ridge interbed between; an ash in the interbed has been fused to a black glass at the base of the Pomona Member. **2.5**
- 82.4 Olympia Street. Continue straight. **1.7**
- 84.1 Elephant Mountain Member on right. Ice Harbor Member above but poorly exposed. **1.4**
- 85.5 Turn right and enter I-82 west. **4.4**
- 89.9 Ice Harbor Member on right for the next mile you will descend through the Ice Harbor Member, Elephant Mountain Member, and Pomona Member. **0.7**
- 90.6 Exit I-82 at Badger Canyon-Clearwater Road. **0.5**
- 91.1 Turn right onto Badger Canyon Road. **1.1**

91.2 Enter Circle (roundabout). Exit at 270° onto Leslie Road. **1.2**

92.4 Turn left onto Meadow Hills Road and proceed up hill to stop sign at Meadow Hills Court. **0.4**

92.8 Meadow Hills Court. Park for Stop 6-D6.

Stop 6-D6: Fault zone along the Olympia-Wallowa Lineament ($46.213004^\circ \text{ N}$, $119.269853^\circ \text{ W}$).

This locality is the frontal fault zone for Badger Mountain, a doubly plunging anticline along the OWL. The rock in this exposure is the Pomona Member and it has been intensely brecciated by thrusting along the OWL (fig. 50). Evidence for recent movement is demonstrated by sediments of the Pleistocene Missoula floods, which have been incorporated in the breccia.

Turn around and return to Leslie Road. **0.3**

93.1 Turn left onto Leslie Road. **1.0**

94.1 Gage Boulevard. Turn left and stay in right lane for turn ahead. **0.1**

94.2 Turn right onto Keene Road. **2.3**

96.5 Turn right onto Queensgate Drive. **0.4**

96.9 Turn right onto I-182 heading east. **0.9**

97.8 Take Exit 4 onto S.R. 240 west. **3.4**

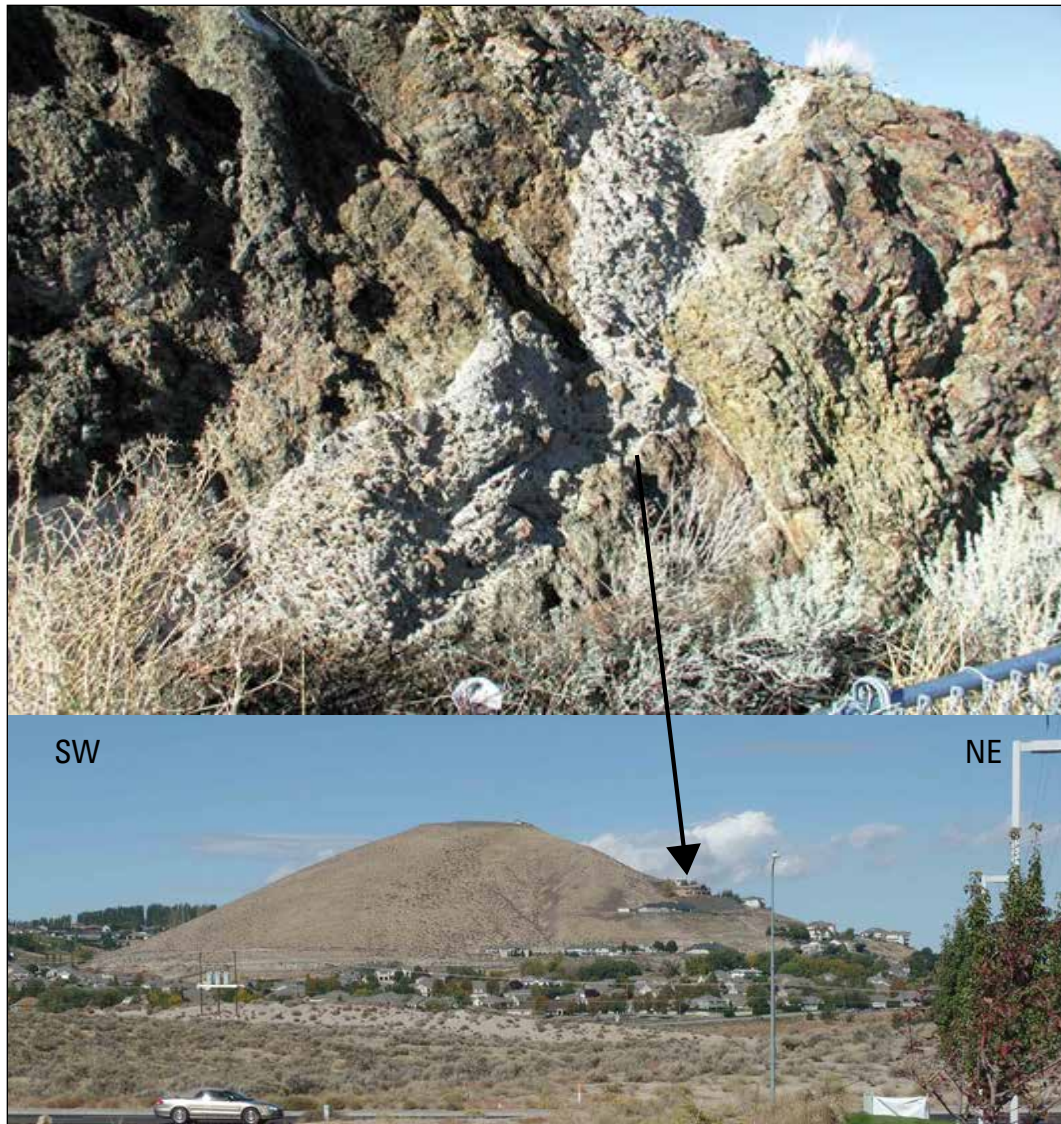


Figure 50. Photograph of thrust fault on the Little Badger Mountain anticline, Kennewick, Washington. Little Badger Mountain is one of the anticlinal folds of the Yakima Fold Belt and forms part of the Olympic-Wallowa Lineament. The anticline is asymmetrical, with a thrust fault on the northeast flank. The upper picture is a close-up of the brecciated 12-Ma Pomona Member, Saddle Mountains Basalt. The breccia zone forms the lower one half of the northeast side of the anticline. The whitish color in the brecciated basalt is sediment from the 1 Ma Missoula floods; this sediment is from Glacial Lake Lewis that formed when the floodwaters were temporally impounded behind Wallula Gap. The thrust moved at this time and the Missoula flood sediments were trapped in the fault zone.

- 101.2 Crossing Van Giessen Road and S.R. 224. Continue straight. **1.4**
- 102.6 Turn left at the intersection of S.R. 240 and Stevens Road onto S.R. 240. **2.3**
- 104.9 The Horn Rapids Dam on the Yakima River is at 9:00. The river eroded a channel across the nose of a small, north plunging anticline and exposed the Ice Harbor, Elephant Mountain, and Pomona Members. This structure continues north across the road (north) where the gently northeast-dipping Elephant Mountain Member can be seen projecting above Pleistocene flood gravels. **4.1**
- 109.0 Milepost 17. View of Rattlesnake Mountain (fig. 51). For the next 1.2 mi, boulders left by Pleistocene floods are visible on the right (east) side of the road. As floodwater that had been temporarily dammed at Wallula Gap began to drain, icebergs carrying boulders and smaller fragments of granite, basalt, and other rock types were left stranded. **9.7**
- 118.7 At 11:00, Snively Basin can be seen between the Rattlesnake Hills and Rattlesnake Mountain. Ahead, you can see the southeast bend in the Yakima Ridge anticline. The fold plunges beneath basin fill (flood sediment and dune sand). Also ahead are several small basalt outcrops of the Elephant Mountain

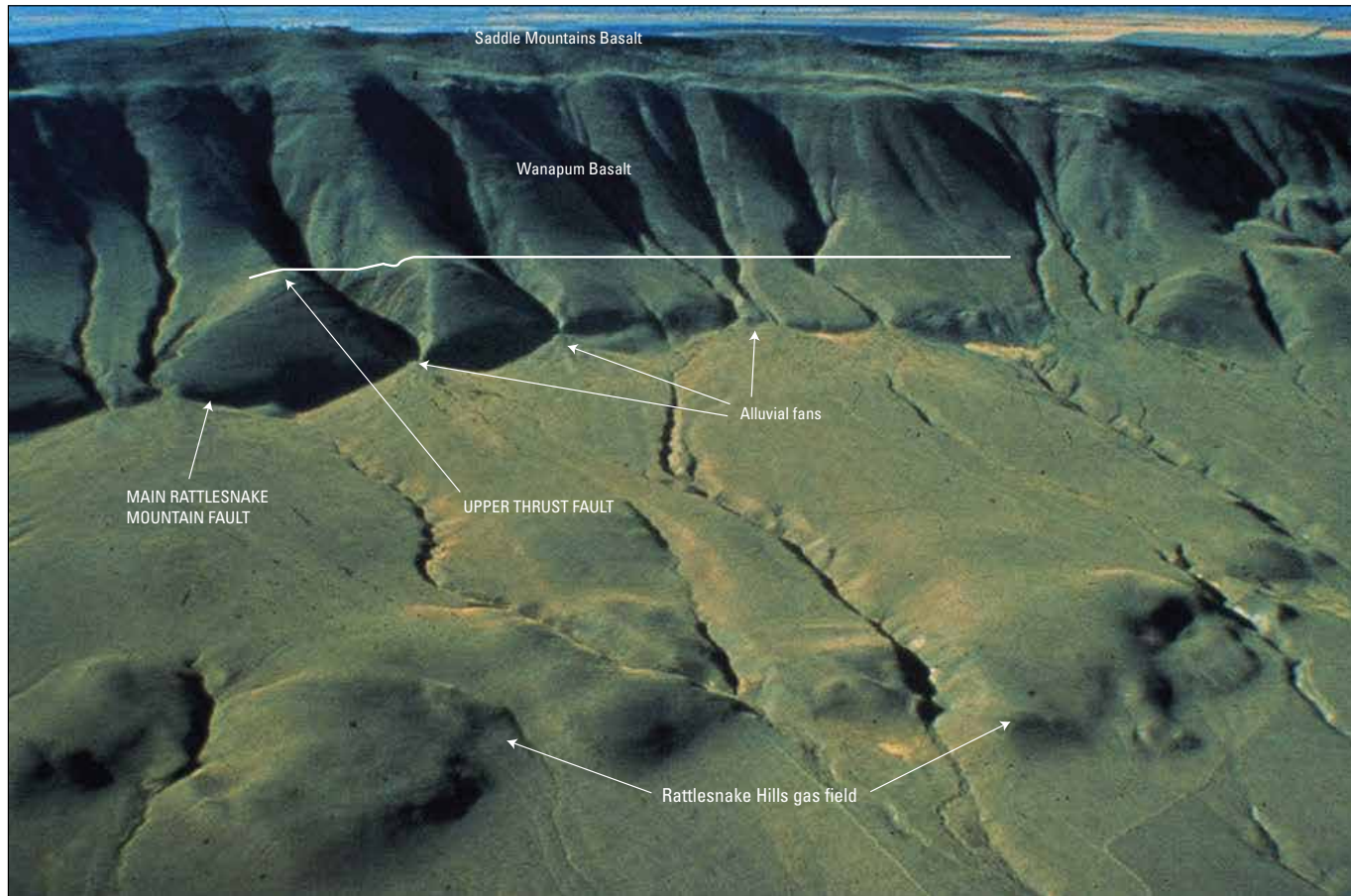


Figure 51. Aerial photograph of Rattlesnake Mountain. Rattlesnake Mountain is one of the tallest anticlines of the Yakima Fold Belt and is very typical of these folds; it also has both an upper and lower thrust fault. The Yakima Fold Belt has been likened to wrinkle ridges, which are found on all terrestrial planets, and especially large igneous provinces. In front (north) of the anticline is a small anticline that was the Rattlesnake Hills gas field, the only commercial gas field in Washington, which was operated in the early part of the 20th century prior to the land being taken over by the military for the site of Manhattan Project facilities in World War II.

- Member at road level along the south side of the road. These are located at the crest of the buried Yakima Ridge anticline. **6.9**
- 125.6 Now climbing onto the Cold Creek bar. Huge gravel bars lie on both sides of the Columbia River where the floodwater spilled out of Sentinel Gap, a narrow gorge in the Saddle Mountains to the north. **0.7**
- 126.3 Junction with S.R. 24 (west) to Yakima and the U.S. Department of Energy's Yakima Barricade, which is an entrance to the Hanford Site. Continue north on S.R. 24 east. The ridge at 12:00 is the Saddle Mountains anticline. A Shell Oil Company well site is at 12:30. The well, drilled to a total depth of more than 5.2 km (17,000 ft), penetrated 3.5 km (11,500 ft) of Columbia River Basalt and passed into prebasalt sedimentary rocks here (Reidel and others, 1989b). **1.8**
- 128.1 At 12:00, is Sentinel Gap, a water gap cut by the Columbia River as the Saddle Mountains were uplifted. **1.8**
- 129.9 At 9:00 is a good view along the north limb of the Umtanum Ridge anticline. Here, flows of the Grande Ronde and Wanapum Basalts dip about 70° to the north. Farther west, the Grande Ronde Basalt is overturned and dips steeply to the south. To the east is Gable Butte, an en echelon anticline along Umtanum Ridge. Pleistocene floodwaters eroded the crest of the anticline producing the small valley visible in the distance. **1.4**
- 131.3 Vernita Bridge over the Columbia River. This is the last free-flowing segment of the Columbia River in Washington, the Hanford Reach, which is part of the Hanford Reach National Monument. **7.0**
- 138.0 Jackson Creek Fish Camp and Stop 7. Turn left onto the gravel road and follow it to the river. Make a right

- turn into the camping and picnic area and pull into the first picnic area on the left. **0.6**
- 138.6 **Stop 7-D6: Overview of Umtanum Ridge Anticline** (46.650111° N, 119.890350° W). Umtanum Ridge extends about 110 km from near the western margin of the Columbia Basin to the Palouse Slope (fig. 52). The structural relief gradually decreases eastward where it becomes a series of en echelon anticlines developed along the dying ridge. In the Priest Rapids Dam area, the north limb is overturned and dips 40° to the south. An upper thrust, the Buck thrust and a lower thrust, the Umtanum thrust, define the overturned part of the fold (Price and Watkinson, 1989). The Buck thrust merges with the Umtanum thrust fault to the east as the overturned part becomes steeply dipping to the north. Drilling constrained the fault's dip to between 30 and 60° to the south.
- To the west is a good view of the thrust faults of the Filey Road area. Many of the thrust faults are partly concealed by landslides, fanglomerates, and loess, but at least one is visible. The thrust faults place the Priest Rapids Member and older rocks onto flows of the Saddle Mountains and Wanapum Basalts. Pleistocene flood gravels near the river level mask the bedrock geology. **0.6**
- 139.2 Return to S.R. 243 and turn left. **7.1**
- 146.3 Traffic circle at intersection of S.R. 243 and County Road 24 SW. At 12:00 is an excellent view of Sentinel Gap. The antecedent Columbia River maintained its course as the Saddle Mountains were uplifted, cutting down through this ridge at Sentinel Gap. At 9:00, the Hansen Creek thrust fault extends to the west shore of the Columbia River. Pleistocene flood bar gravels on this side of the river cover it. This thrust places Priest Rapids and Roza basalt flows over the Priest Rapids flows. The Asotin Member, which crops out at lower elevations of the Saddle Mountains anticline at 10:00, fills a former channel of the Columbia River through Sentinel Gap. **3.9**
- 150.2 At 1:00 along the right (east) side of Sentinel Gap, the Frenchman Springs, Roza, and Priest Rapids Members form the upper cliffs. The bench below the upper cliffs is the result of erosion along an interbed, the Vantage Member of the Ellensburg Formation. The lower cliffs here are flows of the Grande Ronde Basalt. At 11:00, west of Sentinel Gap, the white patch high on the cliff face is the Vantage interbed. Frenchman Springs Member flows lie above it and Grande Ronde Basalt below. **0.7**



Figure 52. Photograph of Umtanum Ridge, an anticlinal ridge similar to Rattlesnake Mountain. This exposure provides an excellent view of the nature of the deformation along the north side of the structure. The upper thrust fault is marked by gently dipping basalt to the south, and overturned and steeply dipping basalt below the thrust. The lower thrust is not exposed, but covered by the Columbia River at this locality.

- 150.9 The road to the right leads to a quarry exposing an interbed of the Ellensburg Formation. The name ‘Beverly’ was formerly applied to this interbed. The name is no longer used because this unit is a composite of several interbeds; the intervening flows are not present. This quarry is a good place to see this 180-ft-thick interbed. The lower part contains conglomerate deposited by the ancestral Columbia River, and the upper part is made up of poorly indurated siltstone, sandstone, and tuff. **2.6**
- 153.5 Turnout. Mazama ash exposed on roadcut on east side of highway. **0.5**
- 154.0 Turn left onto dirt road. **0.5**

Stop 8-D6. Sentinel Bluffs Member, Grande Ronde Basalt (46.805915° N, 119.922231° W). Along the walls of Sentinel Gap are excellent exposures of Grande Ronde Basalt, the Vantage Member interbed, Ellensburg Formation, and the upper part of the Frenchman Springs Member, as well as a good cross-sectional look at the Saddle Mountains. A major thrust fault at the base of the north flank of the Saddle Mountains places Grande Ronde Basalt on top of the Priest Rapids Member. Horizontal shortening is at least several kilometers. The fault cuts across the Columbia River somewhere between here and the town of Schwana. In addition, a north-trending right-lateral strike-slip fault cuts through the ridge at the gap (Reidel, 1984, 1988).

At this stop we will examine lava flows of the Sentinel Bluffs Member (fig. 53). The Grande Ronde Basalt has been divided into 25 mappable units (Reidel and Tolan, 2013). The Sentinel Bluffs Member, the youngest of the Grande Ronde units, consists of flows that have high magnesium contents (mostly 4.5–6.5 percent) relative to other Grande Ronde units; the lavas also have normal polarity. The eruption of the Sentinel Bluffs lavas marked the end of Grande Ronde Basalt volcanism and the end of the greatest period of CRBG volcanism. The Sentinel Bluffs lavas erupted from a northerly trending vent system in eastern Washington and northern Oregon, and flowed westward down an ancestral paleoslope covering more than 169,700 km² of the flood-basalt province and producing more than 10,000 km³ of lava. The Sentinel Bluffs Member is divided into six eruptions that are distinguished by their compositions. The first eruption was the most voluminous and reached the Pacific Ocean (Reidel, 2005). The volume of basalt declined with later eruptions until the final eruption, which produced the second largest volume of basalt.

Compositional variation in individual lavas is relatively small both vertically through each basalt

eruption and over their areal extents. This homogeneity allows the individual eruptions to be recognized throughout the province (Reidel, 2005). One exception is in the central part of the province where four of the eruptions combined to form one local lava, the ‘Cohassett flow’ (fig 53). The Cohassett formed as successive eruptions inflated the first lava to form a new lava that had a compositional zonation that reflected the sequence of eruptions. The compositions of the original lavas remained intact except for mixing where they came into contact. Thin zones of vesicles separate relatively uniform compositional zones. A thick vesicle zone, called the interior vesicular zone, marks the boundary between the last two eruptions and represents a volatile-rich part of the last lava to form the Cohassett (Reidel, 2005).

There are two compositional trends in the eruptions of the Sentinel Bluffs Member that are defined best by TiO₂ and P₂O₅. The six eruptions fall along one or the other trend, but neither trend is defined by the timing of eruptions or location along the vent system. The first and last eruptions follow one trend and the eruptions between follow the other trend. Both trends represent decreasing TiO₂ and P₂O₅ with time.

Day 7 Overview—Geology and Structure of the Yakima Fold Belt

This day will focus on two Yakima folds, Horse Heaven Hills and Columbia Hills, and the volcanic rocks and structures associated with them. Initially, the trip will provide an overview of the Horse Heaven Hills and Yakima folds to the north. The route will then parallel the Columbia Hills Fault Zone where young volcanics (<1 Ma) and flows observed at previous stops will be seen at greater distances from their vent systems. As the day proceeds, the route will enter the Columbia Gorge and the ancestral Columbia River.

Mileage for Day 7 begins at the junction of I-82 and I-182 south of Richland, WA (fig. 54). Geologic maps for this area include Reidel (1988), Reidel and Fecht (1994a), Schuster and others (1997), Schuster (2005) and Walsh and others (1987).

Day 7—Road Log

- 0.0 Mileage begins on I-182 west at Yakima River sign.
- 2.7 Roadcut on left has small upper thrust fault for Badger Mountain Fault. **2.7**
- 3.3 Bear right onto I-82 west. **0.6**
- 9.4 Pass Benton City Exit 96. **6.1**
- 10.5 Elephant Mountain Member on left. **1.1**

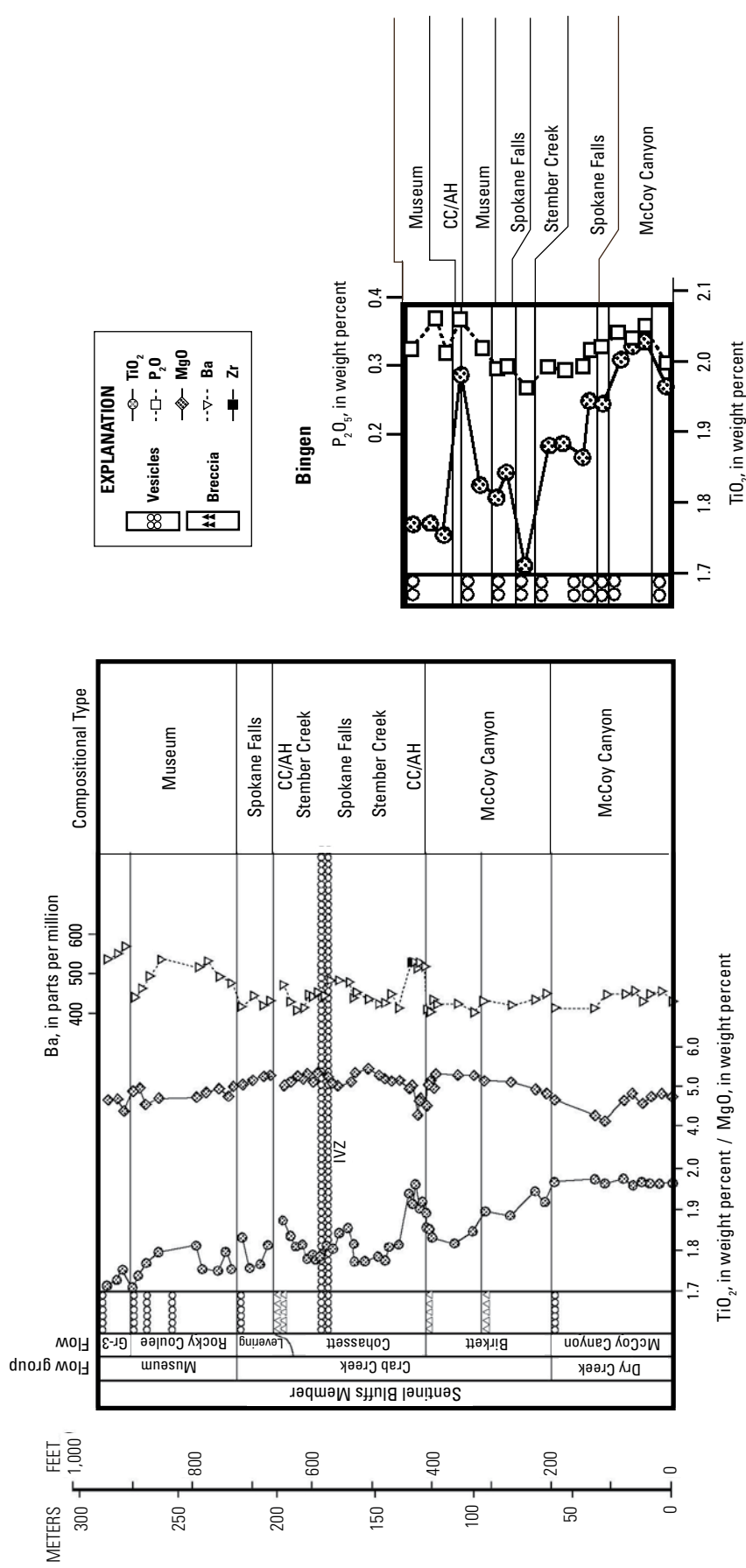


Figure 53. Chemical composition of the Sentinel Bluffs Member (Grande Ronde Basalt) in Sentinel Gap of the Saddle Mountains and the Sentinel Bluffs Member at Bingen, Washington. The Bingen section is drawn at the same vertical scale and is therefore much thinner than the section at Sentinel Gap. Although most of the same compositional types are present in both, the Bingen section is more chaotic, due mainly to all the Sentinel Bluffs Member flows being funneled into the Columbia Gorge. The stratigraphic nomenclature for Sentinel Bluffs in the Pasco Basin is partly based on compositional changes in vertical section. The nomenclature on the left side is from Landon and Long (1989). They used less precise and less accurate x-ray fluorescence (XRF) data restricted to major-element compositions. The nomenclature on the right is from Reidel (2005). This is based on a regional stratigraphy where individual names are derived from the locations of dikes, vents, and the flows that they fed. In addition, compositions are determined using newer, more precise and accurate XRF analyses including major and trace elements. Reidel's (2005) study showed that the Cohassett flow of Landon and Long (1989) is, in reality, a composite flow consisting of three individual flows that inflated an earlier fourth flow. CC, California Creek; AH, Airway Heights; IVZ, internal vesicular zone; GR-3, Grande Ronde Basalt flow here using Landon and Long (1989) nomenclature.

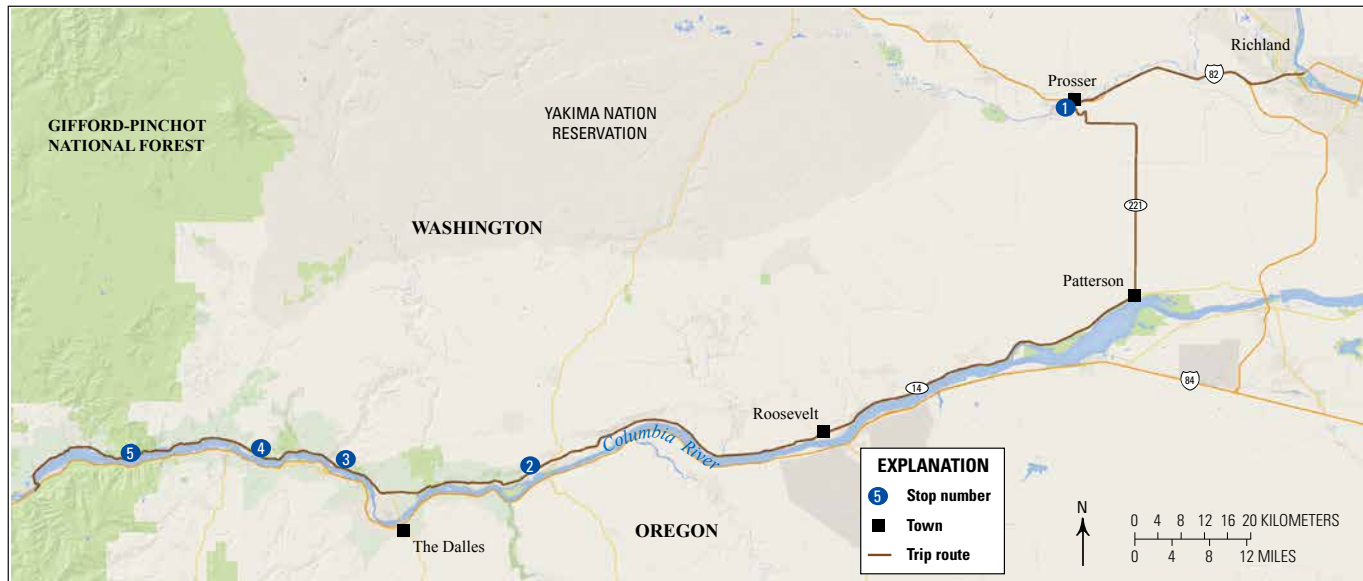


Figure 54. Map of field-trip stops for Day 7.

- 23.4 Take Prosser Exit 82. **12.9**
- 24.0 Left on Wine Country Road (formally U.S. 12). **1.4**
- 24.4 Turn left onto S.R. 22 **0.4**
- 24.9 Turn left on S.R. 221. The road now climbs to the crest of the Horse Heaven Hills. All the roadcuts you pass are landslides until the crest of the hill, which places the Elephant Mountain Member over a thick sedimentary interbed, which in turn overlies the Pomona Member. The sedimentary interbed consists of several paleosols and ash horizons. The ash is from the Cougar Point eruption in the Snake River Plain. **0.5**
- 27.6 Turn left into Yakima Valley Overlook. **3.2**
- Stop 1-D7: Folds of the Olympic-Wallowa Lineament** ($46.205988^\circ \text{ N}$, $119.706626^\circ \text{ W}$). This stop provides an opportunity to view Rattlesnake Mountain and the Rattlesnake Hills to the north, several of the small folds of the OWL that align with Rattlesnake Mountain, the Yakima Valley below, and Toppenish Ridge to the west. Near the crest of all the ridges, there is an abrupt increase in dip of the south slope up to the ridge crest. This increase in dip is due to displacement on the upper thrust fault on these ridges.
- Return to S.R. 221 and turn left.
- 50.9 Patterson, WA. Intersection of S.R. 221 and S.R. 14. Turn right onto S.R. 14, which now follows the Columbia Hills Fault Zone until reaching Stop 2-D7.
- The Columbia Hill anticline is an anomaly for a Yakima fold. Its fault zone is on the south side rather than north side like many other faults. **23.3**
- 56.9 Intersection with Mainline Road. S.R. 14 is now paralleling Canoe Ridge. **6.0**
- 63.2 Intersection with Sonova Road. Entrance to Crow Butte Park. Crow Butte State Park is part of a series of small anticlines that are associated with the Columbia Hills. The main ridge is to the north and a series of small anticlines lie south of the road. Continue west on S.R. 14. **6.3**
- 67.6 Exposures of the clastic sediments of the Selah interbed on the north (right) side of S.R. 14. **4.4**
- 69.0 Intersection with Alderdale Road. Continue west on S.R. 14. **1.4**
- 72.4 S.R. 14 crosses landslides developed on the Selah Interbed. Basalts of the Pomona and Elephant Mountain Members (Saddle Mountains Basalt) are exposed on the south side of the Columbia River. **3.4**
- 78.6 S.R. 14 crosses a breccia zone of the Columbia Hills Fault Zone. **6.2**
- 83.7 Entering the community of Roosevelt, Washington. **5.1**
- 84.0 Intersection with Roosevelt Grade Road. Exposures of the Priest Rapids Member (Wanapum Basalt) along S.R. 14. On the skyline north of the highway, basalt flows of the Pomona Member overlie Selah Formation sediments of the Ellensburg Formation,

- which in turn overlie Umatilla and Priest Rapids Member basalts. **0.3**
- Continue west on S.R.14.
- 90.2 Sundale Park. Arlington-Shetler Butte Anticline. Basalts of the Frenchman Springs Member (Wanapum Basalt) in roadcuts along the highway. **6.2**
- 98.1 Intersection with Rock Creek Road. **7.9**
- 103.8 Luna Butte Fault. Core of a doubly plunging anticline. **5.7**
- 110.9 John Day Dam turnoff. **7.1**
- 116.9 Stonehenge and Mary Hill State Park. **6.0**
- 117.8 U.S. 97 south. Go straight. **0.9**
- 118.3 Crossing U.S. 97 north. **0.5**
- 121.7 Stop 2-D7: Columbia Hills Fault Zone and 900 ka basalt of Haystack Butte flow** (45.669104° N, 120.890150° W). This stop lies within the Columbia River Gorge National Scenic Area. Exposed in the roadcut along the Columbia Hills Fault Zone is a basalt of Simcoe flow, which was erupted from a vent (Haystack Butte) atop the Columbia Hills. This lava flow traveled down the south flank of the Columbia Hills and flowed to the Columbia River, which was at essentially the same elevation as the modern (pre-dam) river; the columnar-jointed basalt at the eastern end of Miller Island (directly below us) is the distal end of the flow. A K-Ar whole rock age of 900 ± 100 ka has been obtained on this basalt flow (Anderson, 1987), indicating that the Columbia River valley had been incised to its present depth by this time. If you look to the northwest from this vantage point, you will see that this basalt of Simcoe flow advanced across a part of what appears to be a truncated alluvial fan before following a ravine down to river level. This truncated fan is one of many that have been mapped along the southern flanks of the Columbia Hills from Dallesport to Rock Creek. These deposits have not been studied in any detail, but the mapped relations indicate they pre-date the 900 ka Simcoe basalt flow. **3.4**
- 124.9 Wishram. **3.2**
- 126.3 Wishram Heights. **1.4**
- 129.7

Optional stop: Cross Laurel Fault and view

Fairbanks Gap. From this location we have an excellent view of Fairbanks Gap (Oregon side) and the Laurel Fault. Fairbanks Gap was created when Missoula floodwaters scoured-out the Laurel Fault Zone. A sketch of the Laurel Fault and stratigraphy at Fairbanks Gap from a detailed study of this feature by Anderson and Tolan (1986) is included as figure 55. Measured sections within the CRBG across this fault zone provided conclusive evidence that the Laurel Fault at this locality was active by 16–15 Ma. In addition, the Frenchman

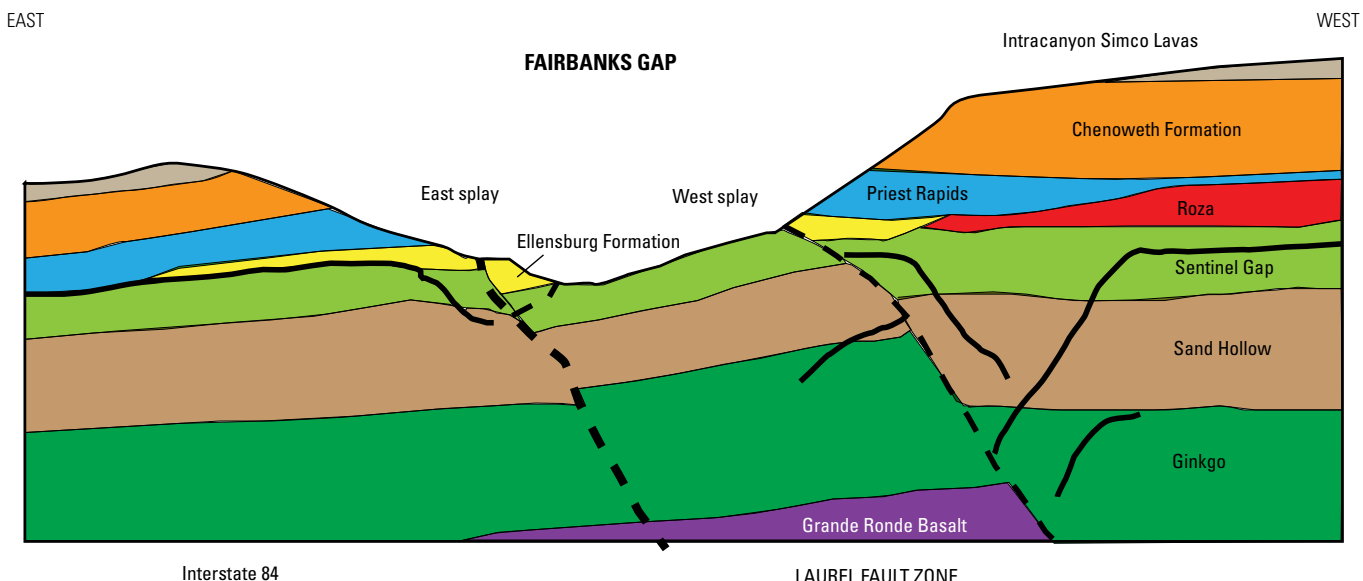


Figure 55. Diagram of the Laurel Fault Zone exposed along Interstate 84 at Fairbanks Gap, Oregon. Anderson and Tolan (1986) found evidence indicating that the fault formed during the time of emplacement of the Columbia River Basalt Group. They observed more than 15 percent thinning of the three Frenchman Springs Member flows: basalt of Ginkgo, basalt of Sand Hollow, and basalt of Sentinel Gap across the fault zone. These Frenchman Springs flows within the central block of the structure are more than 30 percent thinner than outside of the fault zone.

Springs Member thins by more than 15 percent across this fault zone. This thinning is interpreted to reflect contemporaneous deformation along the fault during the emplacement of the Frenchman Springs Member flows. Further evidence of deformation coeval with CRBG flow emplacement includes (1) Inclined basal colonnade in the basalt of Ginkgo flow (Frenchman Springs Member) on the west side of the western fault splay (fig. 55) at a buttress unconformity. Pre-15 Ma movement on the Laurel Fault created an upthrown central block of Sentinel Bluffs Member, Grande Ronde Basalt. The advancing basalt of Ginkgo flow engulfed the uplifted block. The western, near-vertical face of the fault block forms a perpendicular cooling surface that the Ginkgo columns propagated from as the flow cooled. (2) Only a thin (<1 cm thick) layer of sand and pebbles represents the Vantage Member (Ellensburg Formation) interbed within the Laurel Fault. Subsurface data from water wells away from the Laurel Fault suggest that the Vantage Member interbed is 1–6 m thick. These data also would suggest that the Laurel fault at this locality was topographically higher than the immediate surrounding area. Looking west from this location we can see where the Columbia Hills anticlinal ridge changes its structural geometry at the Laurel Fault. The geometry of the anticline reverses, with the asymmetrically steep limb

and frontal fault changing from the southern side to the northern side of the ridge across the Laurel Fault; this explains why we see the dramatic change in character and appearance of the CRBG across the Laurel Fault. 3.4

- 131.4 Basalt of Ginkgo flow. Note jointing style and vesicle sheets. 1.7
- 132.2 Dalles Garbage Dump Road. 0.8
- 133.7 Columbia Hills Historical State Park (formerly Horse Thief Lake State Park.). 1.5
- 134.8 Dalles Mountain Road. 1.1
- 135.7 Cross U.S. 197 south. 0.9
- 137.3 Murdock. 1.6
- 140.8 **Stop 3-D7: The Columbia Hills fault zone and anticline** (45.676817° N, 121.223267° W). At this locality we have an excellent view of the Columbia Hills anticline (a Yakima Fold Belt structure) where it has been bisected by the Columbia River (fig. 56). Our stop is where vertical beds of the Grande Ronde Basalt have been tilted along the Columbia Hills Fault Zone.

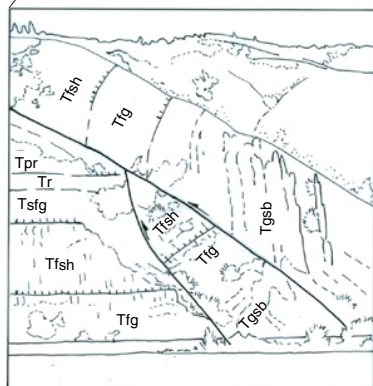
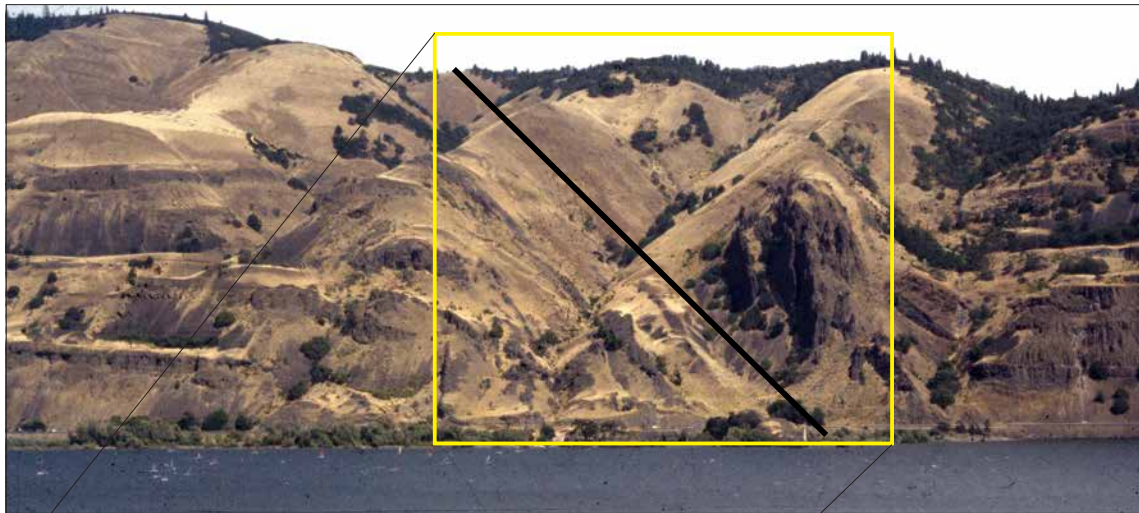


Figure 56. Columbia Hills Fault Zone as viewed from Stop 3 along Washington State Route 14. Grande Ronde Basalt on the north limb of the anticline along the fault has near-vertical dips. The Frenchman Springs Member is exposed at road level on the west; however, the Vantage and Frenchman Springs Member flows are 600 m higher along the crest of the Columbia Hills. Black line on the photograph is the fault. Inset drawing: Tgsb, Sentinel Bluffs Member; Tfg, basalt of Ginkgo; Tfsh, basalt of Sand Hollow; Tfsg, Sentinel Gap; Tr, Roza Member; Tpr, Priest Rapids Member.

- To our right (east) is Grande Ronde Basalt overlain by Frenchman Springs Member flows near the top of the ridge. To our left (west) are Frenchman Springs Member flows overlain by the Roza Member, Priest Rapids Member, all of the Wanapum Basalt, and in turn, overlain by the Pomona Member and sediment of the Chenoweth Formation. This water gap through the Columbia Hills was not initially incised by the ancestral Columbia River, but by the major tributary river (ancestral Snake River). It was not until about 6 million years ago that the ancestral Columbia River was captured farther east at Wallula Gap and began to follow this channel and use this water gap. Scouring of the lower half of the water gap's walls by the Pleistocene cataclysmic floods served to clean-off and accentuate the morphology of the CRBG flows. **3.5**
- 142.7 Lyle. **1.9**
- 145.3 Rest Area. **2.6**
- 148.9 Entering ancestral Columbia River channel. Pomona Member in roadcuts. **3.6**
- 149.7 **Stop 4-D7: Grande Ronde stratigraphy at Bingen Gap** (45.702066° N, 121.428622° W). At this stop, there is an excellent tilted exposure of the upper part of the Grande Ronde Basalt, consisting mainly of Grouse Creek member at the base (to the west), the Winter Water Member, and the Sentinel Bluffs Member (fig. 57). The entire section has been measured and collected for geochemical composition by M. Beeson, C. Fecht, S. Reidel, and T. Tolan. In addition, the section has been drilled for paleomagnetic declination and inclination, which was reported by Wells and others (1989). The Sentinel Bluffs Member section here has been described by Reidel (2005); it is 110 m thick compared to 330 m at Sentinel Gap (fig. 53). Throughout much of the Columbia Basin, the Sentinel Bluffs Member is relatively consistent, with the basal flows being composed of the McCoy Canyon compositional type and the upper flows being composed of the Museum compositional type. Between the two types at Sentinel Gap, the Cohassett flow records an inflation event consisting of four compositional types. However, here, the flows between the Museum and McCoy Canyon types are far more complex, suggesting that the flows consisting of the four compositional types at Sentinel Gap probably arrived at Bingen at about the same time, creating a more chaotic composition in the section. As we proceed along this road, we will pass through two flows of the Winter Water Member and then several flows of the Ortley and Grouse Creek members. **0.8**
- 153.9 Bingen. **4.2**
- 154.2 Hood River Toll Bridge and Rest Area. **0.3**
- 155.8 S.R. 141. White Salmon River. Continue on S.R. 14. **1.6**
- 158.6 View to left of Mitchell Point (fig. 58). Intracanyon Pomona Member.
- View of Mitchell Point on the Oregon side of the Columbia River. Mitchell Point provides a natural cross-section through the southern half of the ancestral Columbia River canyon, which was partly filled by the intracanyon flow of the Pomona Member (Anderson, 1980; Tolan and Beeson, 1984; Anderson and Vogt, 1987). The Pomona Member at Mitchell Point appears to have been advancing down a relatively dry canyon (Anderson and Vogt, 1987), with only occasional hyaloclastic deposits found at the margin of the flow. These minor hyaloclastites appear to have been created when the Pomona intracanyon flow encountered small tributary streams. **2.8**
- 165.6 **Stop 5-D7: Base of Grande Ronde Basalt section exposing flows of the Teepee Butte Member** (45.699364° N, 121.708790° W). Park at Dog Mountain trailhead. Walk back along S.R. 14 (east) approximately 800 m (0.5 mi). Be careful of traffic.
- Dog Mountain exposes more than 1,200 m of Grande Ronde Basalt and is the only known surface exposure that contains flows belonging to all four Grande Ronde MSUs (fig. 57; Anderson, 1987). The oldest R1 Grande Ronde flows exposed at Dog Mountain belong to the Teepee Butte Member. This locality is an excellent place to examine the intraflow structures displayed in the distal part of Teepee Butte flow. Below the thin (<0.3 m) tuffaceous interbed, three Pruitt Draw flows are exposed. Note that they display either entablature/colonnade or blocky jointing patterns. The structure and thickness of flow tops found here are not significantly different from those displayed by these same flows in the eastern part of the flood-basalt province (Stop 8-D4; Reidel and Tolan, 1992). The one exception is the presence of secondary minerals filling vesicles and vugs; these secondary minerals are related to geothermal systems created by Cascadian volcanism (Beeson and Moran, 1979). These flows appear to lack internal features that would suggest they were tube- or conduit-fed flows. **7.0**
- 167.9 Town of Home Valley. **2.3**
- 169.9 Bridge over Wind River. **2.0**
- 172.9 Stevenson. **3.0**
- 177.8 Bridge of the Gods Exit on I-84 Turn left onto Bridge of the Gods. Cascade Locks. Enter I-84 west.

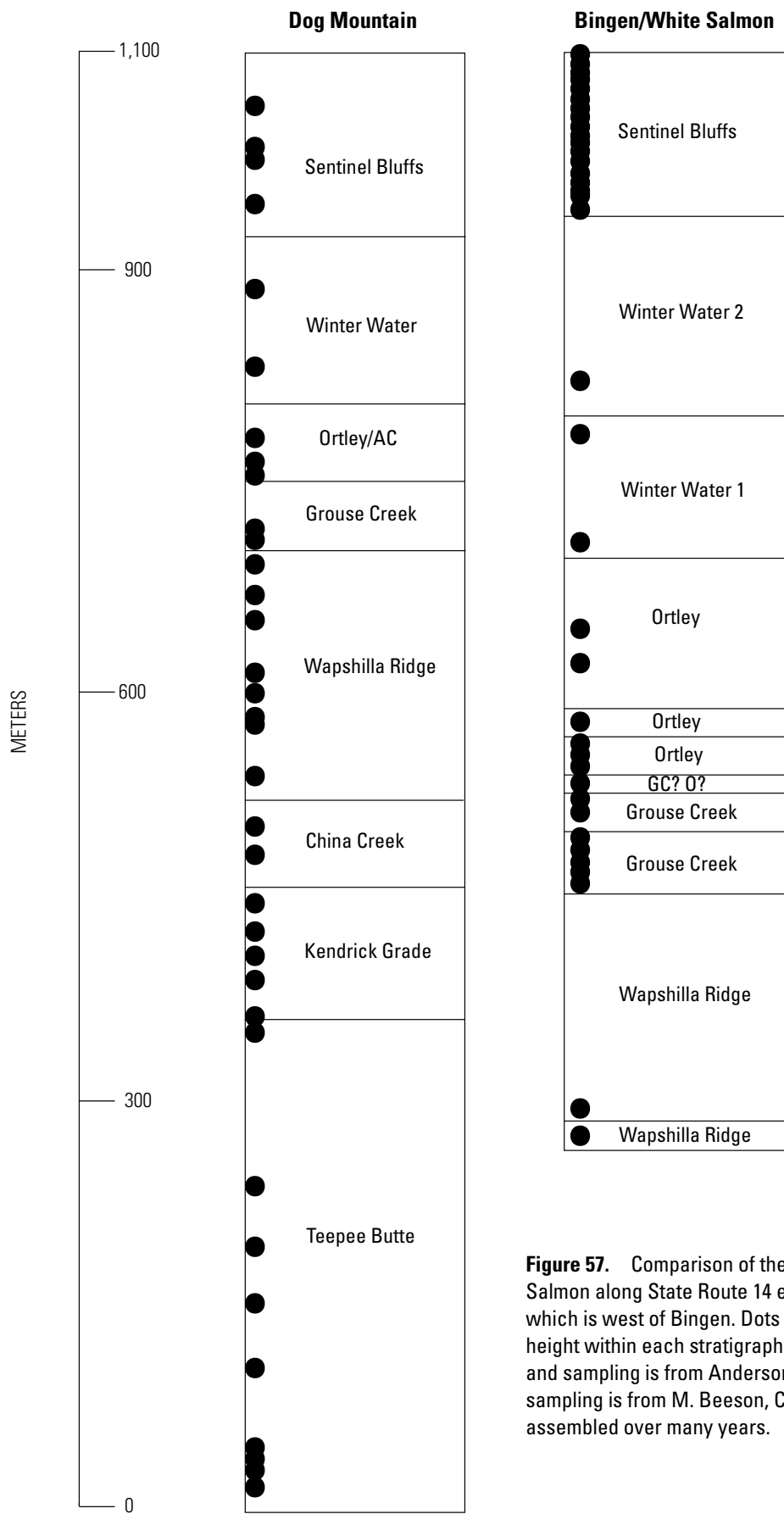


Figure 57. Comparison of the stratigraphy from Bingen/White Salmon along State Route 14 east of Bingen, and Dog Mountain, which is west of Bingen. Dots show x-ray fluorescence sampling height within each stratigraphic unit. Dog Mountain section and sampling is from Anderson (1987). Bingen stratigraphy and sampling is from M. Beeson, C. Fecht, S. Reidel, and T. Tolan, assembled over many years.

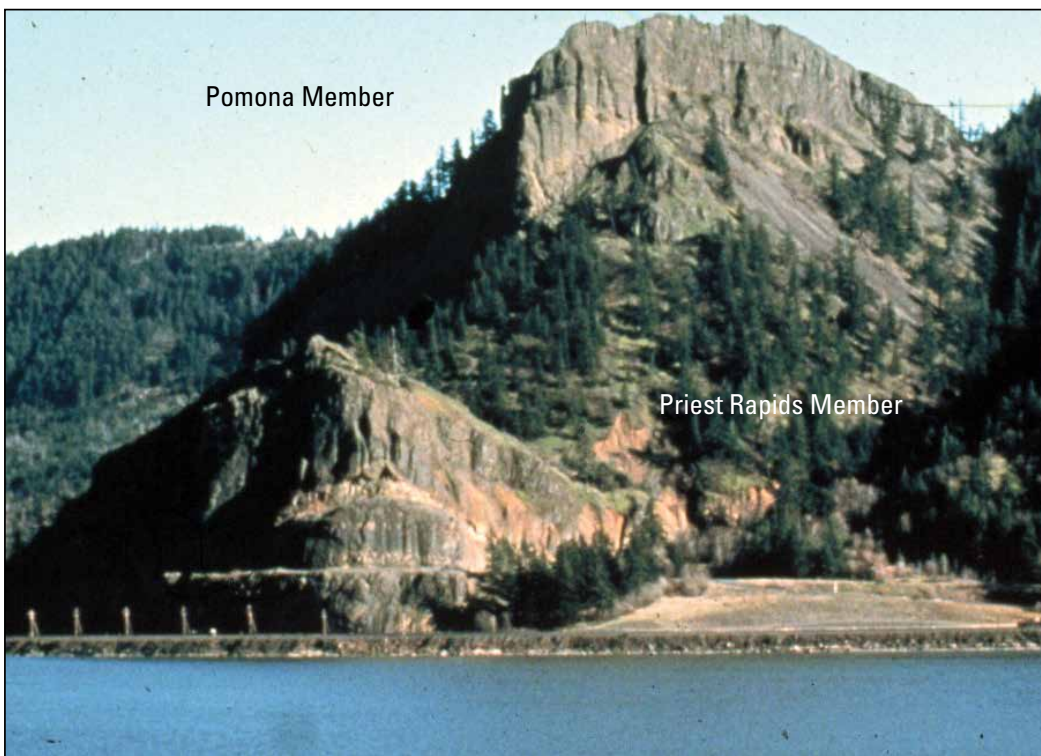


Figure 58. Photograph of Mitchell Point, viewed across the river from Washington State Route 14. Mitchell Point is located south of the Columbia River along Interstate 84 and is composed of intracanyon Priest Rapids Member and intracanyon Pomona Member (Tolan and Beeson, 1984).

References Cited

- Alloway, M.R., Watkinson, A.J., and Reidel, S.P., 2013, A serial cross-section analysis of the Lewiston Structure, Clarkston, Washington, and implications for the evolution of the Lewiston Basin, in Reidel, S.P., Camp, V.E., Ross, M.E., Wolff, J.A., Martin, B.S., Tolan, T.L., and Wells, R.E., eds., The Columbia River Flood Basalt Province: Geological Society of America Special Paper 497, p. 349–362.
- Anderson, J.L., 1980, Pomona Member of the Columbia River Basalt Group—An intracanyon flow in the Columbia River Gorge, Oregon: Oregon Geology, v. 42, p. 195–199.
- Anderson, J.L., 1987, Structural geology and ages of deformation of a portion of the southwest Columbia Plateau: Los Angeles, University of Southern California, Ph.D. dissertation, 283 p.
- Anderson, J.L., and Tolan, T.L., 1986, Ages of wrench faulting in interridge basins, southwest Columbia Plateau, Washington and Oregon [abs.]: Geological Society of America Abstracts with Programs, v. 18, no. 2, p. 82.
- Anderson, J.L., and Vogt, B.F., 1987, Intracanyon flows of the Columbia River Basalt Group in the southwestern part of the Columbia Plateau and adjacent Cascade Range, Oregon and Washington, in Schuster, J.E., ed., Selected papers on the geology of Washington: Washington Division of Geology and Earth Resources, Bulletin 77, p. 249–267.
- Bacon, C.R., and Lanphere, M.A., 2006, Eruptive history and geochronology of Mount Mazama and the Crater Lake region, Oregon: Geological Society of America Bulletin, v. 118, p. 1331–1359. doi:10.1130/B25906.1
- Bailey, M.M., 1989, Revisions to stratigraphic nomenclature of the Picture Gorge Basalt subgroup, Columbia River Basalt Group, in Reidel, S.P., and Hooper, P.R., eds., Volcanism and tectonism in the Columbia River flood-basalt province: Geological Society of America Special Paper 239, p. 67–84.
- Baksi, A.K., 2013, Timing and duration of volcanism in the Columbia River Basalt Group—A review of existing radiometric data and new constraints on the age of the Steens through Wanapum Basalt extrusion, in Reidel, S.P., Camp, V.E., Ross, M.E., Wolff, J.A., Martin, B.S., Tolan, T.L., and Wells, R.E., eds., The Columbia River Flood Basalt Province: Geological Society of America Special Paper 497, p. 67–86.

- Barry, T.L., Kelley, S.P., Reidel, S.P., Camp, V.E., Self, S., Jarboe, N.A., Duncan, R.A., and Renne, P.R., 2013, Eruption chronology of the Columbia River Basalt Group, in Reidel, S.P., Camp, V.E., Ross, M.E., Wolff, J.A., Martin, B.S., Tolan, T.L., and Wells, R.E., eds., The Columbia River Flood Basalt Province: Geological Society of America Special Paper 497, p. 45–66, doi: 10.1130/2013.2497(02).
- Barry, T.L., Self, S., Kelley, S.P., Reidel, S.P., Hooper, P.R., and Widdowson, M., 2010, New $^{40}\text{Ar}/^{39}\text{Ar}$ dating of the Grande Ronde lavas, Columbia River Basalts, USA—Implications for duration of flood basalt eruption episodes: *Lithos*, v. 118, no. 3–4, p. 213–222, doi:10.1016/j.lithos.2010.03.014.
- Beeson, M.H., Fecht, K.R., Reidel, S.P., and Tolan, T.L., 1985, Correlations within the Frenchman Springs Member of the Columbia River Basalt Group—New insights into the middle Miocene tectonics of northwest Oregon: *Oregon Geology*, v. 47, p. 87–96.
- Beeson, M.H., and Moran, M.R., 1979, Stratigraphy and structure of the Columbia River Basalt Group in the Cascade Range, Oregon, in Geothermal resource assessment of Mount Hood, final report: State of Oregon Department of Geology and Mineral Industries Report RLO-1040, p. 5–77.
- Beeson, M.H., Perttu, R., and Perttu, J., 1979, The origin of the Miocene basalt of coastal Oregon and Washington: *Oregon Geology*, v. 41, p. 159–166.
- Benson, T.R., and Mahood, G.A., 2016, Geology of the mid-Miocene Rooster Comb caldera and Lake Owyhee Volcanic Field, eastern Oregon—Silicic volcanism associated with Grande Ronde flood basalt: *Journal of Volcanology and Geothermal Research*, p. 96–117, doi: 10.1016/j.jvolgeores.2015.11.011.
- Benson, T.R., Mahood, G.A., and Coble, M.A., 2013, An intense 16.5–16 Ma episode of rhyolitic volcanism associated with flood basalt dike emplacement at McDermitt caldera field and High Rock caldera complex, Nevada and Oregon [abs.]: American Geophysical Union, no. V33E-2828.
- Benson T.R., Mahood, G.A., Coble, M.A., and Grove, M.J., 2016, New geological mapping and $^{40}\text{Ar}/^{39}\text{Ar}$ geochronology demonstrate that rhyolite volcanism mirrors northward propagation of mid-Miocene Columbia River Flood Basalts [abs.]: Geological Society of America Abstracts with Programs, v. 48, no. 3-2.
- Best, M.G., Christiansen, E.H., Deino, A.L., Gromm, C.S., McKee, E.H., and Noble, D.C., 1989, Excursion 3A-Eocene through Miocene volcanism in the Great Basin of the western United States, in Chapin, C.E., and Zidek, J., eds., Field excursions to volcanic terrains in the western United States, Volume I- Cascades and intermountain west: New Mexico Bureau of Mines and Mineral Resources Memoir 47, p. 91–133.
- Bina, C.R., and Helffrich, G., 1994, Phase-transition clapeyron slopes and transition zone seismic discontinuity topography: *Journal of Geophysical Research*, v. 99, p. 15853–15860, doi:10.1029/94JB00462.
- Binger, G.B., 1997, The volcanic stratigraphy of the Juntura region, eastern Oregon: Pullman, Washington State University, Ph.D. dissertation, 176 p.
- Bingham, J.W., and Grolier, M.J., 1966, The Yakima Basalt and Ellensburg Formation of south-central Washington: U.S. Geological Survey Bulletin 12224-G, p. G1–G15.
- Blakely, R., Sherrod, B.L., Weaver, C.S., Wells, R.E., and Rohay, A.C., 2014, The Wallula fault and tectonic framework of south-central Washington, as interpreted from magnetic and gravity anomalies: *Tectonophysics*, v. 624, p. 32–45.
- Blakely, R., Sherrod, B.L., Weaver, C.S., Wells, R.E., Rohay, A.C., Barnett, E.A., and Knepprath, N.E., 2011, Connecting the Yakima fold and thrust belt to active faults in the Puget Lowland, Washington: *Journal of Geophysical Research*, v. 116, B07105.
- Bondre, N.R., and Hart, W.K., 2008, Morphological and textural diversity of the Steens Basalt lava flows, southeastern Oregon, USA—Implications for emplacement style and nature of eruptive episodes: *Bulletin of Volcanology*, v. 70, p. 999–1019, doi:10.1007/s00445-007-0182-x.
- Brandon, A.D., and Goles, G.G., 1988, A Miocene subcontinental plume in the Pacific Northwest—Geochemical evidence: *Earth and Planetary Science Letters*, v. 88, p. 273–283.
- Brandon, A.D., and Goles, G.G., 1995, Assessing subcontinental lithospheric mantle sources for basalts—Neogene volcanism in the Pacific Northwest, USA as a test case: *Contributions to Mineralogy and Petrology*, v. 212, p. 364–379.
- Brandon, A.D., Hooper, P.R., Goles, G.G., and Lambert, R., 1993, Evaluating crustal contamination in continental basalts—The isotopic composition of Picture Gorge Basalt of the Columbia River Basalt Group: *Contributions to Mineralogy and Petrology*, v. 114, p. 452–464, doi:10.1007/BF003321750.
- Brown, R.J., Blake, S., Thordarson, T., and Self, S., 2014, Pyroclastic edifices record vigorous lava fountains during the emplacement of a flood basalt flow field, Roza Member, Columbia River Basalt Province, USA: *Geological Society of America Bulletin*, v. 126, p. 875–891. [Also available at <http://dx.doi.org/10.1130/B30857.1>.]
- Brown, R.J., Thordarson, T., Self, S., and Blake, S., 2015, Disruption of tephra fall deposits caused by lava flows during basaltic eruptions: *Bulletin of Volcanology*, v. 77, 15 p.
- Brueske, M.E., and Hart, W.K., 2008, Geology and petrology of the mid-Miocene Santa Rosa-Calico volcanic field, northern Nevada: Nevada Bureau of Mines and Geology Bulletin 113, 44 p.

- Burov, E., and Guillou-Frottier, L., 2005, The plume head–continental lithosphere interactions using a tectonically realistic formulation for the lithosphere: *Geophysical Journal International*, v. 161, p. 469–490, doi:10.1111/j.1365-246X.2005.02588.x.
- Burov, E., Guillou-Frottier, L., d’Acremont, E., Le Pourhet, L., and Cloetingh, S., 2007, Plume head–lithosphere interactions near intra-continental plate boundaries: *Tectonophysics*, v. 434, p. 15–38, doi: 10.1016/j.tecto.2007.01.002.
- Camp, V.E., 1976, Petrochemical stratigraphy and structure of the Lewiston Basin area: Pullman, Washington State University, Ph.D. dissertation, 201 p.
- Camp, V.E., 1981, Upper Miocene basalt distribution, reflecting source locations, tectonism, and drainage history in the Clearwater Embayment, Idaho: *Geological Society of America Bulletin*, v. 92, p. 669–678.
- Camp, V.E., 1995, Mid-Miocene propagation of the Yellowstone mantle plume head beneath the Columbia River Basalt source region: *Geology*, v. 23, p. 435–438.
- Camp, V.E., 2013, Origin of Columbia River Basalt—Passive rise of shallow mantle, or active upwelling of a deep-mantle plume, *in* Reidel, S.P., Camp, V.E., Ross, M.E., Wolff, J.A., Martin, B.S., Tolan, T.L., and Wells, R.E., eds., *The Columbia River Flood Basalt Province: Geological Society of America Special Paper 497*, p., 181–199, doi: 10.1130/2013.2497(04).
- Camp, V.E., and Hanan, B.B., 2008, A plume-triggered delamination origin for the Columbia River Basalt Group: *Geosphere*, v. 4, p. 480–495.
- Camp, V.E., and Hooper, P.R., 1981, Geologic studies of the Columbia Plateau: Part I. Late Cenozoic evolution of the southeast part of the Columbia River Basalt Province: *Geological Society of America Bulletin*. v. 92, p. 659–668, doi:10.1130/0016-7606(1981)92<659:GSOTP>2.0.CO;2.
- Camp, V.E., Hooper, P.R., Swanson, D.A., and Wright, T.L., 1982, Columbia River Basalt in Idaho—Physical and chemical characteristics, flow distribution and tectonic implications, *in* Bonnichsen, B., and Breckenridge, R.M., eds., *Cenozoic geology of Idaho*: Idaho Bureau of Mines and Geology Bulletin 26, p. 55–75.
- Camp, V.E., Pierce, K.L., and Morgan, L.A., 2015, Yellowstone plume trigger for Basin and Range extension, and coeval emplacement of the Nevada–Columbia Basin magmatic belt: *Geosphere*, v. 11, doi:10.1130/GES01051.1.
- Camp, V.E., and Ross, M.E., 2004, Mantle dynamics and genesis of mafic magmatism in the intermontane Pacific Northwest: *Journal of Geophysical Research*, v. 109, B08204, doi: 10.1029/2003JB002838.
- Camp, V.E., Ross, M.E., Duncan, R.A., Jarboe, N.A., Coe, S.C., Hanan, B.B., and Johnson, J.A., 2013, The Steens Basalt—Earliest lavas of the Columbia River Basalt Group, *in* Reidel, S.P., Camp, V.E., Ross, M.E., Wolff, J.A., Martin, B.S., Tolan, T.L., and Wells, R.E., eds., *The Columbia River Flood Basalt Province: Geological Society of America Special Paper 497*, p. 87–116, doi: 10.1130/2013.2497(04).
- Camp, V.E., Ross, M.E., and Hanson, W.E., 2003, Genesis of flood basalts and Basin and Range volcanic rocks from Steens Mountain to the Malheur River Gorge, Oregon: *Geological Society of America Bulletin*, v. 115, p. 105–128.
- Campbell, I.H., 2005, Large igneous provinces and the mantle plume hypothesis: *Elements*, v. 1, p. 265–269.
- Carlson, R.W., 1984, Isotopic constraints on Columbia River flood basalt genesis and the nature of subcontinental mantle: *Geochimica et Cosmochimica Acta*, v. 48, p. 2357–2372.
- Carlson, R.W., and Hart, W.K., 1987, Crustal genesis on the Oregon Plateau: *Journal of Geophysical Research*, v. 92, p. 6191–6206.
- Carlson, R.W., Lugmair, G.W., and MacDougall, J.D., 1981, Columbia River volcanism—The question of mantle heterogeneity or crustal contamination: *Geochimica et Cosmochimica Acta*, v. 45, p. 2483–2499.
- Church, S.E., 1985, Genetic interpretation of lead-isotopic data from the Columbia River Basalt Group, Oregon, Washington, and Idaho: *Geological Society of America Bulletin*, v. 96, p. 676–690.
- Coble, M.A., and Mahood, G.A., 2012, Initial impingement of the Yellowstone plume located by widespread silicic volcanism contemporaneous with Columbia River flood basalts: *Geology*, v. 40, p. 655–658, doi:20.2230/G32692.2.
- Coble, M.A., and Mahood, G.A., 2015, Geology of the High Rock caldera complex, northwest Nevada and implications for intense rhyolitic volcanism associated with flood basalt magmatism and the initiation of the Snake River Plain–Yellowstone trend: *Geosphere*, v. 12, doi: 10.1130/GES01162.1.
- Colgan, J.P., 2013, Reappraisal of the relationship between the northern Nevada rift and Miocene extension in the northern Basin and Range Province: *Geology*, v. 41, p. 211–214, doi: 10.1130/G33512.1.
- Colgan, J.P., Dumitru, T.A., McWilliams, M., and Miller, E.L., 2006, Timing of Cenozoic volcanism and Basin and Range extension in northwestern Nevada—New constraints from the northern Pine Forest Range: *Geological Society of America Bulletin*, v. 118, p. 126–139, doi: 10.1130/B25681.1.
- Colgan, J.P., Dumitru, T.A., and Miller, E.L., 2004, Diachroneity of Basin and Range extension and Yellowstone hotspot volcanism in northwestern Nevada: *Geology*, v. 32, p. 121–124, doi:10.1130/G20037.1.

- Cummings, M.L., Evans, J.G., Ferns, M.L., and Lees, K.R., 2000, Stratigraphic and structural evolution of the middle Miocene synvolcanic Oregon-Idaho graben: Geological Society of America Bulletin, v. 112, p. 668–682.
- Darold, A., and Humphreys, E., 2013, Upper mantle seismic structure beneath the Pacific Northwest—A plume-triggered delamination origin for the Columbia River flood basalt eruptions: Earth and Planetary Science Letters v. 365, p. 232–242.
- Davis, K., Wolff, J.A., Rowe, M.C., Boroughs, S., and Self, S., 2013, Flood lavas of R2 magnetostratigraphic interval of Grande Ronde Basalt: new investigations into stratigraphy, eruption mechanisms and volatile release [abs.]: American Geophysical Union, Fall meeting, no. V41D-2844.
- Dickinson, W.R., 1997, Overview—Tectonic implications of Cenozoic volcanism in coastal California: Geological Society of America Bulletin, v. 109, p. 936–954.
- Dodson, A., Kennedy, B.M., and DePaolo, D.J., 1997, Helium and neon isotopes in the Imnaha Basalt, Columbia River Basalt Group—Evidence for a Yellowstone plume source: Earth and Planetary Science Letters, v. 150, p. 443–451.
- Draper, D.S., 1991, Late Cenozoic bimodal magmatism in the northern Basin and Range Province of southeastern Oregon: Journal of Volcanology and Geothermal Research, v. 47, p. 299–328, doi:10.1016/0377-0273(91)90006-L.
- Duncan, R.A., 1982, A captured island chain in the Coast Range of Oregon and Washington: Journal of Geophysical Research, v. 87, p. 10827–10837.
- Eagar, K.C., Fouch, M.J., James, D.E., and Carlson, R.W., 2011, Crustal structure beneath the High Lava Plains of eastern Oregon and surrounding regions from receiver function analysis: Journal of Geophysical Research, v. 116, B02313.
- Evans, J.G., 1992, Geologic map of the Dooley Mountain quadrangle, Baker County, Oregon: U.S. Geological Survey Geologic Quadrangle Map GQ-1694, scale 1:24,000.
- Evans, J.G., and Geisler, T.M., 2001, Geologic field-trip guide to Steens Mountain Loop Road, Harney County, Oregon: U.S. Geological Survey Bulletin 2183, 15 p.
- Faccenna, C., Becker, T.W., Lallemand, S., Lagabrielle, Y., Funiciello, F., and Piromallo, C., 2010, Subduction-triggered magmatic pulses—A new class of plumes?: Earth and Planetary Science Letters, v. 299, p. 54–68, doi:10.1016/j.epsl.2010.08.012.
- Ferns, M.L., Brooks, H.C., Evans, J.G., and Cummings, M.L., 1993, Geologic map of the Vale 30° x 60° quadrangle, Malheur County Oregon and Owyhee County, Idaho: Oregon Department of Geology and Mineral Industries Reconnaissance Map Series RMS-1, scale 1:100,000.
- Ferns, M.L., and McClaughry, J.D., 2013, Stratigraphy and volcanic evolution of the middle Miocene to Pliocene La Grande-Owyhee eruptive axis, in Reidel, S.P., Camp, V.E., Ross, M.E., Wolff, J.A., Martin, B.S., Tolan, T.L., and Wells, R.E., eds., The Columbia River Flood Basalt Province: Geological Society of America Special Paper 497, p. 401–427, doi: 10.1130/2013.2497(16).
- Ferns, M.L., McConnell, V.S., Madin, I.P., and Johnson, J.A., 2010, Geology of the upper Grande Ronde River basin, Union County, Oregon: Oregon Department of Geology and Mineral Industries Bulletin 107, scale 1:100,000, 65 p.
- Ford, M.T., Grunder, A.L., and Duncan, R.A., 2013, Bimodal volcanism of the High Lava Plains and northwestern Basin and Range of Oregon—Distribution and tectonic implications of age-progressive rhyolites: Geochemistry, Geophysics, Geosystems, v. 14, p. 2836–2857, doi:10.1002/gg.20175.
- Geist, D., and Richards, M., 1993, Origin of the Columbia Plateau and Snake River plain—Deflection of the Yellowstone plume: Geology, v. 21, p. 789–792.
- Glazner, A.F., 2007, Thermal limitations on incorporation of wall rock into magma: Geology, v. 35, p. 319–322.
- Goff, F., 1996, Vesicle cylinders in vapor-differentiated basalt flows: Journal of Volcanology and Geothermal Research, v. 71, p. 167–185, doi:10.1016/0377-0273(95)00073-9.
- Gradstein, F., Ogg, J., and Smith, A., 2004, A geologic time scale: Cambridge, UK, Cambridge University Press, 589 p.
- Graham, D.W., Reid, M.R., Jordan, B.T., Grunder, A.L., Leeman, W.P., and Lupton, J.E., 2009, Mantle source provinces beneath the northwestern USA delimited by helium isotopes in young basalts: Journal of Volcanology and Geothermal Research, v. 199, p. 128–140, doi:10.1016/j.volgeores.2008.12.004.
- Greene, R.C., 1973, Petrology of the welded tuff of Devine Canyon, southeastern Oregon: U.S. Geological Survey Professional Paper 792, 26 p.
- Grolier, M.J., and Bingham, J.W., 1971, Geologic map and section of parts of Grant, Adams, and Franklin Counties, Washington: U.S. Geological Survey Miscellaneous Investigations Map I-589, 6 sheets, scale 1:62,500.
- Grolier, M.J., and Bingham, J.W., 1978, Geology of parts of Grant, Adams, and Franklin Counties, east-central Washington: Washington Division of Geology and Earth Resources Bulletin 71, 91 p.
- Gunn, B.M., and Watkins, N.D., 1970, Geochemistry of the Steens Mountain Basalts, Oregon: Geological Society of America Bulletin, v. 81, p. 1497–1516, doi:10.1130/0016-7606(1970)81(1497:GOTSMB)2.0;CO.2.

- Hagstrum, J.T., Sawlan, M., Wells, R.E., Evarts, R.C., and Neim, A.R., 2010, New paleomagnetic and geochemical reference sections in Miocene Grande Ronde Basalt flows on the Columbia Plateau are fundamental to stratigraphic, structural, and tectonic studies in the Portland Metro area and coast ranges of Oregon and Washington [abs.]: American Geophysical Union, no. GP11A-0745.
- Hales, T.C., Abt, D.L., Humphreys, E.D., and Roering J.J., 2005, A lithospheric instability origin for Columbia River flood basalts and Wallowa Mountains uplift in northeast Oregon: *Nature*, v. 438, p. 842–845.
- Hart, W.K., and Carlson, R.W., 1987, Tectonic controls on magma genesis and evolution in the northwestern United States: *Journal of Volcanology and Geothermal Research*, v. 32, p. 119–135.
- Hemphill-Haley, M.A., Page, W.D., Burke, R., and Carver, G.A., 1989, Holocene activity of the Alvord fault, Steens Mountain, southeastern Oregon: Technical report to Woodward-Clyde Consultants, under Contract Grant No. 14-08-0001-G1333, 45 p.
- Ho, A.M., and Cashman, K.V., 1997, Temperature constraints on the Ginkgo flow of the Columbia River Basalt Group: *Geology*, v. 25, p. 403–406. [Also available at [http://dx.doi.org/10.1130/0091-7613\(1997\)025<0403:TCOTGF>2.3.CO;2](http://dx.doi.org/10.1130/0091-7613(1997)025<0403:TCOTGF>2.3.CO;2).]
- Hon, K., Kauahikaua, J., Denlinger, R., and MacKay, K., 1994, Emplacement and inflation of pahoehoe sheet flows—Observations and measurements of active lava flows on Kilauea Volcano, Hawaii: *Geological Society of America Bulletin*, v. 106, p. 351–370. [Also available at [http://dx.doi.org/10.1130/0016-7606\(1994\)106<0351:EAIOPS>2.3.CO;2](http://dx.doi.org/10.1130/0016-7606(1994)106<0351:EAIOPS>2.3.CO;2).]
- Hooper, P.R., 1985, A case of simple magma mixing in the Columbia River Basalt Group—The Wilbur Creek, Lapwai, and Asotin flows, Saddle Mountains formation: *Contributions to Mineralogy and Petrology*, v. 91, p. 66–73.
- Hooper, P.R., 2000, Chemical discrimination of Columbia River basalt flows: *Geochemistry, Geophysics, Geosystems*, v. 1, doi: 10.1029/2000GC000040.
- Hooper, P.R., Binger, G.B., and Lees, K.R., 2002, Ages of the Steens and Columbia River flood basalts and their relationship to extension-related calc-alkaline volcanism in eastern Oregon: *Geological Society of America Bulletin*, v. 114, p. 43–50.
- Hooper, P.R., and Camp, V.E., 1981, Deformation of the southeast part of the Columbia Plateau: *Geology*, v. 9, p. 323–328.m
- Hooper, P.R., Camp, V.E., Reidel, S.P., and Ross, M.E., 2007, The origin of the Columbia River flood basalt province—Plume versus nonplume models, *in* Foulger, G.R., and Jurdy, D.M., eds., *Plates, plumes, and planetary processes: Geological Society of America Special Paper* 430, p. 635–668.
- Hooper, P.R., and Conrey, R.M., 1989, A model for the tectonic setting of the Columbia River basalt eruptions *in* Reidel, S.P., and Hooper, P.R., *Volcanism and tectonism in the Columbia River Flood Basalt Province: Geological Society of America Special Paper* 239, p. 21–53.
- Hooper, P.R., Gillespie, B.A., and Ross, M.E., 1995, The Eckler Mountain basalts and associated flows, Columbia River Basalt Group: *Canadian Journal of Earth Sciences*, v. 33, p. 410–423.
- Hooper, P.R., and Hawkesworth, C.J., 1993, Isotopic and geochemical constraints on the origin and evolution of the Columbia River Basalts: *Journal of Petrology*, v. 34, p. 1203–1246.
- Hooper, P.R., Kleck, W.D., Knowles, C.R., Reidel, S.P., and Thiessen, R.L., 1984, Imnaha Basalt, Columbia River Basalt Group: *Journal of Petrology*, v. 25, p. 473–500.
- Humphreys, E., and Schmandt, B., 2011, Looking for mantle plumes: *Physics Today*, v. 64, no. 8, p. 34–41, doi:10.1063/PT.3.1217.
- James, D.E., Fouch, M.J., Carlson, R.W., and Roth, J.B., 2011, Slab fragmentation, edge flow and the origin of the Snake River Plain hotspot track: *Earth and Planetary Science Letters*, v. 311, p. 124–135, doi:10.1016/j.epsl.2011.09.007.
- Jarboe, N.A., Coe, R.S., Renne, P.R., and Glen, J.M.G., 2010, The age of the Steens reversal and the Columbia River Basalt Group: *Chemical Geology*, v. 274, p. 158–168, doi: 10.1016/j.chemgeo.2010.04.001.
- Jarboe, N.A., Coe, R.S., Renne, P.R., Glen, J.M.G., and Mankinen, E.A., 2008, Quickly erupted volcanic sections of the Steens Basalt, Columbia River Basalt Group—Secular variation, tectonic rotation, and the Steens Mountain reversal: *Geochemistry, Geophysics, Geosystems*, v. 9, doi: 10.1029/2008GC002067.
- John, D.A., Wallace, A.R., Ponce, D.A., Fleck, R., and Conrad, J.E., 2000, New perspectives on the geology and origin of the northern Nevada rift, *in* Cluer, J.K., Price, J.G., Struhsacker, E.M., Hardiman, R.F., and Morris, C.L., eds., *Geology and ore deposits 2000—The Great Basin and beyond, 2000 Symposium Proceedings*: Reno, Nevada, Geological Society of Nevada, p. 127–154.
- Johnson, J.A., 1994, Geologic map of the Kurmbo Reservoir quadrangle, Harney County, southeastern Oregon: U.S. Geological Survey Map MF-2267.
- Johnson, J.A., 1995, Geologic evolution of the Duck Creek Butte eruptive center, High Lava Plains, southeastern Oregon: Corvallis, Oregon, Oregon State University, M.S. thesis, 151 p.
- Johnson, J.A., Hawkesworth, C.J., Hooper, P.R., and Binger, G.B., 1998, Major- and trace-element analyses of Steens Basalt, southeastern Oregon: U.S. Geological Survey Open-File Report 98-482, 30 p.

- Jordan, B.T., 2005, Age-progressive volcanism of the Oregon High Lava Plains—Overview and evaluation of tectonic models, in Foulger, G.R., Natland, J.H., Presnall, D.C., and Anderson, D.L., eds., Plates, plumes, and paradigms: Geological Society of America Special Paper 388, p. 503–515, doi:10.1130/2005.2388(30).
- Jordan, B.T., Grunder, A.L., Duncan, R.A., and Deino, A.L., 2004, Geochronology of age-progressive volcanism of the Oregon High Lava Plains—Implications for plume interpretation of Yellowstone: Journal of Geophysical Research, v. 109, doi: 10.1029/2003JB002776.
- Kauffman, J.D., Garwood, D.L., Schmidt, K.L., Lewis, R.S., Othberg, K.L., and Phillips, W.M., 2009, Geologic map of the Idaho parts of the Orofino and Clarkston 30 x 60 Minute quadrangles, Idaho: Idaho Geological Survey Geologic Map 48, scale 1:100,000.
- Keszthelyi, L., and Self, S., 1998, Some physical requirements for the emplacement of long basaltic lava flows: Journal of Geophysical Research, v. 103, p. 27447–27464. [Also available at <http://dx.doi.org/10.1029/98JB00606>.]
- Keszthelyi, L., Self, S., and Thordarson, T., 2006, Flood lavas on Earth, Io, and Mars: Journal of the Geological Society, v. 163, p. 253–264. [Also available at <http://dx.doi.org/10.1144/0016-764904-503>.]
- King, S.D., and Anderson, D.L., 1998, Edge-driven convection: Earth and Planetary Science Letters, v. 160, p. 289–296, doi: 10.1016/S0012-821X(98)00089-2.
- Kittleman, L.R., Green, A.R., Haddock, G.H., Hagood, A.R., Johnson, A.M., McMurray, J.M., Russell, R.G., and Weeden, D.A., 1965, Cenozoic stratigraphy of the Owyhee region, southeastern Oregon: University of Oregon Museum of Natural History Bulletin 1, 45 p.
- Kittleman, L.R., Green, A.R., Haddock, G.H., Hagood, A.R., Johnson, A.M., McMurray, J.M., Russell, R.G., and Weeden, D.A., 1967, Geologic map of the Owyhee region, Malheur County, Oregon: University of Oregon Museum of Natural History Bulletin, scale 1:250,000.
- Ladderdud, J.A., Wolff, J.A., Rember, W.C., and Brueseke, M.E., 2015, Volcanic ash layers in the Miocene Lake Clarkia beds—Geochemistry, regional correlation, and age of the Clarkia flora: Northwest Science, v. 89, p. 309–323.
- LaMaskin, T.A., Vervoort, J.D., Dorsey, R.J., and Wright, J.E., 2011, Early Mesozoic paleogeography and tectonic evolution of the western United States—Insights from detrital zircon U-Pb geochronology, Blue Mountains Province, northeastern Oregon: Geological Society of America Bulletin, v. 123, p. 1939–1965, doi:10.1130/B30260.1.
- Landon, R.D., and Long, P.E., 1989, Detailed stratigraphy of the N2 Grande Ronde Basalt, Columbia River Basalt Group in the central Columbia Plateau, in Reidel, S.P., and Hooper, P.R., eds., Volcanism and tectonism in the Columbia River flood-basalt province: Geological Society of America Special Paper 239, p. 55–66.
- Langer, V.W., 1991, Geology and petrologic evolution of silicic and intermediate volcanic rocks underneath Steens Mountain Basalt, SE Oregon: Covallis, Oregon State University, M.S. thesis, 109 p.
- Large, A., Streck, M.J., Jenkins, E.N., and Ferns, M.L., 2015, Silicic volcanism at the northern and western extent of the Columbia River Basalt rhyolite flare-up—Rhyolites at Dooley Mountain and Buchanan, Oregon [abs.]: American Geophysical Union, no. V31E-3064.
- Laval, W.N., 1956, Stratigraphy and structural geology of portions of south-central Washington: Seattle, Washington University, Ph.D. dissertation, 208 p.
- Le Bas, M.J., Le Maitre, R.W., Streckeisen, A., and Zanettin, B., 1986, A chemical classification of volcanic rocks based on the total alkali-silica diagram: Journal of Petrology, v. 27, p. 745–750.
- Lees, K.R., 1994, Magmatic and tectonic changes through time in the Neogene volcanic rocks of the Vale area, Oregon, northwestern U.S.A.: Milton Keynes, U.K., Open University, Ph.D. dissertation, 283 p.
- Lewis, R.S., Kauffman, J.D., Keegan, K.L., and Burmester, R.F., 2006, Geologic map of the Sixmile Creek Quadrangle, Clearwater, Idaho, and Lewis Counties, Idaho: Idaho Geological Survey, 1:24,000 scale.
- Liu, L., and Stegman, D.R., 2012, Origin of Columbia River flood basalt controlled by propagating rupture of the Farallon slab: Nature, v. 482, p. 386–389, doi:10.1038/nature10749.
- Long, M.D., Till, C.B., Druken, K.A., Carlson, R.W., Wagner, L.S., Fouch, M.J., James, D.E., Grove, T.L., Schmerr, N., and Kincaid, C., 2012, Mantle dynamics beneath the Pacific Northwest and the generation of voluminous back-arc volcanism: Geochemistry Geophysics Geosystems, v. 13, doi:10.1029/2012GC004189.
- Ludwin, R.S., Weaver, C.S., and Crossen, R.S., 1991, Seismicity of Washington and Oregon, in Slemon, D.B., Engdahl, E.R., Zoback, M.D., and Blackwell, D.D., eds., Neotectonics of North America: Boulder Colorado, Geologic Society of America Decade Map Volume 1, p. 77–98.
- Mackin, J.H., 1961, A stratigraphic section in the Yakima Basalt and Ellensburg Formation in south-central Washington: Washington Division of Mines and Geology Report Investigation 19, 45 p.

- Mahood, G.A., and Benson, T.R., 2016, $^{40}\text{Ar}/^{39}\text{Ar}$ ages of intercalated silicic tuffs to date flood basalts—Precise ages for Steens Basalt Member of the Columbia River Basalt Group: *Earth and Planetary Science Letters*, v. 459, p. 340–351, doi:10.1016/j.epsl.2016.11.038.
- Mangan, M.T., Wright, T.L., Swanson, D.A., and Byerly, G.R., 1986, Regional correlation of Grande Ronde Basalt flows, Columbia River Basalt Group, Washington, Oregon, and Idaho: *Geological Society of America Bulletin*, v. 97, p. 1300–1318. [Also available at [http://dx.doi.org/10.1130/0016-7606\(1986\)97<1300:RCOGRB>2.0.CO;2](http://dx.doi.org/10.1130/0016-7606(1986)97<1300:RCOGRB>2.0.CO;2).]
- Mankinen, E.A., Prevot, M., Gromme, C.S., and Coe, R.S., 1985, The Steens Mountain (Oregon) geomagnetic polarity transition—I. Directional history, duration of episodes, and rock magmatism: *Journal of Geophysical Research*, v. 90, p. 10,393–10,416, doi:10.1029/JB090iB12p10393.
- Mankinen, E.A., Larson, E.E., Gromme, C.S., Prevot, M., and Coe, R.S., 1987, The Steens Mountain (Oregon) geomagnetic polarity transition, 3. Its regional significance: *Journal of Geophysical Research*, v. 92, no. B8, p. 8057–8076, doi:10.1029/JB090iB08p08057.
- Mann, G.M., and Meyer, C.E., 1993, Late Cenozoic structure and correlations to seismicity along the Olympic-Wallowa Lineament, northwest United States: *Geological Society of America Bulletin*, v. 105, p. 853–871.
- Martin, B.S., 1989, The Roza Member, Columbia River Basalt Group—Chemical stratigraphy and flow distribution, in Reidel, S.P., and Hooper, P.R., eds., *Volcanism and tectonism in the Columbia River flood-basalt province*: Geological Society of America Special Paper 239, p. 85–104.
- Martin, B.S., Tolan, T.L., and Reidel, S.P., 2013, Revisions to the stratigraphy and distribution of the Frenchman Springs Member, Wanapum Basalt, in Reidel, S.P., Camp, V.E., Ross, M.E., Wolff, J.A., Martin, B.S., Tolan, T.L., and Wells, R.E., eds., *The Columbia River Flood Basalt Province*: Geological Society of America Special Paper 497, p. 155–179, doi:10.1130/2013.2497
- McCaffrey, R., King, R.W., Payne, S., and Lancaster, M., 2013, Active tectonics of the northwestern US inferred from GPS derived surface velocities: *Journal of Geophysical Research*, v. 118, p. 709–723, doi: 10.1029/2012JB009473.
- McCaffrey, R., King, R.W., Wells, R.E., Lancaster, M., and Miller, M.M., 2016, Contemporary deformation in the Yakima fold and thrust belt estimated with GPS: *Geophysical Journal International*, v. 207, p. 1–11, doi:10.1093/gji/ggw252.
- McKee, E.H., Nobel, D.C., and Silberman, M.L., 1970, Middle Miocene hiatus in volcanic activity in the Great Basin area of the western United States: *Earth and Planetary Science Letters*, v. 8, p. 93–96.
- McQuarrie, N., and Oskin, M., 2010, Palinspastic restoration of NAVDat and implications for the origin of magmatism in southwestern North America: *Journal of Geophysical Research*, v. 115, B10401, doi: 10.1029/2009JB006435.
- McQuarrie, N., and Wernicke, B.P., 2005, An animated tectonic reconstruction of southwestern North America since 36 Ma: *Geological Society of America Bulletin*, v. 1, p. 147–172, doi: 10.1130/GES00016.1.
- Meigs, A., Scarberry, K., Grunder, A., Carlson, R., Ford, M.T., Fouch, M., Grove, T., Hart, W.K., Iademarco, M., Jordan, B., and Millard, J., 2009, Geological and geophysical perspectives on the magmatic and tectonic development, High Lava Plains and northwest Basin and Range, in O'Connor, J.E., Dorsey, R.J., and Madin, I.P., eds., *Volcanoes to vineyards—Geologic field trips through the dynamic landscape of the Pacific Northwest*: Geological Society of America Field Guide 15, p. 435–470.
- Morgan, W.J., 1972, Plate motions and deep mantle convection: *Geological Society of America Bulletin*, v. 132, p. 7–22.
- Nash, B.P., Perkins, M.E., Christensen, J.N., Lee, D.C., and Halliday, A., 2006, The Yellowstone hotspot in space and time—Nd and Hf isotopes in silicic magmas: *Earth and Planetary Science Letters*, v. 247, p. 143–156.
- Niem, A.R., and Niem, W.A., 1985, Oil and gas investigation of the Astoria Basin, Clatsop and northernmost Tillamook Counties, northwest Oregon: Oregon Department of Geology and Mineral Industries OGI-14, scale 1:100 000, 2 plates, 8 p. text.
- North American Commission on Stratigraphic Nomenclature, 2005, *North American Stratigraphic Code*: American Association of Petroleum Geologists Bulletin, v. 89, p. 1547–1591.
- Obrebski, M., Allen, R.M., Pollitz, F., and Hung, S-H., 2011, Lithosphere-asthenosphere interaction beneath the western United States from joint inversion of body-wave traveltimes and surface-wave phase velocities: *Geophysical Journal International*, v. 185, p. 1003–1021, doi: 10.1111/j.1365-246X.2011.04990.x.
- Oldow, J.S., and Singleton, E.S., 2008, Application of terrestrial laser scanning in determining the pattern of late Pleistocene and Holocene fault displacement from the offset of pluvial lake shorelines in the Alvord extensional basin, northern Great Basin, USA: *Geosphere*, v. 4, p. 536–563, doi: 10.1130/GES00101.1.
- Payne, S.J., McCaffrey, R., King, R.W., and Kattenhorn, S.A., 2012, A new interpretation of deformation rates in the Snake River Plain and adjacent Basin and Range regions based on GPS measurements: *Geophysical Journal International*, v. 189, p. 101–122, doi: 10.1111/j.1365-246X.2012.05370.x.

- Personius, S.F., Dart, R.L., Bradley, L-A., and Haller, K.M., 2003, Map and data for Quaternary faults and folds in Oregon: United States Geological Survey Open-File Report 03-095, 550 p.
- Petcovic, H.L., and Grunder, A.L., 2003, Textural and thermal history of partial melting in tonalitic wallrock at the margin of a basalt dike, Wallowa Mountains, Oregon: *Journal of Petrology*, v. 44, p. 2287–2312.
- Pierce, K.L. and Morgan, L.A., 1992, The track of the Yellowstone hot spot: volcanism, faulting, and uplift, *in* Link, P.K., ed., *Regional geology of eastern Idaho and western Wyoming: Geological Society of America Memoir 179*, p. 1–53.
- Pierce, K.L., and Morgan, L.A., 2009, Is the track of the Yellowstone hotspot driven by a deep mantle plume—Review of volcanism, faulting, and uplift in light of new data: *Journal of Volcanology and Geothermal Research*, v. 188, p. 1–25, doi: 10.1016/j.volgeores.2009.07-009.
- Pierce, K.L., Morgan, L.A., and Saltus, R.W., 2002, Yellowstone plume head—Postulated tectonic relations to the Vancouver slab, continental boundaries, and climate, *in* Bonnichsen, B., White, C.M., and McCurry, M., eds., *Tectonic and magmatic evolution of the Snake River Plain Volcanic Province: Idaho Geological Survey Bulletin 30*, p. 5–33.
- Price, E.H., and Watkinson, A.J., 1989, Structural geometry and strain distribution within Umtanum Ridge, south-central, Washington, and its tectonic significance, *in* Reidel, S.P., and Hooper, P.R., eds., *Volcanism and tectonism in the Columbia River flood-basalt province: Geological Society of America Special Paper 239*, p. 265–282.
- Raisz, E., 1945, The Olympic-Wallowa lineament: *American Journal of Science*, v. 243-A, p. 479–485.
- Ramos, F.C., Wolff, J.A., Starkel, W., Eckberg, A., Tollstrup, D.L., and Scott, S., 2013, The changing nature of sources associated with Columbia River Basalts—Evidence from strontium isotope ratio variations in plagioclase phenocrysts, *in* Reidel, S.P., Camp, V.E., Ross, M.E., Wolff, J.A., Martin, B.S., Tolan, T.L., and Wells, R.E., eds., *The Columbia River Flood Basalt Province: Geological Society of America Special Paper 497*, p. 231–257.
- Ramos, F.C., Wolff, J.A., and Tollstrup, D.L., 2005, Sr isotope disequilibrium in Columbia River Basalts—Evidence for rapic, shallow-level, open-system processes: *Geology*, v. 33, p. 457–460, doi:10.1130/G1512.1.
- Reidel, S.P., 1982, Stratigraphy of the Grande Ronde Basalt, Columbia River Basalt Group, from the lower Salmon River and northern Hell's canyon area, Idaho, Washington, and Oregon, *in* Bonnichsen, B., and Breckenridge, R.M., eds., *Cenozoic geology of Idaho: Geological Survey of Idaho Bulletin 26*, p. 77–101.
- Reidel, S.P., 1983, Stratigraphy and petrogenesis of the Grande Ronde Basalt from the deep canyon country of Washington, Oregon, and Idaho: *Geological Society of America Bulletin*, v. 94, p. 519–542.
- Reidel, S.P., 1984, The Saddle Mountains—The evolution of an anticline in the Yakima Fold Belt: *American Journal of Science*, v. 284, p. 942–978, doi:10.2475/ajs.284.8.942.
- Reidel, S.P., 1988, Geologic map of the Saddle Mountains, south-central Washington: *Division of Geology and Earth Resources Geologic Map GM-38*, 28 p., 5 plates, scale 1:48,000.
- Reidel, S.P., 1998, Emplacement of Columbia River Flood Basalt: *Journal of Geophysical Research*, v. 103, p. 27393–27410. [Also available at <http://dx.doi.org/10.1029/97JB03671>.]
- Reidel, S.P., 2005, A lava flow without a source—The Cohassett flow and its compositional components, Sentinel Bluffs Member, Columbia River Basalt Group: *Journal of Geology*, v. 113, p. 1–21.
- Reidel, S.P., 2015, Igneous rock associations 15. The Columbia River Basalt Group—A flood basalt province in the Pacific Northwest, USA: *Geoscience Canada*, v. 42, p. 151–168. [Also available at <http://dx.doi.org/10.12789/geocanj.2014.41.061>.]
- Reidel, S.P., Camp, V.E., Ross, M.E., Wolff, J.A., Martin, B.S., Tolan, T.L., and Wells, R.E., 2013c, eds., *The Columbia River Flood Basalt Province: Geological Society of America Special Paper 497*, 440 p.
- Reidel, S.P., Camp, V.E., Tolan, T.L., Kauffman, J.D., and Garwood, D.L., 2013b, Tectonic evolution of the Columbia River flood basalt province, *in* Reidel, S.P., Camp, V.E., Ross, M.E., Wolff, J.A., Martin, B.S., Tolan, T.L., and Wells, R.E., eds., *The Columbia River Flood Basalt Province: Geological Society of America Special Paper 497*, p. 293–324, doi: 10.1130/2013.2497(12).
- Reidel, S.P., Camp, V.E., Tolan, T.L., and Martin, B.S., 2013a, The Columbia River flood basalt province—Stratigraphy, areal extent, volume, and physical volcanology, *in* Reidel, S.P., Camp, V.E., Ross, M.E., Wolff, J.A., Martin, B.S., Tolan, T.L., and Wells, R.E., eds., *The Columbia River Flood Basalt Province: Geological Society of America Special Paper 497*, p. 1–43, doi: 10.1130/2013.2497(01).
- Reidel, S.P., Campbell, N.P., Fecht, K.R., and Lindsey, K.A., 1994a, Late Cenozoic structure and stratigraphy of southcentral Washington, *in* Cheney, E., and Lasmanis, R., eds., *Regional geology of Washington State: Washington Division of Geology and Earth Resources Bulletin 80*, p. 159–180.
- Reidel, S.P., and Fecht, K.R., 1987, The Huntzinger flow—Evidence of surface mixing of the Columbia River basalt and its petrogenetic implications: *Geological Society of America Bulletin*, v. 98, p. 664–667.

- Reidel, S.P., and Fecht, K.R., 1994a, Geologic map of the Richland 1:100,000 quadrangle, Washington: Washington Division of Geology and Earth Resources Open File Report 94-8, 21 p., 1 plate.
- Reidel, S.P., and Fecht, K.R., 1994b, Geologic map of the Priest Rapids 1:100,000 quadrangle, Washington: Washington Division of Geology and Earth Resources Open File Report 94-13, 22 p., 1 plate.
- Reidel, S.P., Fecht, K.R., Hagood, M.C., and Tolan, T.L., 1989a, The geologic evolution of the central Columbia Plateau, *in* Reidel, S.P., and Hooper, P.R., eds., Volcanism and tectonism in the Columbia River flood-basalt province: Geological Society of America Special Paper 239, p. 247-264.
- Reidel, S.P., and Hooper, P.R., eds., 1989, Volcanism and tectonism in the Columbia River flood-basalt province: Geological Society of America Special Paper 239, 386 p.
- Reidel, S.P., Scott, G.R., Bazard, D.R., Cross, R.W., and Dick, B., 1984, Post-12 million year clockwise rotation in the central Columbia Plateau, Washington: Tectonics, v. 3, no. 2, p. 251-273, doi:10.1029/TC003i002p00251.
- Reidel, S.P., and Tolan, T.L., 1992, Eruption and emplacement of flood basalt—An example from the large-volume Teepee Butte Member, Columbia River Basalt Group: Geological Society of America Bulletin, v. 104, p. 1650-1671, doi: 10.1130/0016-7606(1992)104<1650:EAEFOB>2.3.CO;2.
- Reidel, S.P., and Tolan, T.L., 2013, The Grande Ronde Basalt, Columbia River Basalt Group, *in* Reidel, S.P., Camp, V.E., Ross, M.E., Wolff, J.A., Martin, B.S., Tolan, T.L., and Wells, R.E., eds., The Columbia River Flood Basalt Province: Geological Society of America Special Paper 497, p. 117-153, doi:10.1130/2013.2497(05).
- Reidel, S.P., Tolan, T.L., and Beeson, M.H., 1994b, Factors that influenced the eruptive and emplacement histories of flood basalt flows—A field guide to selected vents and flows of the Columbia River Basalt Group, *in* Swanson, D.A., and Haugerud, R.A., eds., Geologic field trips in the Pacific Northwest: Geological Society of America Annual Meeting Field Guide, p. 1B-1-18.
- Reidel, S.P., Tolan, T.L., Hooper, P.R., Beeson, M.H., Fecht, K.R., Bentley, R.D., and Anderson, J.L., 1989b, The Grande Ronde Basalt, Columbia River Basalt Group—Stratigraphic descriptions and correlations in Washington, Oregon, and Idaho, *in* Reidel, S.P., and Hooper, P.R., Volcanism and tectonism in the Columbia River Flood Basalt Province: Geological Society of America Special Paper 239, p. 21-53.
- Ross, M.E., 1975, The structure of Yakima basalts in a portion of the Grande Ronde River region of northeastern Oregon and southeastern Washington [abs.]: Geological Society of America Abstracts with Programs, v. 7, p. 366.
- Ross, M.E., 1978, Stratigraphy, structure, and petrology of the Columbia River basalt in a portion of the Grande Ronde River-Blue Mountains area of Oregon and Washington: Moscow, University of Idaho, Ph.D. thesis, 407 p.
- Ross, M.E., 1979, Large scale strike-slip faulting of Columbia River Basalt in northeast Oregon [abs.]: Geological Society of America Abstracts with Programs, v. 11, p. 51.
- Ross, M.E., 1980, Tectonic controls of topographic development within Columbia River basalts in a portion of the Grande Ronde River-Blue Mountains region, Oregon and Washington: Oregon Geology, v. 42, no. 10, p. 167-171.
- Ross, M.E., 1983, Chemical and mineralogical variations within four dikes of the Columbia River Basalt Group: Geological Society of America Bulletin, v. 94, p. 1117-1126.
- Ross, M.E., 1989, Stratigraphic relationships of subaerial, invasive, and intracanyon flows of Saddle Mountains Basalt in the Troy Basin, Oregon and Washington, *in* Reidel, S.P., and Hooper, P.R., eds., Volcanism and tectonism in the Columbia River flood-basalt province: Geological Society of America Special Paper 239, p. 131-142.
- Rytuba, J.J., and McKee, E.H., 1984, Peralkaline ash flow tuffs and calderas of the McDermitt volcanic field, southeast Oregon and north central Nevada: Journal of Geophysical Research, v. 89, p. 8616-8628.
- Scarberry, K.C., Meigs, A.J., and Grunder, A., 2010, Faulting in a propagating continental rift—Insight from the late Miocene structural development of the Aber Rim fault, southern Oregon, USA: Tectonophysics, v. 488, p. 71-86, doi: 10.1016/j.tecto.2009.09.025.
- Schmandt, B., Dueker, K., Humphreys, E., and Hansen, S., 2012, Hot mantle upwelling across the 660 beneath Yellowstone: Earth and Planetary Science Letters, v. 331, p. 224-236, doi: 10.1016/j.epsl.2012.03.025.
- Schmincke, Hans-Ulrich, 1967, Stratigraphy and petrography of four upper Yakima basalt flows in south-central Washington: Geological Society of America Bulletin, v. 78, p. 1385-1422.
- Schuster, J.E., 1994, Geologic map of the Walla Walla 1:100,000 quadrangle, Washington: Washington Division of Geology and Earth Resources Open File Report 94-3, 21 p., 1 plate.
- Schuster, J.E., 2005, Geologic map of Washington State: Washington Division of Geology and Earth Resources Geologic Map GM-53, scale 1:500,000.
- Schuster, J.E., Gulick, C.W., Reidel, S.P., Fecht, K.R., and Zurendo, S., 1997, Geologic map of Washington - southeast quadrant: Washington Division of Geology and Earth Resources Geologic Map GM-45, 20 p., 3 plates.

- Schwartz, J.J., Snee, A.W., Frost, C.D., Barnes, C.G., Gromet, L.P., and Johson, K., 2010, Analysis of the Wallowa-Baker terrane boundary—Implications for tectonic accretion in the Blue Mountains province, northeastern Oregon: Geological Society of America Bulletin, v. 122, p. 517–536, doi:10.1130/B26493.1.
- Self, S., Keszthelyi, L., and Thordarson, T., 1998, The importance of pāhoehoe: Annual Reviews of Earth Planetary Science, v. 26, p. 81–110.
- Self, S., Thordarson, T., Keszthelyi, L., Walker, G.P.L., Hon, K., Murphy, M.T., Long, P., and Finnemore, S., 1996, A new model for the emplacement of Columbia River basalts as large, inflated pahoehoe lava flow fields: Geophysical Research Letters, v. 23, p. 2689–2692. [Also available at <http://dx.doi.org/10.1029/96GL02450>.]
- Shaw, H.R., and Swanson, D.A., 1970, Eruption and flow rates of flood basalts, in Gilmour, E.H., and Stradling, D.F., eds., Proceedings of the second Columbia River Basalt symposium: Cheney, Eastern Washington State College Press, p. 271–299.
- Shervais, J.W., and Hanan, B.B., 2008, Lithospheric topography, tilted plumes, and the track of the Snake River-Yellowstone hot spot: Tectonics, v. 27, TC5004, doi:10.1029/2007TC002181.
- Shubat, M.A., 1979, Stratigraphy, petrochemistry, petrography and structural geology of the Columbia River Basalt in the Minam-Wallowa River area, northeastern Oregon: Pullman, Washington State University, M.S. thesis, 156 p.
- Sigloch, K., McQuarrie, N., and Nolet, G., 2008, Two-stage subduction history under North America inferred from multiple-frequency tomography: Nature Geoscience, v. 1, p. 458–462, doi:10.1038/ngeo231.
- Smith, A.D., 1992, Back-arc convection model for Columbia River Basalt genesis: Tectonophysics, v. 207, p. 269–285.
- Smith, R.B., Jordan, M., Steinberger, B., Puskas, C.M., Farrell, J., Waite, G.P., Husen, S., Wu-Lung, C., and O'Connell, R., 2009, Geodynamics of the Yellowstone hotspot and mantle plume—Seismic and GPS imaging, kinematics, and mantle flow: Journal of Volcanology and Geothermal Research, v. 188, p. 26–56, doi:10.1016/j.volgeores.2009.08.020.
- Stoffel, K.L., 1984, Geology of the Grande Ronde lignite field, Asotin County, Washington: Washington Department of Natural Resources Report of Investigations 27, 79 p.
- Streck, M.J., and Ferns, M., 2004, The Rattlesnake Tuff and other Miocene silicic volcanism in eastern Oregon, in Haller, K.M., and Wood, S.H., eds., Geological field trips in southern Idaho, eastern Oregon, and northern Nevada: United States Geological Survey Open-File Report 2004-1222, p. 5–19.
- Streck, M.J., Ferns, M., and McIntosh, W., 2015, Large, persistent rhyolitic magma reservoirs above Columbia River Basalt storage sites—The Dinner Creek Tuff eruptive center, eastern Oregon: Geosphere, v. 11, doi: 10.1130/GES01086.1.
- Streck, M.J., and Grunder, A.L., 1995, Crystallization and welding variations in a widespread ignimbrite sheet; the Rattlesnake Tuff, eastern Oregon, USA: Bulletin of Volcanology, v. 57, p. 151–169.
- Streck, M.J., McIntosh, W., and Ferns, M.L., 2016, Co-CRBG rhyolite volcanism reassessed [abs.]: Geological Society of America, Rocky Mountain Section, Abstracts with Programs, v. 48, no. 3–3.
- Swanson, D.A., 1973, Pahoehoe flows from 196901971 Mauna Ulu eruption, Kilauea volcano, Hawaii: Geological Society of America Bulletin, v. 84, p. 615–626.
- Swanson, D.A., Anderson, J.L., Camp, V.E., Hooper, P.R., Taubeneck, W.H., and Wright, T.L., 1981, Reconnaissance geologic map of the Columbia River Basalt Group, northern Oregon and western Idaho: U.S. Geological Survey Open-File Report I-797, scale 1:250,000.
- Swanson, D.A., and Wright, T.L., 1976, Guide to field trip between Pasco and Pullman, Washington emphasizing stratigraphy, vent areas, and intracanyon flows of Yakima Basalt: Geological Society of America Cordilleran Section Field Guide no. 1, 32 p.
- Swanson, D.A., and Wright, T.L., 1981, The regional approach to studying the Columbia River Basalt Group, in Subbarao, K.V., and Sukheswala, R.N., eds., Deccan volcanism and related basalt provinces in other parts of the world: Geological Society of India Memoir 3, p. 58–80.
- Swanson, D.A., Wright, T.L., Camp, V.E., Gardner, J.N., Helz, R.T., Price, S.M., Reidel, S.P., and Ross, M.E., 1980, Reconnaissance geologic map of the Pullman and Walla Walla quadrangles, southeast Washington and adjacent Idaho: U.S. Geological Survey Miscellaneous Investigations Series Map I-1139, scale 1:250,000, 2 sheets.
- Swanson, D.A., Wight, T.L., and Helz, R.T., 1975, Linear vent systems and estimated rates of magma production and eruption of Yakima Basalt on the Columbia Plateau: American Journal of Science, v. 275, p. 877–905, doi:10.2475/ajs.275.8.877.
- Swanson, D.A., Wright, T.L., Hooper, P.R., and Bentley, R.D., 1979, Nomenclature of the Columbia River Basalt Group: Geological Survey Bulletin 1457-G, 59 p.
- Takahashi, E., Nakajima, K., and Wight, T.L., 1998, Origin of the Columbia River basalts—Melting model of a heterogeneous plume head: Earth and Planetary Science Letters, v. 162, p. 63–80, doi: 10.1016/S0012-821X(98)00157-5.

- Taubeneck, W.H., 1970, Dikes of the Columbia River Basalt in northeastern Oregon and southeastern Washington, in Gilmore, E.H., and Stradling, D., eds., Proceedings of the second Columbia River Basalt symposium: Cheney, Eastern Washington State College Press, p. 73–96.
- Taubeneck, W.H., 1987, The Wallowa Mountains, northeastern Oregon, in Hill, M.L., Cordilleran Section of the Geological Society of America: Boulder, Colo., Geological Society of America Centennial Field Guide, v. 1, p. 327–332.
- Thordarson T., and Self S., 1996, Sulfur, chlorine and fluorine degassing and atmospheric loading by the Roza eruption, Columbia River Basalt Group, Washington, USA: Journal of Volcanology and Geothermal Research, v. 74, p. 49–73.
- Thordarson, T., and Self, S., 1998, The Roza Member, Columbia River Basalt Group—A gigantic pahoehoe lava flow field formed by endogenous processes?: Journal of Geophysical Research, v. 103, p. 27411–27445.
- Tian, Y., and Zhao, D., 2012, P-wave tomography of the western United States—Insight into the Yellowstone hotspot and the Juan de Fuca slab: Physics of the Earth and Planetary Interiors, v. 201, p. 72–84, doi: 10.1016/j.pepi.2012.04.004.
- Tikoff, B., Benford, B., and Giorgis, S., 2008, Lithospheric control on the initiation of the Yellowstone hotspot—Chronic reactivation of lithospheric scars: International Geology Review, v. 50, p. 305–324, doi:10.2747/0020-6814.50.3.305.
- Tolan, T.L., and Beeson, M.H., 1984, Intracanyon flows of the Columbia River Basalt Group in the lower Columbia River Gorge and their relationship to the Troutdale Formation: Geological Society of America Bulletin, v. 95, p. 463–477.
- Tolan, T.L., Martin, B.S., Reidel, S.P., Kauffman, J.D., Garwood, D.L., and Anderson, J.L., 2009, Stratigraphy and tectonics of the central and eastern portions of the Columbia River Flood-basalt Province—A primer for the GSA Columbia River Basalt Group field trips, in O'Connor, J.E., Dorsery, R.J., and Madin, I.P., eds., Volcanoes to vineyards—Geologic field trips through the dynamic landscape of the Pacific Northwest: Geological Society of America Field Guide 15, p. 645–672.
- Tolan, T.L., Reidel, S.P., Beeson, M.H., 1989, Revisions to the estimates of the areal extent and volume of the Columbia River Basalt Group, in Reidel, S.P., Camp, V.E., Ross, M.E., Wolff, J.A., Martin, B.S., Tolan, T.L., and Wells, R.E., eds., The Columbia River Flood Basalt Province: Geological Society of America Special Paper 497, p. 1–20, doi:10.1130/2013.2497(05).
- Yye-Brown, C., Self, S., and Barry, T.L., 2013, Architecture and emplacement of flood basalt flow fields—Case studies from the Columbia River Basalt Group, NW USA: Bulletin of Volcanology, v. 75, article 697, doi:10.1007/s00445-013-0697-2.
- Wacaster, S., Streck, M.J., Belkin, H.E., and Bodnar, R.J., 2011, Compositional zoning of the Devine Canyon Tuff, Oregon [abs.]: American Geophysical Union, Fall Meeting, no. V21C–2517.
- Walker, G.P.L., 1971, Compound and simple lava flows and flood basalts: Bulletin of Volcanology, v. 35, p. 579–590.
- Walker, G.W., 1979, Revisions to the Cenozoic stratigraphy of Harney Basin, southeastern Oregon: U.S. Geological Survey Bulletin 1475, 35 p.
- Walker, G.W., and MacLeod, N.S., 1991, Geologic map of Oregon: U.S. Geological Survey, scale 1:500,000, 2 sheets.
- Walker, G.W., and Nolf, B., 1981, Roadlog for High Lava Plains, Brothers fault zone to Harney Basin, Oregon, in Johnston, D.A., and Donnelly-Nolan, J.M., eds., Guides to some volcanic terranes in Washington, Idaho, Oregon, and northern California: U.S. Geological Survey Circular 838, 189 p.
- Walsh, T.J., Korosec, M.A., Phillips, W.M., Logan, R.L., and Schasse, H.W., 1987, Geologic map of Washington-Southwest quadrant: Washington Division of Geology and Earth Resources Geologic Map GM-34, scale 1:250 000, 2 sheets, 28 p. text.
- Waters, A., 1961, Stratigraphic and lithologic variations in the Columbia River Basalt: American Journal of Science, v. 259, p. 583–611, doi: 10.1475/ajs.259.8.583.
- Watkins, N.D., and Baksi, A.K., 1974, Magnetostratigraphy and orocinal folding of the Columbia River, Steens, and Owyhee basalts in Oregon, Washington, and Idaho: American Journal of Science, v. 274, p. 148–189.
- Webb, B.M., Streck, M.J., McIntosh, W.C., and Ferns, M.L., 2016, Flow units of the Littlefield Rhyolite, eastern Oregon, constraining age and storage sites of Grande Ronde Basalt magmas [abs.]: Geological Society of America Abstracts with Programs, v. 48, no. 28-1.
- Wells, R.E., Bukry, D., Friedman, R., Pyle, D., Duncan, R., Haeussler, P., and Wooden, J., 2014, Geologic history of Siletzia, a large igneous province in the Oregon and Washington Coast Range—Correlation to the geomagnetic polarity time scale and implications for a long-lived Yellowstone hotspot: Geosphere, v. 10, doi:10.1130/GES01018.1.
- Wells, R.E., and Heller, P.L., 1988, The relative contribution of accretion, shear, and extension to Cenozoic tectonic rotation in the Pacific Northwest: Geological Society of America Bulletin, v. 100, p. 325–389.
- Wells, R.E., and McCaffrey, R., 2013, Steady rotation of the Cascade arc: Geology, v. 41, p. 1027–1030, doi: 10.1130/G34514.1.

- Wells, R.E., Niem, A.R., Evarts, R.C., and Hagstrum, J.T., 2009, The Columbia River Basalt Group—From the gorge to the sea, in O'Connor, J.E., Dorsey, R.J., and Madin, I.P., eds., Volcanoes to vineyards—Geologic field trips through the dynamic landscape of the Pacific Northwest: Geological Society of America Field Guide 15, p. 737–774.
- Wells, R.E., Simpson, R.W., Bentley, R.D., Beeson, M.H., Mangan, M.T., and Wright, T.L., 1989, Correlation of Miocene flows of the Columbia River Basalt Group from the central Columbia River Plateau to the coast of Oregon and Washington, in Reidel, S.P., and Hooper, P.R., eds., Volcanism and tectonism in the Columbia River Flood-Basalt Province: Geological Society of America Special Paper 239, p. 113–130.
- Wells, R.E., Weaver, C.S., and Blakely, R.J., 1998, Fore-arc migration in Cascadia and its neotectonic significance: Geology, v. 26, p. 759–762, doi:10.1130/0091-7613(1998)026<0759:FAMICA>2.3.CO;2.
- White, R.S., and McKenzie, D.P., 1989, Magmatism at rift zones—The generation of volcanic continental margins and flood basalts: Journal of Geophysical Research, v. 94, p. 7685–7729.
- White, R.S., and McKenzie, D.P., 1995, Mantle plumes and flood basalts: Journal of Geophysical Research, v. 100, p. 17,543–17,586, doi: 10.1029/95JB01585.
- Wolff, J.A., and Ramos, F.C., 2013, Source material for the main phase of the Columbia River Basalt Group—Geochemical evidence and implications for magma storage and transport, in Reidel, S.P., Camp, V.E., Ross, M.E., Wolff, J.A., Martin, B.S., Tolan, T.L., and Wells, R.E., eds., The Columbia River Flood Basalt Province: Geological Society of America Special Paper 497, doi: 10.1130/2013.2497(11).
- Wolff, J.A., Ramos, R.C., Hart, G.L., Patterson, J.D., and Brandon, A.D., 2008, Columbia River flood basalts from a centralized crustal magmatic system: Nature Geoscience, v. 1, no. 2, doi: 0.2038.ngeo124.
- Wright, T.L., Grolier, M.J., and Swanson, D.A., 1973, Chemical variation related to the stratigraphy of the Columbia River basalt: Geological Society of America Bulletin, v. 84, p. 371–386.
- Wright, T.L., Mangan, M., and Swanson, D.A., 1989, Chemical data for flows and feeder dikes of the Yakima Basalt Subgroup, Columbia River Group, Washington, Oregon, and Idaho, and their bearing on a petrological model: U.S. Geological Survey Bulletin 1821, 71 p.
- Wright, T.L., Swanson, D.A., and Fruchter, J.S., 1976, Petrogenesis of Yakima Basalt in southeastern Washington [abs.]: Geological Society of America Abstracts with Programs, v. 8, no. 3, p. 422.
- Wyld, S.J., and Wright, J.E., 2001, New evidence for Cretaceous strike-slip faulting in the United States Cordillera and implications for terrane-displacement, deformation patterns, and plutonism: American Journal of Science, v. 301, p. 150–181.
- Wypych, A., Hart, W.K., Scarberry, K.C., McHugh, K.C., Pasquale, S.A., and Legge, P.W., 2011, Geologic map of the Hawks Valley-Lone Mountain Region, Harney County, Oregon: Oregon Department of Geology and Mineral Industries Open-File Report 0-11-12, scale 1:24,000-scale.
- Yaxley, G.M., 2000, Experimental study of the phase and melting relations of homogeneous basalt + peridotite mixtures and implications for petrogenesis of flood basalts: Contributions to Mineralogy and Petrology, v. 139, p. 326–338, doi:10.1007/s004100000134.

Menlo Park Publishing Service Center, California
Manuscript approved April 19, 2017
Edited by Kate Jacques
Design and layout by Cory Hurd

